CRANFIELD INSTITUTE OF TECHNOLOGY
SCHOOL OF INDUSTRIAL AND MANUFACTURING SCIENCE

Ph.D. THESIS

Academic Year 1990-91

J. CHAPPLES

ELECTROCHEMICAL AND CHEMICAL METHODS OF METALLIZING PLASTIC FILMS

Supervisor: Prof. H. Block

September 1991

ABSTRACT

This thesis describes two novel techniques for the metallization of non-electroactive polymer films and thicker sectioned polyethylene and nylon substrates.

In the first approach, non-electroactive polymer substrates were impregnated with surface layers of polypyrrole and polyaniline, using electrochemical and chemical methods of polymerization. The relative merits of both these approaches are discussed and compared with other methods in the literature. The resultant composite materials exhibited sufficient conductivity to permit the direct electrodeposition of metal surface coats. Polypyrrole coated substrates were also metallized using chemical methods.

Cyclic voltammetry studies and scanning electron microscopy of metal coated polypyrrole, showed that metal deposition occurred mainly at the polymer surface by a mechanism of instantaneous nucleation and growth. Using optimized deposition conditions, both electrochemical and chemical metal deposition methods were used to deposit highly reflecting and coherent metal layers onto conducting polymer coated materials.

The second approach of metallizing polymers, was the metallization of non-electroactive polymer films by the electroreduction of silver from non-aqueous based silver plating solutions. The effects of the electrode substrate, the deposition potential, and the concentration of metal ions in solution were investigated to determine suitable metal salt/solvent, and polymer film/solvent combinations. The resultant metallized polymer films were evaluated using optical and scanning electron microscopy, ac impedance, and reflectance measurements. These studies enabled the optimum deposition conditions to be determined, and these were subsequently used for the preparation of high quality, uniform, and reflective metal coated films.

The results for the electrodeposition of silver into polymer films using the latter approach are compared with those obtained from alternative electrochemical and chemical methods of metallizing polymer films.

He that to what he sees, adds observation, and to what he reads reflection, is on the right road to knowledge.

Caleb Colton

Acknowledgements

The author would like to express his thanks to his supervisor, Prof. H. Block for his advice and support during the course of this work, Dr. R.G. Compton for valuable discussion and his invitation to use facilities at Oxford University, and Dr. A.M. Waller at Oxford for his assistance with practical aspects of the work.

Grateful thanks are also expressed to SERC and CIT for their financial support, to GEC Avionics for supplying materials, and Kodak Ltd for use of their facilities. Finally the author would like to thank Dr. R. Tidswell for proof reading.

To My Parents

CONTENTS

Page.

FIGURES

TABLES

PLATES

CHAPTER 1

ELECTROPLATING OF PLASTICS

1.1 Introduction.

It has been stated that "as long as there have been plastics there have been efforts to electroplate them"[1]. Early methods of plating plastics were derived from processes which were originally developed to plate materials as diverse as wood, glass, leather, leaves, flowers, etc[2-5]. These methods were intricate, required skilled workers, and were not suited to mass production. Furthermore, the bond between the plastic substrate and metal was poor, which meant that metallization was restricted to small scale decorative or artistic applications. With these, the low adhesion between substrate and deposit was not important, and total encapsulation was used to keep the metal coating in place.

The modern era of electroplating of plastics dates from work in the mid 1960's by Narcus[6], Saubestre[7], and Jensen[8]. They successfully combined the newly developed 2-phase acrylonitrile-butadiene-styrene (ABS) polymers with existing chemical conditioning pretreatment techniques, to produce metal coats which had a strong adhesion to the plastic substrate. The advantages afforded by these plastics was such, that the subsequent developments in metallizing plastics were almost entirely focused on ABS, and on improvements in the chemical conditioners and etchants that were required for their pretreatment. Indeed, as late as 1966, approximately 95% of the plastic items that were plated were ABS[9]. As a result of the considerable research effort that had gone into improving the techniques and processes for plating on plastics, the industry developed from small scale specialised plating, into large scale mass production in only five years[10]. During this time, several hundred formulations and processes were reported in U.S. patents, for the pretreatment, activation, and metal coating of ABS, polyesters, nylon, polyethylene and polypropylene[9,11]. More recently, attention has focused on the metallization of polyimides, as these are widely used in the electronics industry as dielectric and passivation films[12].

The purpose of this chapter is to outline traditional and recent techniques which have been developed to metallize non-conductors. Particular emphasis is focused on plastics and polymer films in order to provide a background to the work which is described in chapters 5, 6, 7 and 8 of this thesis.

Classical methods of plating non-conductors are described in section 1.2.1. The principles behind these processes still form the basis of many of the current methods of plating on plastics. Modern methods of plating plastics are covered in section 1.3; finally, current developments in metallizing polymers and polymer films are discussed in section 1.5.

1.2 Metallizing Processes.

Plastics and other non-metallic materials can only be electroplated after the application of an initial conducting layer to the surface to be plated. Once this is achieved, one or more other metal layers are subsequently deposited to reach the required deposit thickness and finish, depending on the intended application. This section describes classical methods which have been developed, although it should be noted that these techniques are now seldom used, having been largely superseded by the processes described in section 1.3.

1.2.1 Classical Methods.

Classical methods of plating non-conductors were used primarily for decorative purposes, or for plating items such as buttons, in which adhesion of the metallic coat was not crucial[2,13,14,15]. These techniques required several steps which were usually performed by hand, hence the processes were labour intensive and time consuming. The initial stage in any of these techniques was surface preparation. This was vital for achieving non-porous, defect free deposits. Smooth surfaces needed to be mechanically roughened to provide adhesion for subsequent layers. This was accomplished by either sanding or shot blasting. Porous substrates were then sealed with a surface coat of wax or varnish. The next stage was to render the surface electrically conductive so as to permit the application of an electrolytic deposit. This could be achieved by several means, and the most common are described below;

1.2.1.1 Polishing with Powdered Graphite.

Graphite was commonly used to form an initial conducting layer. It possessed the advantages of being cheap, and more importantly, it readily adheres to a wide variety of different materials. Finely divided graphite powder was brushed onto the substrate surface, and then polished to a high lustre, completely encapsulating the article. Electrolytic reinforcement of the surface coat was then carried out in the conventional manner[3,4,15].

1.2.1.2 Immersion Techniques.

Immersion plating (also called displacement) techniques were also used[3,4,16]. A fine powder of a metal which was more electropositive than the one to be plated, was mixed with either varnish or a special lacquer, and coated onto the substrate surface. Typical examples included iron, which could be used to form an immersion deposit of copper from copper sulphate solution, or in a technique known as "bronzing", copper was used to immersion plate silver.

1.2.1.3 Spray Techniques.

Several spray techniques have been utilised to metallize non-conductors[3,4,16]. "Spray silvering" was a technique in which low adhesion silver layers were applied as undercoats to the surface of plastics. Silver was deposited by the chemical reduction of ammoniacal silver nitrate with a solution of formaldehyde or hydrazine. Both these solutions were simultaneously sprayed by aerosol so that mixing occurred on the surface to be plated. The metallic silver coats produced by this method were generally thin, and needed to be overplated with other metals to increase the coating thickness.

Alternative dry spray techniques, known as the "Schoop process" or "Flame spraying", have been known since 1910[3,16]. In these techniques, molten metal was sprayed by compressed air on to a plastic substrate, with solidification occurring on contact with the surface. This process possessed certain advantages over wet methods,

namely it was exceedingly fast and it could also be used to plate metals such as aluminium which could not be deposited using other methods. However, in common with other techniques, the metal coats possessed only poor substrate adhesion, and depending on the type of process that was used to spray the substrate, the porosity of the deposit could be high.

1.3 Modern Techniques.

Modern methods of plating plastics were developed in the mid 1960's after the work of Narcus[6], Saubstre[7] and Jensen[8]. These employ chemical methods to form an initial conducting metallic layer which can then be over plated using conventional electroplating.

1.3.1 Chemical (Electroless) Pretreatment.

Chemical or electroless pretreatment is used prior to conventional electroplating to impart a highly adhering conductive metallic layer, with a thickness of a few tens of microns onto the surface of a non conducting substrate. Although several stages are involved, they can be divided into three main processes[9]. These include etching, activation, and the electroless deposition of metal. The combination of these stages is collectively referred to as chemical or electroless pretreatment to distinguish it from the subsequent electroplating stage. The processes involved in each of these procedures are discussed below, with particular reference being made to the sequence of operations which are used to electroplate acrylonitrile-butadiene-styrene (ABS) copolymers.

1.3.1.1 Etching.

After thorough cleaning of the sample, the first stage is the application of an etching solution of chromic/sulphuric acid[15,17]. This preferentially oxidizes the butadiene phase that is distributed in ABS, thus creating sites of anchorage for the subsequent metal coating. This is illustrated in Figs. 1 and 2.

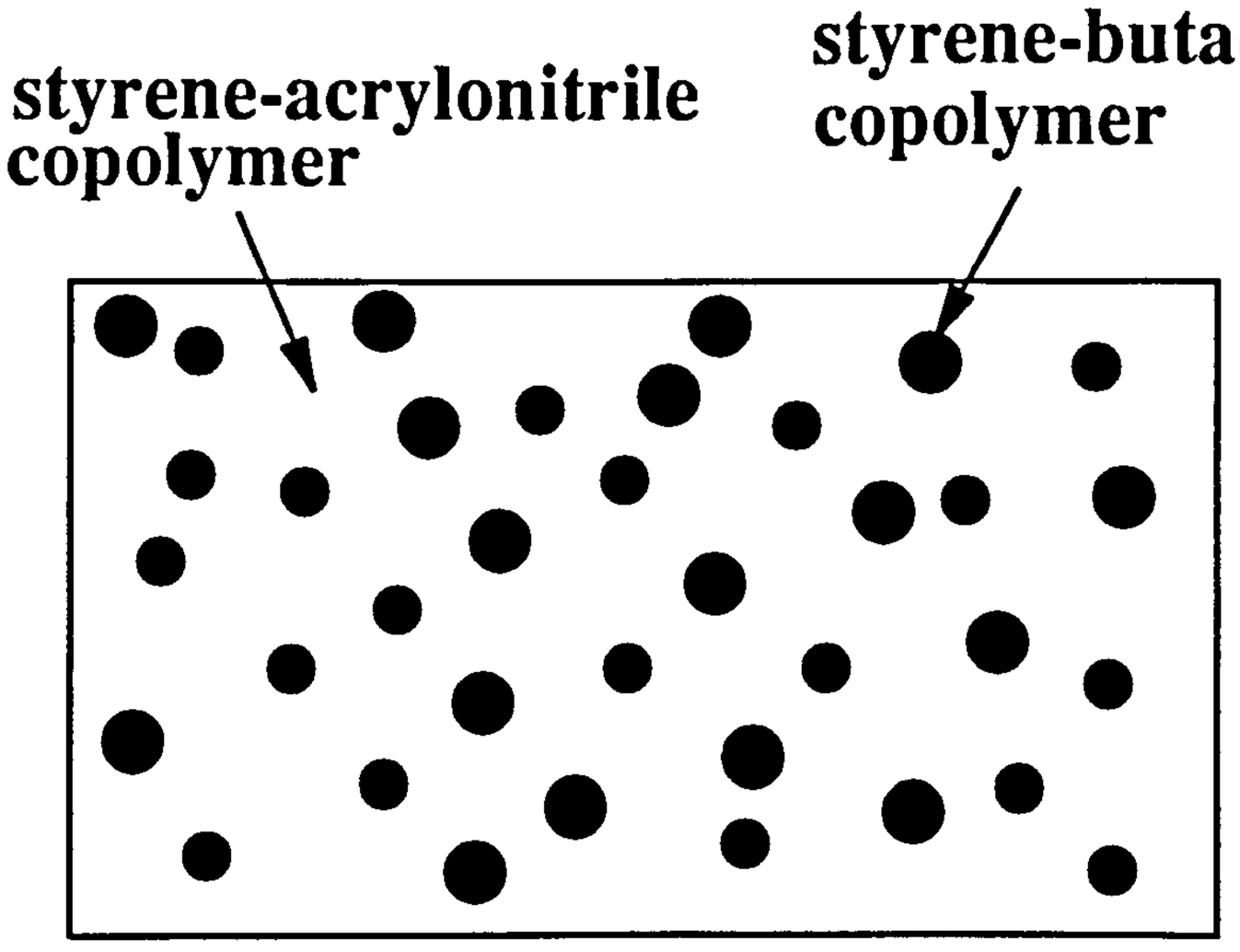

Fig. 1. Schematic showing butadiene phase in ABS before etch.

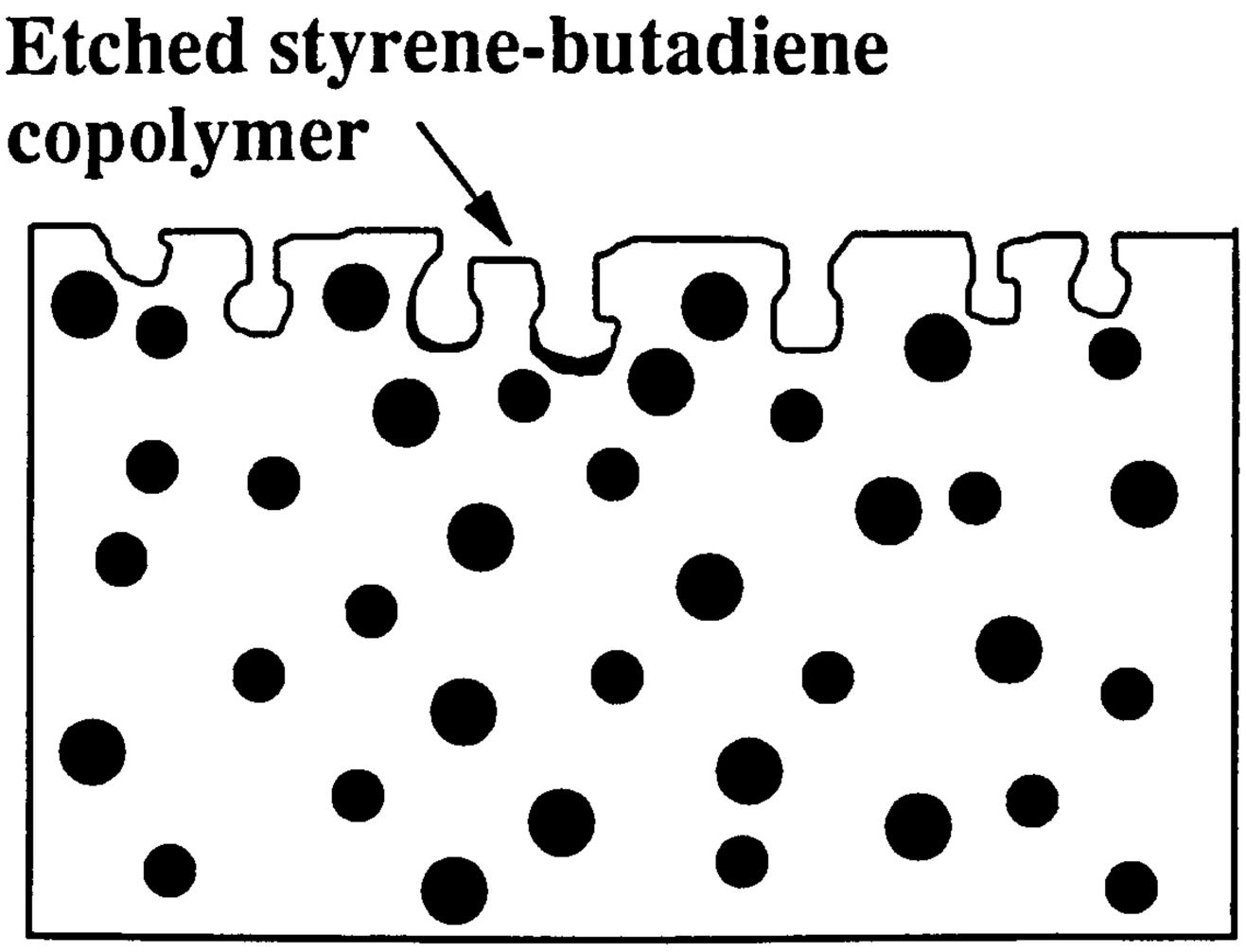

Fig. 2. Schematic showing surface of ABS after chromic/sulphuric acid etch.

1.3.1.2 Activation.

This stage involves the formation of precious metal nuclei on the etched surface. These are required in order to catalyse the subsequent electroless metal deposition step, and are formed in two discrete stages[17,18]. The first stage is often referred to as sensitisation, and involves the adsorption of a reducing agent, usually tin(II) chloride onto the surface of the substrate. After rinsing, the substrate is immersed in a solution of either palladium chloride or silver nitrate. The adsorbed tin(II) chloride is then readily oxidised, producing catalytic metal nuclei within the micro-cavities of the etched plastic. The half reactions for the formation of metal nuclei are given below.

$$Sn^{2+} + 2Ag^{+} = Sn^{4+} + 2Ag^{o} \qquad (1.1)$$

$$Sn^{2+} + Pd^{2+} = Sn^{4+} + Pd^{o} \qquad (1.2)$$

The major disadvantage of this process, is that activation is non specific[15], with metal deposition also occurring on the jigs supporting the work being plated. Modifications which overcome this disadvantage combine both the etching and activation steps into a single stage, by the addition of the noble metal to the etchant, and are referred to as "straight through processes"[15]. Using these methods activation is restricted to the etched plastic only, so that the same jig can be used for both chemical pretreatment and the subsequent electroplating stages. This saves both time and cost. A comparison of both these processes is shown in Fig. 3.

1.3.1.3 Electroless Deposition.

Electroless deposition may be defined as the sequence of steps which is used to deposit a metallic coat by controlled catalytic chemical reduction[19]. The process differs from conventional electroplating, in that deposition does not require an external source of current. Since its discovery by Brenner in 1946[20,21], electroless deposition has become a commercially important and integral part of the process of plating on plastics.

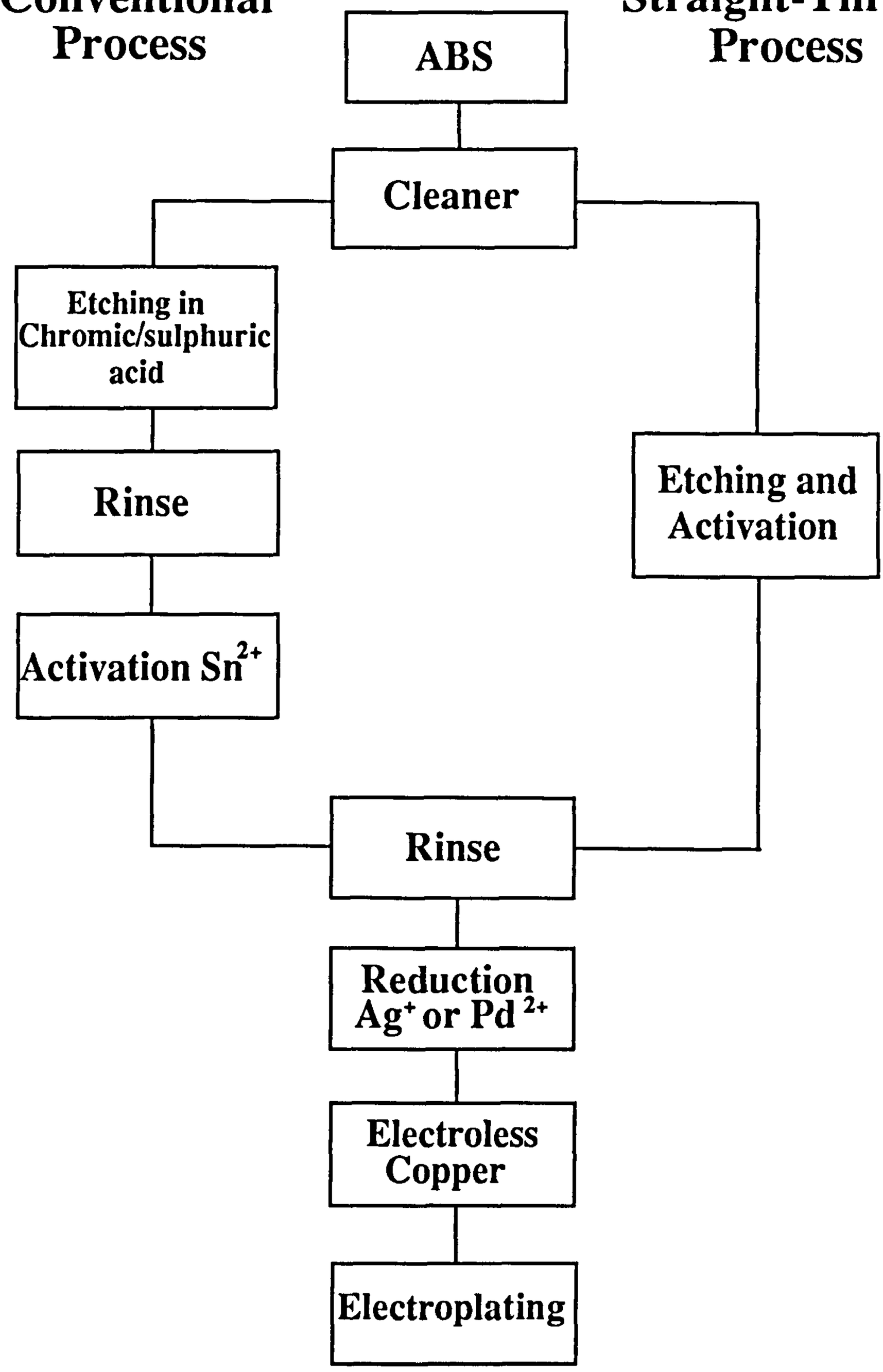

Fig. 3. Comparison of the steps involved in conventional and straight-through processes that are used to metallize acrylonitrile-butadiene-styrene (ABS).

Once the surface of the plastic substrate has been activated, a thin conducting metallic layer is applied by electroless deposition. A typical formulation of an electroless copper plating solution is given below[18];

Copper sulphate	10-50 g/l
Ethylenediamine tetraacetic acid, tetrasodium salt (EDTA)	10-50 g/l
or Sodium potassium tartrate (Rochelle salt)	10-50 g/l
Sodium hydroxide	pH 10.5-12
Formaldehyde	10-100 g/l

Commercial compositions of electroless plating solutions are usually proprietary and exact formulations are not disclosed[18]. In addition to the above reagents, plating solutions also contain brighteners to improve the overall finish[22,23], and stabilisers which retard spontaneous decomposition of the plating solution[22,23].

Copper is the most widely used metal for electroless deposition, and consequently has been most thoroughly investigated. The stoichiometry of the reaction for the reduction of copper(II) ions has been investigated by several workers[24-26] and is represented by[27]

$$Cu^{2+} + 2HCHO + 4OH^- \rightarrow Cu^o + H_2 + 2H_2O + 2HCO_2^- \qquad (1.3)$$

However, the detailed reaction mechanism is complex, and no consensus has been reached on the precise reactions involved in the reduction process[24].

Electroless deposition is terminated once the metal coat achieves a thickness in the range (0.1 to 5 μm). At this stage, the metal coat has sufficient conductivity for electrolytic deposition to be used to build up the thickness of the metal layer.

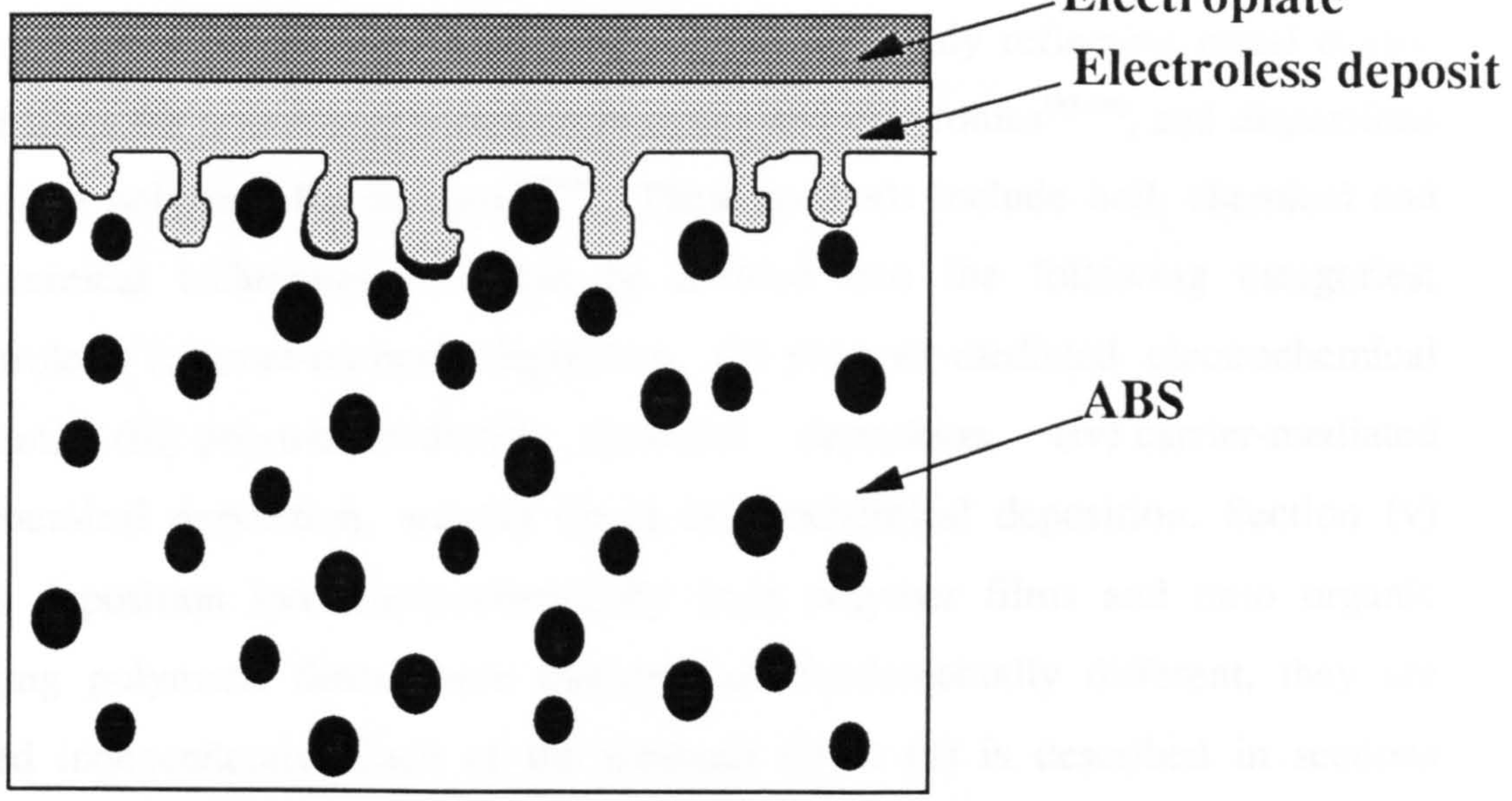

Fig. 4. Schematic representation of metallized ABS, showing electroless and electroplated metal layers.

1.4 Other Polymers.

Following the success of plating on ABS, other polymers were investigated to determine their suitability for being plated. The techniques used to plate other plastics are adaptations of the process used to plate ABS. The major problem is the selection of an etchant, capable of etching single phase plastics which have no equivalent of the butadiene phase in ABS. Polypropylene has been successfully plated by taking advantage of fillers such as zinc oxide, which can be etched out to provide anchorage sites[28-31]. Unfilled polypropylene brands have also been plated with limited success. In this instance, amorphous regions, or low molecular weight polypropylene interspersed in high molecular weight polypropylene are selectively etched. Other polymers that have been plated include acetals, acrylics, fluoroplastics including PTFE, polyamides, polyesters, polyethylene, polysulphone and polystyrene[4,9,11,23,32].

1.5 Current Developments.

In addition to the conventional plating processes described in sections 1.2 and 1.3, a number of novel techniques have been developed for the metallization of polymer films. These have been used to produce highly reflecting metal coated polymer films for possible applications in optics and electronics[33-39], and dispersions of metals in polymers for catalysis[40-46]. These methods include both chemical and electrochemical techniques, and can be divided into the following categories; (i) Electroless (counter-current) deposition, (ii) polymer-mediated electrochemical deposition, (iii) polymer-mediated chemical deposition, (iv) carrier-mediated electrochemical deposition, and (v) direct electrochemical deposition. Section (v) includes deposition into electrochemically inert polymer films and onto organic conducting polymers. Since these methods are fundamentally different, they are discussed independently. Each of the methods (i) to (v) is described in sections 1.5.1 - 6, although a discussion of the relative merits of each of these approaches is reserved until chapter 8.

1.5.1 Electroless (Counter-Current) Deposition.

An electroless method of metal deposition (also referred to as counter current deposition) has been described by Manring[47]. This is a chemical process which is used to deposit a conductive metallic 'interlayer' within the bulk of a preformed polymer film. The process is accomplished by simultaneous diffusion of metal ions [M^+], and a reducing agent [R] into a film from opposite surfaces. Metal is deposited on contact of both reagents, with the locus of deposition being governed by the concentration of reactants and magnitude of diffusion coefficients. Under optimized reaction conditions, sharp metallic interlayers have been formed which are both conductive and reflective. A schematic representation of the formation of a metal interlayer by this technique is shown in Fig. 5.

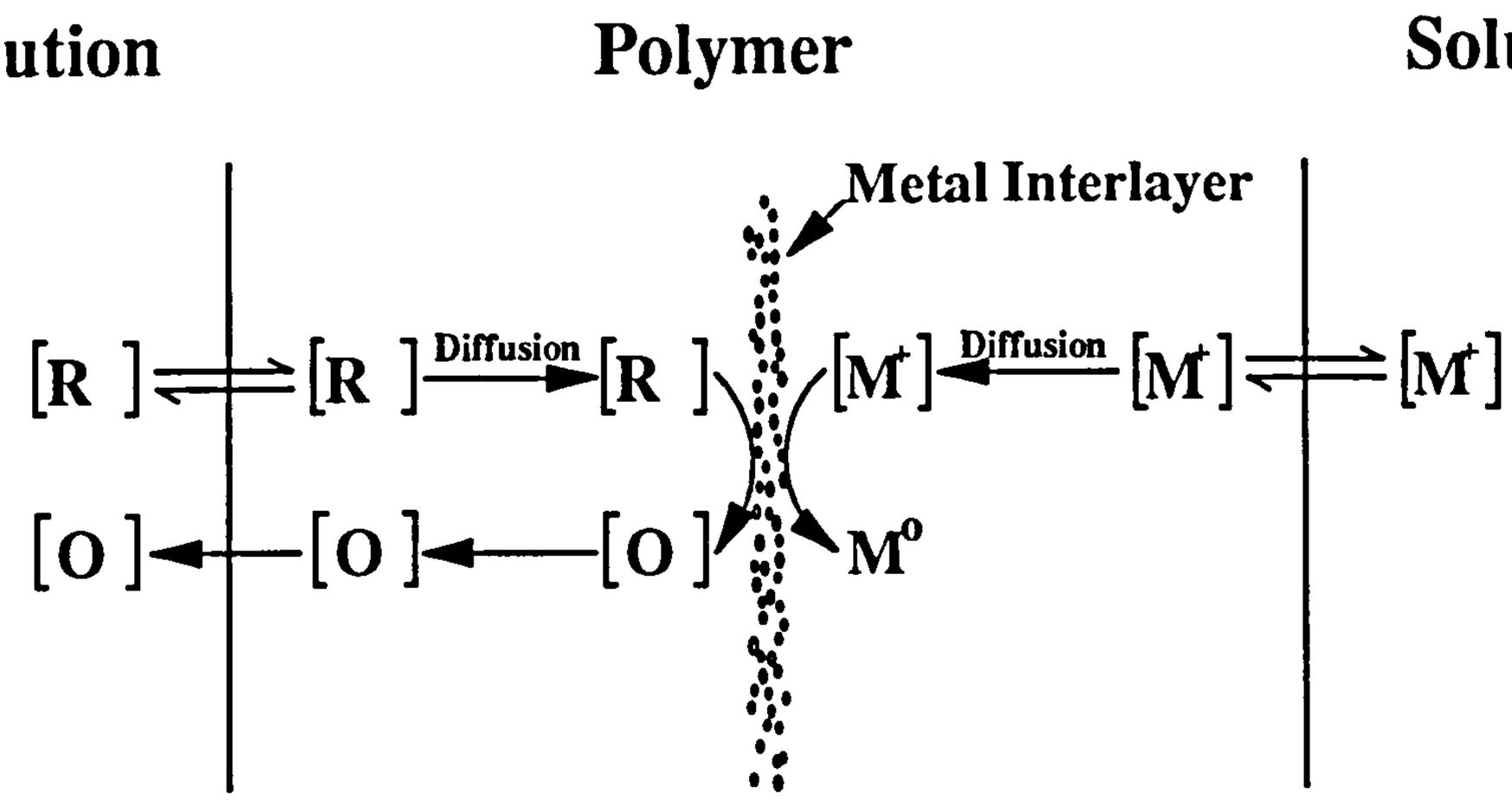

Fig. 5. Schematic of electroless counter current deposition[47].

1.5.2 Polymer-Mediated Electrodeposition (PMED).

Polymer-mediated electrodeposition involves the injection of electrons into a redox-active polymer from a cathode. The electrons diffuse through the polymer via reversible redox exchange reactions, until they encounter and reduce metal ions which have permeated into the polymer from solution. This is illustrated schematically in Fig. 6.

Metal interlayers produced by this method are more diffuse and less conductive than those prepared chemically, and are composed of spherical microparticles 10-40 nm in diameter. Reich *et al*[49] used an annealing process to sinter silver interlayers formed in polyimide by this method. This dramatically improved both the conductivity and reflectivity of the metallic interlayer.

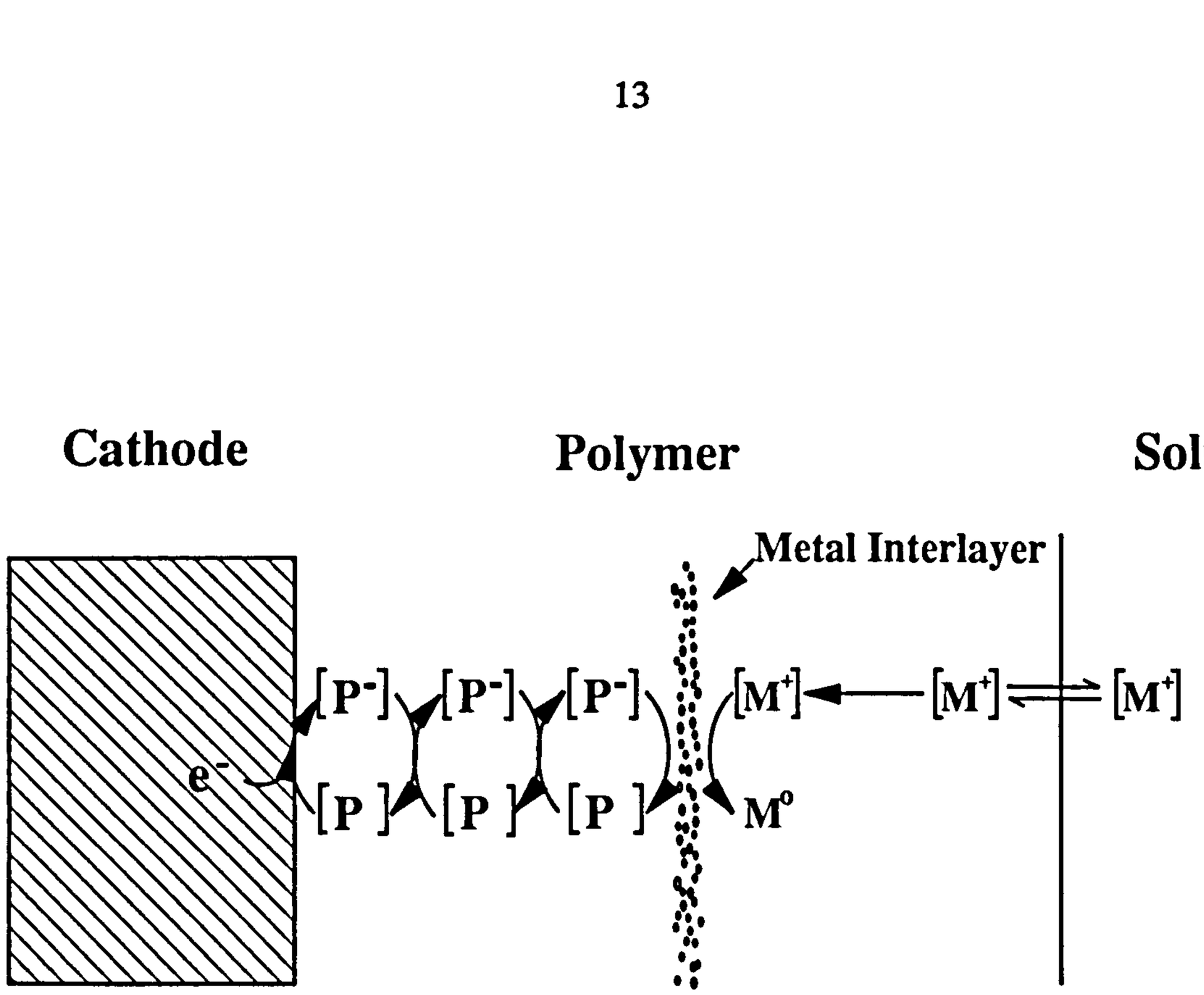

Fig. 6. Schematic of polymer mediated electrodeposition[48].

The electro-catalytic properties of organic and organometallic redox active polymers have been investigated by several groups. Wrighton *et al*[50,51] described the deposition of both Pt and Pd particulates onto an electroactive polymer $[(PQ^{2+})_n]$ derived from an N,N'-dialkyl-4,4' bipyridinium monomer. Metal was deposited onto the outermost portion of the polymer by potentiostating at a potential sufficient to effect the reduction $(PQ^{2+}/PQ^{+})_n$. The overall deposition process for platinum can then be represented by the following equations. The first stage involves ion exchange of the polymer with $PtCl_6^{2-}$ (Eqn 1.4).

$$[(PQ^{2+}\cdot 2Br^{-})_n)]_{surf} + nK_2PtCl_6 \rightarrow [(PQ^{2+}\cdot PtCl_6^{2-})_n)]_{surf} + 2nK^{+}Br^{-} \qquad (1.4)$$

followed by reduction of Pt(IV) to Pt(0) (Eqn 1.5)

$$[(PQ^{2+}\cdot PtCl_6^{2-})_n)]_{surf} + 4ne^{-} \rightarrow [(PQ^{2+}\cdot 2Cl^{-}\cdot Pt(0)_n)]_{surf} + 4nCl^{-} \qquad (1.5)$$

Pickup *et al*[37] studied the electrodeposition of Cu, Ag, Co and Ni onto poly-$[Ru(bpy)_2(vpy)_2]^{2+}$ using cyclic voltammetry [bpy=2,2'bipyridine;

vpy=4-vinylpyridine]. In this example, the Ru(I) and Ru(0) states of the polymer were used to mediate metal ion reduction. Mazur and Reich[52] produced highly reflecting metallic interlayers of Cu, Ag and Au in polyimide films derived from pyromellitic dianhydride (PMDA) and 4,4'oxydianiline (ODA). The position of the metallic interlayer could be varied by altering the electrode potential and metal ion concentration in solution.

1.5.3 Carrier-Mediated Electrodeposition (CMED).

Metal ion reduction can also be accomplished by carrier-mediated electrochemical deposition. This is a technique which is similar to that described in section 1.5.2, except that an electroactive solute [O], is added to the electrolyte solution to effect reduction. This permeates through the polymer film to the electrode surface where it is reduced. The reduced form of the redox couple [R], then diffuses outward from the electrode surface until it encounters and reduces metal ions from solution, being re-oxidised in the process. This approach is depicted in Fig. 7.

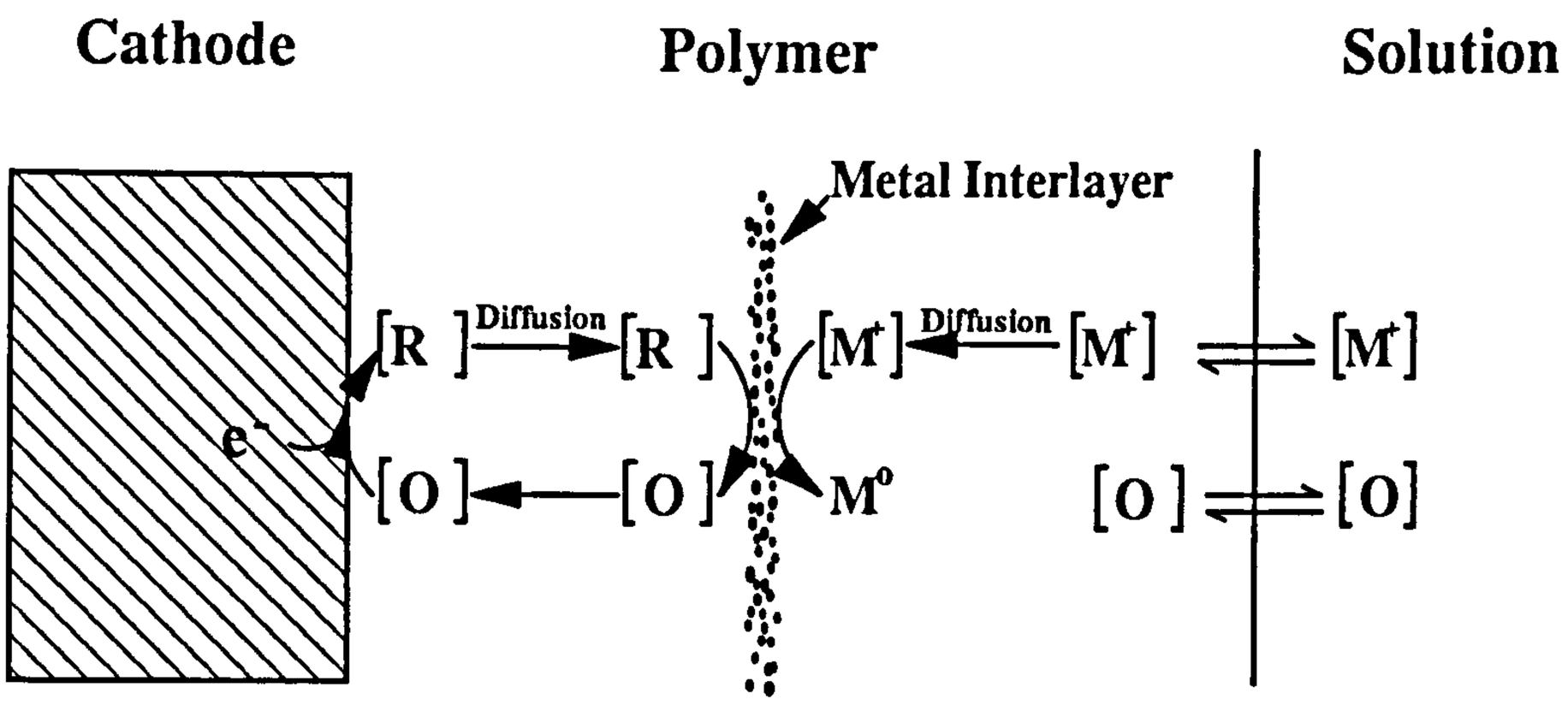

Fig. 7. Schematic representation of carrier-mediated metal deposition[48].

Levy *et al*[48] employed a variety of quinones as redox reagents to deposit Ag and Au interlayers into electrochemically inert polymers such as PVC and PVDF. A combination of this technique with polymer-mediated electrodeposition was also utilized by Pickup *et al*[37], to enhance the deposition rate of copper onto poly-$[Ru(bpy)_2(vpy)_2]^{2+}$, compared to that obtained solely with polymer-mediated deposition.

1.5.4 Polymer-Mediated Chemical Deposition (PMCD).

Polymer mediated chemical processes are analogous to polymer mediated electrochemical processes, except that chemical reducing agents rather than electrochemical methods are used to effect the reduction of an electroactive polymer.

Haushalter and Krause[53] described the reduction and subsequent metallization of films of polyimide by exposure to the highly reducing potassium salts of Zintle anions. These have the general formula given by $K_n(M)_x^{n-}$, where $(M)_x^{n-}$= $(Sn)_9^{4-}$, $(Bi)_4^{2-}$, $(Sb)_7^{3-}$, and $(Tl_4Te_2)^{2-}$. The authors classified the metallization reactions into three categories. In type (I) reactions, main group elements, Sn, Bi, and Sb, derived from oxidation of the Zintle ions were deposited on the surface of the polymer. This process was accompanied by the simultaneous incorporation of potassium cations into the reduced polymer film in order to maintain overall charge neutrality. The reduced and partly metallized films produced by type (I) depositions were then used to further reduce other more noble metal ions from solution, thus yielding bi-metallic surface layers. These were termed type (II) reactions. They also reported that it was possible to reduce polyimide with Zintle anions without surface metallization occurring. The reduced films were then used to reduce metal anions other than those incorporated within the Zintle anions, such as Co, Pt, or Pd, by immersion of the film in an appropriate metal salt solution. A variation of this last approach has been employed by Viehbech *et al*[54], who used electrochemically generated chemical reducing agents to effect the reduction of polyimide. The reduced polyimide was then exposed to various metal salt solutions, resulting in metal deposition at the polymer surface. This latter method of metal deposition is shown in Fig. 8.

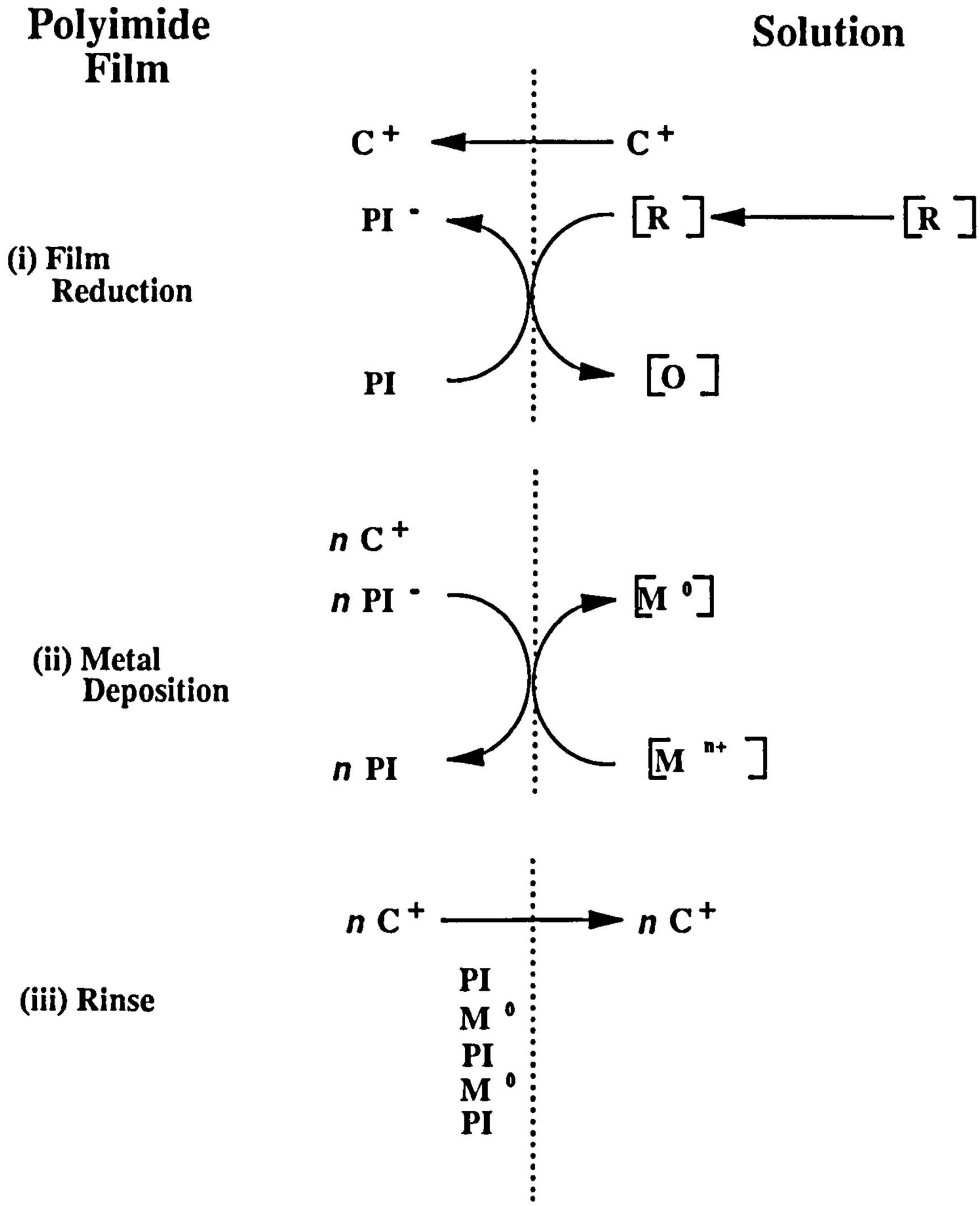

Fig. 8. Schematic representation of the steps involved in the metallization of polyimide film[54].

Auerbach[55], and Macfarlane *et al*[56] have also used chemical methods to effect metallization of polyimide films. Polyimide precursors (3,3'4,4'-benzophenone-tetracarboxylic acid dianhydride; BDTA) and ODA were doped with soluble metal salts of either silver or palladium. The metal cation was then reduced to the metallic state during the cure cycle of the film. Improvements in the reflectivity of the metallic coat were obtained by covering the films with a blanket of carbon powder, in order to aid the reduction of the metal cation during the final high temperature bake which was used to effect imidization.

1.5.5 Direct Electrochemical Deposition.

The electro-reduction of metals at polymer coated electrodes has also been reported for polymers which are not intrinsically electroactive, but which are permeable to metal ions in solution. The mechanism of deposition involves ingress of metal ions from solution, through the matrix of the polymer film to the electrode surface where reduction occurs. This is illustrated schematically in Fig. 9.

Using this method, Kuwana *et al*[43-45] described the direct deposition of metallic microparticles of Pt, Pd, Ag, Ni, Cd, and Pd-Pt (a bimetallic) into poly(vinyl-acetic acid) (PVAA), and Pt into poly(4-vinylpyridine) (PVP) films coated onto glassy carbon electrodes. The authors reported an increased catalytic activity towards the electrochemical generation of H_2, and the reduction of O_2 compared to that obtained with deposition onto non polymer coated metallized graphite electrodes.

Bard and co-workers[39] used a modification of this technique, in which the tip of a cathodically biased scanning tunnelling microscope was used to deposit highly resolvable (*ca.* 0.5 μm) metallic conducting patterns on the surface of a nafion membrane impregnated with metal silver nitrate. This procedure is illustrated in Fig. 10. It was suggested that with further refinement, the technique might be applied to the production of lithographic masks.

1.5.6 Organic Conducting Polymers.

The use of organic conducting polymers as substrates for metal deposition has recently been described[38,41,46,57-60]. It has been proposed that such materials might be used in applications such as rectifying bilayer electrodes[37] or molecular based micro electrode devices[61-63], thus opening up new possibilities for technological applications.

The electrocatalytic properties of conducting polymer/metal composites have been investigated by several authors. These materials have superior catalytic properties compared to the type of redox active polymers described in section (1.5.2), since electronic charge is conducted directly through the polymer matrix, rather than indirectly through diffusion controlled electron transfer processes. The use of

conducting polymers also permits the formation of three dimensional polymer/metal composites, thus increasing the potential catalytic surface of these types of materials.

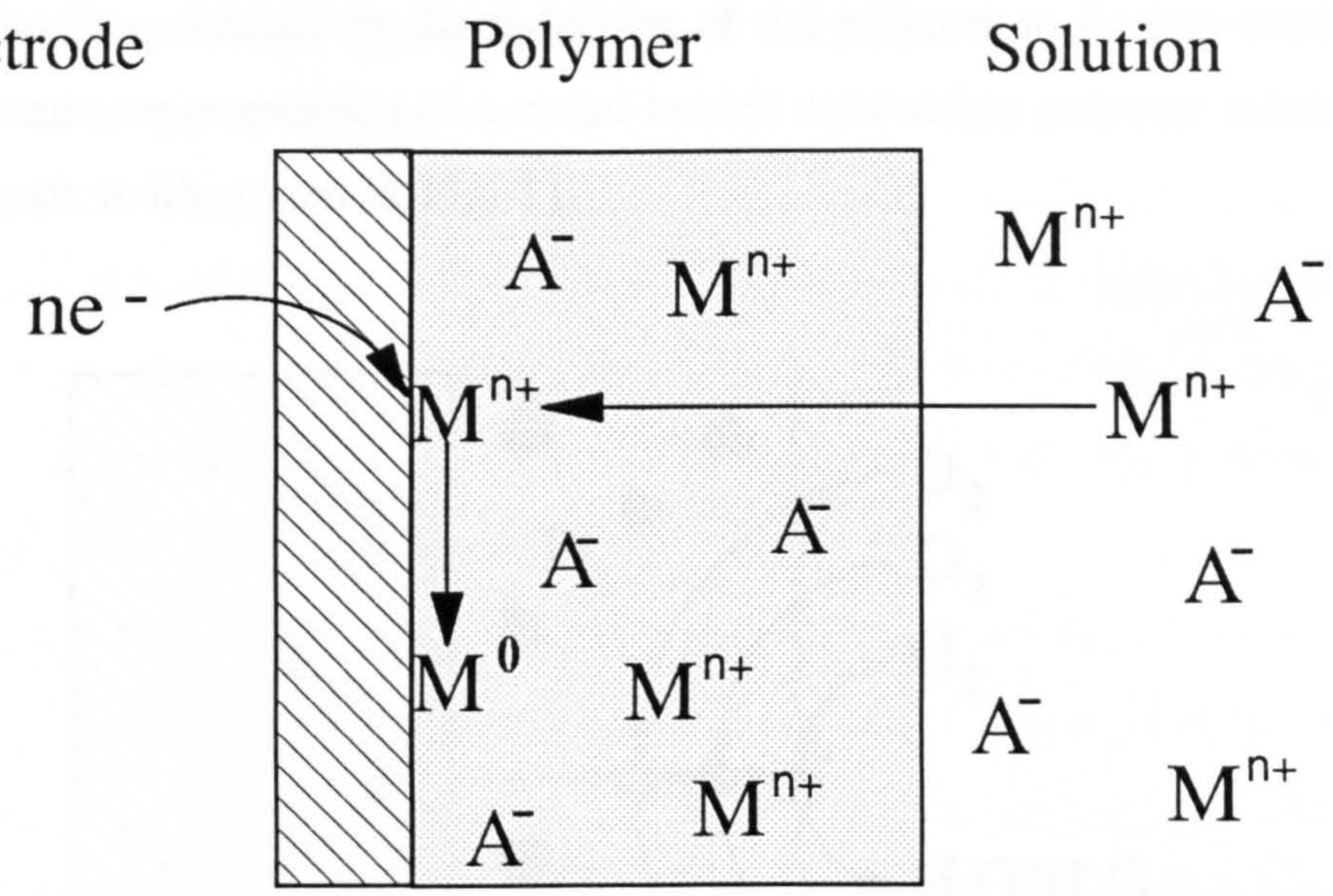

Fig. 9. Schematic representation of direct electrodeposition at a polymer-coated electrode.

Fig. 10. Direct electrodeposition at a polymer surface using the tip of a scanning tunnelling microscope to effect the reduction of metal ions contained in a polymer membrane[39].

Holdcroft and Funt[46] described the incorporation of metallic aggregates of Pt into polypyrrole, and the resultant films were found to be catalytic towards O_2 reduction within a narrow potential window. However, the rate of reduction of O_2 was limited at cathodic potentials by the reduction of the polymer to its non-conducting state. A schematic representation of a metal loaded conducting polymer substrate as used for catalysis is illustrated in Fig. 11.

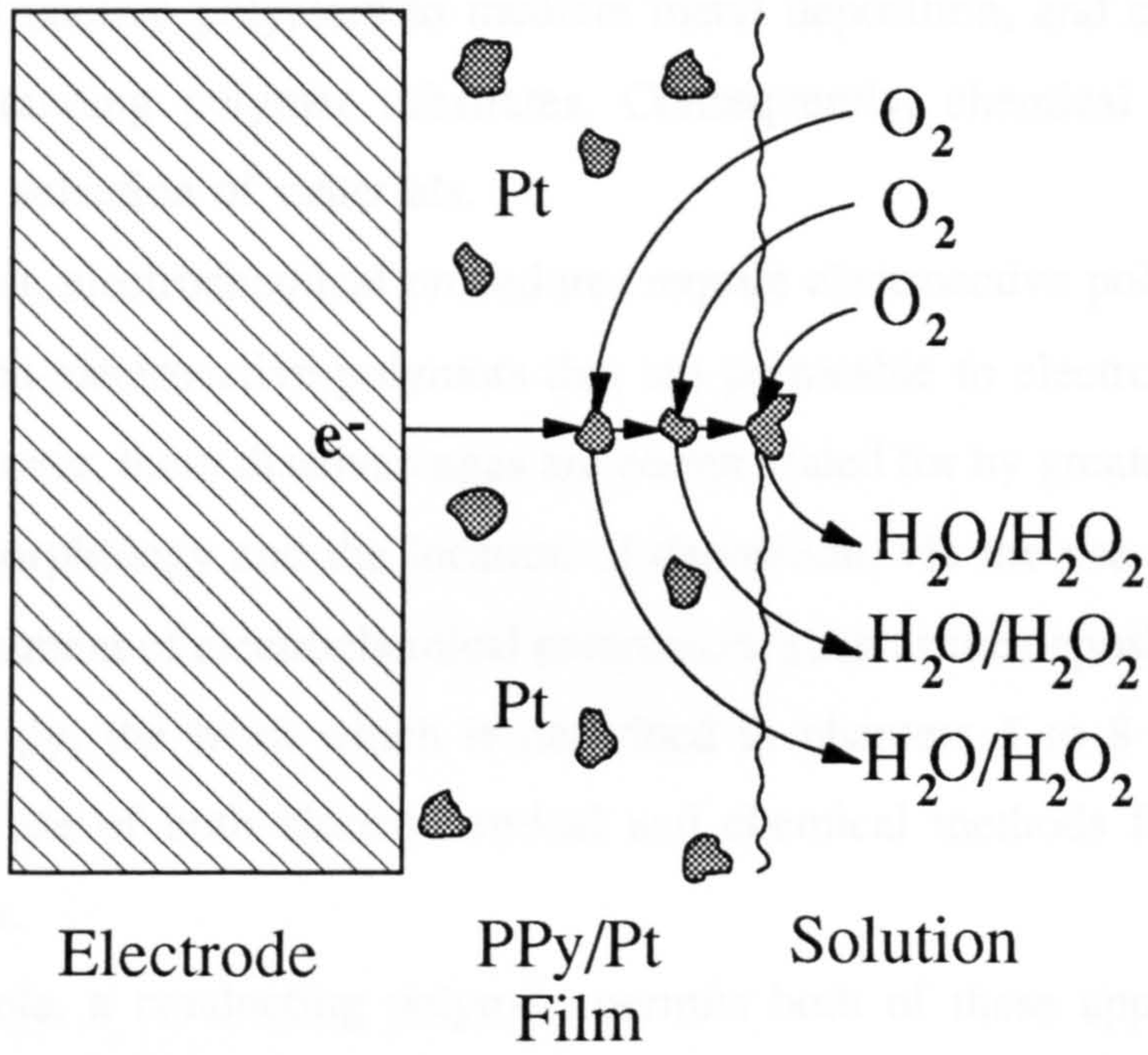

Fig. 11. Schematic illustration of the application of metallized polypyrrole in the catalytic reduction of O_2[46].

Tourillon and Garnier[41] overcame the problem of the low conductivity of the reduced state of the polymer, by co-depositing Ag and Pt into poly(3-methylthiophene) (PMeT), to produce [PMeT-Ag-Pt] bi-metallic composites. Ag aggregates located along the polymer fibres provided sufficient conductivity at potentials where P-MeT was in the reduced state, to enable the catalytic reduction of H^+ in acidic solutions. Finally, Bedioui *et al*[40] utilised various pyrrole-substituted cobalt porphyrins, to incorporate Pt and Ag aggregates. The catalytic activity of these polymers was investigated towards the reduction of H^+ at pH 0, and similar results were obtained to those achieved by Tourillon and Garnier.

1.6 Summary.

This chapter has reviewed traditional and more recent developments in the metallization of plastic materials.

Recent developments have utilized both chemical and electrochemical procedures to effect the deposition of metal into polymer film substrates. Of the approaches that are described in section 1.5, chemical methods are more versatile, do not require electroactive polymers to mediate metal deposition, and can be used to metallize free standing polymer substrates. Consequently, chemical processes are suited to a wide selection of materials.

In contrast, electrochemical procedures require electroactive polymers such as polyimide, or non-electroactive polymers that are permeable to electroactive species in solution. However, these disadvantages are compensated for by greater control over the thickness, morphology and the location of deposition, via the use of coulometry and careful adjustment of electrochemical parameters, such as the deposition potential.

Accordingly, the work which is described in chapters 5 to 8 of this thesis, investigates the use of both electrochemical and chemical methods for metallizing plastic substrates.

Polypyrrole, a conducting polymer, permits both of these approaches to be tried, since the material is conducting when in the oxidized state, and can serve directly as an electrode material for the reduction of metal ions from solution[38,57]. It is also a redox-active, and can be used in an analogous fashion to the procedure described by Haushalter and Krause[53] in section 1.5.4 to metallize polyimide.

The second approach which is used to metallize polymer films is an adaptation of the direct electroreduction technique described by Kuwana *et al*[43-45] to hydrophobic polymer substrates. The use of hydrophobic polymer substrates in conjunction with non-aqueous electroplating solutions, is expected to increase the applicability of this method to a much wider selection of polymer substrate materials.

CHAPTER 2
POLYPYRROLE

2.1 Introduction.

Traditionally, polymers have been regarded as insulators, and have found wide commercial application exploiting this property. However, the discovery by MacDiarmid *et al*[64] in 1977, that the conductivity of polyacetylene could be increased by up to 13 orders of magnitude when treated with suitable chemical oxidants, has led to a considerable amount of research focusing on the conducting nature of organic polymeric materials. The number of these polymeric materials is now numerous, and includes polymers based on polyaromatics, such as poly(p-phenylene)[65,66], poly(p-phenylene sulphide)[67], polyazulene[68], and polyaniline[69], and polyheterocyclics, including polypyrrole[70,71] and polythiophene[72], and their derivatives. The most well known conducting polymers are shown in Fig. 12.

The literature on conducting polymers is voluminous and rapidly expanding, hence a complete review covering all aspects of synthesis, polymer morphology, electronic structure, transport properties, etc, is beyond the scope of this chapter. Also, several excellent reviews have been recently published which thoroughly cover these areas[73-77], and therefore this chapter is focused on specific aspects of the chemistry and electrochemistry of polypyrrole which are pertinent to the experimental work described in chapters 5, 6 and 7.

Polypyrrole and polyaniline were chosen as materials to investigate due to their ease of synthesis by both chemical and electrochemical methods[73], and their relative stability under ambient conditions when compared to other conducting polymers[78-81]. Aniline also has the advantage of being relatively cheap industrial chemical, which makes it attractive when considering potential commercial applications.

The areas covered in this chapter are the synthesis of polypyrrole by both electrochemical (section 2.2.1) and chemical methods (section 2.3), the electrochemistry of polypyrrole is described in section 2.2.4, and reaction stoichiometry in section 2.2.2. The preparation of conducting polymer composite materials is covered in section 2.4, and finally, the chemical treatment of polypyrrole with base is discussed in section 2.5.

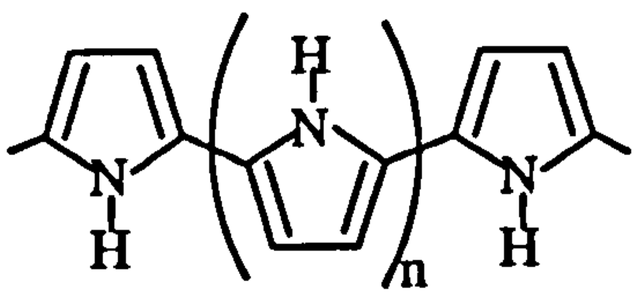

Polypyrrole

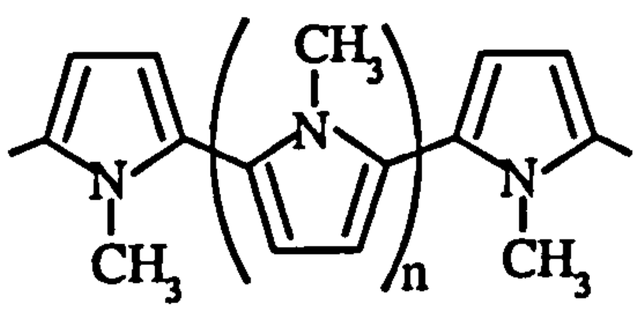

Polymethylpyrrole

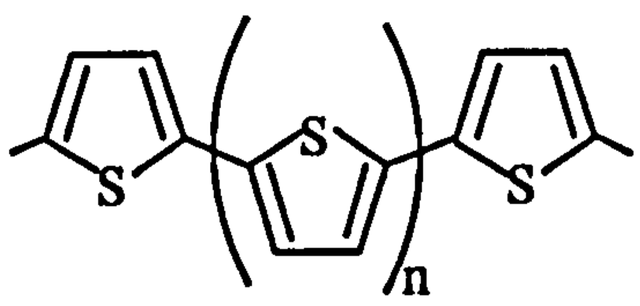

Polythiophene

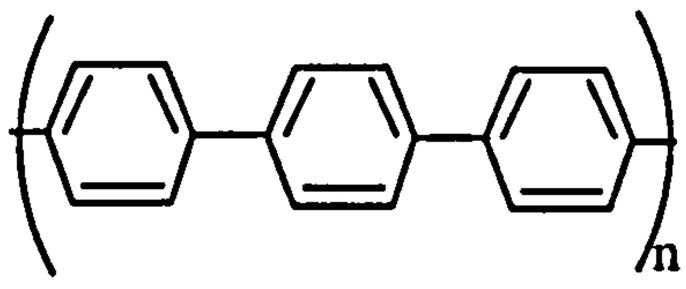

Poly(p-phenylene)

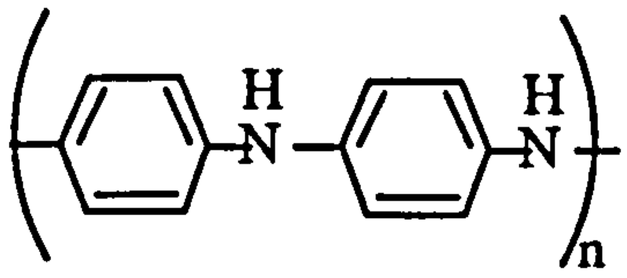

Polyaniline

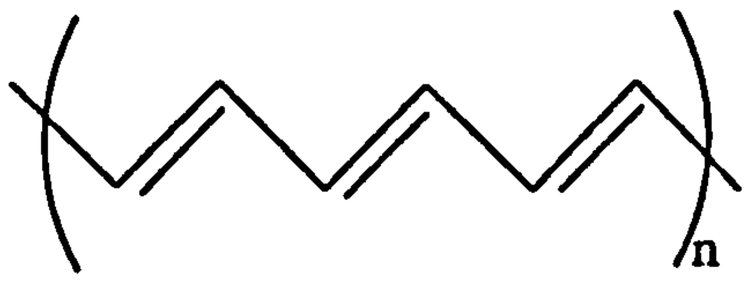

Trans polyacetylene

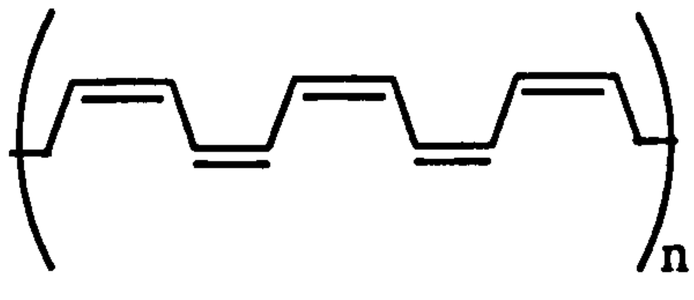

Cis polyacetylene

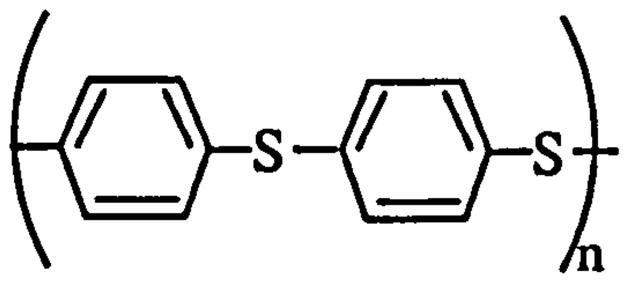

Poly(p-phenylene) sulphide

Fig. 12. Chemical structures of common conjugated polymers that conduct on doping.

2.2 Polypyrrole.

2.2.1 Electrochemical Synthesis.

The first mention of the electrochemical synthesis of polypyrrole, or "pyrrole black" as it was then called, dates back to Lund in 1961. He reported the formation of a polymeric residue during the anodic oxidation of pyrrole in acetonitrile. However, the conducting nature of this material was not recognised until 1968, when polypyrrole was prepared by the electrochemical oxidation of pyrrole in aqueous sulphuric acid[82]. It was found to have a conductivity of 8 Scm^{-1}, and exhibited a strong electron spin resonance (ESR) signal which signified that the material contained unpaired electrons. Surprisingly, the electronic properties of this polymer were not investigated further until the first of a series of papers was published by Diaz *et al*[70] in 1979. Using a modification of the method employed by Dall'Olio, flexible free standing films of polypyrrole were prepared which exhibited conductivities of up to 100 Scm^{-1}. As a consequence, the electrochemical method of synthesis has become a widely established technique for preparing this, and other highly conducting organic polymers.

A standard procedure for the preparation of polypyrrole films, based on the method employed by Diaz *et al*[76] is given below. Oxidation was usually carried out in a single compartment electrochemical cell, either potentiostatically at a potential sufficient to oxidise the pyrrole monomer, (usually greater than 0.65 V *vs*. SCE), or galvanostatically, with current densities varying from 10 μAcm^{-2} to 10 $mAcm^{-2}$ [75]. Platinum was commonly used as a working electrode material, with either gold or carbon counter electrodes. Electrode potentials were measured versus a calomel reference electrode (SCE). Polymerization was carried out in non-aqueous conditions since, oxidation was reported to be sensitive to the nucleophilic nature of the surrounding media[83]. Typical solvent/electrolyte combinations included acetonitrile

as a choice of solvent, with quaternary ammonium salts, usually 0.1 M tetraethylammonium tetrafluoroborate electrolyte ($TEABF_4$), or soluble metal salts of non-nucleophilic anions as supporting electrolyte. Water was also added at concentrations of up to 1%, as this was reported to increase the mechanical properties polymer and decrease the surface roughness[78].

The influence of different preparative conditions on polypyrrole film formation has been studied by several groups[57,78,80,83-91], with much of the emphasis of research being to improve the ambient stability and mechanical properties of these materials. The effects of different experimental parameters on the properties of polypyrrole films are discussed in the following sections.

2.2.1.1 The Nature of the Working Electrode.

Polypyrrole is readily formed at most electrode surfaces which remain inert during electrosynthesis. The most common choice of working electrode material is platinum, since this produces films with good mechanical strength and high conductivity[83,92]. Other electrode materials which have been used include gold, titanium and aluminium[92], alloys such as stainless steel[93], and graphite and vitreous carbon electrodes which permit the use of high voltages and high current densities[38,80,94]. Semiconductor electrodes such as gallium arsenide[95], indium tin oxide and n-type polysilicon[96] have also been used.

The nature of the working electrode (anode) substrate material is often overlooked as a factor which is able to affect the physical and electrochemical properties of polypyrrole. Early work by Prejza *et al*[97] demonstrated that film morphology was dependent on the choice of substrate. This was subsequently confirmed by Cheung *et al*[92] who reported differing microstructures for polypyrrole films polymerized on different electrode substrates, and Witkowski *et al*[94], who found that different forms of the same substrate material (glassy carbon and rough pyrolytic

graphite) could produce different polymer morphologies with dissimilar electrochemical behaviour. Polymerization kinetics and redox behaviour have also been shown to be affected by the choice of substrate material[92,97].

2.2.1.2 Effects of Solvent and Counteranions.

Early synthetic studies demonstrated that polypyrrole films prepared in aqueous electrolytes suffered from poor stoichiometry, and generally had lower conductivities than those prepared in non-aqueous conditions[78]. Consequently, the majority of studies on polypyrrole prior to 1986 were carried out in acetonitrile.

The presence of water during synthesis has a marked influence on the kinetics of polymerization[98], film morphology[83], conductivity[87,89,90,98] and mechanical properties[80,88,91]. Using totally anhydrous dry box conditions with the rigorous exclusion of oxygen, Street *et al*[99] showed that the formation of polypyrrole was completely inhibited. This indicated that either oxygen or water was necessary to provide a reducible species for the counter electrode reaction. The surface morphology of polypyrrole is also strongly dependent on the water content of the solvent. Films grown in anhydrous acetonitrile are rough and exhibit dendritic growth, whereas the addition of 1% of water produces films with much smoother and more uniform surfaces[76,100]. However, the presence of water in acetonitrile is only beneficial at relatively low concentrations (of the order of a few percent). For example, Diaz and Hall[87] found that increasing the water content to 33% produced detrimental effects on the conductivity of the film, which decreased by approximately two orders of magnitude and also on the mechanical properties. The effects of the volume fraction of water on the conductivity of polypyrrole films prepared in acetonitrile/water co-solvents is shown in Fig. 13.

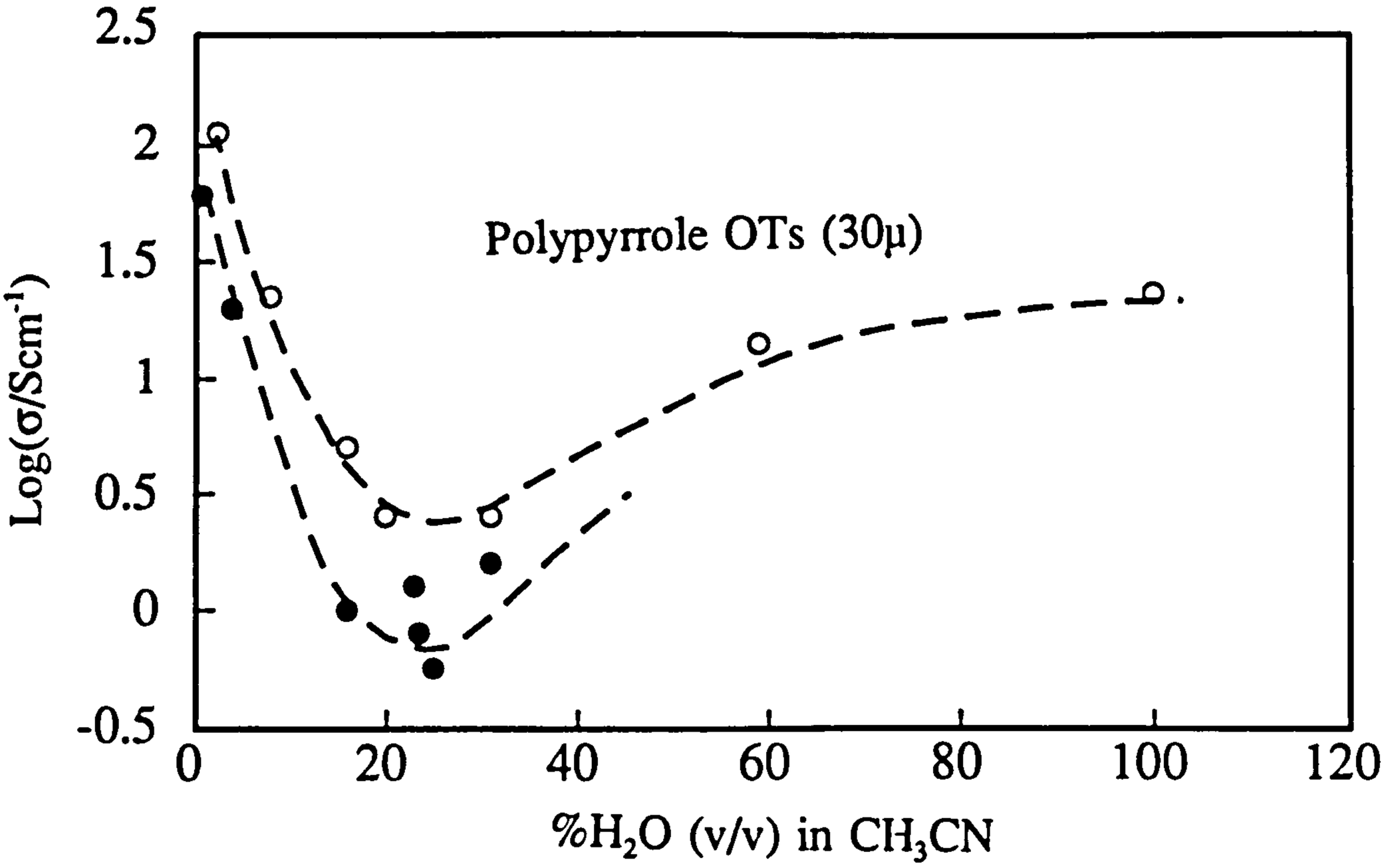

Fig. 13. Dependence of the conductivity values of two 30 μm thick polypyrrole toluene-sulphonate films prepared in electrolyte solutions containing varying amounts of water[87].

More recently, attention has turned to films prepared in entirely aqueous environments, since this permits the use of a much wider selection of electrolytes[101-103]. In contrast with previous studies, Pletcher *et al*[104] obtained highly conducting polypyrrole with good mechanical properties from aqueous acid solutions of H_2SO_4, HCl and HBr. A variety of other anions have since been utilized, including conventional anions such as AsF_6^-, ClO_4^-, BF_4^-, SO_3^{2-} and NO_3^-, which are commonly used in non-aqueous preparations[104,105], organic acids and soluble metal salts of these acids such as *p*-toluene sulphonic acid and sodium-*p*-toluene sulphonic acid[80,90,91] and complex polyanions and surfactants[103,106].

The anion content of oxidised polypyrrole films incorporating univalent anions is typically in the range 0.25 to 0.33 anions per pyrrole moiety. This is equivalent in some cases to weight fractions of anions in excess of 50%. Therefore it is not surprising that both the morphology and mechanical properties of polypyrrole are affected by the choice of counteranion[107,108]. The stoichiometry of various polypyrroles incorporating different anions is listed in Table 1.

Table 1. Composition of polypyrrole films with various anions.

Anion	Anions per pyrrole ring	Weight fraction of anion	ref.
BF_4^-	0.22	0.23	(107)
PF_6^-	0.25	0.36	(a)
AsF_6^-	0.31	0.48	
ClO_4^-	0.30	0.31	
HSO_4^-	0.30	0.31	
FSO_3^-	0.36	0.31	
$CF_3SO_3^-$	0.31	0.42	
$BrC_6H_4SO_3^-$	0.33	0.54	
$CH_3C_6H_4SO_3^-$	0.32	0.52	
CF_3COO^-	0.25	0.30	
$H(CH_2)_{12}OSO_3^-$	0.24 to 0.26	0.51	(109)
$H(CH_2)_4SO_3^-$	0.29	0.38	(b)
$H(CH_2)_{10}SO_3^-$	0.33	0.53	
$H(CH_2)_{16}SO_3^-$	0.26	0.55	
$^-O_3S(CH_2)_{10}SO_3^-$	0.125	0.36	
SO_4^{2-}	0.15	0.18	(104)
Cl^-	0.4	0.18	(b)
Br^-	0.8	0.50	
Cl^-	0.28	0.13	(108)
NO_3^-	0.20	0.16	(b)
$CH_3C_6H_4SO_3^-$	0.32	0.52	

Key: a=films prepared in non-aqueous media
b=films prepared in aqueous media

Polypyrrole prepared in non-aqueous conditions incorporating spherical anions such as ClO_4^-, BF_4^-, PF_6^- tends to be brittle[83]. Street[80] and Buckley[88] have shown that the mechanical properties of polypyrrole can be improved by incorporating toluene sulphonate as the counter anion, and depending on electrolysis conditions, conductivities as high as 500 Scm^{-1} have been obtained[105]. The increase in conductivity is probably because planar anions impose some local order, and allow for closer interchain packing[88,51].

2.2.1.3 Effects of Electrode Potential.

Results presented by several workers indicate that the electrical, electrochemical, and mechanical properties of polypyrrole are dependent on the applied potential during deposition[57,86,88,105].

The effects of the anodic potential limit on the conductivity of polypyrrole during the formation of polymer in aqueous conditions have been studied by various groups[57,86,104]. In all cases, it was noted that oxidative degradation and loss of electroactivity occurred if the anodic potential of the film exceeded 1.0 V *vs.* SCE. Typical results illustrating this effect are shown in Fig. 14[104].

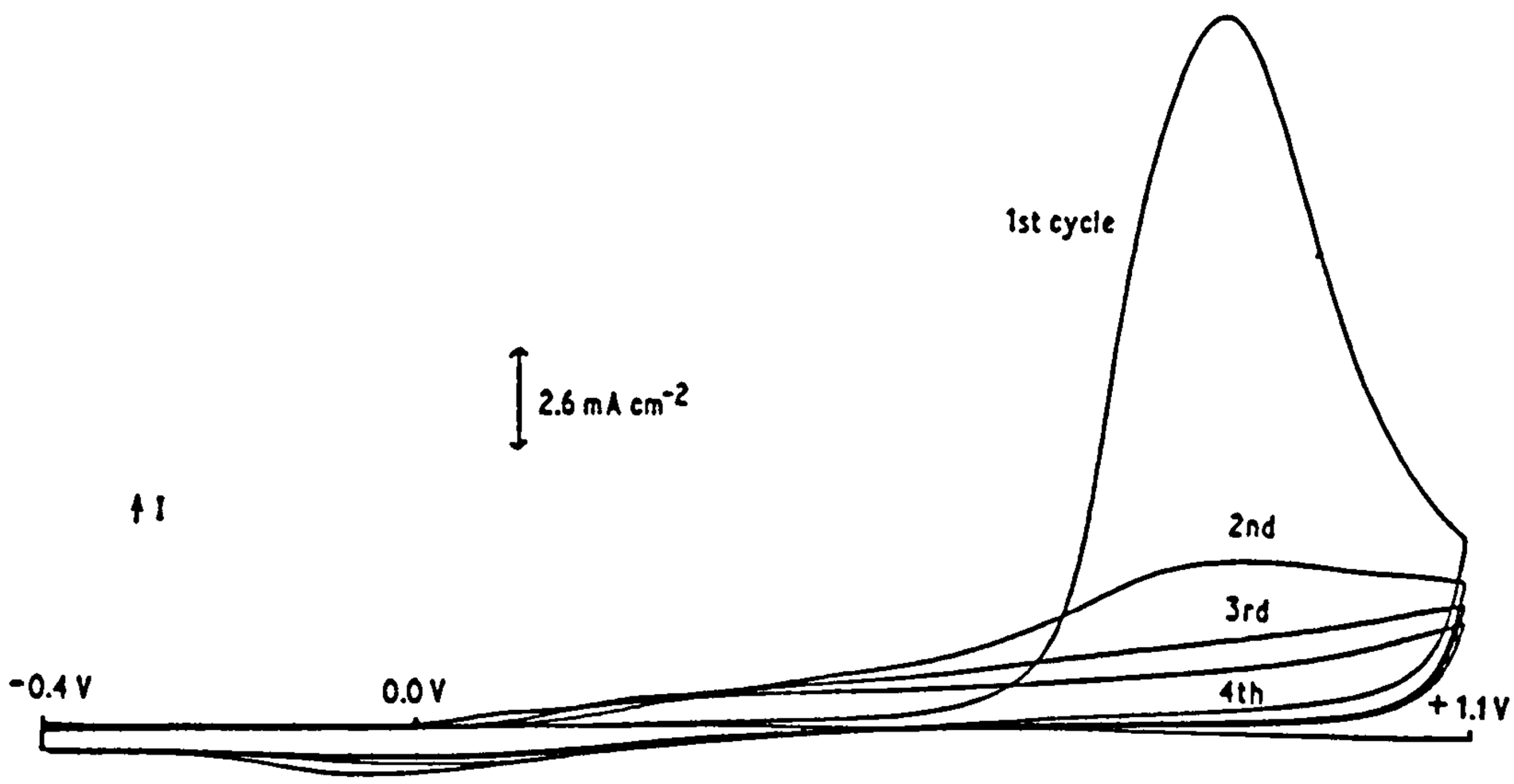

Fig. 14. Successive cyclic voltammograms of polypyrrole in aqueous electrolyte, showing a decrease in electroactivity caused by cycling at electrode potentials greater than 1.0 V[104].

This loss of electroactivity is in accord with the results of Satoh[105] in Fig. 15, which shows that the conductivity of polypyrrole decreases as the anodic potential limit is increased beyond 0.7 V. The decrease in conductivity at potentials greater than 0.7 V was attributed to nucleophilic attack by water, leading to ring opening and loss of conjugation[86,92]. Interestingly, the optimum potential range for the preparation of highly conducting films (0.6 to 0.7 V *vs.* SCE), corresponds to electrode potentials at

the foot of the current-voltage response for polypyrrole films prepared by cyclic voltammetry[104], as illustrated in Fig. 14.

Mechanical properties as determined by the tensile strength, are also dependent on the electrode potential during deposition[88,105]. Observations made by Bloor *et al*[91] and Buckley[88] show an increase in tensile strength as the current density and corresponding deposition potential decreased. The changes in mechanical properties being assigned to probable variations in the molecular weight of the oxidized polymer, changes in the numbers of defects, morphological changes and/or variations in the degree of crystallinity.

2.2.1.4 The Effect of Preparation Temperature.

Only a few studies have focused on the effects of the preparation temperature during the oxidation of pyrrole. However, these indicate that the both the conductivity and mechanical properties of polypyrrole are sensitive to the temperature of polymerization. For depositions in aqueous conditions with paratoluene sulphonate anion, the highest conductivities have been obtained at around 10°C, decreasing fivefold as the preparation temperature was increased to 40°C (See Fig. 16)[105].

Dramatic improvements in both conductivity and mechanical properties were reported by Ogasawa[85] for films electropolymerized in propylene carbonate, at temperatures in the range -40 to 10°C. Films prepared at -20°C could be extended by as much as 70% and sometimes in excess of 100%, with the conductivities of these stretch aligned films being reported to be excess of 1000 Scm^{-1}[85]. The increase in conductivities at lower temperatures being considered to be due to fewer side reactions and less defects.

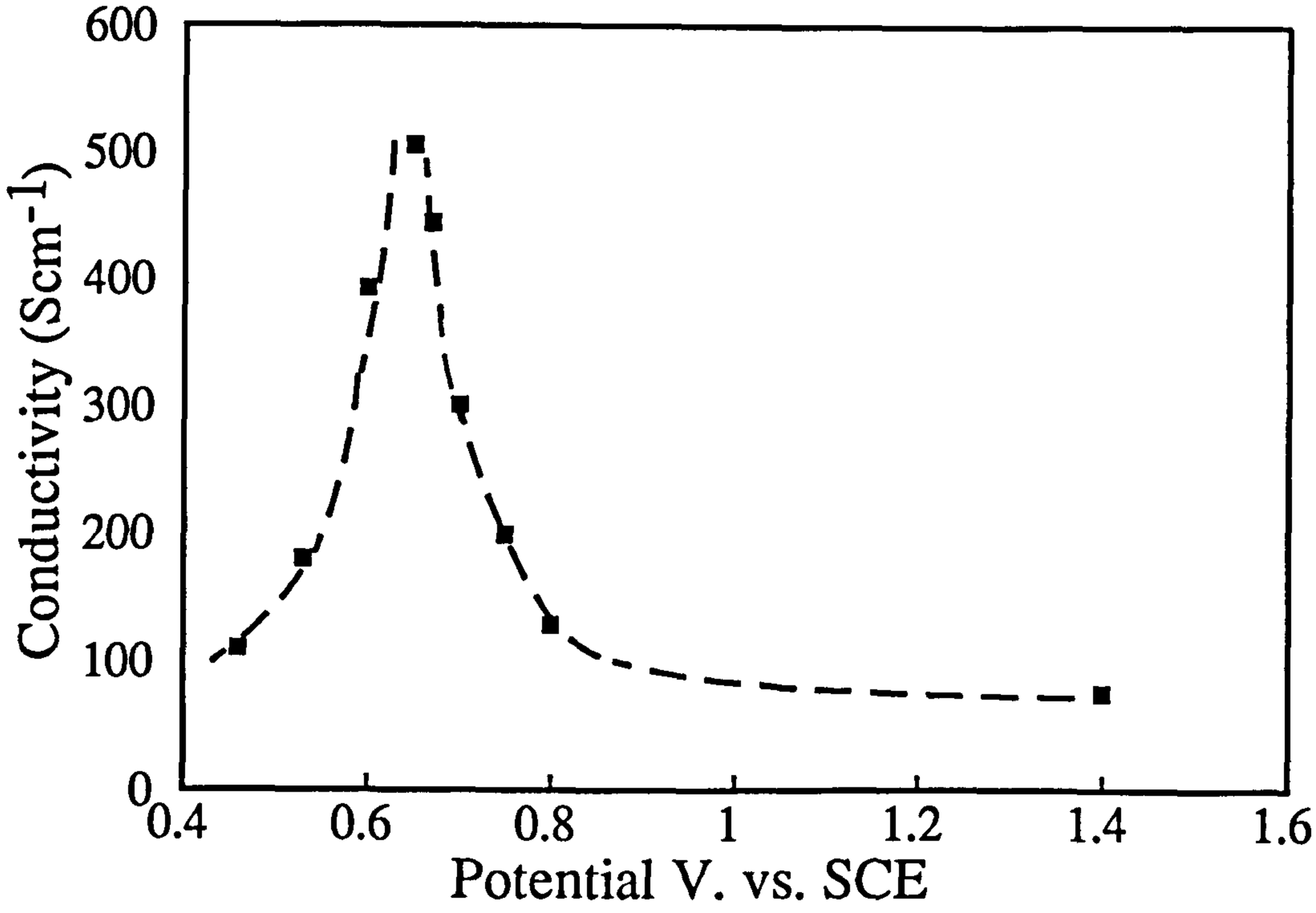

Fig. 15. Dependence of the conductivity of polypyrrole toluene sulphonate films on the applied potential during polymerization[105].

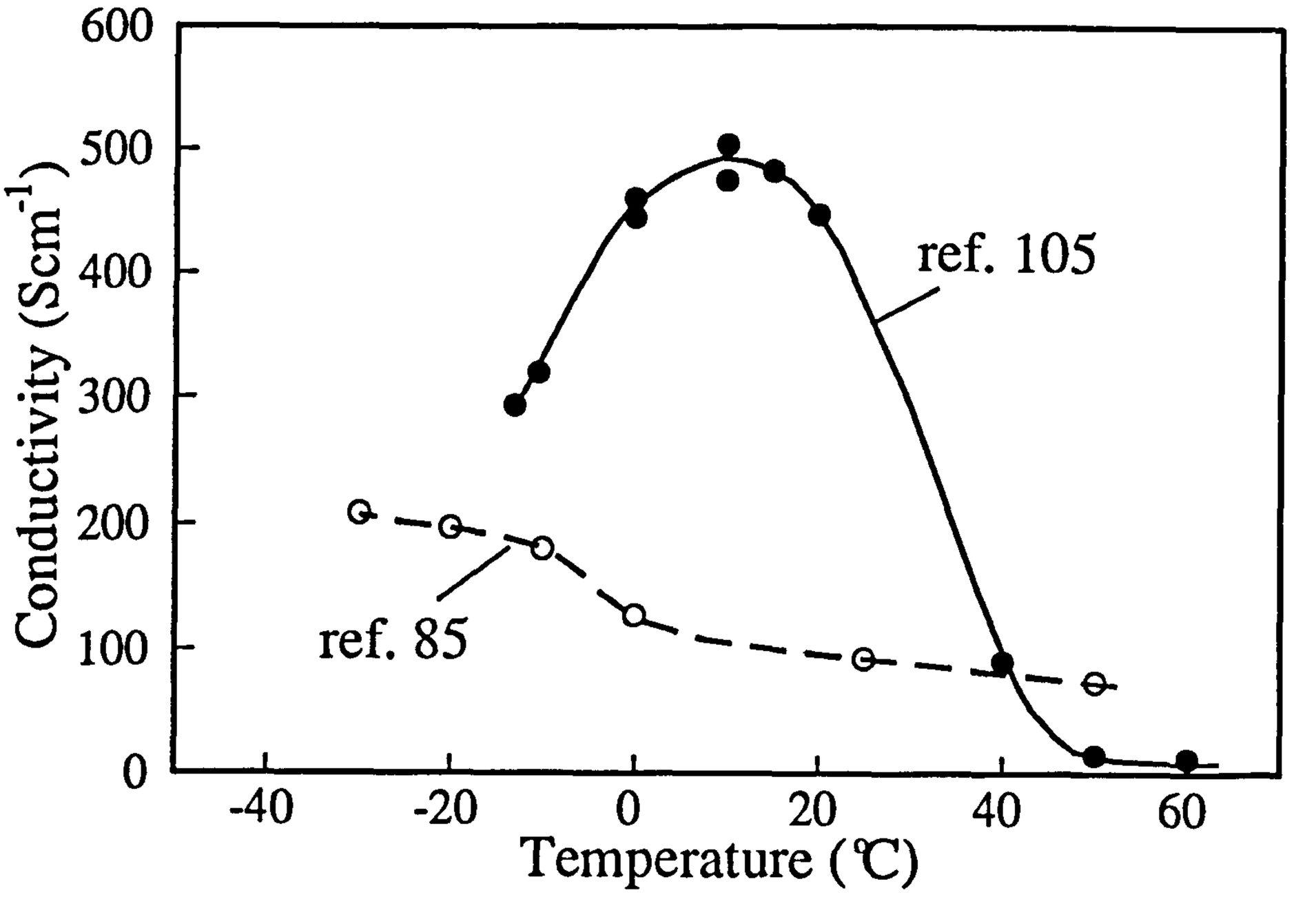

Fig. 16. Electrical conductivity of polypyrrole films prepared by electrochemical polymerization as a function of the preparation temperature. After refs.[85,105].

2.2.2 Stoichiometry of Polymerization.

The electrochemical oxidation of pyrrole is stoichiometric and can be represented by the following formalization[83]. For large n values, approximately two electrons per pyrrole ring are involved in the formation of the polymer (Eqn. 2.1), and a further (x) electrons are consumed during oxidation (Eqn. 2.2). Chemical analysis of polypyrrole indicates that (x) typically varies between 1/3 and 1/4 and is dependent on the nature of the dopant anion.

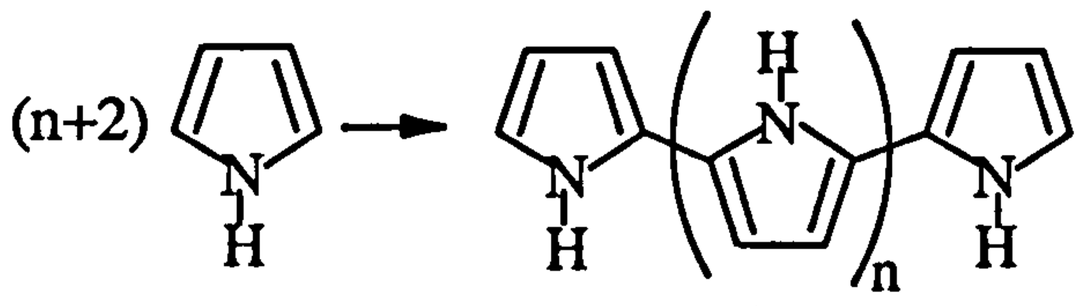

(2.1)

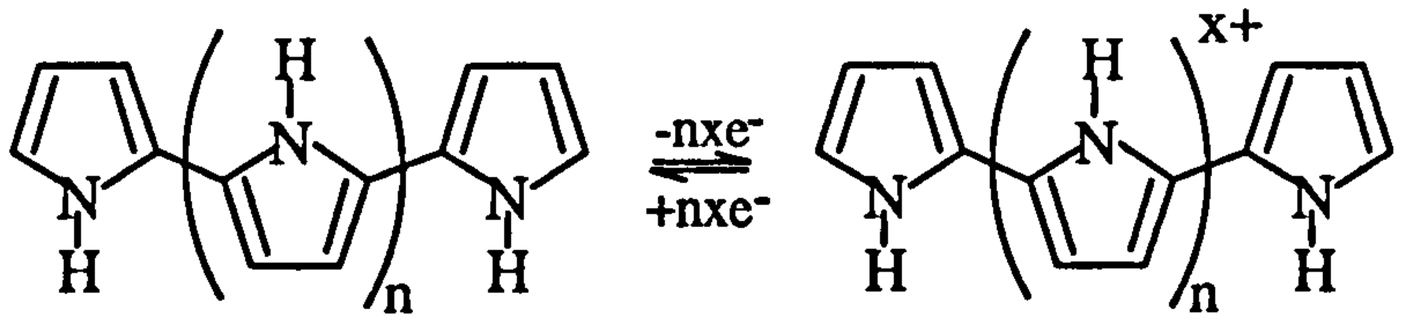

(2.2)

$x \approx \frac{1}{3}$ to $\frac{1}{4}$

This reaction scheme is also consistent with cyclic voltammetry studies[110] which show that the formation of the polymer involves the consumption of between 2.2 and 2.4 F/mol of pyrrole, of which 2 F/mol is consumed during the formation of the polymer film, with the remaining 0.2-0.4 F/mol being involved in the oxidation of the polymer.

2.2.3 Mechanism of Polymerization.

The polymerization of polypyrrole is complex, and involves a series of oxidation and deprotonation steps. Various studies to establish the mechanism have proved inconclusive and some times contradictory[57,97,110], however, the reaction scheme shown in Fig. 17 for the initial stages of oxidation is still commonly accepted. Potential step experiments and cyclic voltammetry studies[57,86] suggest that in aqueous conditions, the formation of polypyrrole on a platinum electrode surface occurs first by a nucleation step, followed by three dimensional growth at the electrode surface

to form a space filling layer. Since polypyrrole is only formed at potentials which are more anodic than that required to oxidize the monomer, it is proposed that polymerization proceeds via a radical cation coupling mechanism, followed by deprotonation to regenerate the aromatic system[111,112] (step 2). This is then followed by further coupling reactions between radical cations of pyrrole and oligomers of pyrrole, which have a lower oxidation potential than the parent monomer (step 3).

As the molecular weight of the polymer increases, it becomes increasingly insoluble in the reaction medium, and eventually precipitation occurs at the working electrode surface. Since the oxidation potential of polypyrrole is less than that required to oxidize pyrrole, polymerization is also accompanied by the simultaneous incorporation of anions into the film to balance the net positive charge on the oxidized polymer. Chain growth then continues until deposition is terminated, or until the reactive centre becomes sterically blocked[113], or undergoes side reactions[83,92] and is prevented from reacting further (step 4).

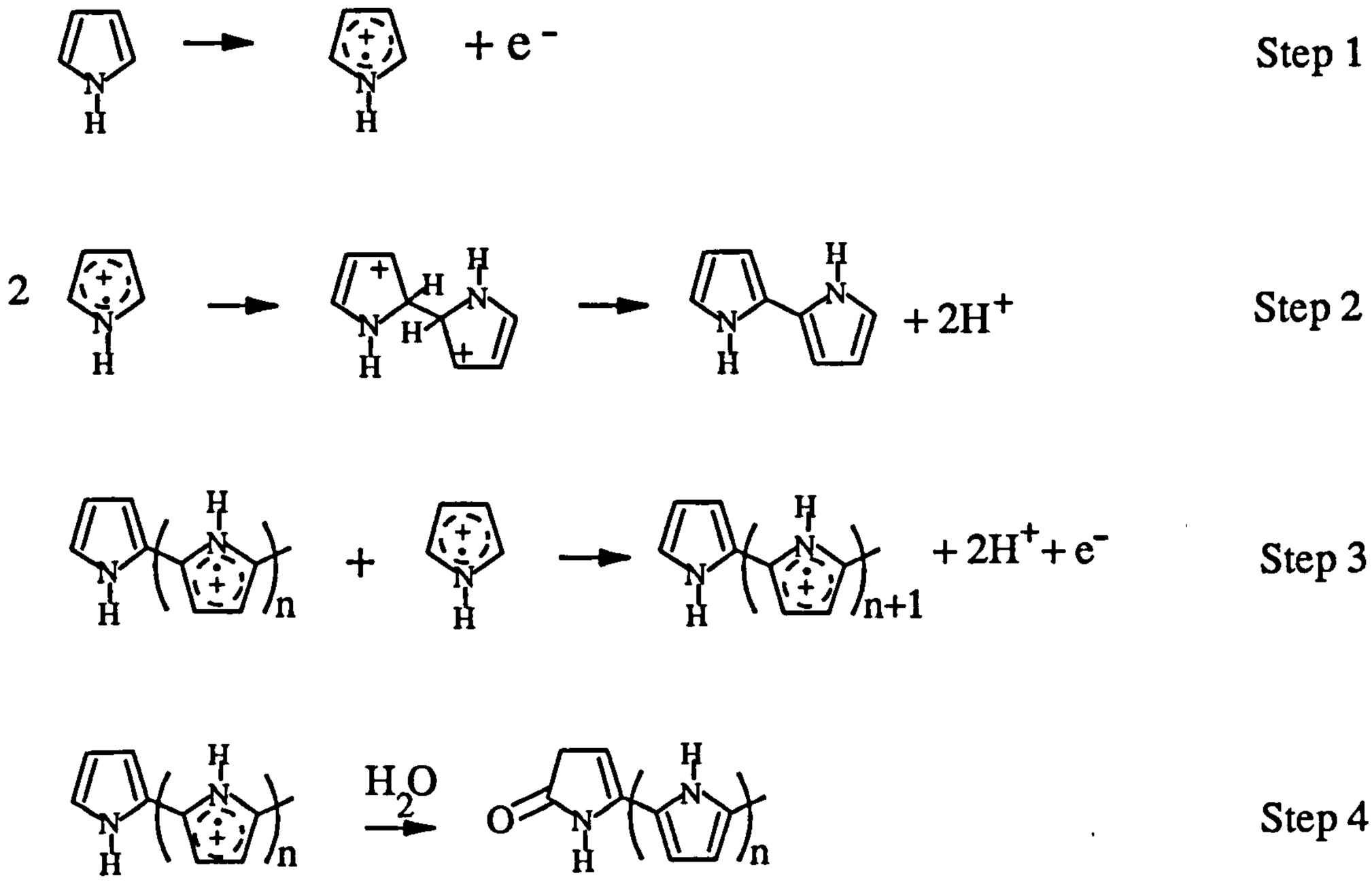

Fig. 17. Schematic representation of the initial stages of the electropolymerization of polypyrrole, after refs.[111,112].

2.2.4 Electrochemistry of Polypyrrole.

Polypyrrole belongs to a class of polymers which are inherently electroactive due to the extended π-conjugation along the polymer backbone which is capable of being oxidized[71,114]. As a result, electron transfer occurs rapidly and directly between the polymer and electrode substrate when the polymer is in an oxidized (conducting) state, and not via redox-mediation processes such as those described in section 1.5.2.

The electrochemistry of polypyrrole has been studied in aqueous[115-118] and non-aqueous solvents[119-121], and in particular by Diaz *et al*[71,114], who demonstrated that in the absence of oxygen, thin films of polypyrrole (0.02 - 0.1 μm thick) could be repeatedly cycled between the electronically insulating (neutral) and electronically conducting (oxidized) oxidation states. This switching process was shown to involve approximately 6% of the total charge required to form the polymer[71], and is accompanied by the simultaneous diffusion of anions between the film and bulk solution, so as to preserve overall film neutrality as the polymer is cycled.

This transition is accompanied by a colour change from brown/black of the oxidized film, to a pale yellow/bronze for the neutral film. Consequently, these materials offer the potential for use in electrochromic displays[115].

Cyclic voltammograms of polypyrrole in acetonitrile exhibit broad but well defined current peaks for the reduction and oxidation processes[71,83,114]. These are centred around -0.2 V *vs.* a sodium chloride calomel electrode in acetonitrile, and -0.4 V *vs.* a SCE in aqueous electrolytes, although exact values are often complicated by multiple peaks [57,114,115]. Peak heights for the oxidation (i_{pa}) and reduction (i_{pc}) waves have been shown to scale linearly with scan rate (v) (within 5%), for scan rates between 10 and 100 mVs^{-1}. This correlation suggests that the electrochemical processes involved during cycling are surface localised[114,115]. Peak potential values (E_p) for the oxidation and reduction processes are non equivalent, and are found to be dependent on the nature of the electrolyte[57,114,115]. This redox electrode process is non-Nernstian and was originally interpreted in terms of a simple counteranion diffusion process by Genies *et al*[112], on the basis that the values of diffusion coefficients for charge transport were dependent on the nature of the anion in the supporting

electrolyte. More recent research has shown the switching processes involved in cycling the film are more complex than was originally assumed, and that explanations of the current-voltage behaviour need also to consider the capacitive contribution to the overall current[122-124].

The origin of the large capacitive current in polypyrrole is still the matter of some debate. Models based on double layer capacitance[125], which require polypyrrole to have a porous fibrillar structure to account for the capacitance have been criticised for being physically unrealistic[123,126], since there is no experimental evidence to support such a structure. Mermilliod[123] and Tanguay[124] studied the capacitance of polypyrrole using ac impedance, and concluded that the capacitive current was more likely to originate from the transport of ions within the polymer.

2.3 Chemically Prepared Polypyrrole.

The chemical synthesis of polypyrrole represents an efficient means of producing large quantities of material, and hence, possesses the potential for bulk production[127]. For this reason, chemical polymerization has attracted attention from several groups[128-131].

Chemical methods of preparing "Pyrrole black" materials precede those obtained by electrochemical methods, and date back to Ciamician[132] in 1912. It was observed that conspicuous amounts of black polymer formed as a result of the atmospheric oxidation of pyrrole in water. Angeli *et al*[133] (1916), also reported the formation of a black precipitate when hydrogen peroxide was bubbled through a mixture of acetic acid and pyrrole. These reactions, and other early literature for the oxidation of pyrrole and pyrrole related compounds by peroxides, lead dioxide, nitrous acid, quinones, diazonium salts, ferric(III) chloride, Cr(VI) and Mn(VII) salts have been covered in a comprehensive review by Gardini[134].

In general, the reactions of pyrrole with more potent oxidizing agents, such as potassium permanganate and potassium dichromate are less specific, and complete oxidative degradation may occur, along with the formation of maleimide and other reaction products[135]. Since highly potent oxidizing agents are more likely to induce a greater proportion of side reactions, the recent trend in synthesis has been to utilize

less powerful transition metal compounds as oxidants[136-138]. In particular, various Fe(III) and Cu(II) complexes are commonly used. In each case, emphasis been to improve the conductivity of polypyrrole by optimization of reaction conditions[127,128,130,131,139,140].

Depending on the preparative conditions, the conductivities of chemically prepared polypyrrole can range from that of insulators or semi-conductors ($\sigma=10^{-15}$ to 10^{-6} Scm^{-1}), to values approaching that obtained from electrochemical polymerization ($\sigma=10^{1}$ Scm^{-1})[128]. The highest conductivity reported so far is 61 Scm^{-1} for the oxidation of pyrrole by $Fe(III)[CH_3(C_6H_4)SO_3]_3$ in methanol at room temperature[131]. This compares well with conductivities obtained by electrochemical methods.

2.3.1 The Effects of the Reaction Medium On the Formation of Polypyrrole.

The physical properties relating to chemically oxidized polypyrrole in instances where pyrrole has been oxidized by salts of metal ions, have been shown to be dependent on; (i) the choice of metal ion[128,137,140], (ii) the nature of the accompanying counteranion[131], (iii) the solubility and concentration of the oxidant[139,141], (iv) the solvent medium[128,141] and (v) the polymerization temperature[128,140].

In addition to being sensitive to the nature of the metal cation employed during polymerization, the formation of polypyrrole has also been shown to be dependent on the accompanying counteranion. This was demonstrated in a series of experiments by Walker[131], who used Fe(III) complexed with different anions to initiate polymerization. The conductivity of the resultant polypyrrole was found to parallel the Fe^{2+}/Fe^{3+} redox potential. Strong acid anions, such as R_fSO_3H, where R_f=fluorinated alkyl, and HCl, which do not strongly coordinate to Fe^{3+}, provided the most oxidizing Fe^{3+} species, and also produced the highest conducting polypyrrole.

The nature of the solvent medium in which polymerization is carried out can also have a significant effect on the resultant material. Factors such as solvent basicity[142], dielectric properties, and solvation effects of the solvent on the oxidant[128], have all been shown to affect the properties of the final material. Strong donor solvents such as dimethylsulfoxide, dimethylacetamide, and pyridine, which complex

strongly to Fe(III), completely inhibit the formation of polypyrrole[128]. This low reactivity was considered to be due a combination of steric effects and the influence of the solvent on the relative stability of the oxidation states of the metal ion, i.e the change in the redox potential caused through solvation. This effect was demonstrated by Castillo[127], who effected the oxidation of pyrrole by the addition of acetonitrile to a solution of $Cu(ClO_4)_2$ dissolved in tetrahydrofuran. This was because acetonitrile strongly stabilizes the Cu^+ oxidation state over the Cu^{2+} state, thus increasing the oxidizing capability of Cu^{2+}.

2.3.2 Reaction Stoichiometry.

An idealized general equation for the polymerization of pyrrole by ferric ions is given below[131].

$$(2+m)n\cdot Fe^{3+} + mn\cdot A^- + n\cdot C_4H_5N \rightarrow [(C_4H_3N)^{m+}\cdot mA^-]_n + 2n\cdot H^+ + (2+m)n\cdot Fe^{2+} \quad (2.3)$$

where A^- is the counteranion and m is the fractional dopant concentration. A wide range of different values for m have been reported by different workers[128,143,144], even in cases where the same oxidant has been used. This would seem to indicate that the polymerization reaction is sensitive to the initial reaction conditions, and also to differences in types of work up procedures that are used to purify the material after preparation.

Characterization of the resultant polymers by conventional methods is complicated by the insoluble and amorphous nature of the final product[129], and spectroscopic techniques such as IR and Raman spectroscopies have only yielded limited information[113]. The insoluble nature of polypyrrole also precludes the use of conventional purification techniques, such as precipitation and crystallization. This renders it difficult to eliminate impurities from the final product, with the possible consequence of obtaining potentially misleading elemental analysis data. Hence, is not surprising that differences exist between proposed dopant species and dopant levels in these materials. For example, the exact nature of the dopant species in polypyrrole oxidized with $FeCl_3$ is still subject to some uncertainty. Mossbauer spectroscopy

studies[143,144,145] indicate Cl^- as the sole dopant anion, with an idealized stoichiometry of $[(C_4H_3N)_4^+Cl^-]_n$. This form of polypyrrole was found to be still reactive towards metal halides, and treatment with $FeCl_3$ in non-aqueous solvents produced polypyrrole with a stoichiometry given by $[(C_4H_3N)^+_2(FeCl_4^-)_xCl^-_y]_n$ (where x+y=1). Other dopant species such as $FeCl_4^-$[128,143,141], and even $FeCl_6^{3-}$[128] have been proposed by other workers. In view of these discrepancies, it is suggested that caution be exercised when deciding on the nature of the counteranion on elemental analysis data alone. Indeed, it seems unlikely that the nature of polypyrrole oxidized with ferric chloride is $(C_4H_3N)^+_{8.3}\ FeCl_4^-$ and $(C_4H_3N)^{3+}_{16.5}\ FeCl_6^{3-}$, as suggested by Myers.

Elemental analysis also shows that a large amount of oxygen, and sometimes hydrogen are incorporated into the polymer during polymerization. The origin of these excesses is still not fully understood, but probably arises from the formation of pyrrolin-2-one groups[129], and low molecular weight reaction products which are formed as products of side reactions of pyrrole with strong oxidants[134].

Excess oxygen and hydrogen has also been attributed to "water of hydration" which is incorporated within the polymer during preparation[127,134]. This is considered feasible, as studies have shown that polypyrrole is hygroscopic, incorporating up to 10% wt./wt. of moisture. Evidence for the presence of trapped water in chemically prepared polypyrrole has been found by Walker[131] using thermogravimetric analysis. IR studies on the same samples also indicates the presence of pyrrolidone absorptions between 1650 and 1700 cm^{-1}, and this would suggest that both of the above explanations are valid in accounting for the excess oxygen and hydrogen content.

2.3.3 Polymerization Mechanisms.

Although polypyrrole has been the subject of great interest, the majority of studies have concentrated on the preparation and characterization of samples prepared by electrochemical methods. Because of this, the mechanism of the chemical oxidation process, and factors which influence this, are not yet fully understood. Most workers[127,142] assume that chemical oxidation proceeds in an analogous manner to that of electrochemically oxidized polypyrrole, and a free radical mechanism for the initial

stage of oxidation of pyrrole by $Cu(II)(ClO_4)_2$ has been recently proposed by Castillo[127]. Evidence that the mechanism does actually involve free radical intermediates comes from early work by Dascola[146] who used ESR to study the oxidation of pyrrole by H_2O_2 in acetic acid.

The mechanism proposed by Castillo[127] involves the generation of radical cations of pyrrole by reaction with the chemical oxidant ($Cu(ClO_4)_2$). This is followed by deprotonation and coupling reactions, which yield oligomers of pyrrole. These are then successively oxidatively coupled in a continuation of the above process. Myers[128] suggests that the initial stage of oxidation is likely to involve a solvent-$FeCl_3$-pyrrole intermediate, on the basis of the Lewis acidity of $FeCl_3$ coupled with the basic nature of pyrrole, and also because of a marked dependence of polymer yield and conductivity on the solvent medium. A similar mechanism is proposed by Gregory *et al*[142], who suggests that polymerization proceeds via an outer sphere activated complex, involving solvent, pyrrole, and Fe(III). The rate of reaction is then determined by the electron transfer step between the pyrrole and Fe(III) complex. Differences in experimentally observed reaction rates were explained in terms of the following acid/base equilibrium of the Fe(III) complex.

$$[Fe(H_2O)_6]^{3+} \rightleftharpoons [Fe(H_2O)_5OH]^{2+} + H^+ \qquad (2.4)$$

Factors which shifted the equilibrium position towards the acidic form of the hydrated Fe(III), such as the addition of acid, promoted the reaction of pyrrole with $[Fe(H_2O)_6]^{3+}$ and increased the rate of polymerization. In contrast, high pH environments were reported to retard reaction rates.

Despite the ease of synthesis of chemically prepared polypyrrole, and the ability of being able to prepare large quantities of material rapidly and at low cost, chemically prepared materials have on their own, found little practical application. One possible way of improving the potential for application, is in the preparation of conducting polymer composite materials, these are discussed in the following section.

2.4 Polypyrrole Composite Materials.

Electrically conducting polymeric materials with reasonable environmental stability have now been known for about a decade. However, as yet there are still few commercial applications which utilize these materials, (with the exception of battery applications of polyaniline[147-149]. The reasons for this are undoubtably due to the poor mechanical properties of organic conducting polymers, coupled with their infusible and insoluble nature. This has meant that conventional fabrication and processing techniques cannot be used with these materials. Modifications to conducting polymer materials in order to improve their mechanical properties and ambient stability, have since been the focus of much research. One approach has been the formation of composite materials which combine the conducting properties associated with these materials, with the mechanical properties of a non-conducting matrix. This method has the advantage that cheaper and more versatile chemical methods can be used to prepare conducting polymers on preformed substrate.

2.4.1 Electrochemical Methods of Preparation.

The electrochemical approach for producing composites was first developed by Niwa and Tamamura[150], and involves the polymerization of pyrrole on an electrode coated with an insulating polymer film. The prime requirement of this technique is the need for the polymer film to be permeable to the electroactive constituents within the electrolyte solution. Pyrrole is then able to diffuse to the electrode surface where oxidation/polymerization occurs. Growth then proceeds outwards from the electrode surface into the host matrix as electrolysis is continued.

The range of conducting composites that have been prepared using this method are now numerous, and includes poly(vinylidene chloride) copolymers, polystyrene, polymethacrylates, phenol resins[150], PVC[150-152], poly(vinylidene fluoride) and vinylidene fluoride tetrafluoroethylene (60-40) co-polymer[93], polyacetylene[153], poly(vinylalcohol)[154] and polyether/polyester elastomers[155]. A summary of data for composite materials prepared by electrochemical methods is given in Table 2.

Table 2. Comparison of electrochemical methods of preparing conducting polymer composite films.

Film substrate	Electrolyte	Deposition potential (V)	Duration of electrolysis	Conductivity (Scm^{-1})	ref.
PVC (1.2 μm thick) poly(vinylidene chloride) polystyrene polymethacrylates poly(vinyl ethers)	acetonitrile, TEAP	----	6 minutes ---- ---- ---- ----	12 --- --- --- ---	150
PVC (4-17 μm thick) PVC + plasticizer 30% wt.	acetonitrile, pyrrole (0.006 M) $TEABF_4$ (0.1 M) ---	1.15 V *vs.* SSCE	30 - 120 minutes	5 to 50 18	151,152
PVC (~20 μm thick)	acetonitrile, pyrrole (1 M) TEA(*p*-TsO^-) (0.3 M)	1.5 V *vs.* SCE	---	---	156
PVC (1.8 μm thick) + 5% wt. $TEABF_4$	acetonitrile, pyrrole (0.1M) $TEABF_4$ (0.2 M)	2 V	5 - 20 minutes	10^{-2} to 10	157
NIGT (25 μm thick)	acetonitrile, pyrrole (0.74 M) $TEABF_4$ (0.1 M)	0.8 V *vs.* SCE	---	20 to 50	158
Polyacetylene	acetonitrile, ClO_4^-, BF_4^-	---	---	20 to 40	153
Poly(vinyl alcohol) (3-4 μm thick)	water, pyrrole (0.1 M) $CuSO_4$ (0.1 M)	---	---	0.1 to 10	154
Polyether/polyester elastomer (50-70 μm thick)	acetonitrile, pyrrole (0.1 M) $TEABF_4$ (0.1 M)	---	5 - 60 minutes	0.2	155
Nafion (50 μm thick)	acetonitrile, pyrrole (0.005 M) $TBABF_4$ (0.2 M)	potential sweep -0.6 to 1.0 V *vs.* Ag	---	---	159

KEY: PVC=Poly(vinylchloride); NIGT=Nafion-impregnated gortex
$TEABF_4$=tetraethylammonium tetrafluoroborate
$TBABF_4$=tetrabutylammonium tetrafluoroborate
TEA(*p*-TsO^-)=tetraethylammonium para-toluenesulphonate
TEAP=tetraethylammonium perchlorate

In each case, the polymer coat is applied to the electrode surface either through a dip coating method, or via spin coating techniques. Preformed commercial films of PVDF have also been used as hosts, but with limited success[93,158]. This was attributed to the low permeability of pyrrole through these materials.

Conductivity studies by Wang[157] have shown that composites produced by electrochemical methods may suffer from a highly non-uniform polypyrrole loading, with the greatest content of polypyrrole being located adjacent to the electrode surface. Efforts to improve the uniformity of the polypyrrole content within these films have centred on the introduction of "ionic centres" into films. This may be achieved either through straightforward addition of electrolyte to the polymer solution[157], or by impregnation of the surface polymer with an ionically conducting phase such as nafion (perfluorinated ion-exchange membrane)[158]. This approach has the beneficial effect of decreasing the ohmic drop within the film, thus aiding diffusion of pyrrole and electrolyte within the polymer, and as a consequence reduces deposition time. Although the electrochemical technique has proved to be a convenient method for producing such composites, its applicability is severely limited by the use of electrodes, coupled with the fact that long polymerization times are required to produce the composites. These constraints have been partly over come using chemical methods.

2.4.2 Chemical Methods of Preparation.

Chemical synthesis is a versatile approach to the preparation of conducting composites. Possible advantages of this method include the use of low cost reagents, the possibility of preparing large areas of conducting film, the preparation of composites with conductivities that are comparable to that obtained using electrochemical methods, and short reaction times[140].

Although a variety of methods have been developed for the preparation of conducting polymer composites, these are essentially based on only three different techniques (see Table 3). These are designated as "in situ" polymerization, chemical impregnation, and emulsion polymerization.

Table 3. Comparison of chemical methods of preparing conducting polymer composits.

Method of Preparation	Substrate	Oxidant	Conductivity Scm^{-1}	Comment	Ref.
1	Polyurethane emulsion	$FeCl_3$ (2-18% wt.)	0.2	Highly non uniform surface, poor mechanical properties	160
	Polyurethane emulsion with polyacrylamide		< 0.2	less porous, improved mechanical properties	
1	Methylcellulose emulsion	$FeCl_3$ (3.5% wt.)	< 0.2	globular polypyrrole embedded in thin flakes of methylcellulose	161
2	Sulphonated polyethylene film (100 μm thick)	$FeCl_3$ (~9% wt.)	10	globular surface morphology	162
2	Nylon-6 fibres	$FeCl_3$ (1.13% wt.)	----	Uniform surface coat, less than 1 μm thick, long preparation times required	144
2	Polystyrene latex particles (0.13 μm diameter)	SO_3^- COO^-	10^{-6} to $2.5x10^{-1}$ $3x10^{-3}$ to $7x10^{-2}$ 0.25, bulk conductivity of particles	Uniformly coated particles	163
3	Polyethylene, latex rubber film (0.1-0.2 mm thick) wood, paper, cloth	$FeCl_3$ (20-30% wt.)	10 to 30 50	Flexible, optimum preperation temperature 0-10°C	142

Method of Preparation	Substrate	Oxidant	Conductivity Scm^{-1}	Comment	Ref.
3	Nylon-66 film (70 µm thick)	$FeCl_3$ (~30% wt.) 24hrs	10^{-9} to 10	Non-uniform deposition, 5 µm thick coat. Increase in Young's modulus	164
3	Cellulose paper	various ferric(III) salts, $Ce(SO_4)_2$, CrO_3, $H_3PMo_{12}O_{40}$	---	$FeCl_3$ in 0.01 M HCl gives highest conductivities	138
3	Filter paper	Ferric(III) salts (20-30% wt.)	1 to 20	---	143
3	Polystyrene solid substrates	$FeCl_3$ (20-40% wt.) aq. and non-aq. solvents	10^{-3} to 10^{-1}	Highly porous and non-uniform polymer coats	165
3			0.8		
3	poly(4-vinylpyridine) film	$FeCl_3$ $CuCl_2$	10^{-3} to 10^{-1} 5 to 150	uneven polymerization, highly conductive	139
3	Cellulose paper	$FeCl_3$ (20% wt.), 0.01 M HCl	2	porous, highly uneven surface	165
3	Poly(vinyl alcohol) (2 µm thick film)	$FeCl_3$ (5 to 30% wt.)	8	Vapour phase polymerization, transparent films, Rough surface at high concentrations of oxidant	166

Key: 1= emulsion polymerization
2= In-situ polymerization
3= chemical impregnation

In-situ polymerization is where pristine substrates are immersed in solutions containing both oxidant and monomer. Polymerization is then effected at the surface of the substrate by absorption of polymeric cations of conducting polymer from solution. Gregory *et al*[142] used this method for coating the surface of nylon fibres, in order to produce conductive textiles (10 Scm^{-1}) for anti-static applications. Polymerization can also be made to occur preferentially at the substrate surface, by covalent attachment of anionic groups such as carboxylic acid or sulphonic acid groups[162,163]. Surfaces treated in this way have been shown to catalyse the formation of conducting polymer, and XPS analysis has shown that the covalently attached groups function as dopants, preferentially doping polypyrrole over Cl^- or other oxidizing species in solution. Because the anionic groups are covalently bonded to the substrate surface, the resultant polypyrrole coats are also highly adherent.

A variation of in-situ polymerization was employed by Bocchi and Gardini[140] for the preparation of composite polypyrrole/polyethylene and polypyrrole/latex rubber films. Conductivities comparable to those produced by electrochemical methods (30 Scm^{-1}) were achieved by effecting polymerization in a host film which was placed at the interface of an aqueous solution containing a chemical oxidant and an organic phase containing pyrrole. Polymerization then occurs via diffusion of pyrrole through the film to the aqueous solution. This approach has the advantage of not requiring prior impregnation of the substrate with either monomer or oxidant.

Impregnation techniques involve permeating the host substrate with either monomer or oxidant, followed by subsequent exposure to another solution containing monomer or oxidant to effect polymerization. Using this method, composite materials have been prepared from cellulose paper[136,137] wood, cloth[140], inorganic materials such as porcelain, plastics including polystyrene[141], and cast epoxy resin[137]. The conductivity of the coated substrates that can be obtained using impregnation methods has been shown to be dependent on parameters such as the solvent, concentration of the oxidant, and the reaction temperature during synthesis. A list detailing the effects of these variables on paper and polystyrene composites is given in Table 4.

Table 4. Effects of various experimental parameters on the conductivity of polypyrrole composites.

Oxidant	Concentration % (wt./wt.)	Solvent	Temperature (°C)	Conductivity (Scm^{-1})	Ref.
$FeCl_3$	10	water	0	4	139
	15			12	(a)
	20			20	
	25			20	
	30			18	
	35			3	
$Fe(NO_3)_3$	20			5	
$Fe(ClO_4)_3$	25			13	
$Fe(SO_4)_3$	saturated			1	
$FeCl_3$	10	water	20	$3x10^{-2}$	136
	10	0.01 M HCl		$1.5x10^{-1}$	137
	10	acetonitrile		$3x10^{-3}$	(b)
	10	ethanol		$3x10^{-4}$	
	10	dimethyl-sulphoxide		no polymer	
CrO_3	10	water		$1x10^{-5}$	
$Ce(SO_4)_2$	10	water		$2x10^{-4}$	
$K_3Fe(CN)_6$	10	water		$5x10^{-3}$	
$H_3PMo_{12}O_{40}$	10	water		$5x10^{-3}$	
$FeCl_3$	20	cyclohexane	RT	$2.1x10^{-1}$	141
	20	chloroform		$3.0x10^{-1}$	(c)
	20	methanol		$1.4x10^{-1}$	
	20	ether		$3.1x10^{-1}$	
$FeCl_3$	40	water		$4.1x10^{-2}$	
	40	acetone		$3.9x10^{-3}$	
	20	acetonitrile		$2.7x10^{-1}$	
I_2	2	acetonitrile		$5.3x10^{-4}$	

Key: a=filter paper substrate saturated with pyrrole prior to exposure to oxidant
b=filter paper saturated with oxidant prior to exposure to pyrrole vapour
c=polystyrene host impregnated with oxidant prior to exposure to pyrrole solvent

Conductivities of up to 50 Scm^{-1} have been achieved for substrates which are doped with monomer prior to oxidation[140]. In contrast, when the oxidant is incorporated into the substrate, high concentrations of oxidant (up to 90%) are usually required to achieve a reasonable conductivity. Even then, the conductivities that have been reported are between two and three orders of magnitude lower than samples which are impregnated with monomer (see Table 4).

Substantial improvements in the conductivity of substrates permeated with oxidant were reported by Salanek *et al*[167] who used stretch aligned films of poly(4-vinylpyridine) complexed with metal ions of Cu^{2+} or Fe^{3+} to impose an ordered

structure on polypyrrole. Using this "template" method, they were able to achieve composite films with electrical conductivities of up to 100 Scm^{-1}.

The third technique of preparing composites involves the preparation of an emulsion which is then blended with chemically prepared conducting polymer. Emulsions prepared in this way can then be cast in to films or applied to the surfaces of other materials to produce conductive surface coats[141,160,168,161]. Initial conductivities of these materials range from ~10^{-6} to 2 Scm^{-1}, which is comparable to other chemical methods. Studies have also shown that the conductivity of colloidal polypyrrole is less environmentally stable compared to that of bulk polypyrrole powder, with the conductivity decreasing with time. The relatively high interfacial areas of these materials (~32 m^2g^{-1}) has been suggested as a possible explanation of this phenomenon[168].

2.5 Chemical Modification of Polypyrrole with Base.

Several studies have recently been conducted on polypyrrole treated with base. Such treatment has been shown to effect changes in the optical, physical and electrochemical behaviour of these materials. For instance, the electrical conductivity of base treated polypyrrole has been reported to be decreased by up to six orders of magnitude for electrochemically prepared polypyrrole[169-171], and by up to nine orders of magnitude for chemically prepared material[127]. The difference in magnitude of effect possibly being due to the greater surface area and porosity of chemically prepared materials. The decrease in conductivity is also accompanied by a reduction in film size and a loss of up to 40% in weight. Both of these effects have been attributed to the loss of the counteranion from within the film[169-171] on the basis of results from dispersive X-ray spectroscopy (see Fig. 18).

The decrease in weight and loss of conductivity were found to be largely reversible and could be almost fully restored by subsequent treatment with either Bronstead or Lewis acids. This reversible behaviour for alternate acid and base treatment is illustrated in Fig. 19.

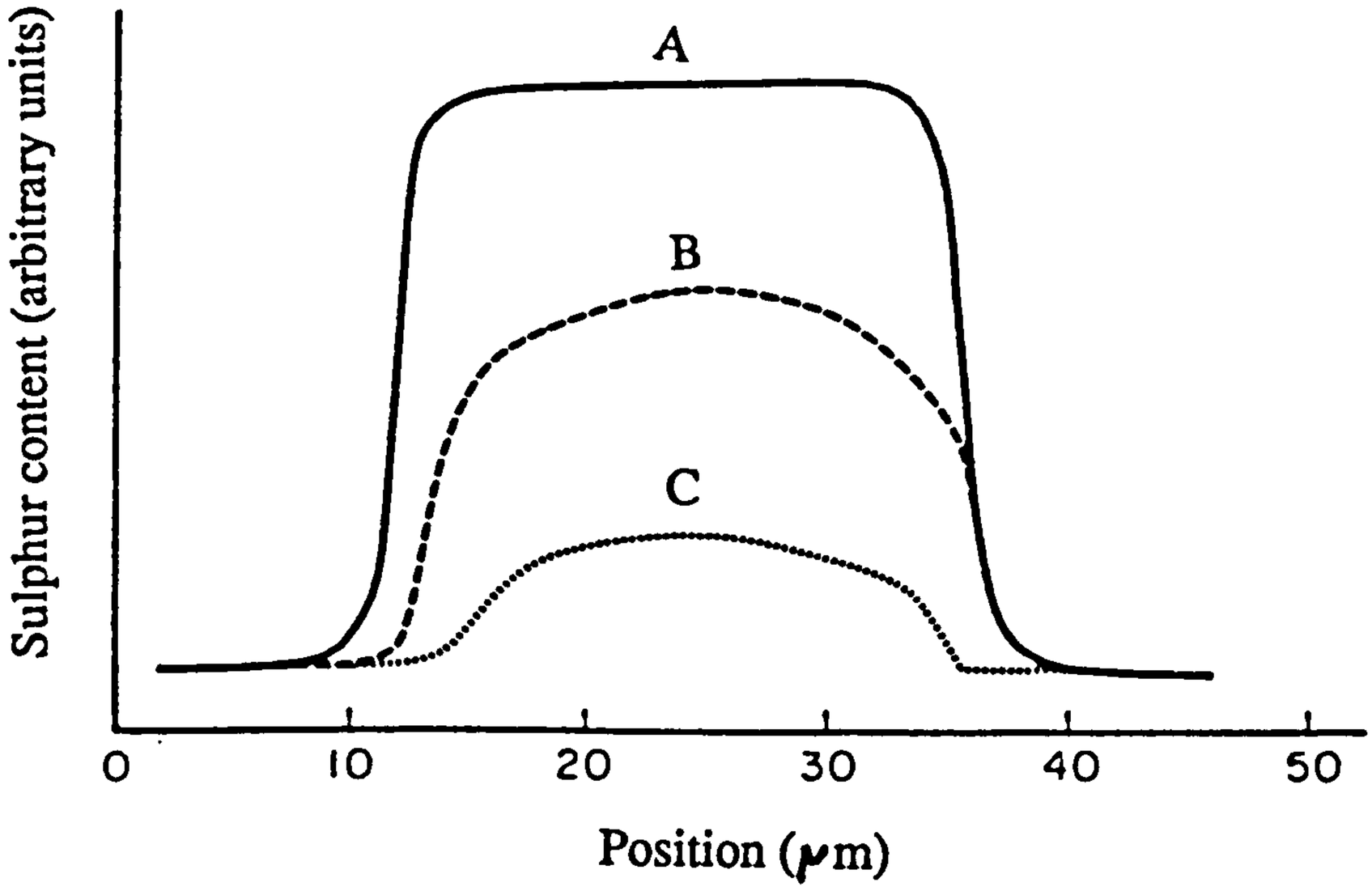

Fig. 18. Dispersive X-ray spectroscopy results showing sulphur distribution of poly(pyrrole phenylsulphonate) films of thickness ~30 μm after treatment with 2% aqueous NaOH solution for different times. A, initial sample; B, treated for 120 min; C, treated for 240 min[169].

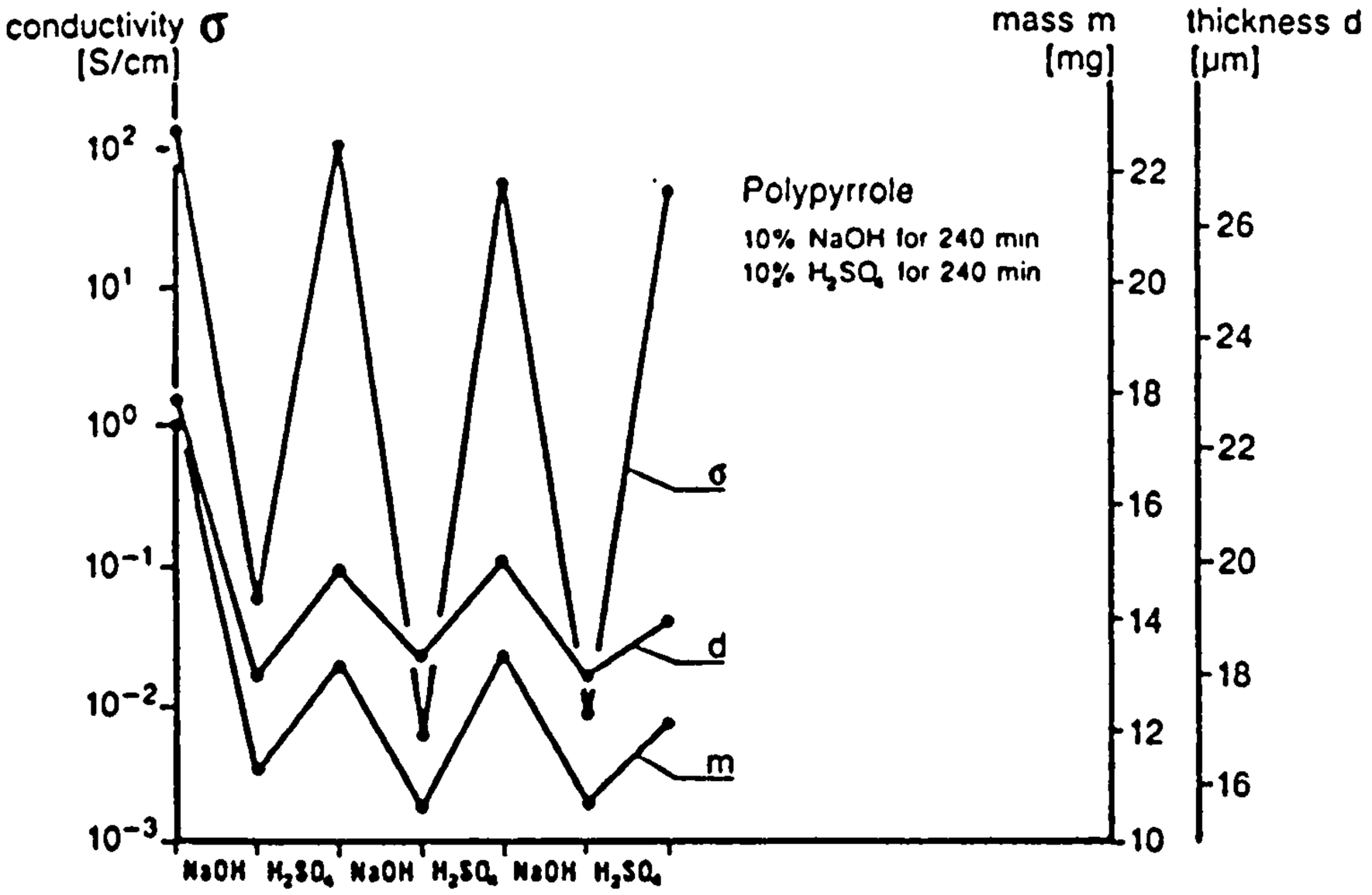

Fig. 19. Changes in conductivity, mass, and thickness of a poly(pyrrole phenylsulphonate) film of 30 μm thickness by alternating exposures to aqueous sodium hydroxide and sulphuric acid solution[169,170].

Experimental results of dispersive X-ray spectroscopy (see Fig. 18), elemental analysis[169,172], X-ray photoelectron spectroscopy (XPS), Fourier transform infrared spectroscopy (FT-i.r)[173], and in-situ visible near infrared spectroscopy[172], suggest that base treatment effects either complete or partial loss of the original counter-anion from polypyrrole. The extent of this loss is dependent on the original film thickness, the concentration of base employed, and duration of contact of the film with the solution. This reaction is generally considered to involve some form of chemical compensation effect, whereby the original film counter-ion is either expelled or exchanged with OH^- from solution[169,172,173]. However, the detailed nature of this process is complex and has yet to be fully elucidated. Munstedt[169] proposed the insertion of OH^- into the polymer, which it is then suggested forms covalent bonds with polypyrrole, resulting in a reduced conjugation length and decrease in conductivity. Qian *et al*[172] consider this to be unlikely, and, on the basis of in-situ vis-n.i.r and cyclic voltammetry, propose the exchange of the original counteranion from the film by OH^-. This, they suggest has a low conductivity in comparison to other anion-intercalated forms of polypyrrole.

Inganas *et al*[171,173] studied the interaction of polypyrrole with NH_3 and NaOH using several spectroscopic techniques. They concluded that the interaction with NaOH and NH_3 was more complex than that suggested by other workers, and proposed the following reactions for interaction with ammonia. At low concentrations of base and short exposure times, they suggest that oxidized polypyrrole interacts reversibly with ammonia according to either of the following reactions.

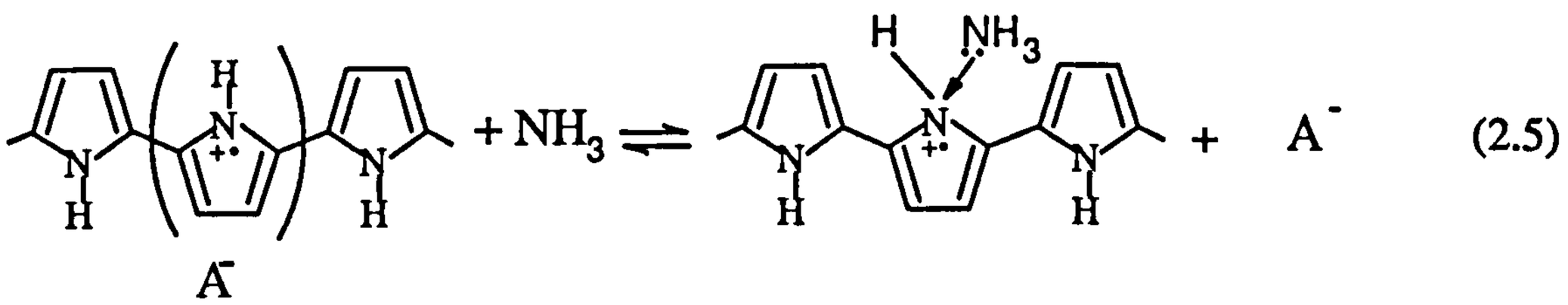

(2.5)

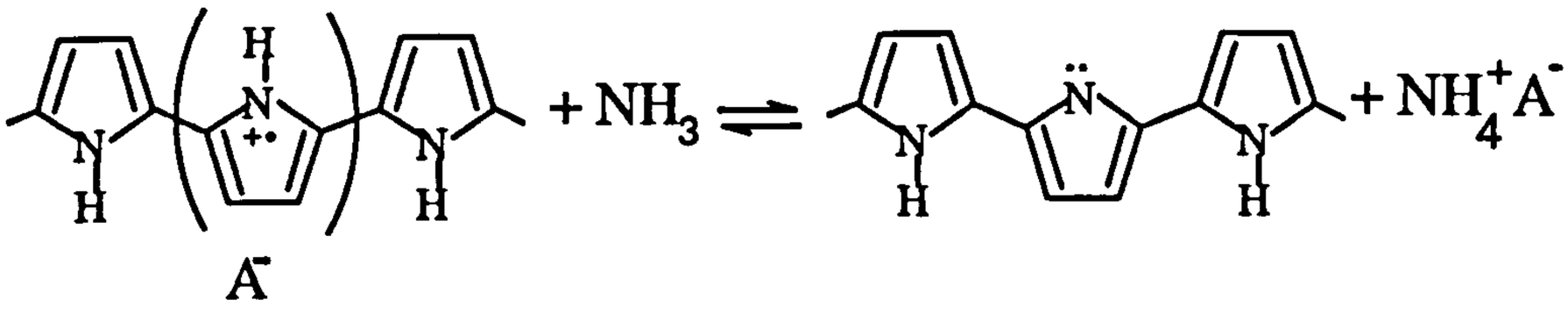

(2.6)

In Eqn. 2.5, ammonia molecules which are electron donating, act as n-type dopants, and decrease the doping level of the polymer chain by compensating the effect of the original dopant. Eqn. 2.6 involves abstraction of a proton from the pyrrole nitrogen, leaving a negative charge on the chain. This then has the possibility of combining with the positive charge on the polymer backbone, resulting in a reduction in conductivity and simultaneous "undoping" of the polymer so as to preserve overall charge neutrality. This mechanism is consistent with conductance measurements of base treated polypyrrole which show a dramatic increase in resistivity between pH 12 and 13, which is in accordance with their estimation of the pK_a for the NH group in the polymer. At longer times of exposure to base, F.T.-i.r and XPS spectroscopies indicated that degradation of the polymer had occurred.

2.5.1 Electrochemistry of Base Treated Polypyrrole.

The electrochemistry of polypyrrole has been shown to be pH dependent[115,172-175]. Qian *et al*[176] used cyclic voltammetry coupled with vis-n.i.r spectroscopy, to follow changes in the absorption of $PPy^+(NO_3^-)$ in $NaNO_3$ solutions at different pH, whilst it was cycled between the oxidized and reduced states. At pH < 7, the electrochemical and spectral responses were shown to be reversible over several cycles, whereas in neutral solutions a decrease in absorbence was observed at potentials which corresponded to the reduced state of the film. This indicated that polypyrrole was more completely reduced in neutral solution. At pH > 7 the CV response and absorption spectra were found to be similar to those obtained from base treated polypyrrole. From this, the authors suggested probable anion exchange of OH^- with NO_3^-.

Voltammograms of base treated polypyrrole show reversible behaviour in the potential range -0.2 to -1.0 V, for scan rates less than 20 mVs^{-1}[172]. Reduction and oxidation peaks which have been attributed to the PPy^+/PPy^o redox couple are observed at -0.63 V and -0.50 to -0.56 V, depending on the pH of the solution. At potentials more anodic than +0.35 V, base treated polypyrrole undergoes irreversible oxidation which results in a loss of electroactivity. The lack of electroactivity of base

treated polypyrrole has also been confirmed by Witkowski *et al*[94] for GC-PPy electrodes treated with 0.5 M NaOH.

The quantity of charge that can be cycled during cyclic voltammetry is also found to be strongly pH dependent[106,175]. At pH 5 the electrochemistry of polypyrrole appears to be quasi-reversible, and the amount of charge that could be continually cycled remained almost constant at about 90% of the theoretical maximum available charge, Q_{rev}. At pH 9 this decreased to 39% Q_{rev} after only 9 cycles, which suggested that polypyrrole had undergone chemical change. One other effect of the base treatment of polypyrrole is a reduction in oxidative stability. This is indicated by decrease in the anodic peak potential E_{pa}, at pH > 9, as shown in Fig. 20.

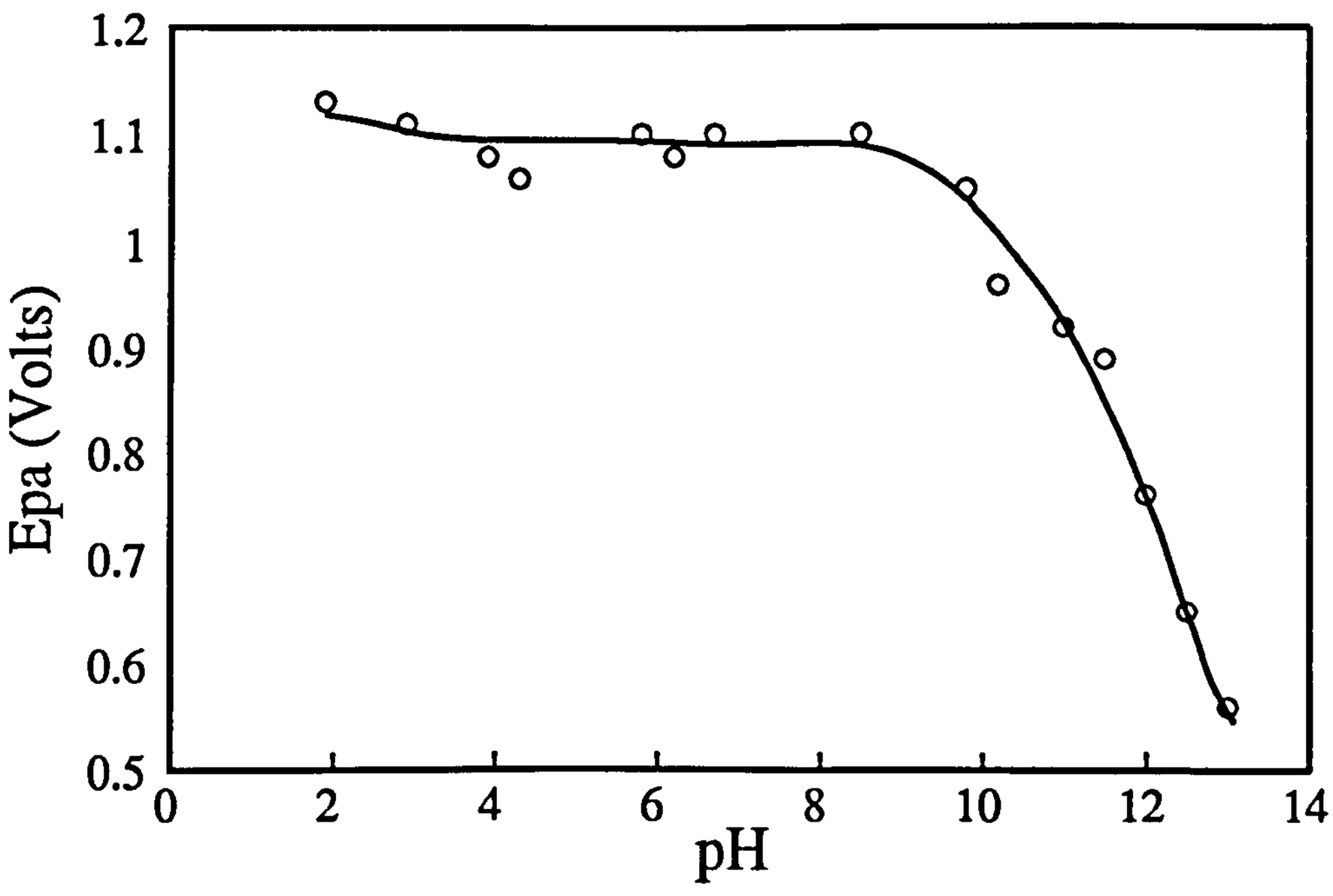

Fig. 20. Effect of solution pH on E_{pa} of Polypyrrole toluenesulphonate.

CHAPTER 3

EXPERIMENTAL

3.1 Introduction.

This chapter describes general experimental procedures that were used throughout this thesis. Section 3.2 lists the solvents and reagents that were used. The design of the electrochemical cells that were used to prepare metallized polymer film, and conduct cyclic voltammetry measurements are described in section 3.4. The procedures used for the preparation and coating of electrodes are detailed in section 3.5 and sections 3.6. Instrumentation is described in Section 3.7. Metallized polymer film and conducting polymer composite materials were characterized using both optical and scanning electron microscopy, these methods are detailed in sections 3.8 and 3.9. The preparation of polypyrrole substrates for cyclic voltammetry studies and metallization are described in sections 3.10 and 3.11. A variety of different methods were used to prepare polymers for impregnation with polypyrrole and polyaniline prior to metallization, these are discussed in sections 3.12 and 3.14; metal deposition on coated substrates is described in section 3.15. Finally, the procedure used to conduct reflectance measurements on metallized polymer films is detailed in section 3.17. More specific descriptions of experimental procedures are contained in the relevant sections of the discussion.

3.2 Solvents and Reagents.

All solvents and reagents were supplied by either British Drug Houses (B.D.H), or Aldrich Chemical Co Ltd. These were of Analar grade and were used as received unless otherwise stated. Electrolytes, and solvents that were used to coat polymer films onto electrode surfaces were dried prior to use using the following procedures.

p-Toluene sulphonic acid monohydrate (98%) was slowly recrystallised twice from hot toluene. The filtered product was dried under dynamic vacuum at 40°C and stored under nitrogen in a desiccating jar. Potassium nitrate was dried and stored in an oven which was maintained at 60°C to keep dry. Tetraethylammonium tetrafluoroborate ($TEABF_4$) and tetrabutylammonium tetrafluoroborate ($TBABF_4$) were used as received and were periodically dried under vacuo at 50°C. Silver fluoroborate

was stored under nitrogen since it is unstable to oxidation, and silver perchlorate was stored at 0°C.

Ethyl acetate was dried over anhydrous potassium carbonate, filtered and freshly distilled, with the second fraction being collected at 75°C. Acetonitrile, (Fisons freeze dried distilled grade) was used as received. Methanol was dried over anhydrous magnesium sulphate, filtered, and then distilled before use. 1-2 dichloroethane was doubly distilled and collected in the temperature range 82-83°C. All solvents were stored over molecular sieve (type 4A), before use.

Oxygen free B.O.C (white spot grade) nitrogen was used throughout to thoroughly degas all solutions unless otherwise indicated. De-ionised water was used in aqueous electrochemistry, and was obtained from an Elgastat Spectrum water purifier (Elga LTD, Bucks.). Pyrrole monomer was used as received and stored in the dark under a nitrogen atmosphere at 0°C to prevent oxidation.

3.3 Polymers.

A number of different polymer films were selected for plating trials. The materials which were tested included both free standing and solvent cast films. A list is given below.

Poly(vinylidene fluoride-trifluoroethylene) copolymer (60-40) $P(VF_2/VF_3)$ and 9 μm thick polyvinylidene fluoride (PVDF) plastic film were supplied by GEC Marconi, PVC (chromatographic grade, unplasticized) was obtained from Polysciences, and copolymethylmethacrylate/butylacrylate (polyacrylate) was supplied by 3M Co.

3.4 Electrochemical Cells.

Two different types of electrochemical cell were used throughout the work in this thesis. These were a general purpose, single compartment cell that was used to prepare 4.9 cm^2 discs of metallized polymer films, and also free standing films of polypyrrole. The second cell was a smaller single compartment cell that was used for cyclic voltammetry studies. Each of these cells is discussed below.

3.4.1 General Purpose Cell.

This was designed for use in conjunction with an external rotating disc electrode system (RDE), (Thompson Electrochem Ltd), for the preparation of 4.9 cm^2 discs of metallized plastic film under an inert atmosphere. Preliminary studies had shown that in order to achieve uniform metal deposition into the film, close contact between the film and the metal surface was vital. This was achieved by securing the film in place with a close fitting collar placed over the edge of the electrode. A schematic diagram of the electrochemical cell and electrode assembly is shown in Fig. 21.

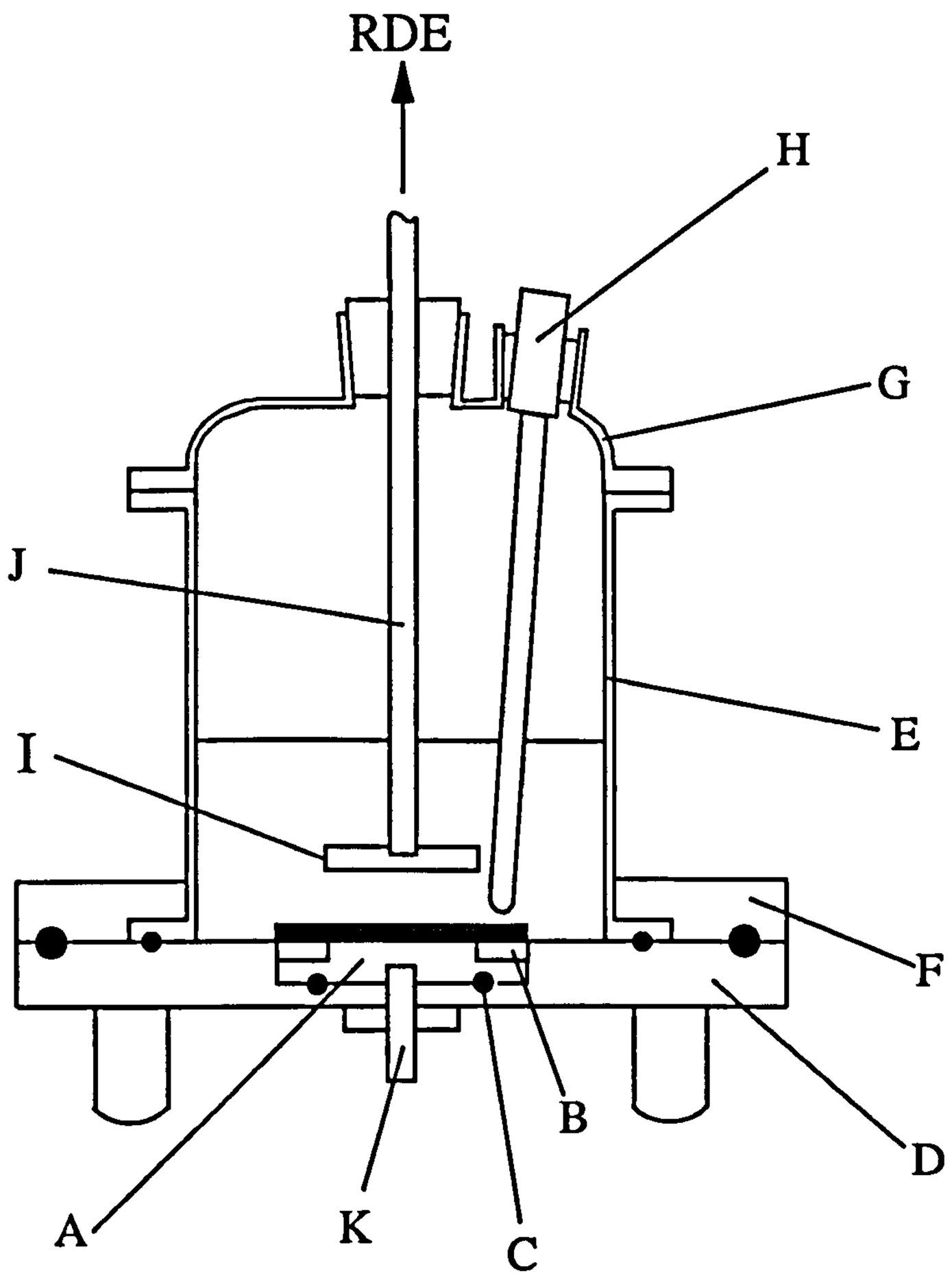

Fig. 21. General purpose electrochemical cell as used for metallizing plastic films and also for the preparation of free standing polypyrrole films.

The working electrode (A) was a type 316 stainless steel disc recessed to contain a close fitting PTFE collar (B), and a neoprene rubber 'O' ring seal (C). The plastic collar was used to maintain close contact of preformed commercial films to the electrode surface throughout electrolysis. The electrode was mounted to fit flush in a poly(propylene) base plate (D). The glass parts of the cell were made from borosilicate (Pyrex) glass by Wesley Co Wingents Ltd, Cambridge. These consisted of a glass cylindrical electrolyte vessel (E) which was mounted securely to the base plate by tightening flange plates (F). The cell lid (G) contained one central (B_{19}) glass joint which housed the rotatable counter electrode, and an off centre (B_{24}) joint which housed the reference electrode (H). This inlet also doubled as a nitrogen purge inlet. The counter electrode (I) was a 25 mm diameter type 316 stainless steel disc which screwed onto a threaded 6 mm diameter stainless steel rod, (J). This was connected to a Thompson Electrochem rotating disc electrode system (RDE). Electrical contact to the working electrode was made via a stainless steel screw (K) threaded into the reverse of the working electrode. Electrical contact to the counter electrode was via the RDE system which was connected internally to the autostat.

For experiments which were conducted under a nitrogen atmosphere, the cell was made air tight by mounting the saturated calomel reference electrode (SCE) in a B_{24} cone glass joint with heat shrink sleeving, and inserting the counter electrode through a conical thermometer gland. The reference electrode was inserted through a rubber seal for the same reasons. The flanges of the cell lid were lightly greased before use.

3.4.2 Cyclic Voltammetry Cell.

Cyclic voltammetry was performed in a single compartment (100 cm^3) glass electrochemical cell. This was sealed with parafilm "M" (Aldrich Chemical Company) to provide an air tight seal.

3.5 Preparation of Electrodes.

This section details the preparation of stainless steel and graphite electrodes that were used for cyclic voltammetry and metallization experiments.

3.5.1 Stainless Steel Electrodes.

Stainless steel was chosen as an electrode material to study the deposition of metal into polymer films for the reasons described in section 8.2.3. It was also used to prepare free standing polypyrrole films, since previous work[93] had shown that it was resistant to oxidation at anodic potentials in the presence of chloride ions[93].

In order to obtain highly reflective metal deposits, it was essential that the stainless steel working electrode (WE) was highly polished and free of grease before being coated with polymer solution. This was achieved using the following procedure.

The electrode surface was polished to a 1 μm finish by first roughly polishing with 1200 grade grit paper, and then successively with 6 μm and 1 μm diamond paste smeared onto Hyprocel paper and cloth surfaces (Engis Ltd, Maidstone, Kent). Care was taken to clean the electrode surface before changing to a finer grade of abrasive, by first washing with detergent, followed by ultrasonic cleaning for approximately 1 minute in water in order to remove any remaining diamond paste. The electrode was finally rinsed in deionised water and dried under a steam of warm air.

The counter electrode (CE) was stainless steel and was cleaned prior to use by scouring with 1200 grit paper, this was then thoroughly rinsed and dried before use.

3.5.2 Graphite Electrodes.

Graphite carbon (GC) electrodes were used for cyclic voltammetry studies as supports for polypyrrole films. The working electrode (area 0.28 cm^2) was an 8 cm vitreous carbon rod (Ultra 'F' purity carbon, Johnson Matthey), fitted with an epoxide bonded polypropylene sleeve (2 mm wall thickness). This was prepared prior to use using an analogous procedure to that described for the preparation of stainless steel electrodes.

The counter electrode was a 10 cm carbon rod. This was cleaned by abrading with well worn 1200 grit paper, and then thoroughly rinsed with distilled water prior to use.

3.5.3 Reference Electrodes.

A standard saturated calomel reference electrode (SCE) (Russell pH Ltd) was used for all measurements unless otherwise specified. This was filled and stored in 3.8 M KCl when not in use. A copper wire/copper sulphate reference electrode, with a potential of +0.077 V with respect to the calomel reference, was used in instances where the electrolyte solution contained Cu^{2+} ions, in which a SCE is poisoned. This was stored in saturated $CuSO_4$ when not in use. A silver wire quasi-reference electrode was used for measurements in non-aqueous solvent systems to avoid problems of precipitation in the fritted junction, and the introduction of unstable junction potentials[177]. This type of electrode has been widely used in acetonitrile in conjunction with silver nitrate or silver perchlorate and exhibits rapid and reversible electrode kinetics[177]. The electrode potential is +0.30 V relative to the SCE[178].

3.5.4 Placements of Electrodes Within the Cell.

Care was taken regarding the placement of the electrodes within the electrochemical cells. The working and counter electrodes were kept parallel to each other to ensure a uniform current distribution at the surface of the WE[179]. The distance of separation of electrodes was about 6 mm. The tip of the reference electrode was sited as close as possible to the WE in order to minimise ohmic resistance of the electrolyte solution[179].

3.6 Preparation of Polymer Films.

Electrode surfaces were coated with polymer film substrates in one of two ways depending on whether the films were free-standing or cast from solution.

Preformed films such as commercial PVDF or poly(ethylene) were degreased with either 1-2 dichloroethane or petroleum ether, before being mounted on the electrode.

Solution cast films were prepared by the dropwise addition of approximately 10% wt./vol. polymer solution onto the surface of a stainless steel electrode, followed by evaporation. To achieve a uniform thickness of cast film, the rate of evaporation of solvent was controlled by placing the coated electrode in a glass container, this also served to protect the drying film from dust. Finally, to ensure complete evaporation, films were heated for a further 30 minutes under an infra-red lamp.

In order maintain a standard polymer film thickness for plating, the thickness of the polymer coat was measured prior to use with a graduated dark field microscope by focusing on the upper and lower surfaces of the films. Plated film thicknesses were obtained from micrographs of cross-sections.

Solution cast polymer films were also used as substrates in the preparation of conducting polymer composite materials, (described in chapter 7). The procedure that was used for preparation was identical to that which was used to coat stainless steel electrodes.

3.7 Electrochemical Measurements.

All electrochemical measurements except that detailed in section 3.7.1, were carried out using a Thompson electrochemical autostat, model (253), interfaced to a BBC microcomputer. Output from the experiments was displayed on VDU or a Yokogawa PL1000, X-Y plotter. A schematic of the electrochemical set up is shown in Fig. 22.

Cyclic voltammetry was performed with software supplied from Thompson Electrochem Ltd, but which had been adapted to enable more rapid data acquisition at higher scan speeds. Software for constant potential electrolysis and chrono-amperometric experiments was custom written to enable automatic control of data acquisition and analysis.

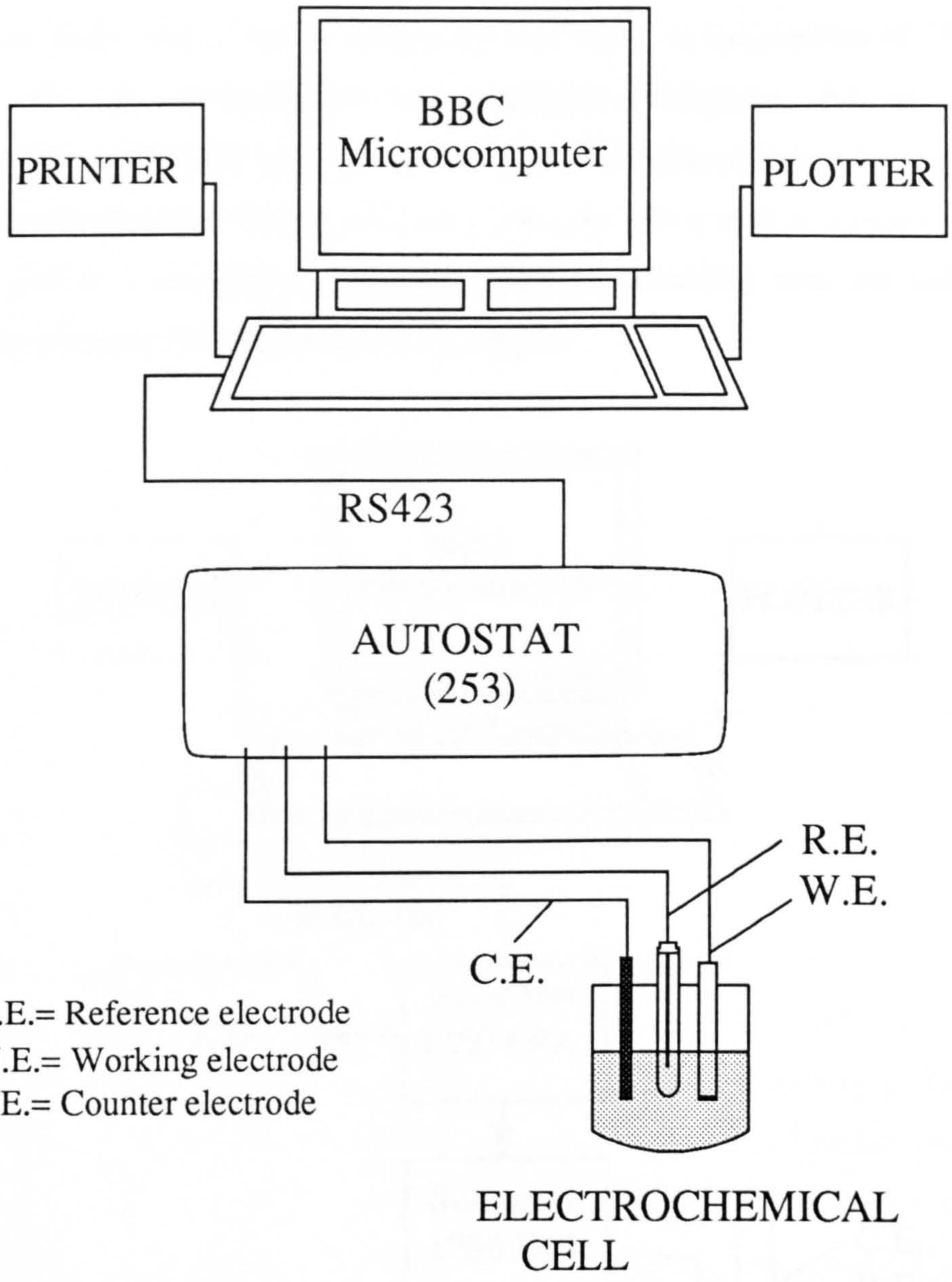

Fig. 22. Schematic representation of the electrochemical system that was used for cyclic voltammetry studies in chapter 5, and for the metallization of plastic films in chapter 7.

3.7.1 AC-Impedance Measurements.

The system used to obtain ac impedance data is shown schematically in Fig. (23). AC impedance measurements at the electrode/silver/polymer interface were performed using a Solartron 1286 electrochemical interface coupled to a Solartron

1250 frequency analyzer. The ac potential applied to the disc (potentiostatted at 0.0 V *vs*. SCE) was a 10 mV amplitude sine wave, at frequencies of 100 mHz to 65 kHz. Full IR compensation was employed throughout. All ac impedance measurements were made in the presence of 0.1 M tetrabutylammonium perchlorate in methanol/acetonitrile (90:10 vol./vol.) with no electroactive species present in solution, and at a temperature of 25°C. Prior to recording data the solution was thoroughly purged with prepurified BOC argon.

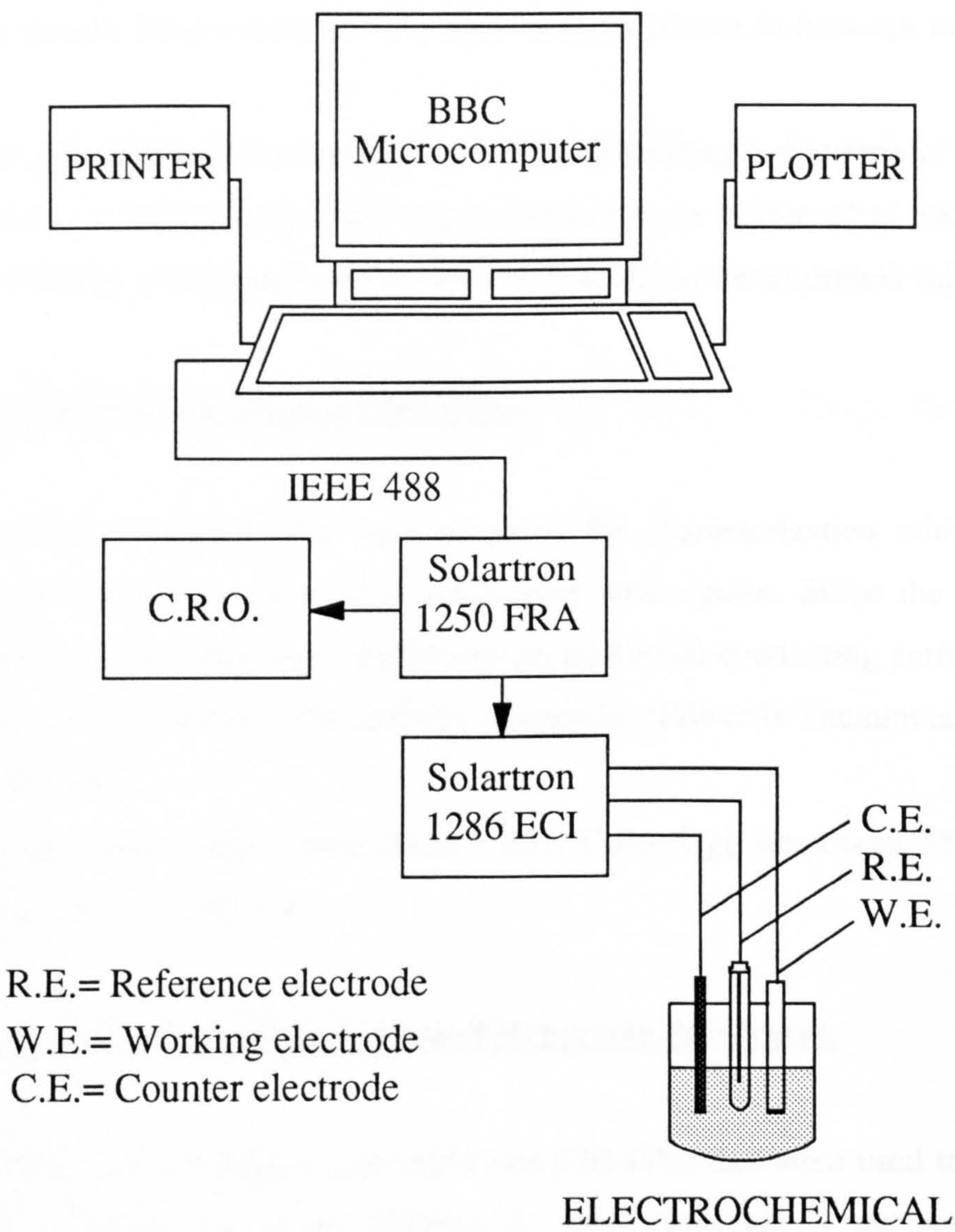

Fig. 23. Schematic representation of the electrochemical system employed for ac impedance measurements.

3.8 Optical Microscopy.

Optical microscopy proved a useful technique in determining both the surface and cross-sectional morphologies of metallized polymer films.

Micrographs of surfaces of metallized film were obtained by cutting approximately 6 mm square sections of film, and then mounting these on a glass slide with the metal layer facing upwards. To obtain sharp images it was found necessary to keep the film and slide surfaces in close contact. This was achieved by the action of surface tension from a drop of iso-propanol/water placed in between the film and slide.

Cross-sections of films were obtained by embedding a thin strip of the coated plastic film in a cold setting "SW" type polyester resin before ultra micro-toming (Riechert OMU3). Photographs were taken with a Nikon metallurgical microscope.

3.9 Scanning Electron Microscopy (SEM).

Sections of coated film were prepared for characterization with SEM by mounting on aluminium stubs with conducting silver paste. Since the embedded cross-sections of film were non-conducting, an additional conducting surface coat of graphite was evaporated onto the surfaces of samples (Edwards Vacuum coater) prior to use in the SEM.

Electron micrographs were taken with a Cambridge stereoscan 250 Mk (III) scanning electron microscope.

3.10 Preparation of Graphite Carbon-Polypyrrole Substrates.

Graphite carbon-polypyrrole substrates (GC-PPy) that were used to study the deposition of copper and silver (Chapter 5), were prepared by the potentiostatic deposition of polypyrrole from a 50 cm^3 aqueous solution containing ($6x10^{-2}$ M) pyrrole and (10^{-1} M) supporting electrolyte. An appropriate electrolyte was chosen in order to maintain a common anion between that incorporated in polypyrrole during

polymerization, and that of the metal being deposited. Sulphuric acid and potassium nitrate were used for the deposition of copper and silver from their respective sulphate and nitrate salts. Sodium sulphate was also tried as a possible source of sulphate anion, but the resultant polymer films were of inferior quality when visually inspected, and required much longer polymerization times to produce equivalent film thicknesses compared to those produced using sulphuric acid.

Oxidation was carried out at +0.75 V versus a saturated potassium chloride calomel reference electrode (SCE), in a single compartment electrochemical cell which housed the electrode assembly. The cell temperature throughout electrolysis was maintained in the range 0 to 3°C by placing the cell in an external salt/ice bath. Electrodes (WE area 0.28 cm^2) were prepared according to the procedures previously described in section 3.5.1. In all instances, the cell was left open to the atmosphere and no attempt was made to de-oxygenate solutions before use.

3.11 Cyclic Voltammetry of Graphite Carbon-Polypyrrole Electrodes.

Polypyrrole is electroactive in the same potential region as that for which the deposition and stripping reactions of copper and silver occur. Therefore, prior to recording voltammograms in solutions containing Cu^{2+} or Ag^{+} ions, the response of GC-$PPy^{+}(SO_4^{2-})$ and GC-$PPy^{+}(NO_3^{-})$ substrates was determined in 0.1 M supporting electrolyte devoid of other electroactive species.

Scans were recorded at 1.66 mVs^{-1} unless otherwise specified, on electrodes with polypyrrole coat thicknesses ranging between 0.05 and 5 μm.

Following cyclic voltammetry measurements, the current-voltage response of GC-PPy electrodes was determined in the presence of 0.01 M metal salt solutions containing (i) copper sulphate with 0.1 M H_2SO_4 background electrolyte, and (ii) silver nitrate with 0.1 M KNO_3 supporting electrolyte. Electrode potentials in copper sulphate solution were measured *vs.* a $Cu/CuSO_{4(sat)}$ reference electrode, since the SCE is poisoned in the presence of Cu(II)[177]. The potential of this electrode is +0.077 V compared to a SCE[180]. A SCE electrode was used to record all other measurements.

3.12 Preparation of Thin-Sectioned Conducting Composite Materials.

Electrochemical and chemical methods were used to prepare conducting composite films and solid plastic substrates. The composite materials were investigated as possible substrates for (i) autocatalytic (electroless copper deposition) from copper/formaldehyde based plating solutions, as described in section 6.3, (ii) the direct electrochemical deposition of copper, from copper sulphate plating solutions (section 5.3.2), and (iii) chemical deposition from solutions containing copper or silver ions (section 6.6).

3.12.1 Electrochemical Preparation.

Poly(vinylidene fluoride-trifluoroethylene copolymer 60-40, P(VF_2/VF_3), was chosen as the substrate material for electrochemical insertion, as this has previously been shown to form composite materials which possessed excellent mechanical properties and uniformity of polypyrrole content[93].

Electropolymerization was carried out at P(VF_2/VF_3) 60-40 copolymer coated stainless steel substrates (WE area 4.9 cm^2), which were prepared according to the protocol previously described in section 3.6. The electrode potential was +1.2 V *vs.* a SCE reference electrode, and the electrolyte was 0.01 M pyrrole, with 0.1 M $TBABF_4$ supporting electrolyte dissolved in 1-2 dichloroethane/acetonitrile (20:80 vol./vol.). A co-solvent system proved necessary due to the solubility of P(VF_2/VF_3) 60-40 copolymer in neat acetonitrile.

Following deposition, PPy/P(VF_2/VF_2) composite films were removed from the electrode surface and rinsed with dichloroethane/acetonitrile solution to remove excess electrolyte and unreacted monomer. These were then left to dry under ambient conditions.

3.12.2 Chemical Preparation.

Materials which were investigated as substrates for impregnation included P(VF_2/VF_3) 60-40 copolymer, PVC (Polysciences, chromatographic grade), polyvinylidene fluoride (PVDF; 9 μm thick unpolled), polyester "Cling film", polyethylene and filter paper. PVC and P(VF_2/VF_3) 60-40 copolymer films were prepared by casting from solution according to the procedure previously described in section 3.6. Film thicknesses of the cast films ranged from between 50-100 μm.

Materials were impregnated with pyrrole monomer using four different approaches, these are described below;

(i) PVC and P(VF_2/VF_3) 60-40 copolymer films were immersed in neat pyrrole monomer for 6 hours at room temperature (~20°C). After removing excess monomer from the film surface, samples were then transferred to aqueous ferric(III) chloride solution (10% wt.vol), and left to stand at room temperature, for ~24 hours.

(ii) The same experiment was repeated with another PVC membrane, except that 5% vol./vol. of tetrahydrofuran (THF), a solvent for PVC, was added to the pyrrole to swell the film.

(iii) The third method involved stoppering one end of a glass tube with sections of the above films. Neat pyrrole was then introduced into the tube so as to contact the film on one surface only. This was then immersed in ferric(III) chloride solution (10% wt./Vol.), and kept at 0°C for 24 hours. After oxidation was completed, samples were removed and rinsed with acetonitrile, with the exception of P(VF_2/VF_3) 60-40 copolymer films which were rinsed with 1-2 dichloroethane/acetonitrile (20:80 vol./vol.). These were then left to stand under ambient conditions to dry, before making conductivity measurements. This method is illustrated in Fig. 24.

(iv) The final method of preparing composite materials was similar to a technique described by Bjorklund and Lundstrom[136]. Filter paper was impregnated with aqueous metal salt solutions of either 2 M $CuNO_3$ or $CuClO_4$, and then contacted with neat pyrrole monomer at room temperature. A dark precipitate of polypyrrole was immediately formed on contact. Samples were then removed and left to dry for between 12 and 24 hours under ambient conditions.

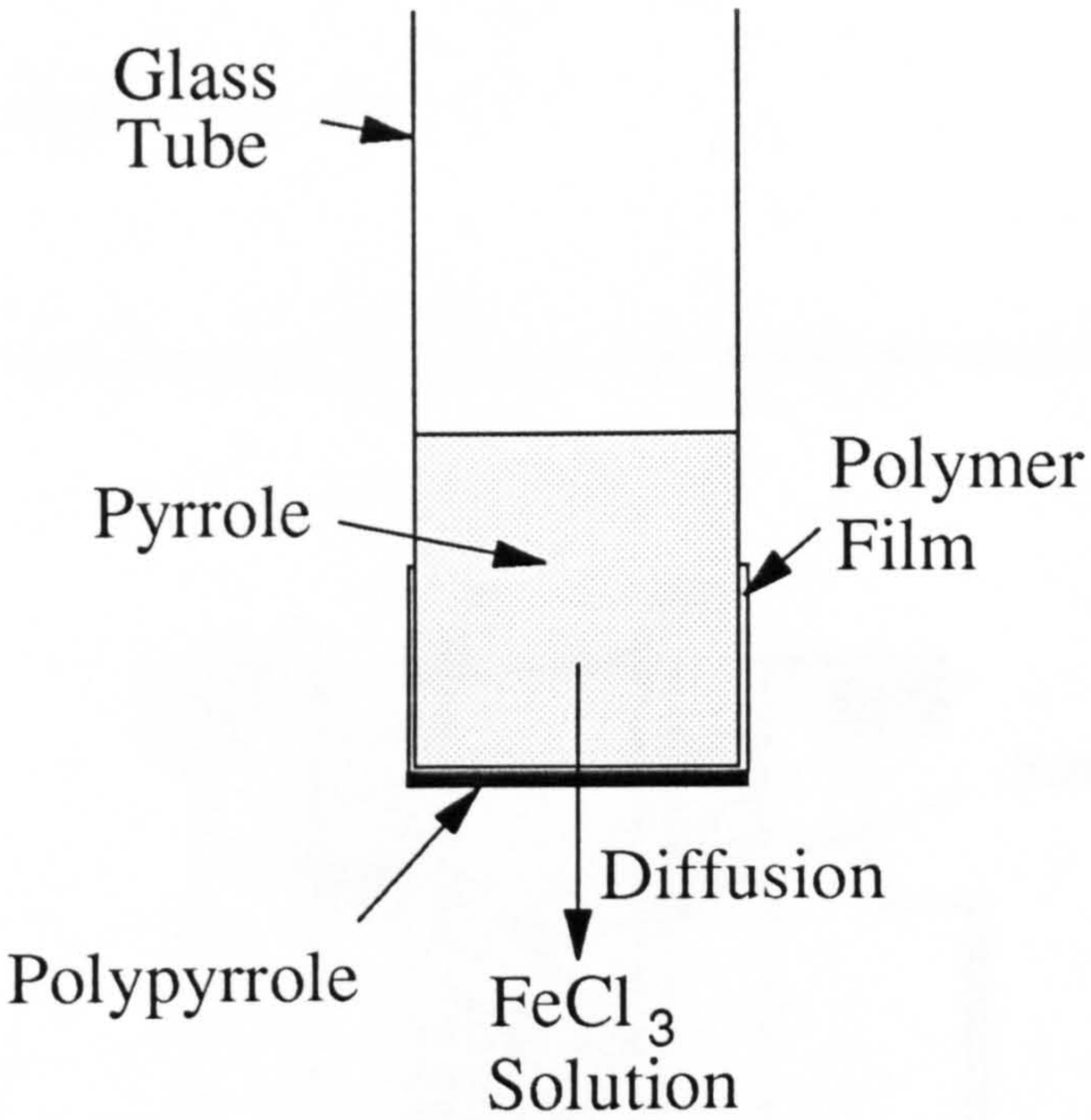

Fig. 24. Illustration of the method used in section 3.12.2(iii) for the impregnation of plastic films with polypyrrole.

3.13 Conductance Measurements.

The effectiveness of electrochemical and chemical methods of preparing composite materials was determined by measuring the electrical conductivity of coated samples.

Measurements were performed with the apparatus shown in Figs. 25 and 26. This consisted of a DC power source, a sample holder, and two digital multimeters for current and voltage measurements. The arrangement is multipurpose and was

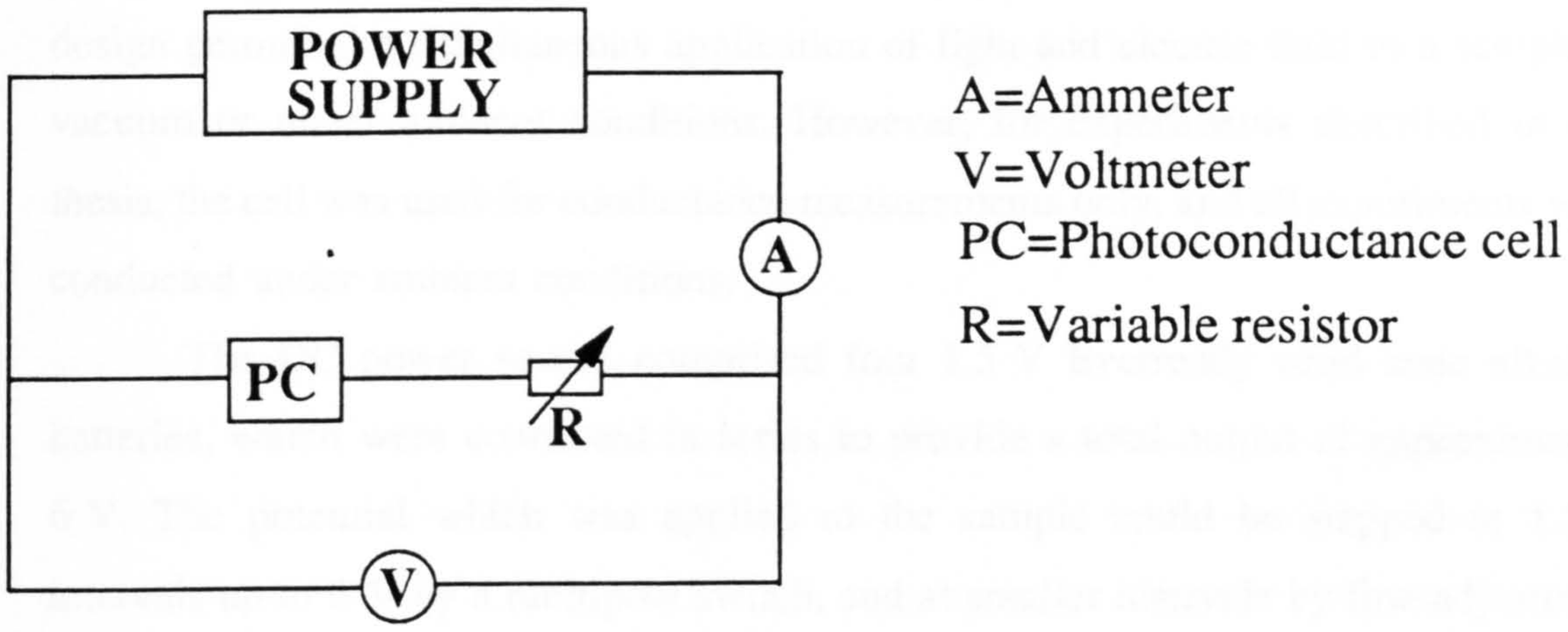

Fig. 25. Schematic representation of the circuit used to measure the conductivity of polypyrrole composite films.

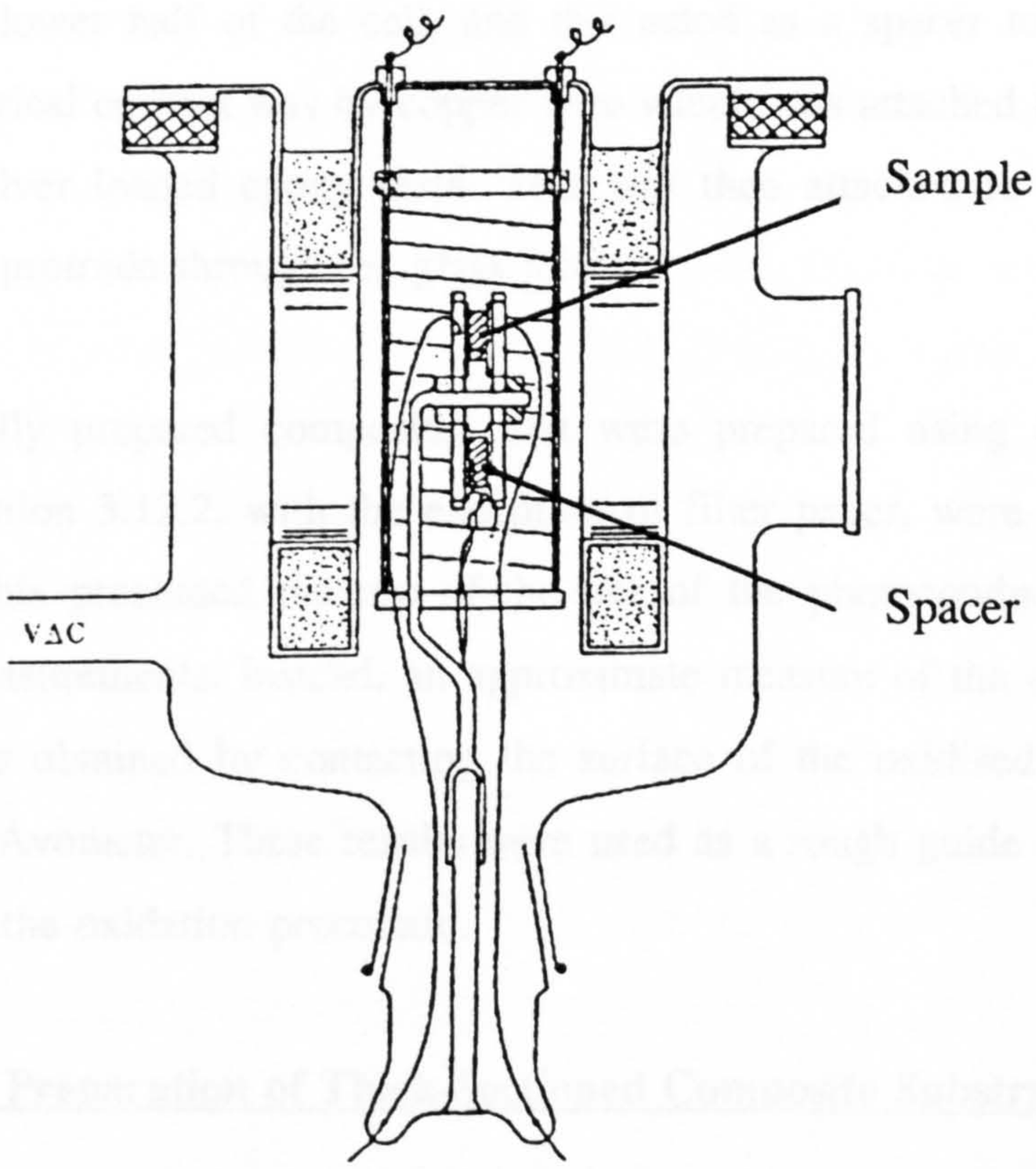

Fig. 26. Schematic representation of the photoconductance cell as used for measuring the conductivity of polypyrrole composite films.

constructed by previous workers[181] for photoconductance measurements. The cell design permits the simultaneous application of light and electric field to a sample in vacuum or under ambient conditions. However, for experiments described in this thesis, the cell was used for conductance measurements only, and all experiments were conducted under ambient conditions.

The DC power source comprised four 1.5 V Everready solid state alkaline batteries, which were connected in series to provide a total output of approximately 6 V. The potential which was applied to the sample could be stepped at 1.5 V intervals up to 6 V by a multipole switch, and at smaller intervals by fine adjustment of the variable resistor connected in series with sample holder arrangement.

Measurements were made on approximately 6 mm square sections of PPy/P(VF_2/VF_3) film, which were mounted in the upper half of the sample holder between two gold plated quartz glass slides. A similarly sized sample was also inserted in the lower half of the cell, and this acted as a spacer to prevent short circuiting. Electrical contact was by copper wire which was attached to the edges of the slides by silver loaded epoxy resin. This was then attached to tungsten feed-throughs which protrude through the glass joints.

Chemically prepared composites that were prepared using the techniques described in section 3.12.2, with the exception of filter paper, were coated on one surface only. This precluded the use of the use of the photoconductance cell for conductivity measurements. Instead, an approximate measure of the conductivity of the samples was obtained by contacting the surface of the oxidised film with the terminals of an Avometer. These results were used as a rough guide only, as to the effectiveness of the oxidation procedure.

3.14 Chemical Preparation of Thick-Sectioned Composite Substrates.

The thicker cross-section of solid plastic objects precludes the use of electrochemical preparation, since polymerization times will be prohibitively long. Consequently, this necessitates the use of chemical methods of preparation.

This section details the methods that were used to prepare solid plastic substrate materials. Polyethylene and nylon substrate materials were chosen in order to investigate the applicability of this technique, as method of preparing both hydrophobic and hydrophillic conducting composite materials.

Ferric(III) chloride solution was primarily used as the oxidant for pyrrole and aniline impregnated substrates, since this is a common choice for the oxidation of pyrrole (see Table 3), and yields polypyrrole impregnated composites with conductivities comparable to that obtained using electrochemical methods[140]. Acidified ammonium persulphate[182] and copper(II) salts[127] were also investigated.

3.14.1 Polyethylene Co-axial Cable.

Polyethylene co-axial cable substrates were prepared for impregnation by removing the outer protective plastic sheath, and then stripping off the copper braiding from the surface. The inner core of copper wire was not removed so as to restrict monomer permeation to the outer surface of the cable only. Stripped samples were then cut to approximate 25 mm lengths before ultrasonic cleaning in petroleum spirit 60-80. These were then immersed in either neat pyrrole or aniline monomer and heated to 100°C for up to 30 minutes. After impregnation, excess monomer was removed from the surface by rinsing in de-ionised water.

Chemical oxidation was carried out at 0°C and 20°C in both aqueous ferric(III) chloride solution (25% wt./vol.), and also with acidified ammonium persulphate solution (5% wt.vol.). Solutions of copper(II) nitrate and copper (II) perchlorate (25% wt./vol.) were also tried (after ref.[127]), but did not effect polymerization.

3.14.2 Nylon-6, Nylon-12, and Polyethylene.

Plastic samples of nylon 6 (Nivionplast polyamide 6, 403 W High viscosity), nylon 12 (Rislan) and polyethylene (AR1057, ICI) were prepared according to the following procedure. Workable sized samples were first cut to approximate size from larger areas of material. These were then polished to remove scratches using 1200

grade grit paper and 6 μm diamond paste. All samples were then thoroughly cleaned with detergent, rinsed with warm water, and finally cleaned in an ultrasonic bath containing petroleum spirit 60-80° for 30 minutes. This ensured surface were free of contamination by grease. Cleaned samples were then left to dry for a minimum of 24 hours in a desiccating jar which was maintained at 50°C. After drying, the weights and dimensions were accurately measured with a five figure analytical balance and micrometer.

Impregnation with monomer was effected under a nitrogen atmosphere, at temperatures in between 10 and 90°C, for up to 60 minutes. Neat monomer was also purged with nitrogen prior to heating as both pyrrole and aniline are unstable to atmospheric oxidation. After impregnation, samples were wiped with absorbent tissue and then reweighed to determine the amount of monomer which was absorbed.

Chemical oxidation of pyrrole was carried out at 0°C and 20°C by immersion in aqueous ferric(III) chloride solution (25% wt./vol.) for 24 hours with occasional stirring. The resultant coated substrate materials were then washed thoroughly with de-ionised water, followed by acetone, and dried under a stream of N_2. These were then left to stand for a further 24 hours under a nitrogen atmosphere at 50°C before reweighing.

3.15 Metal Deposition on Coated Substrates.

3.15.1 Polyethylene Co-axial Cable.

Copper deposition on polypyrrole and polyaniline coated co-axial cable was carried out in an aqueous copper sulphate bath containing 4g $CuSO_4.5H_2O$ and 10g concentrated H_2SO_4 at 20°C. The coated co-axial cable was the cathode, and this was connected to two 1.5 V Everready batteries connected in series via crocodile clips. The counter electrode was a copper anode.

3.16. Metal Deposition on Free-Standing Polypyrrole Films.

Free standing films of polypyrrole (~20 μm thick) were metallized using electrochemical methods. These methods are described in the following sections.

3.16.1 Electrochemical Metallization.

After preparation, samples were thoroughly rinsing with de-ionised water to remove any remaining pyrrole or electrolyte. The films were then transferred to a single compartment electrochemical cell containing 0.32 M $CuSO_4.5H_2O$, 2 M H_2SO_4 supporting electrolyte, and 10^{-4} M sodium 3-mercaptopropane-1-sulphonic acid. This was added to increase the brightness of the deposit, since copper plating solutions do not yield reflective deposits without additives.

Copper deposition was carried out at -0.9 V (*vs.* $Cu/CuSO_4$ ref.). By adjusting the position of the polypyrrole film relative to the cathode, highly reflective and cohesive deposits were formed on the smooth surface of the polypyrrole film.

3.16.2 Chemical Metallization.

Two methods were used to chemically metallize polypyrrole. These were autocatalytic or electroless deposition from copper formaldehyde based electroless plating solutions, and the chemical oxidation of base treated polypyrrole films with metal salt solutions of copper and silver ions.

3.16.2.1 Autocatalytic (Electroless) Copper Deposition.

After preparation, samples were transferred to a conventional formaldehyde based electroless plating solution, which comprised;

100 cm^3 H_2O (deionised)

(0.02 M) Copper(II) sulphate, $CuSO_4.5H_2O$

(0.089 M) Sodium potassium tartrate, $KNaC_4H_4O_6.4H_2O$

(0.18 M) Sodium hydroxide, NaOH

(0.12 M) Formaldehyde, HCHO, 37%

The addition of other reagents such as brightening agents and bath stabilizers was avoided, because the effects of these are difficult to predict. Also, unless the reaction conditions are specially optimized, metal deposition can be seriously retarded, or even inhibited by the addition of inappropriate quantities of additive. Samples were immersed until deposition was observed, or until the plating solution decomposed.

3.16.2.2 The Chemical Oxidation of Base Treated Polypyrrole.

Base treated polypyrrole films were metallised by immersion in solutions containing Cu^{2+} and Ag^{+}. Several different systems were tried in order to find an optimum plating solution. The composition of these solutions is given below.

$[Cu(II)(H_2O)_6]^{2+}$ was prepared by dissolving 2g of $CuSO_4.5H_2O$ in 50 cm^3 of distilled water.

$[Cu(II)(NH_3)_4]^{2+}$ was prepared by adding excess NH_4OH (conc) solution to 50 cm^3 of 0.16 M $CuSO_4$ solution until the precipitate of $Cu(OH)_2$ dissolved.

$[Cu(II)(EDTA)]^{2-}$ was prepared by adding 1.75g of EDTA to 50 cm^3 of 0.12 M $CuSO_4$ solution, (EDTA = ethylenediaminetetraacetic acid $(HO_2CCH_2)_2NCH_2CH_2N(CH_2CO_2H)_2$).

The oxidation of base treated polypyrrole by Ag^{+} was carried out using ammoniacal silver nitrate solution at 50°C. This was prepared by adding excess NH_4OH (conc) solution to 50 cm^3 of 0.16 M $AgNO_3$ until the precipitate of Ag_2O dissolved.

3.17 Reflectance Measurements.

In order to obtain a more quantitative measure of the quality of metallized samples, reflectance measurements were carried out using the configuration shown in Fig. 27.

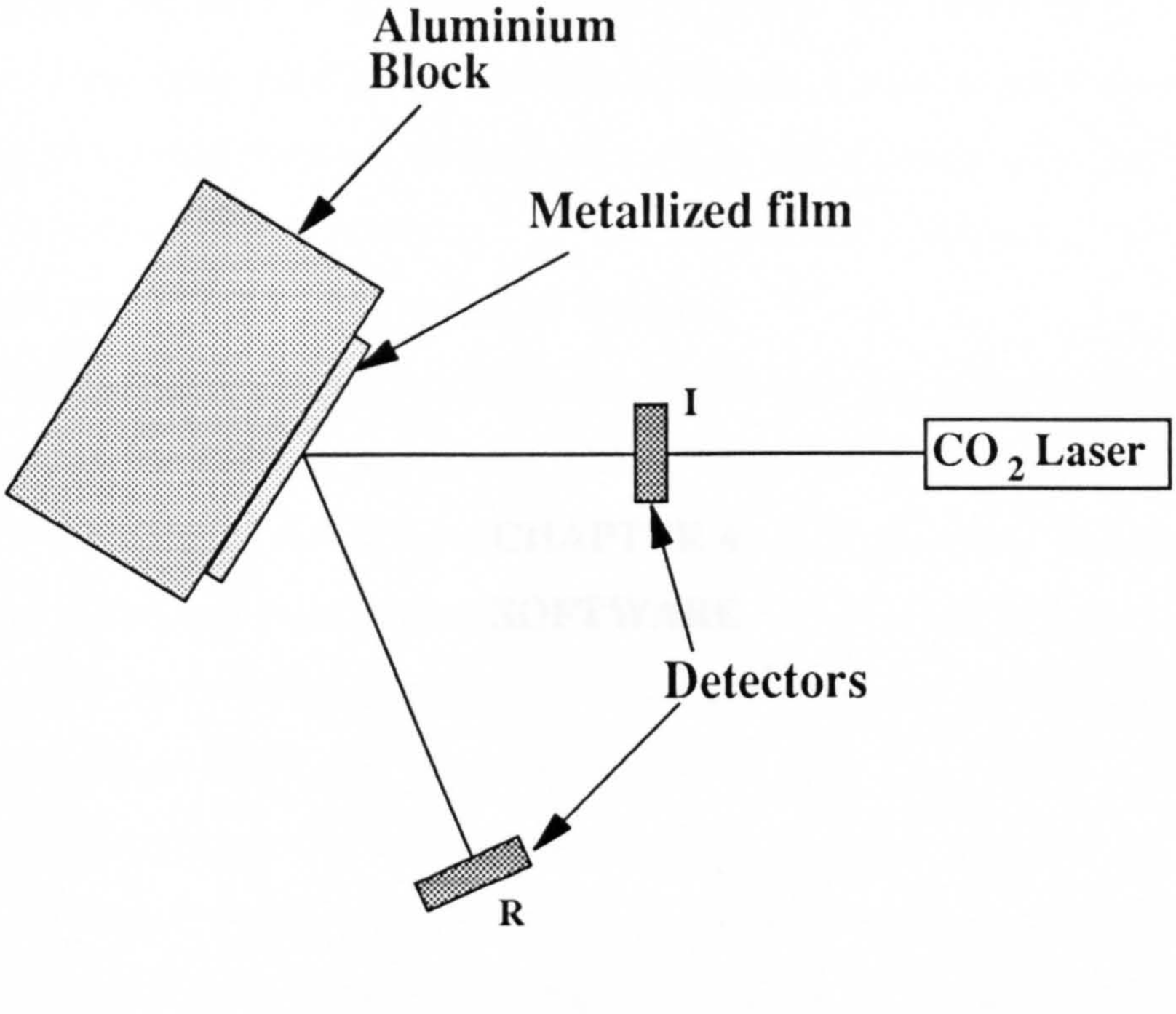

Fig. 27. Schematic representation of the optical system used to measure the reflectivity of silver coated $P(VF_2/VF_3)$ 60-40 copolymer films.

A silvered film was attached to an aluminium heat sink using silicon grease. This was then irradiated using a 2.6 W CO_2 laser at a wavelength of 10.6 μm. The incident and reflected powers, I and R, were measured using a calorimeter type laser power probe. The reflectivity was then calculated from an average of several measurements taken at different places over the surface of the film.

CHAPTER 4
SOFTWARE

4.1 Introduction.

As mentioned in section 1.6, one of the major benefits of electrochemical methods of preparing composite materials, is the ability to accurately control the thickness of deposits using coulometry. This is most conveniently carried out using computer control, since it permits rapid and accurate acquisition of data, facilitates data processing once tests are completed, and saves a considerable amount of time compared to manual methods of data acquisition and analysis. For these reasons, a significant part of the experimental procedure was the preparation of a computer program to enable coulometry and data analysis.

The following chapter describes software which was custom written to enable automatic control of data acquisition and analysis on the Thompson Electrochem autostat. "Coulometry" is a program which records current versus time data, in order to obtain a direct and reliable measure of the amount of metal which was deposited during controlled potential electrolysis. Data can then be processed using the data analysis programs, "Data-lister" and "Multiplot".

Cyclic voltammetry was performed using software supplied by Thompson Electrochem Ltd, but which was adapted to enable more rapid data acquisition at high scan rates, and display current-voltage data with the electrode potential along the abscissa. Programs were written in BBC BASIC for use on either BBC "B" or "Master" series microcomputers.

4.2 Data Acquisition Programs.

4.2.1 Coulometry.

"Coulometry" is a data acquisition program which measures voltage and current with respect to time. The total amount of charge consumed during electrolysis is then calculated by integration of the current versus time response using trapezoidal integration. The program offers a choice of selecting either time, or the amount of coulombs passed for determining the duration of the experiment. If the time control

option is chosen, current and voltage are recorded versus time, at a fixed time interval which is input from the keyboard by the user. Integration of the current time transient can then be performed using **Data-lister**, once the program has terminated. If the coulomb control option is selected, integration is performed continuously throughout electrolysis, and the amount of charge consumed is displayed on VDU. In both of these options, data is continuously stored on disc throughout electrolysis. The maximum number of data points which can be taken during each experiment is set to 750. The main procedures contained in "coulometry" are discussed in the following section.

On start up, the title of the program which has been accessed is displayed at the top of each page. **PROCtest_autostat**, checks the status of the autostat and indicates on the VDU whether or not the autostat is set to run. This is repeated until communications with the autostat are established.

PROCSEND("Q") cancels all existing autostat control parameters and resets them to their start up values.

An experimental title is requested before the program will proceed. This is the title under which all subsequent data is stored and retrieved.

PROCcurrent_range selects the current range for the duration of the experiment. The operator has a choice of low, medium and high current ranges. Low range has a maximum output current of 32.766 μA and a resolution of 2 nA. Mid range has a maximum output of 32.76 mA and a resolution of 2 μA, and high range has a maximum output of 3 A and a resolution of 200 μA. The current range which is selected, is displayed on the VDU throughout the experiment.

PROCset_potential sets the control potential of the working electrode with respect to the reference electrode. This is limited to ± 5 V by the output of the autostat. If a control potential outside this range is requested, the command is repeated until a legitimate input is made. The input potential is then converted to millivolts, and sent to the autostat using the routine **PROCSEND("P")**. The procedure **PROCSEND("S1")** selects the voltage follower for measurement, and the potential of the working electrode is then measured and displayed on the VDU using the

routines **PROCreadpot, PROCADCV,** and **PROCget.** Values of the control potential which are different from the requested value usually indicate a loose fitting connection, or a misplacement of the reference electrode in the cell. If the fault causing the error is not located, the operator has an option to abort the experiment.

PROCexpt_cond requests the experimental conditions under which electrolysis is being carried out.

PROCdisc requests the insertion of a data disc in drive 1. Two files are created, a header file for the storage of experimental parameters and experimental conditions, and a data file which is suffixed with the letter "d", for the storage of data. If for any reason the computer is unable to create these files, the program is terminated, and the error message "Disc files not opened" is displayed on the VDU.

PROCexpt offers a choice of controlling the duration of the experiment by pressing "T", which selects the time control option, and calls **PROCtime_rtn,** or by pressing "C" which calls **PROCcoulomb** and selects coulomb control.

PROCtime_rtn measures current and voltage versus time. The duration of the experiment is input in hours and minutes and the time interval between readings is input in minutes and seconds. The total number of data points which will be taken is then calculated, if this exceeds 750, the space available for data storage in the arrays, an error message is displayed on the VDU. The user is then requested to re-enter both these parameters. On confirmation of the duration of experiment and time interval between readings, the VDU message "*Autostat Ready*" is displayed. Data collection may then be initiated by inputting "S" from the keyboard. This calls **PROCSEND("R")** which connects the cell to the autostat for current and voltage measurement, and simultaneously sets the autostat to "run" mode.

The time between readings is measured in hundredths of a second on the computer's internal clock. This is set to zero when the experiment is commenced, and also at the start of each control loop. When the time multiplied by a calibration factor, is greater than or equal to the time interval between readings input from the keyboard, current and voltage measurement is initiated, and these values, together with the time of measurement are stored on disc. The clock was calibrated versus an accurate stop clock to take into account the finite time which is needed to run the loop. The

calibration factor "cal", is then set accordingly prior to each experiment. Cal= 0.93, 0.82, 0.76, 0.66, and 0.30 for a time interval between readings of 5, 4, 3, 2, and 1 seconds respectively. For recording data at time intervals less than 1 second, a modified version of the program was used. The number of data points taken, and current versus time data are displayed continuously on the VDU while the experiment is in progress. The program is terminated once the required number of readings taken, is equal to that previously calculated. The programme can also be terminated at any stage during a cycle, without losing data by pressing "Q".

PROCcoulomb measures current and voltage versus time, at a fixed preset time interval, dt, throughout the duration of the experiment. The current integral $Q_t=\int i.dt$, is then calculated using trapezoidal integration.

PROCsum_area employs the following equation to integrate the current integral, Q_t:

$$Q_{t(j)} = Q_{t(j-1)} + dQ_t \qquad (4.1)$$

in which $Q_{t(j)}$, the value of the current integral is calculated by adding the increment of charge, dQ_t, which was accumulated over the time interval dt, to the previous value of the current integral $Q_{t(j-1)}$. The increment in charge dQ_t is calculated from,

$$dQ_t = \frac{dt(i_{(j-1)}+i_{(j)})}{2} \qquad (4.2)$$

where $i_{(j)}$ is the value of the current after j readings. When the value of $Q_{t(j)}$ is equal to or greater than the predetermined value of Q_t, the procedure for taking current and voltage measurement is terminated.

PROCend_rtn isolates the cell from the autostat, and displays the message "scan completed" on the VDU. All remaining data stored within the computer's buffer memory is then filed to disc, and both the header and data files are closed. When this is complete the message "filing completed" is displayed. After a short duration, the menu option is run to enable selection of data processing programs.

"Coulometry" is limited to data collection at time intervals of about 1 second and above. Some sections of the program were modified so that data acquisition at 0.2 seconds could be achieved. This was achieved by,

(i) Replacing real variables with integer variables where possible.

(ii) Data was stored in an array, and only filed to disc at the end of the experiment, rather than continuously throughout the experiment.

(iii) The control loop for data acquisition was considerably shortened by using more efficient routines, and by leaving out commands which are non essential to data collection, such as displaying data on the VDU.

4.3 Data Processing Programs.

4.3.1 Data Lister.

This program lists experimental details and data to the VDU, or to the printer if a hard copy is required. On entering the program, a catalogue of the data files which are stored on the disc in drive 1 is displayed. After selection of the appropriate file, data is listed/printed under the appropriate headings in columns. An option of integrating the current-time data is available once the data has been listed. This is necessary if the time option of controlling the duration of the experiment was chosen for data acquisition, since this option does not provide a readout of the amount of charge consumed during electrolysis.

4.3.2 Multiplot.

Multiplot plots autostat data on the PL1000 X-Y plotter in the form of a current versus time graph. Current versus time data can be plotted for individual data

files, or up to a maximum of fifteen data files can be plotted on the same axes for comparison. Data can be plotted on either auto-scaled axes or user-defined axes if any section of data needs to be examined in greater detail. Current can be plotted either as absolute current or current density. After plotting is complete, labels can be added to identify individual data. The major routines in "Multiplot" are discussed below.

PROCdiscstatus reports the status of the disc in drive 1, by indicating the number of unused files which are available for data storage, and the amount of bytes they contain.

PROCenter_files catalogues a list of data files in disc drive 1, and allows up to 15 files to be entered for simultaneous display on the same axis.

PROCsetup gives the option of plotting current or current density on either user-defined or auto-scaled axes.

PROCuserscales is a routine which allows any section of the current-time plot to be examined in closer detail, by defining the maximum and minimum current/time limits.

PROCset_plotter resets the PL1000 to its initial (ready) status and initialises the plotter for data transmition. Prior to operation, the plotter should be connected to the BBC via the RS423 port. Paper needs to be inserted into the plotter manually, and the user is requested to press the space bar to acknowledge that the plotter is ready. Once this has been pressed, the data transmission rate is set at 4800 baud and the paper format is set to A4.

PROCoutline draws a double border on the paper, prints the figure title, and labels the graphs axes. The file name, date of experiment, and control potential can also be plotted.

PROCdraw_x_axis and **PROCdraw_y_axis** draws and scales both of the x and y axes.

PROCplot opens both the header and data files and plots current versus time data.

PROClabel allows labels to be added to the graph after the data has been plotted. The label title is input from the keyboard and printed on the plot by pressing

the return key. In order to enable manual control of the pen, the plotter must be set to "local" mode. The position of the label can then be set using the appropriate keys on the plotter. The program is terminated by typing "999".

4.4 Summary.

In summary, controlled potential coulometry software was written for a Thompson Electrochem Autostat, in order to enable data acquisition and processing using a BBC Master microcomputer. Software supplied with the autostat for the purpose of cyclic voltammetry, was also modified to enable a faster rate of data acquisition at high scan rates, and to plot *i-E* data in the conventional manner, with the electrode potential axis as the abscissa.

CHAPTER 5

ELECTROCHEMICAL METALLIZATION OF POLYPYRROLE.

5.1 Introduction.

The electrodeposition of metal particles onto polymer films is of both theoretical and practical importance, and consequently has attracted much interest. Possible uses include electronic device applications[37,38], as well as applications in catalysis[40-46].

Several recently developed techniques which utilize polymers as substrates for metal deposition have been previously discussed in section 1.5. Of these methods, the use of conducting organic polymers as substrates show most promise, as these can be easily synthesized by both electrochemical and chemical techniques. In particular, polypyrrole would seem ideal, since it is stable, is reported to be non-porous, and exhibits rapid surface-substrate electron transfer kinetics[71,183].

In this chapter, the electrodeposition of copper and silver at graphite carbon-polypyrrole (GC-PPy) substrates will be studied using cyclic voltammetry. The deposition of these metals has previously been reported at other polymer coated electrode surfaces, but not as yet at polypyrrole. In order to interpret the electrochemical behaviour of polypyrrole in metal salt solutions, the electrochemical behaviour of GC-PPy substrates was first studied in inert electrolyte solution (section 5.3). This is followed by a discussion of the electrodeposition of copper at bare graphite electrodes (section 5.3.2), and a comparison is made with copper deposition at GC-$PPy^{+}(SO_4^{2-})$ electrodes.

The effects of copper sulphate solution on the electrochemical behaviour of polypyrrole are discussed in section 5.6. The electrodeposition of silver is also considered in section 5.8, and contrasted with that of copper.

5.2 Preparation of Graphite Carbon-Polypyrrole Substrates.

Graphite carbon-polypyrrole substrates (GC-PPy) were prepared for metal deposition studies according to the method in section 3.10

Films were prepared with thicknesses estimated to be in the range 0.05 - 10 μm, as calculated from Eqn. 5.1, by controlling the number of coulombs passed during oxidation.

$$d = \frac{Q_{form}(m_1 + x m_2)}{2 F \rho A} \qquad (5.1)$$

Where d is the film thickness, m_1 the molecular weight of a repeating pyrrole unit, m_2 the molecular weight of the dopant anion, x the weight proportion of anion in the film, *F* is Faraday's constant, ρ the estimated density of the doped polypyrrole film, and A the electrode area; The charge consumed in the formation of the film is given by,

$$Q_{form} = Q_{tot} - Q_{ox} \qquad (5.2)$$

where Q_{tot} is the total charge passed during electrolysis, and Q_{ox} is the charge associated with the electrochemical doping of the polymer. This is assumed to be equal to $z.x/Q_{tot}$, where z is the valency of the dopant anion. Typical values for the ratio of dopant anion to pyrrole moiety vary between 0.25 - 0.33 for a wide variety of univalent anions (See Table 1).

After deposition, black films of polypyrrole were visible on all working electrode (anode) surfaces, except for the 0.05 μm coat. This was semi transparent in appearance.

5.3 Cyclic Voltammetry of GC-PPy^{+}(SO_4^{2-}) Electrodes.

After preparation, graphite carbon-polypyrrole electrodes (GC-PPy) were thoroughly rinsed in distilled water to remove residual electrolyte and unreacted monomer, before being transferred to another cell for cyclic voltammetry. All measurements were performed at ambient temperature, in solutions which had been thoroughly purged with oxygen free nitrogen prior to use.

The effect of the thickness of the polypyrrole coat on the deposition of copper was investigated first, since this parameter has been shown to affect the electrochemical response of redox active species in solution[38,114]. It is reported that

thin films (< 1 μm thick) are switched to the insulating state when cycled at potentials sufficient to cause reduction, and thus inhibit electrochemistry[71], whereas thicker films (*ca.* 1 μm thick) are resistant to reduction and remain in the conducting state[114].

This section investigates the potentiodynamic response of GC-$PPy^{+}(SO_4^{2-})$ electrodes with thicknesses in the range 0.05 - 5 μm, prior to the study of the deposition of copper at the same electrodes.

5.3.1 Electrochemical Response in H_2SO_4 Background Electrolyte.

Polypyrrole is electroactive in the same potential region as that for which the deposition and stripping reactions of copper and silver occurs. Therefore, the response of substrates in 0.1 M H_2SO_4 supporting electrolyte devoid of other electroactive solution species, will be discussed prior to the cyclic voltammetry of GC-$PPy^{+}(SO_4^{2-})$ in copper sulphate solution.

Fig. 28 shows cyclic voltammograms of a 0.05 μm substrate at various scan rates between 10 and 100 mVs^{-1}.

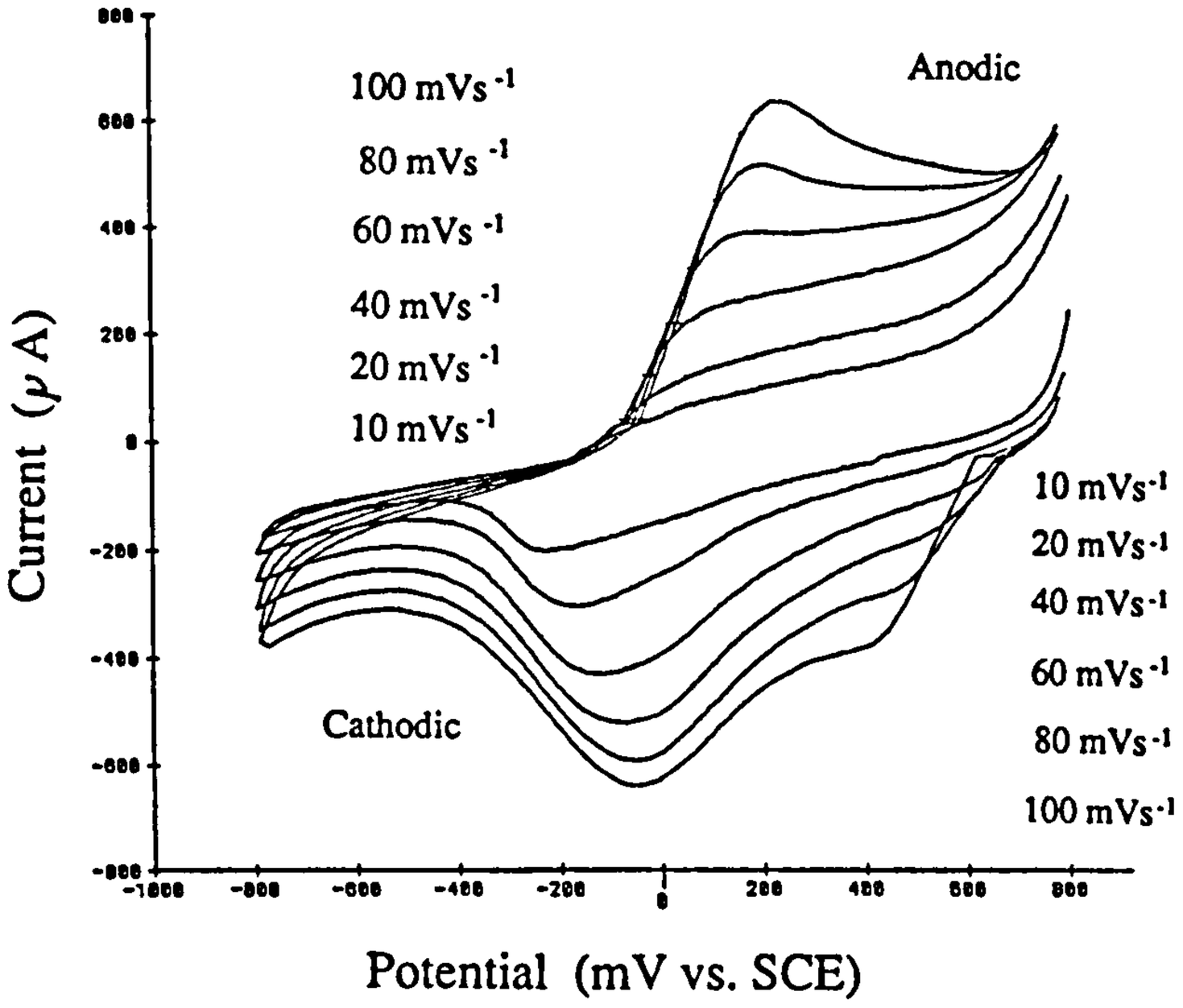

Fig. 28. Cyclic voltammograms of a 0.05 μm thick GC-$PPy^{+}(SO_4^{2-})$ electrode in 0.1 M H_2SO_4, at scan rates between 10 and 100mVs^{-1}.

Characteristic broad and non-symmetrical redox waves were observed in both the anodic and cathodic scan directions as the film was cycled between its oxidised and neutral states. These correspond to the reduction and oxidation of the delocalised π-system associated with polypyrrole[71], and extend from between +0.6 to -0.5 V, and from -0.1 to +0.6 V in the cathodic and anodic potential scan directions respectively. This response is typical of that observed previously for polypyrrole in aqueous solution[38,92,115]. The peak positions (E_p) on the anodic and cathodic scans were well defined for scan rates above 40 mVs^{-1}, but were partially obscured at lower scan rates by the high background capacitive current which was observed in the anodic potential region. The broadness of the reduction and oxidation waves, in conjunction with the large capacitive currents, makes it difficult to accurately determine peak heights (i_p) and the charges involved in the redox process. For this reason, i_p values were measured from the zero current baseline.

Fig. 29 shows the dependence of i_p values on the scan rate (v). For a reversible diffusion controlled wave, the peak current (i_p) is directly proportional to the square root of the scan rate ($v^{1/2}$), and the ratio of the peak anodic current (i_{pa}) and peak cathodic current (i_{pc}) is equal to unity and is independent of the scan rate. Conversely, for a surface localised reaction, i_p is directly proportional to v. The cathodic peak currents (i_{pc}) scale linearly with $v^{1/2}$, suggesting that the reduction process is diffusion controlled, whereas the peak anodic currents (i_{pa}) vary directly with v. The direct dependence of i_{pa} values with scan rate is indicative of a process involving surface localisation[114]. However, some degree of caution should be exercised in interpretation of this type of behaviour, since the charging current (i_c) is also directly proportional to v, so that at faster scan rates, i_c becomes relatively more important compared to i_p[184]. Thus, at high scan rates it can be difficult to distinguish the origin of the current.

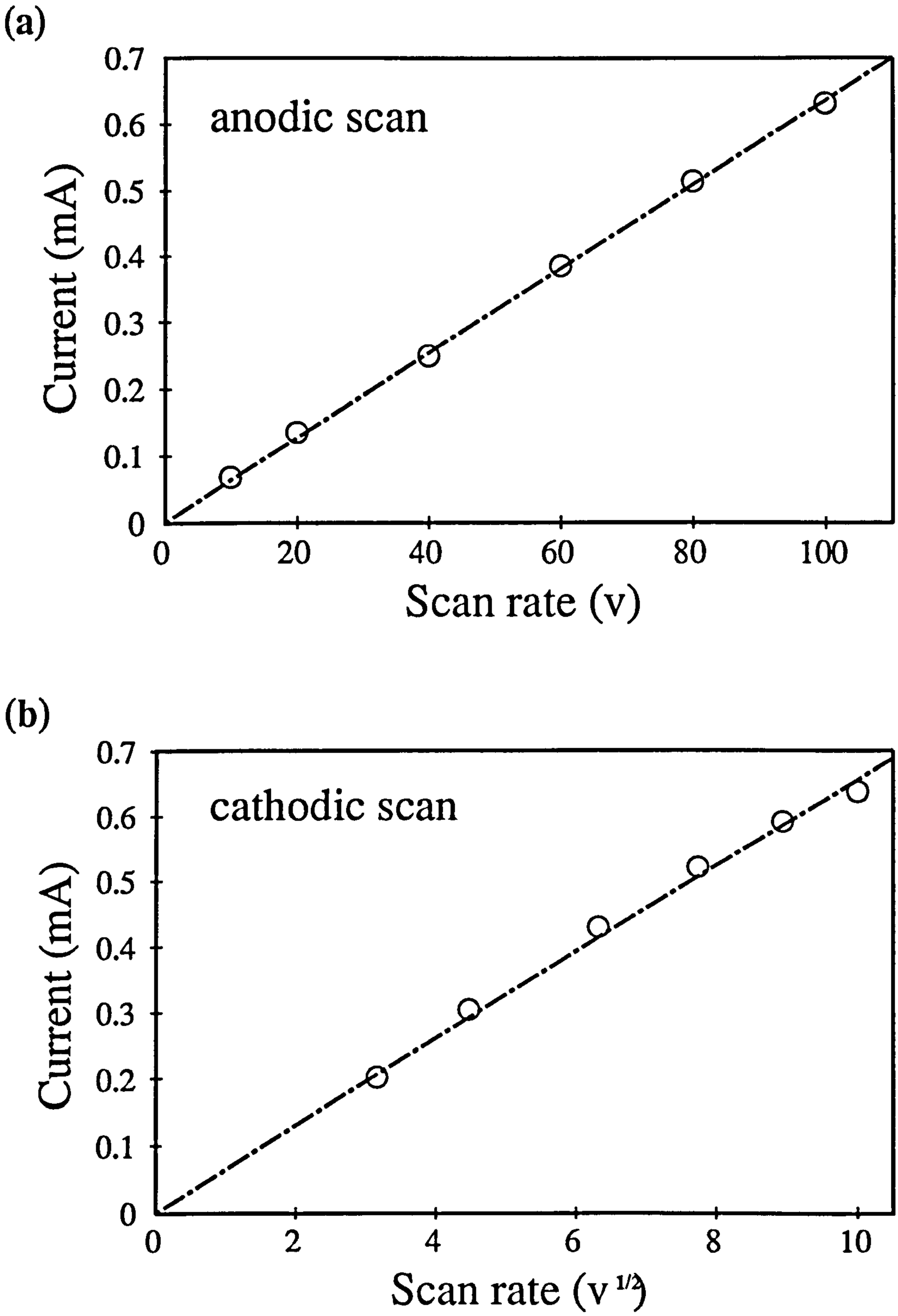

Fig. 29. Peak current values for a 0.05 μm thick GC-$PPy^{+}(SO_4^{2-})$ substrate in 0.1 M H_2SO_4 supporting electrolyte as a function of the scan rate (v). (a) anodic peak current values, (b) cathodic peak current values.

Figs. 30 shows voltammograms for the first and second scans of GC-$PPy^{+}(SO_4^{2-})$ electrodes in 0.1 M H_2SO_4 supporting electrolyte, for polypyrrole coat thicknesses ranging between 0.05 and 5 μm. Electrodes were cycled between +0.60 and -0.65 V at a scan rate of 3.33 mVs^{-1}.

As observed previously, all voltammograms exhibit broad redox waves, superimposed over the large background capacitive current which is associated with the redox processes[124]. Cathodic waves extend from between +0.10 to -0.50 V, and multiple reduction waves are apparent on the first scan on some voltammograms. These were most noticeable for films having thicknesses less than 0.5 μm and are clearly visible in Fig. 30(a) for the reduction of the 0.05 μm thick film. At thicknesses greater than this, individual waves are less easily resolved, with the less cathodic of the two reduction waves tending to appear as a shoulder on the more cathodic peak. In these instances, the more cathodic reduction peak has a maximum centred roughly between -0.35 to -0.40 V, with the less cathodic of the reduction waves exhibiting a maximum approximately +0.35 V less negative. On the second and subsequent scans only a single broad cathodic peak is observed. This extends from about +0.10 to -0.50 V, with the peak maximum centred approximately around -0.30 V. Multiple redox waves of this type have previously been reported for sulphate anions (Na_2SO_4, K_2SO_4 and Li_2SO_4) in aqueous electrolytes, and have been attributed to the divalent nature of the sulphate anion[115].

The anodic wave accompanying the re-oxidation process is less well defined than that obtained for reduction, and becomes smeared into a broad envelope at film thickness greater than about 0.25 μm. This broadening is to be expected, since ion diffusion is more rapid during the reduction of the oxidised film compared than during oxidation of the neutral film, as has been reported previously[98,112]. Except for the increased background capacitive current, the features of the voltammograms remain the same as those obtained with thinner films.

(a)

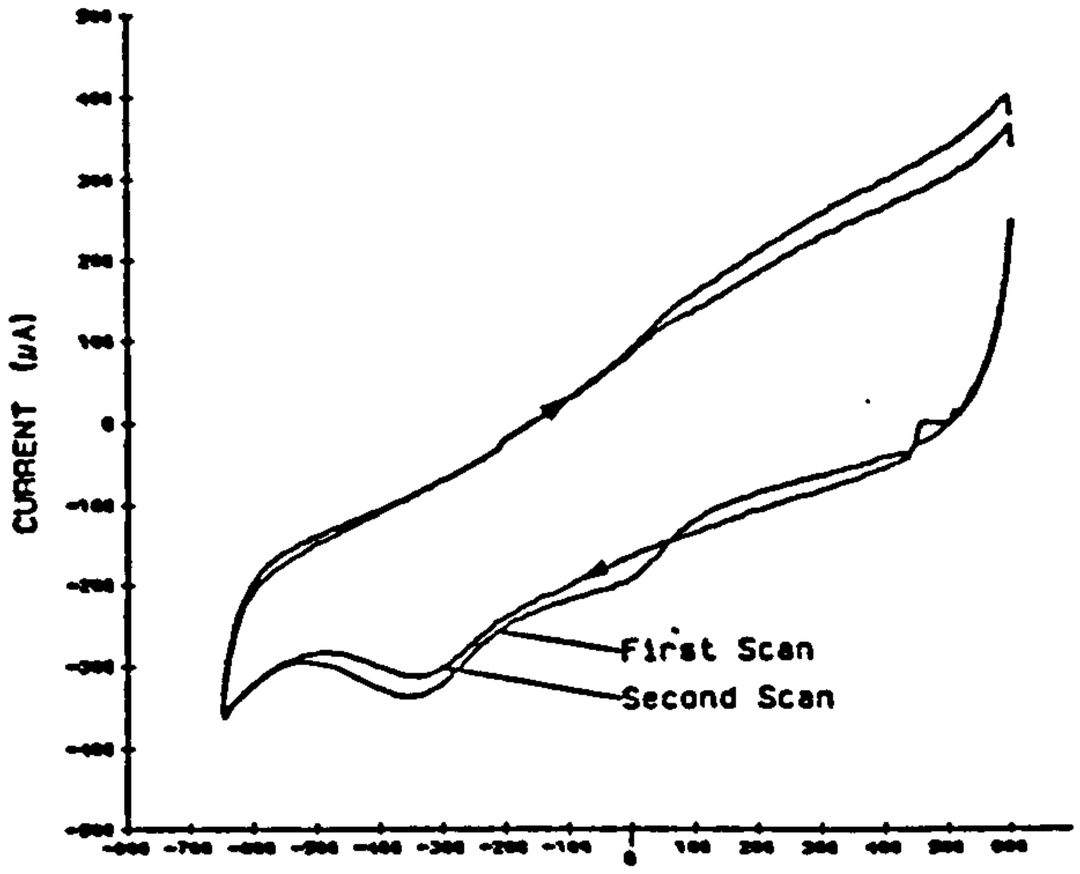

(b)

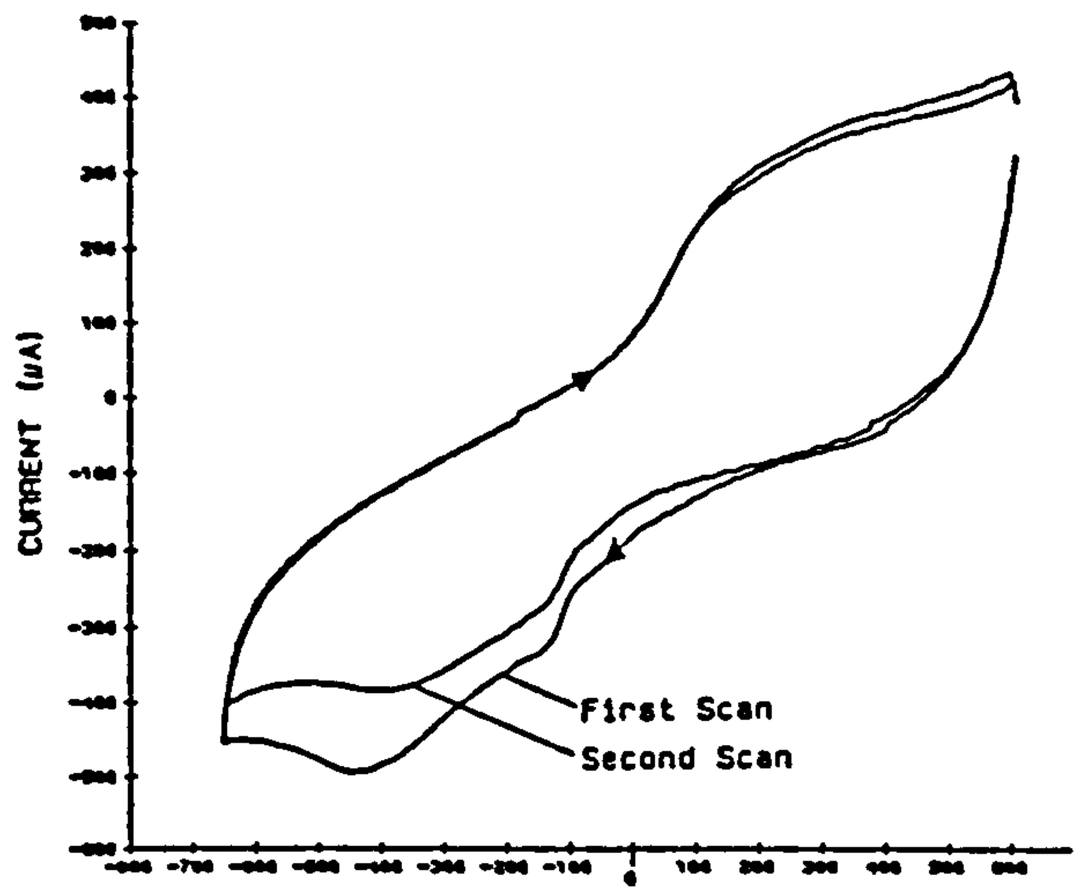

(c)

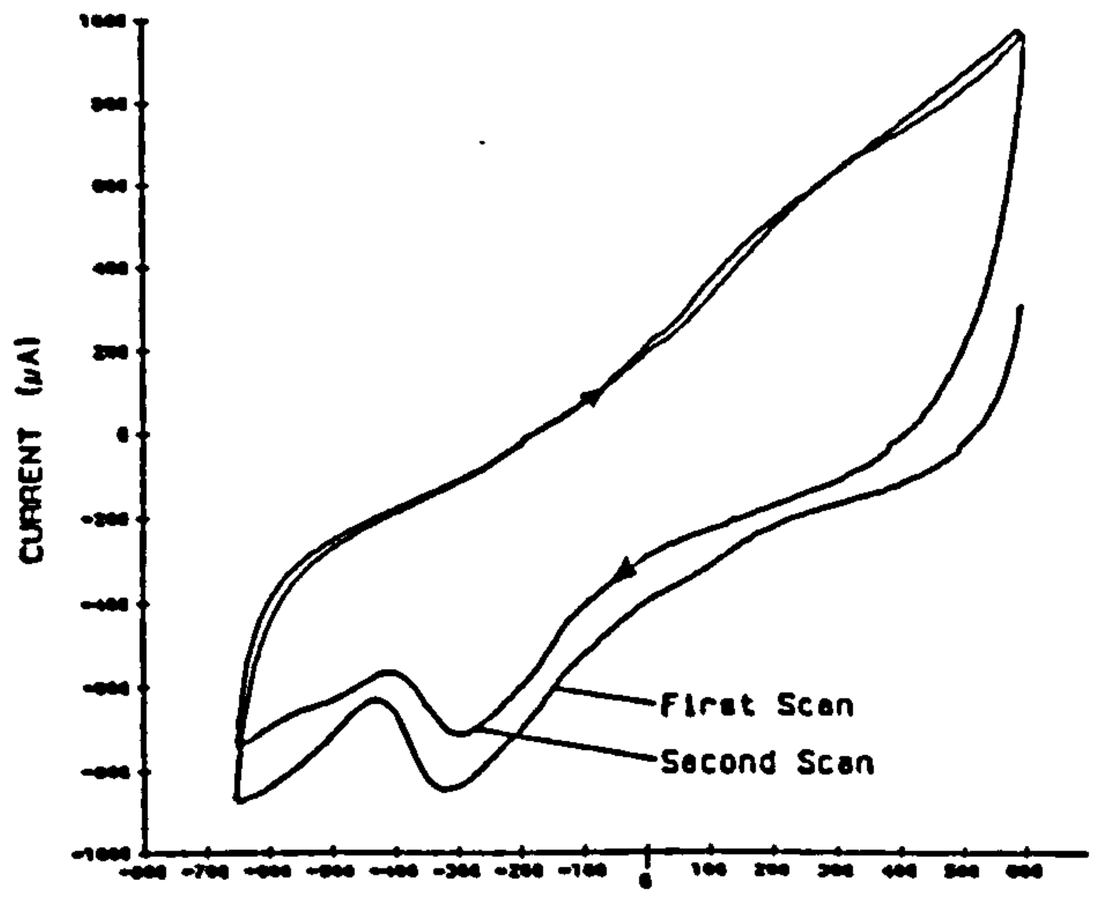

Figs. 30. Cyclic voltammograms of GC-$PPy^{+}(SO_4^{2-})$ electrodes in 0.1 M H_2SO_4 supporting electrolyte. (a) 0.05 μm thick polypyrrole layer (b) 0.5 μm, (c) 5 μm. Scan rates are 3.33 mVs^{-1}.

5.3.2 Electrochemical Response in Copper Sulphate solution.

Having discussed the cyclic voltammetry of GC-$PPy^{+}(SO_4^{2-})$ in inert electrolyte, the cyclic voltammetry of copper on bare GC is considered, and compared with that obtained at GC-$PPy^{+}(SO_4^{2-})$ electrodes.

Fig. 31 shows a cyclic voltammogram of the deposition and stripping reactions of copper, for copper sulphate (0.01 M) in 0.1 M sulphuric acid background electrolyte. The *i-E* response was recorded at a scan rate of 1.67 mVs^{-1}, and the electrode potential was measured *vs.* a $Cu/CuSO_{4(sat)}$ reference electrode.

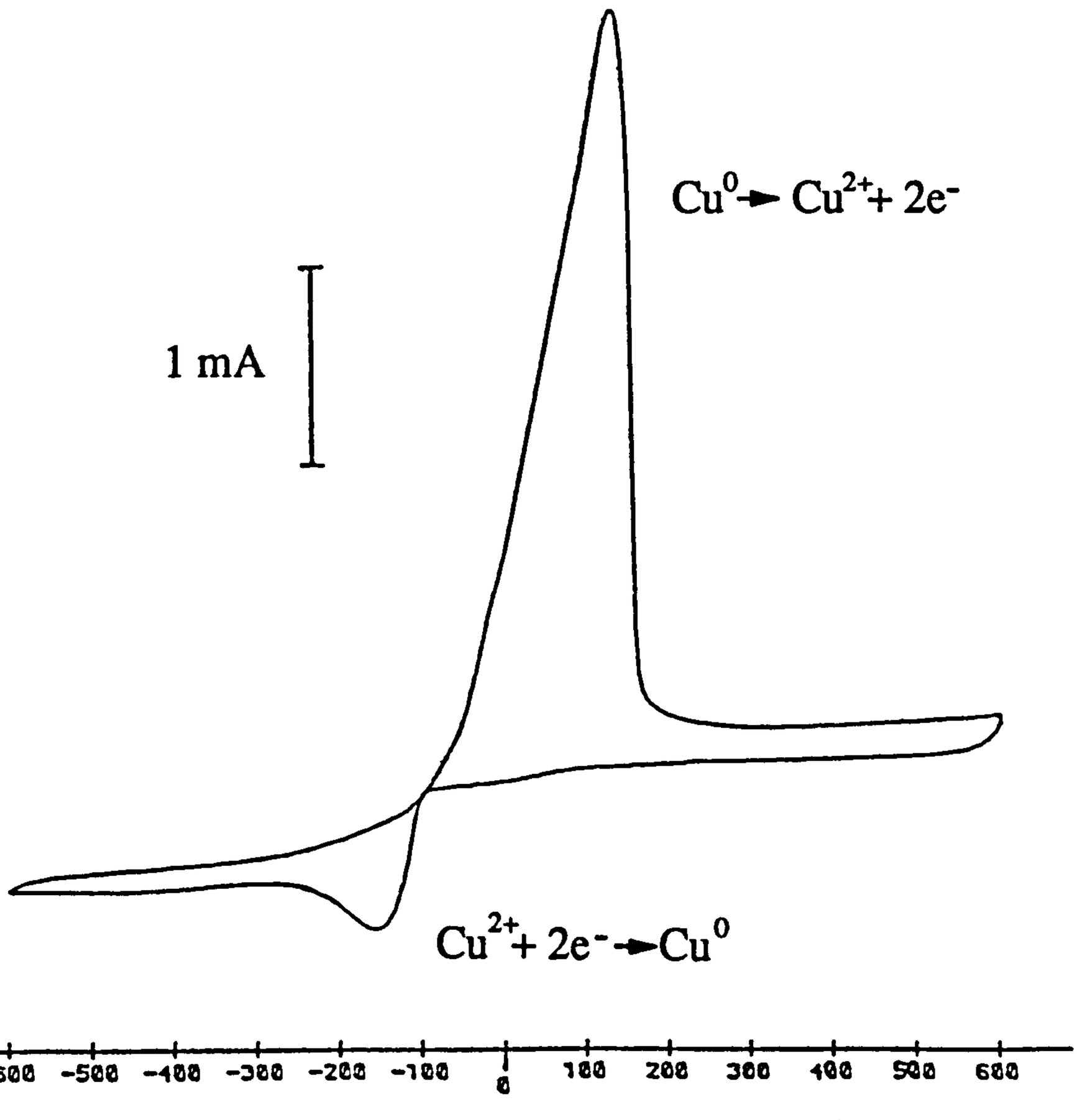

Fig. 31. Cyclic Voltammogram of the deposition and stripping reactions of copper at a bare graphite carbon (GC) electrode, in 0.01 M copper sulphate with 0.1 M sulphuric acid background electrolyte. Scan rate =1.67 mVs^{-1}.

The voltammogram of the deposition of copper on bare graphite (Fig. 31) displays a cathodic peak for the deposition of copper at potentials more cathodic than E_{pc} ~-0.15 V, and is assigned to the reduction $Cu^{2+} \rightarrow Cu^{0}$ according to Eqn. 5.3. In aqueous copper sulphate solution, this reaction has been demonstrated to occur exclusively via two single-electron transfer steps[185,186], with the rate determining step being the reduction of Cu^{2+} to Cu^{+} (step A). The peak centred at E_{pa} = +0.12 V is the corresponding anodic stripping peak. The narrow peak shape is characteristic of a surface localised process[184], such as might be expected from the stripping of copper.

$$Cu^{2+} \overset{(A)}{\rightarrow} Cu^{+} \overset{(B)}{\rightarrow} Cu^{o} \qquad (5.3)$$

Following Cyclic voltammetry measurements at bare GC electrodes, the electrochemical response of Cu^{2+} was studied at GC-$PPy^{+}(SO_4^{2-})$ electrodes, with polypyrrole coat thicknesses between 0.05 and 10 μm. Copper deposition was readily accomplished in all instances.

Figs. 32 (a-c), displays voltammograms for the deposition of copper at GC-$PPy^{+}(SO_4^{2-})$ electrodes with polypyrrole coat thicknesses of 0.05, 0.5, and 5 μm. The general features of the voltammograms remain the same as that exhibited at bare GC, in spite of the fact that the deposition of copper on graphite (-0.095 V) occurs at a potential more cathodic than the onset potential for the reduction of polypyrrole. The resemblance of the CV response of Cu^{2+} at GC-$PPy^{+}(SO_4^{2-})$, to that obtained on bare GC implies that the mechanism of copper deposition is similar in both instances, and that copper deposition on GC-$PPy^{+}(SO_4^{2-})$ electrodes is also described by Eqn. 5.3.

The characteristics of the deposition and stripping processes remain essentially unchanged as the thickness of the polypyrrole coat is increased more than 100 fold, although the redox processes of the underlying substrate do, however, become more apparent with increasing polypyrrole coat thickness. This is reflected by the increased current at potentials more positive than the copper stripping peak, coupled with the appearance of an additional redox peak centred at E_{pc} = -0.35 V, which corresponds to the reduction of the polymer.

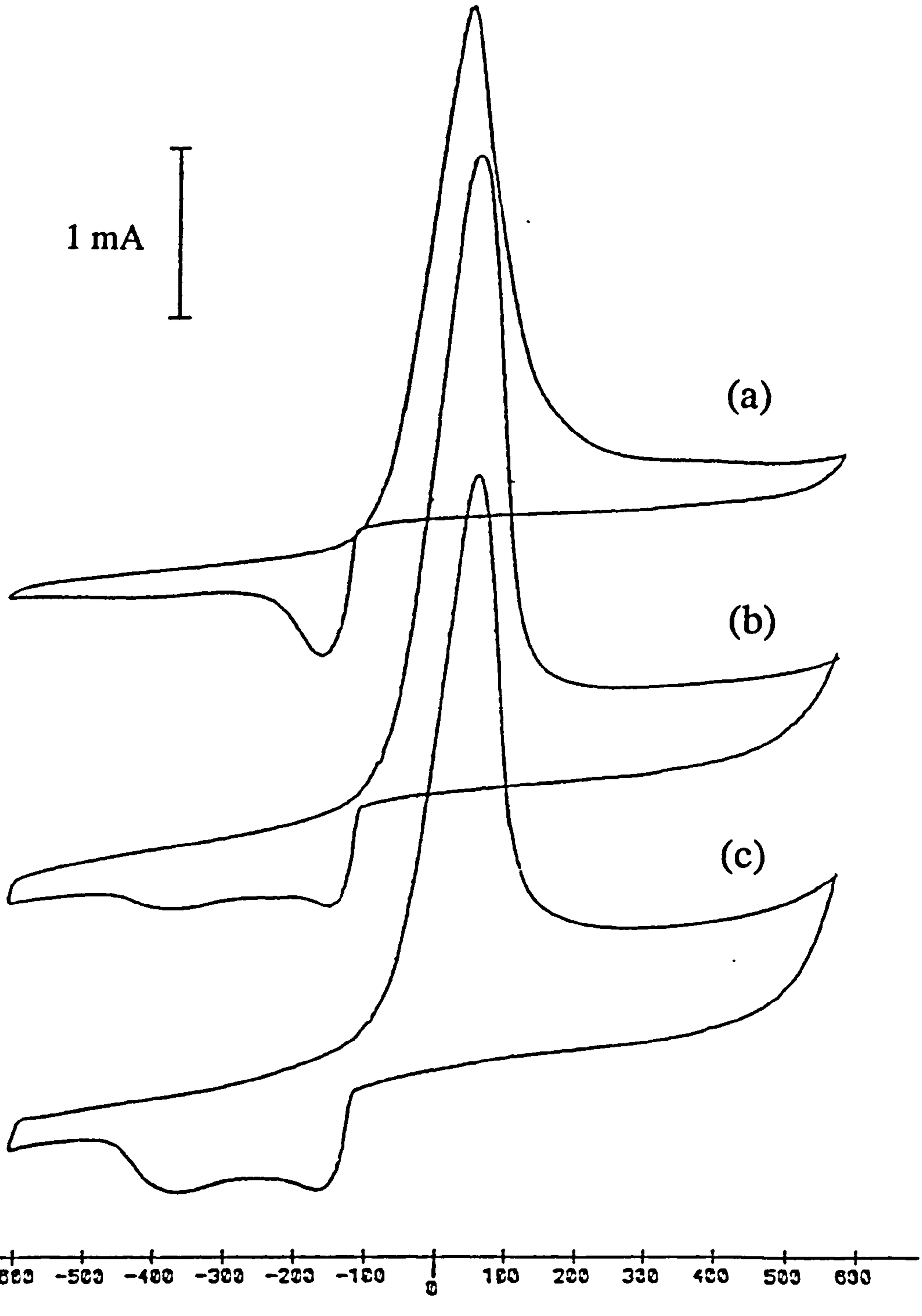

Fig. 32. Cyclic voltammograms of Cu^{2+} in 0.01 M copper sulphate, at GC-$PPy^{+}(SO_4^{2-})$ electrodes with polypyrrole coat thicknesses of; (a) 0.05 µm, (b) 0.5 µm, and (c) 5 µm. Scans are recorded at v=1.67 mVs^{-1}.

Table (5) details how the E_p and i_p values vary with the polypyrrole coat thickness.

Table 5. E_p and i_p values for the deposition of copper on GC-PPy$^+$(SO_4^{2-}) electrodes.

Polypyrrole Coat Thickness (μm)	Onset (V)	E_{pc} (V)	i_{pc} (mA)	E_{pa} (V)
Bare GC	-0.095	-0.153	-0.88	0.125
0.05	-0.105	-0.158	-0.94	0.053
0.1	-0.109	-0.185	-0.80	0.087
0.25	-0.103	-0.164	-0.94	0.056
0.5	-0.106	-0.154	-0.88	0.061
1	-0.105	-0.173	-0.66	0.066
2.5	-0.119	-0.182	-0.87	0.058
5	---	-0.144	-0.81	0.063
10	-0.163	-0.163	-0.94	0.073

As shown, there was no direct correlation between film thickness and E_p and i_p values. This absence of correlation between i_{pc} values and substrate thickness for the reduction of Cu^{2+} is in contrast to cyclic voltammograms obtained with GC-PPy$^+$(SO_4^{2-}) electrodes in supporting electrolyte only (see Fig. 30), which show an increase in i_p values with film thickness. This suggests that the area of the polypyrrole electrode which is accessible to Cu^{2+} from solution remains relatively constant, and implies that the deposition of copper is largely confined to the outer surface of the film. If polypyrrole was porous to Cu^{2+}, the peak current values would be expected to decrease with increasing film thickness, since the diffusion of ions to the electrode surface would be more impeded[37].

Only one other report of the redox chemistry of Cu^{2+} at a polypyrrole coated electrode is contained in the literature[187]. In this work, the *i-E* behaviour of aqueous $CuCl_2$ (10^{-3} M) in 0.1 M $NaClO_4$ was studied on 0.1 μm thick polypyrrole films. No mention of copper deposition was reported, and the redox process centred around 0.0 V *vs.* SCE, was attributed to the single electron reduction and oxidation of Cu^{2+} according to Eqn. 5.4:

$$Cu^{2+} + e^- = Cu^+ \qquad (E^\circ = 0.319\ V\ vs.\ SCE) \qquad (5.4)$$

This assertion seems implausible for several reasons. Firstly, the mechanism is in contradiction to the generally accepted view for the reduction of copper in aqueous conditions[185,186]. The proposed mechanism corresponds to a situation in which the Cu^+ oxidation state is more stable than Cu^{2+}, and implies that step B of Eqn. 5.3 is rate determining for metal deposition (such as with the electrodeposition of copper from acetonitrile). Secondly, ClO_4^- has a greater affinity for the Cu^{2+} compared to Cu^+ and is thus expected to stabilise the Cu^{2+} oxidation state[185,188]. The mechanism is also inconsistent with the *i-E* response published by the same authors. If it is assumed that the reduction is due to the Cu^{2+}/Cu^+ redox couple as proposed, redox peaks for the reduction of Cu^+ to Cu° should also be evident in the potential range over which was scanned (+0.8 to -1.0 V). This is supported by the fact that the reduction of Cu^+ to metallic copper occurs at E_p = -0.52 V in acetonitrile, a solvent which is known to stabilise the Cu^+ oxidation state[37,185]. Moreover, the narrow symmetrical wave shape which is reported to display diffusion of Cu^+ at the electrode surface is in fact characteristic in shape of a metal stripping peak[38]. In view of this, it seems more likely that the redox process was misinterpreted and is in fact due to the reduction of Cu^{2+} to Cu° as proposed in this section.

Copper deposition has also been reported on poly(3-methylthiophene), a close analogue of polypyrrole. Fontaine *et al*[60] studied the formation of metallic clusters by prolonged cathodic polarization using energy dispersive X-ray absorption spectroscopy. The electro-reduction of copper from $CuCl_2$ (10^{-3} - 10^{-2} M) in acetonitrile, with $N(Bu)_4SO_3CF_3$ electrolyte was reported to proceed through the following series of reduction steps Cu(II)→Cu(I)→Cu(0), with metallic clusters being formed via the disproportionation of Cu^+ according to the reaction:

$$2\ Cu^+ \rightarrow Cu^{2+} + Cu^\circ \qquad (5.5)$$

This mechanism is not in contradiction to the mechanism of copper deposition given in Eqn. 5.3, since acetonitrile, $N(Bu)_4SO_3CF_3$, and poly(3-methylthiophene) all strongly stabilise the Cu^+ oxidation state[60], so that appreciable concentrations of Cu^+ are able to form in the vicinity of the electrode surface. Conversely, in aqueous H_2SO_4 solution, the Cu^{2+} state is stabilised by SO_4^{2-}, which does not covalently bond to $Cu^+_{(aq)}$ [188]. Further evidence that the results of Fontaine *et al*[60] are not in conflict with data obtained for the deposition in aqueous conditions, is obtained from a comparison of the kinetics of copper deposition. In acetonitrile, copper deposition was only observed after ~600 seconds, as compared to near instantaneous deposition in aqueous conditions. This dissimilarity in the time scale of deposition is consistent with different mechanisms of copper deposition, as described by Eqns. 5.3 and 5.5 for aqueous and non-aqueous deposition.

5.4 Nucleation of Copper at GC-$PPy^+(SO_4^{2-})$.

Although the deposition of copper was readily accomplished on all GC-$PPy^+(SO_4^{2-})$ electrodes, the effect of the polypyrrole layer is to retard nucleation. This is indicated by two factors. Firstly the slight increase in overpotential for the deposition of copper at GC-$PPy^+(SO_4^{2-})$ electrodes compared to that obtained on graphite only, and secondly, the larger current in the reverse (anodic) scan direction at potentials between -0.11 and -0.07 V, for 0.05, 0.1 and 0.25 μm thick GC-$PPy^+(SO_4^{2-})$ substrates. This increase in current indicates that the reduction of copper takes place more readily once an initial seed layer of metal has been nucleated[36,38]. Further deposition then occurs preferentially at existing copper nuclei, rather than by the nucleation of new growth centres.

In this section, the nucleation of copper at GC-$PPy^+(SO_4^{2-})$ electrodes was examined in detail using a reduced scan rate of (0.33 mVs^{-1}). The lower scan rate was chosen in order to reduce the effects of the capacitive charging current on the overall *i-E* response. Fig. 33 shows two consecutive scans for a 1 μm GC-$PPy^+(SO_4^{2-})$ substrate cycled between ± 0.30 V. The upper (anodic) potential limit was chosen to be +0.30 V so that the stripping of copper from the electrode surface would be

incomplete. This was confirmed by visible traces of copper on the electrode surface prior to commencing the second scan. Both voltammograms exhibit a region at around -0.1 V where the current in the reverse (anodic) scan direction is greater than that for the corresponding cathodic scan direction. This phenomenon is not uncommon in CV scans involving the deposition of metal on a foreign substrate, and is commonly referred to as a form of hysteresis[37,38]. Since the hysteresis effect is also apparent in the second scan, the overpotential for the deposition of copper has not been entirely eliminated. However, it has been reduced, as indicated by the slightly anodic shift (0.015 V) in the foot of the deposition wave, and the reduction of area enclosed within the second hysteresis loop.

The increase in the overall cathodic current density on the second scan may arise from either an increase in the number of copper nuclei at the electrode surface, or else from continued growth of the existing copper phase. The reduction in the overpotential for copper deposition on the second scan suggests the latter as being more likely, and micrographs in section 5.7, which show a uniform size distribution for copper nuclei electrochemically deposited onto polypyrrole support this.

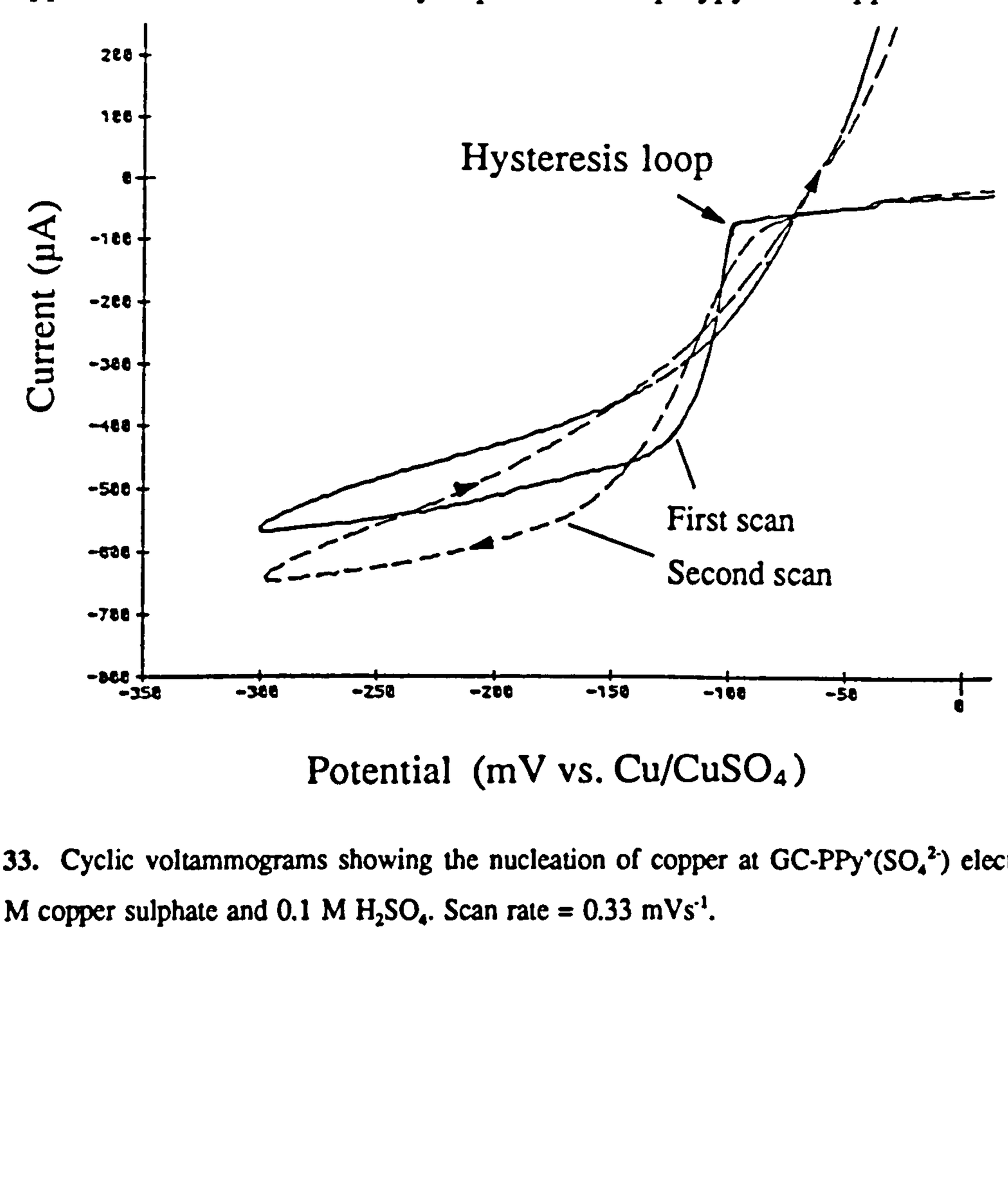

Fig. 33. Cyclic voltammograms showing the nucleation of copper at GC-PPy^{+}(SO_4^{2-}) electrodes in 0.01 M copper sulphate and 0.1 M H_2SO_4. Scan rate = 0.33 mVs^{-1}.

5.5 Kinetics of Copper Deposition.

The kinetics of the copper deposition process were examined in greater detail by varying the potential scan rate between 0.33 and 1.66 mVs^{-1}. Fig. 34 displays successive cyclic voltammograms that were recorded in 0.01 M $CuSO_4$ solution with 0.1 M H_2SO_4 supporting electrolyte. The potential limits were +0.60 and -0.40 V (*vs.* $Cu^{2+}/CuSO_4$ ref.), with the upper (anodic) potential limit chosen in order to ensure that the copper stripping reaction was complete. A single 0.5 µm thick GC-$PPy^+(SO_4^{2-})$ electrode was used to record all scans.

The principal features of the voltammograms remain the same as the scan rate is increased, except for the slight increase in cathodic current between -0.25 and -0.40 V, and the appearance of an additional anodic wave between +0.10 and +0.35 V. This additional current becomes more pronounced as the scan rate is increased and corresponds to the redox processes of the underlying GC-$PPy^+(SO_4^{2-})$ substrate, as previously stated.

Analysis of the deposition and stripping of copper, in terms of i_p values, and the charges involved during cycling, is complicated by capacitive charging currents, and the redox processes associated with the polypyrrole substrate. It was not possible to compensate for this extra current by simply subtracting the current contribution from a scan made in supporting electrolyte from that made in copper solution, since the scans do not superimpose. Indeed, i_p values for the reduction of copper cannot be determined absolutely, since there is no clear way of separating the total current into individual contributions[114]. As a result, only qualitative aspects of copper deposition at GC-$PPy^+(SO_4^{2-})$ electrodes can be discussed. In view of this complication, i_{pc} values were measured as the difference between the baseline of the charging current and the peak of each wave. Fig. 35 shows a plot of the measured i_{pc} values as a function of $v^{1/2}$. The linear relationship indicates that copper reduction is diffusion controlled between the above scan rates, and not limited by kinetic aspects of the polypyrrole layer. The positive intercept on the current axis at zero scan rate represents the additional redox current associated with the reduction of the polypyrrole substrate.

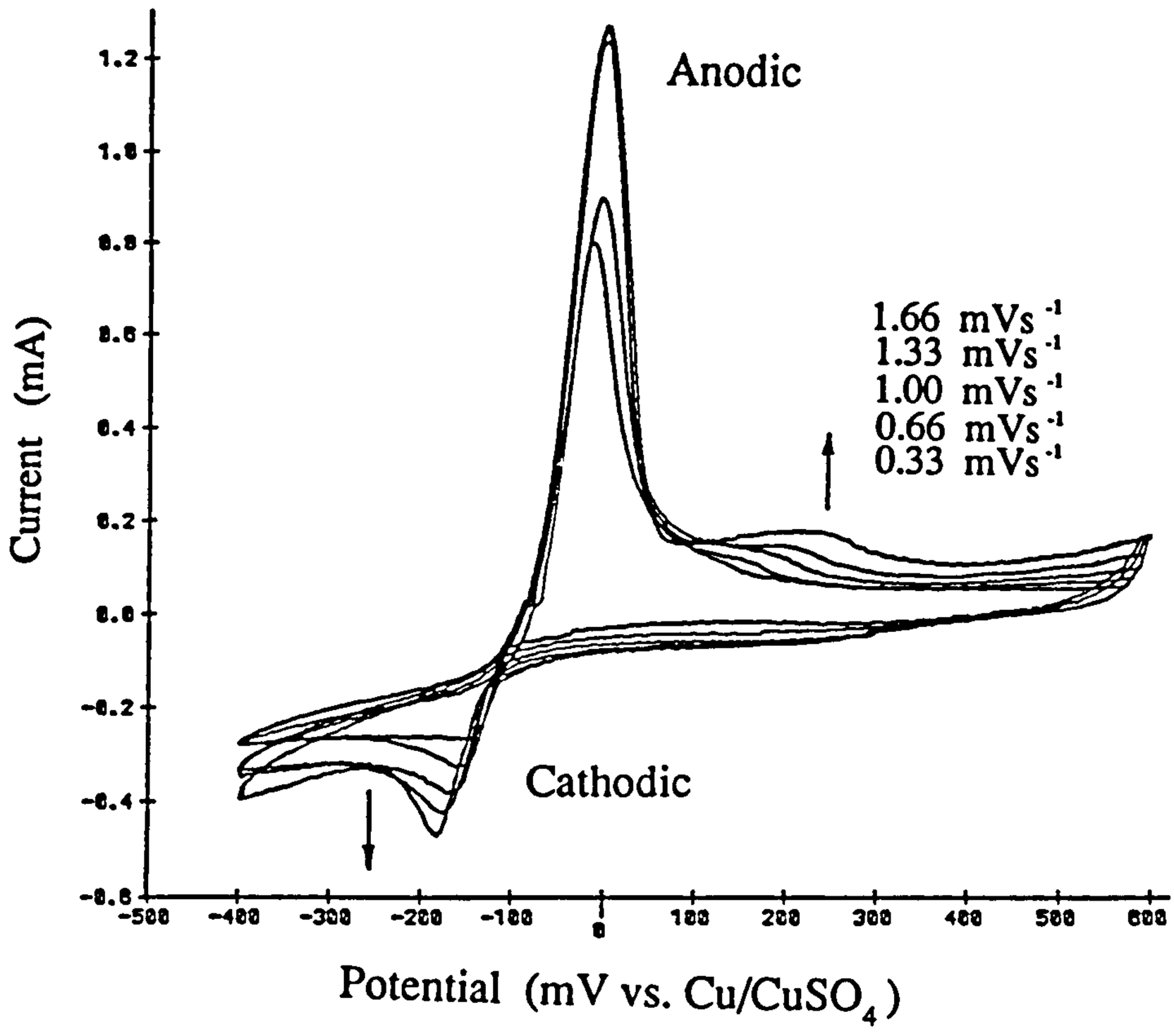

Fig. 34. Successive cyclic voltammograms of a 0.5 µm thick GC-$PPy^{+}(SO_4^{2-})$ electrode in 0.01 M $CuSO_4$ with 0.1 M H_2SO_4 supporting electrolyte, for scan rates between 0.33 and 1.66 mVs^{-1}.

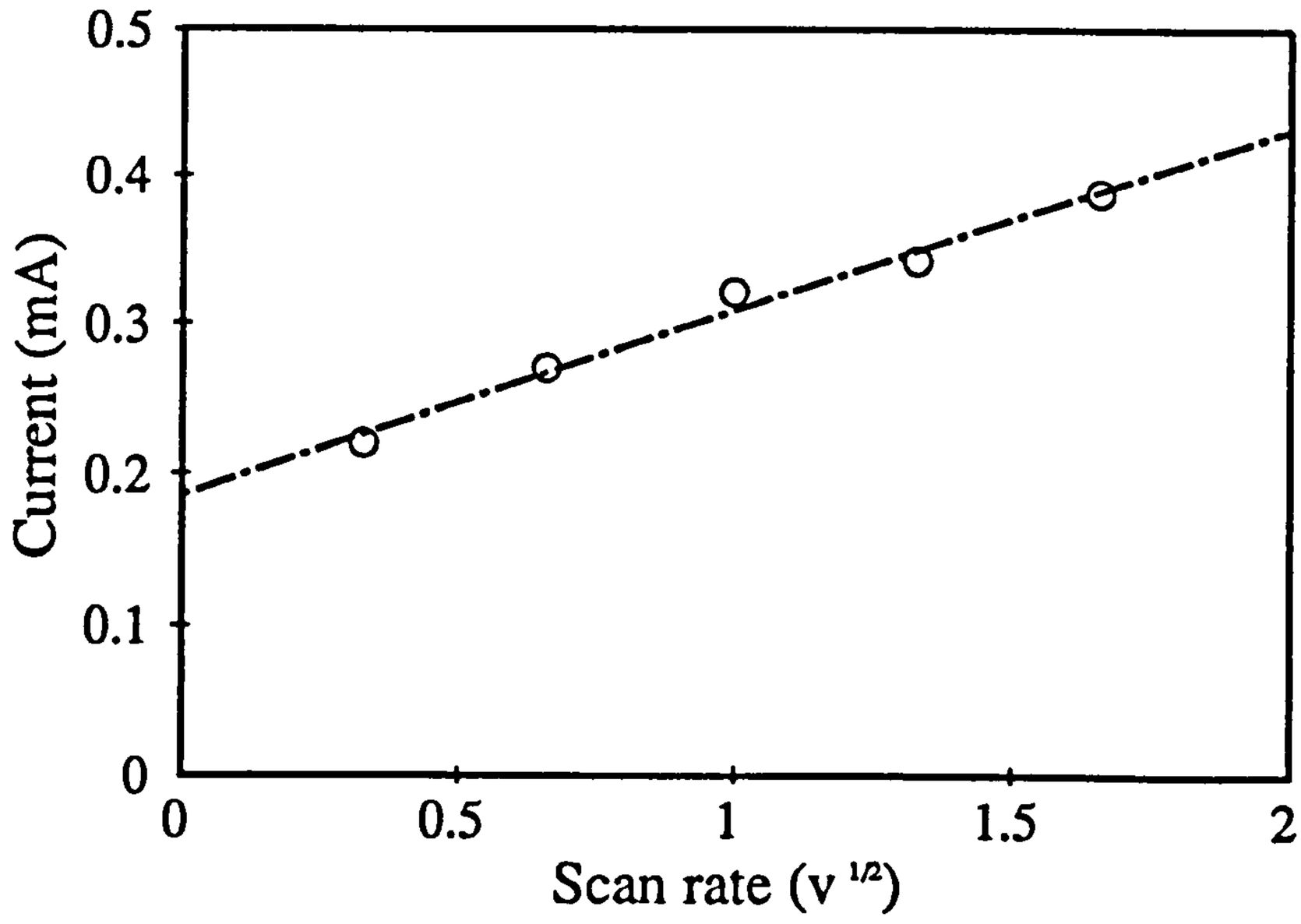

Fig. 35. Peak cathodic current values for a 0.5 µm thick GC-$PPy^{+}(SO_4^{2-})$ substrate in 0.01 M $CuSO_4$ 0.1 M H_2SO_4 supporting electrolyte as a function of the scan rate ($v^{1/2}$).

This is not adequately accounted for by subtracting the baseline charging current, since the redox peak for the reduction of the film occurs at a more cathodic potential than the onset potential for copper deposition.

The peak anodic current values (i_{pa}), which were also measured from the base line of the charging current, do not exhibit any particular scan rate dependence. This could be due to several reasons. One possibility is that some copper is deposited internally within the matrix of the polymer as well as on the polymer surface. The i_{pa} values would then be a combination of surface dissolution, for which i_p is proportional to v, and diffusion from within the polymer, which would generate an i_p versus $v^{1/2}$ dependence[189]. However, the symmetrical shape of the anodic stripping peak suggests that internal diffusion can be disregarded in this instance. Another possibility is that not all Cu^{2+} is reduced to Cu° on the cathodic cycle, but some Cu^{+} is also formed. On the time-scale of this experiment, it is most probable that any Cu^{+} formed in the vicinity of the electrode surface would have either diffused into bulk solution before the anodic scan, or else have undergone disproportionation. The latter reaction occurs rapidly (< 1 second) in aqueous conditions[188]. Another equally plausible explanation is that some surface copper re-dissolves after deposition, according to equation 5.6.

$$Cu^{\circ} + Cu^{2+} \rightleftharpoons 2Cu^{+} \qquad (5.6)$$

This reaction has an accepted value of $1x10^{-6}$ for the equilibrium constant[185]. Thus, at the equilibrium potential of Cu° in 0.01 M Cu^{2+}, the concentration of Cu^{+} is $1x10^{-4}$ M, and the copper electrodeposit will tend to dissolve in order to maintain this concentration.

The deposition of copper was also investigated over a wider range of scan rates (10 - 70 mVs^{-1}) to ascertain whether copper reduction was impeded by the substrate. Voltammograms recorded in 0.01 M $CuSO_4$ gave peaks that were indistinguishable from the background current, and hence the concentration of copper was increased to 0.06 M. Fig. 36 shows a succession of voltammograms cycled between ± 0.70 V in 0.06 M $CuSO_4$ with 0.1 M H_2SO_4 supporting electrolyte. The shapes of the deposition and stripping peaks are distorted from that exhibited in Fig. 34, for scan rates between

0.33-1.67 mVs^{-1}, due to the increased charging current, plus some kinetic limitations of the GC-$PPy^{+}(SO_4^{2-})$ electrode at potentials more cathodic than E_{pc}. This is particularly evident for the stripping reaction, which now appears as a plateau rather than a narrow symmetrical peak.

Quantitative analysis of the anodic wave for the stripping reaction is precluded due to the absence of a baseline from which to measure i_{pa} values, plus the additional contribution of capacitive current from the underlying polypyrrole substrate. The peak cathodic current i_{pc} values were measured as the difference between the base line of the charging current and the limiting current plateau. These were found to scale linearly with $v^{1/2}$ between the above scan rates (10 - 70 mVs^{-1}) see Fig. 37, which indicates that deposition is diffusion controlled for deposition potentials less cathodic than E_{pc}.

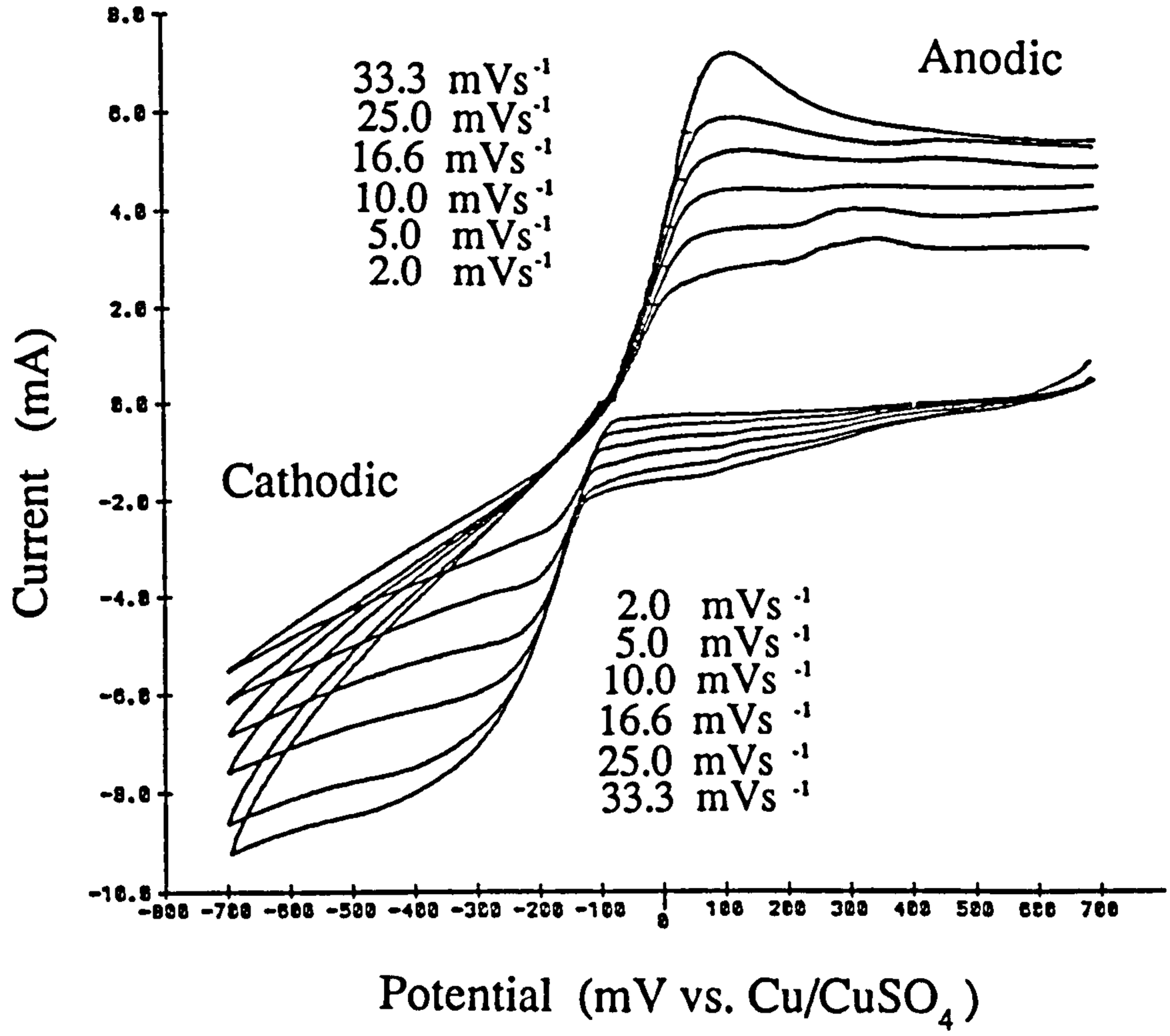

Fig. 36. Successive cyclic voltammograms of a 0.5 μm thick GC-$PPy^{+}(SO_4^{2-})$ electrode in 0.06 M $CuSO_4$ with 0.1 M H_2SO_4 supporting electrolyte, for scan rate between 10 and 70 mVs^{-1}.

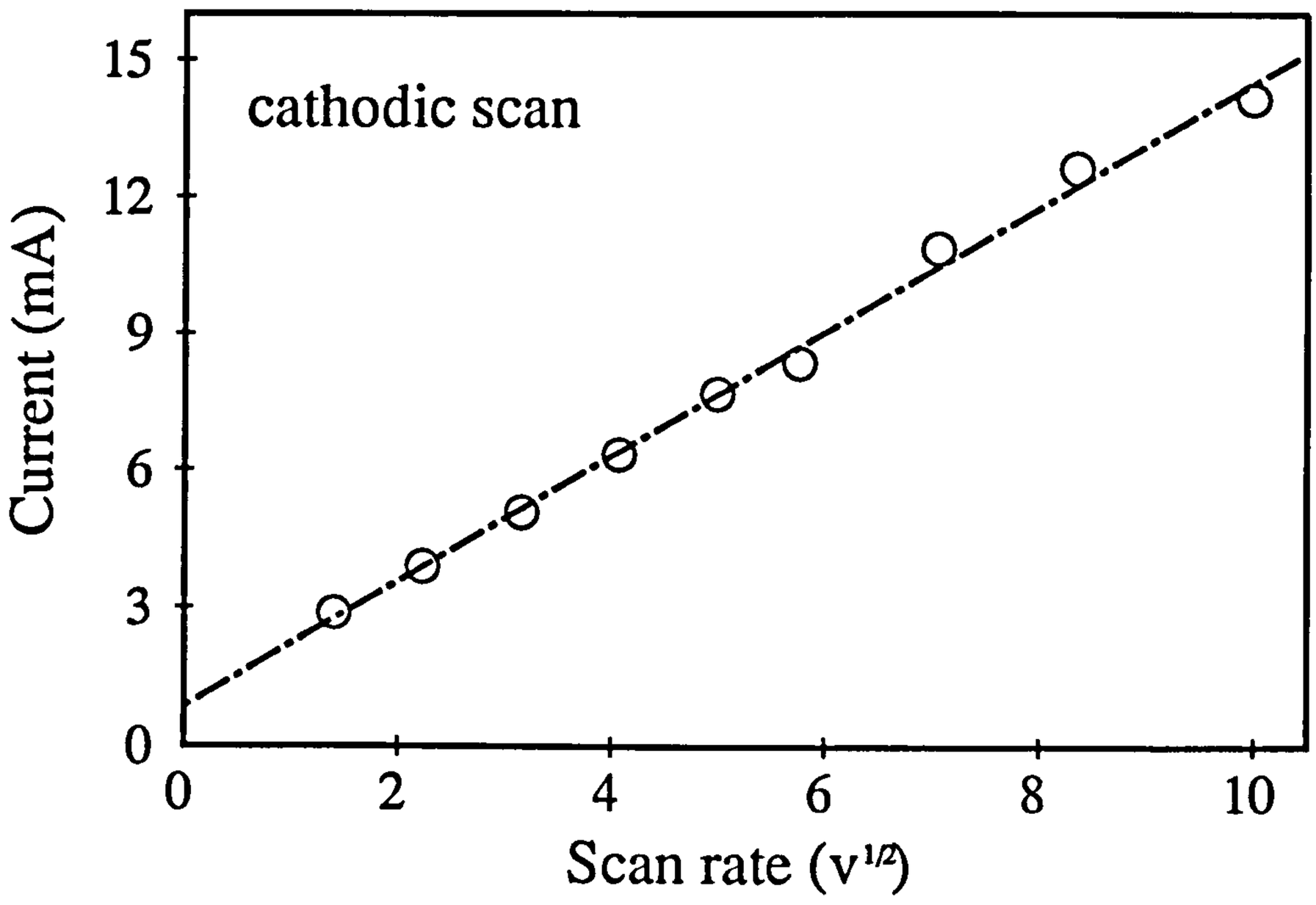

Fig. 37. Peak cathodic current values for the deposition of copper at a 0.5 µm thick GC-$PPy^{+}(SO_4^{2-})$ electrode in 0.06 M $CuSO_4$ with 0.1 M H_2SO_4 supporting electrolyte. Scans were measured at scan rates between 10 and 70 mVs^{-1}.

5.6 The Effects of Copper Sulphate Solution on the Electrochemical Behaviour of GC-$PPy^{+}(SO_4^{2-})$ Electrodes.

The electrochemical and chemical behaviour of polypyrrole in the presence of anions in solution, other than that initially incorporated within the film during synthesis, has been recently investigated by several groups[108,116,169,170,190]. In these studies, the exchange of the original film based counteranions has been demonstrated with other non-identical anions from bulk solution.

In addition to the exchange of counteranions, polypyrrole is also reported to incorporate additional electrolyte from solution, in excess to that required to maintain overall charge neutrality of the film[119,121]. As a consequence, polypyrrole may be expected to incorporate Cu^{2+} from solution, either during cyclic voltammetry, or by simple immersion in solutions containing Cu^{2+} ions. The effects of this are expected to be twofold. Firstly, the ingress of copper ions into polypyrrole will complicate the interpretation of voltammograms of GC-$PPy^{+}(SO_4^{2-})$ electrodes made in the presence of Cu^{2+}, since an additional current response of these ions will need to be considered.

Secondly, in addition to the surface deposition of copper, any absorbed Cu^{2+} may be reduced within the polypyrrole matrix to Cu°, if the polymer is subsequently subjected to a cathodic potential more negative than the Cu^{2+}/Cu° redox couple. For these reasons, the effects of copper ions on the electrochemical response of polypyrrole were studied using cyclic voltammetry.

5.6.1 Incorporation of Cu(II) by Polypyrrole During Cyclic Voltammetry.

The effects of cycling a polypyrrole substrate between its oxidised and reduced states were studied using a 1 μm thick GC-$PPy^{+}(SO_4^{2-})$ substrate, prepared according to the procedure outlined in section 3.10. Cyclic voltammetry was performed in de-oxygenated 0.01 M $CuSO_4$ solution containing 0.1 M H_2SO_4 supporting electrolyte, and also in 0.1 M H_2SO_4 devoid of other electroactive species.

Fig. 38 shows voltammograms of the GC-$PPy^{+}(SO_4^{2-})$ substrate in 0.1 M H_2SO_4 prior to cycling in copper solution (scan a), and in the same electrolyte solution after successive scans in the presence of Cu^{2+} (scans b-e).

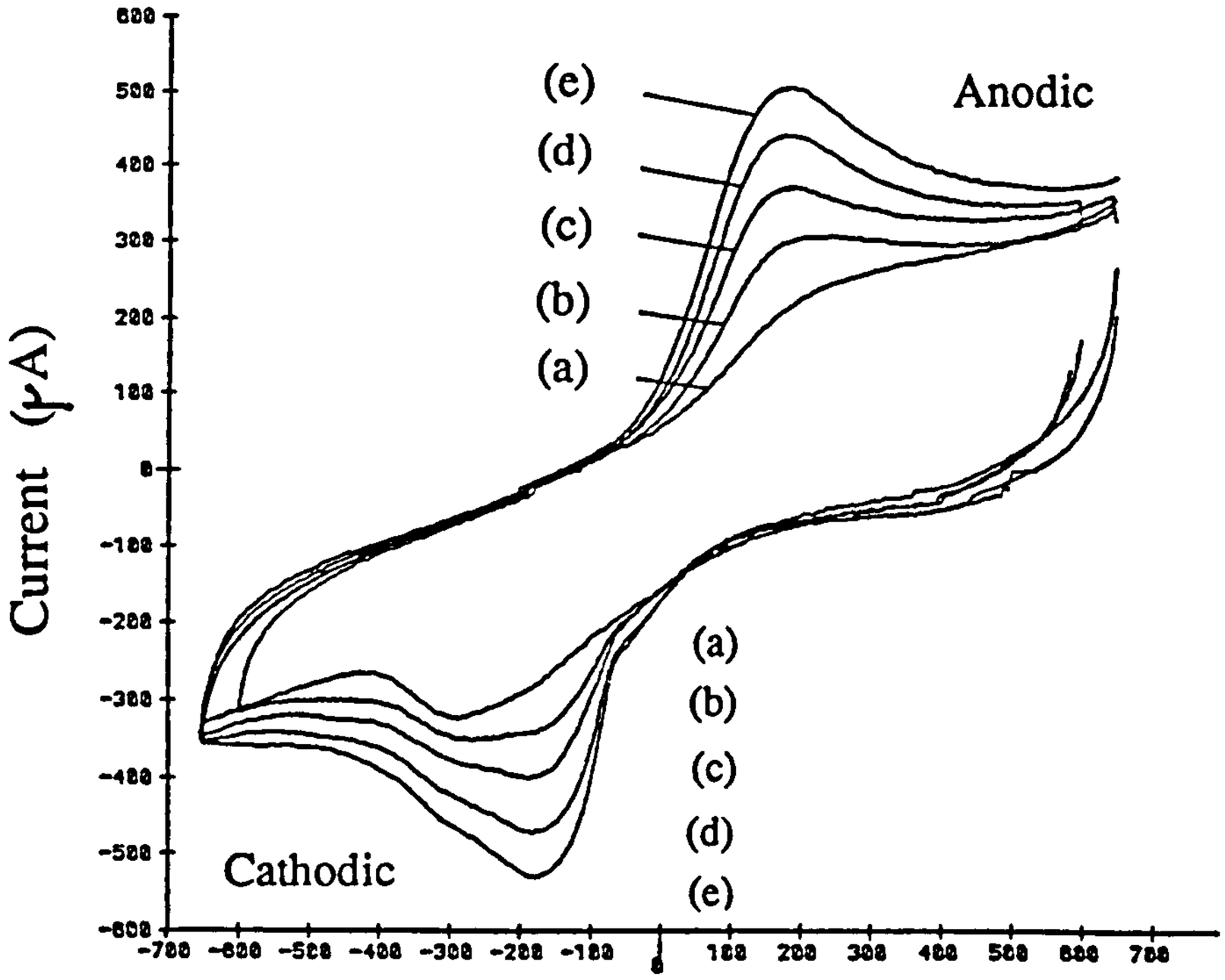

Fig. 38. Cyclic voltammograms of a 1 μm thick GC-$PPy^{+}(SO_4^{2-})$ substrate showing the incorporation of Cu^{2+} from solution. Scans were recorded at 1.67 mVs^{-1}.

Two newly formed broad anodic and cathodic waves are clearly visible superimposed over the redox response of the polypyrrole substrate. The ratio of i_{pa} and i_{pc} values for these peaks is found to be equal to unity, and E_p values are centred at E_{pc} ~-0.185 V and E_{pa} = +0.158 V, with E^o equal to +0.05 V *vs.* SCE. A comparison with E_p values for the deposition/stripping of copper at an equivalent thickness GC-$PPy^+(SO_4^{2-})$ substrate (E_{pc} ~ -0.096 V and E_{pa} = +0.25 V *vs.* SCE) shows that this redox process is not due to residual surface copper from the previous scan, but is in fact the result of reduction/oxidation of Cu^{2+} which has been incorporated internally within the polypyrrole matrix.

Figs. 39 and 40 shows how the amount of charge, and i_p values vary as a function of the number of cycles in copper solution. The linear increase in both i_p and Q_{red} with the number of scan cycles, indicates that a saturation limit for the incorporation of Cu^{2+} by polypyrrole has not been reached, and it is conceivable that the final capacity of the film could be significantly higher. This data also implies that at low levels of incorporation of Cu^{2+}, copper ions are not expelled by cycling polypyrrole between its oxidised and reduced states, as might initially be expected on the basis of equation 2.2.

The ratio of the current associated with the reduction of Cu^{2+} incorporated in the polypyrrole film, compared to the i_{pc} value for the reduction of Cu^{2+} in 0.01 M solution containing 0.1 M H_2SO_4 supporting electrolyte, is 0.18 (at a scan rate of 3.33 mVs^{-1}). Although this is not of sufficient magnitude to significantly distort the visual appearance of wave shapes obtained from cyclic voltammetry measurements, this additional current needs to be taken into account in quantitative measurements of electroactive species in bulk solution, especially if multiple measurements are made with the same electrode in solutions containing electroactive ions.

The quantity of charge involved in the redox process (Q_{red}) may be calculated from integration of the areas under the redox peaks after subtracting the redox contribution from the GC-$PPy^+(SO_4^{2-})$ substrate. The value of Q_{red} = 5.44 mC, obtained on the first scan after cycling in copper solution compares with 7.24 mC for the charge cycled during the reduction of the $PPy^+(SO_4^{2-})$ substrate.

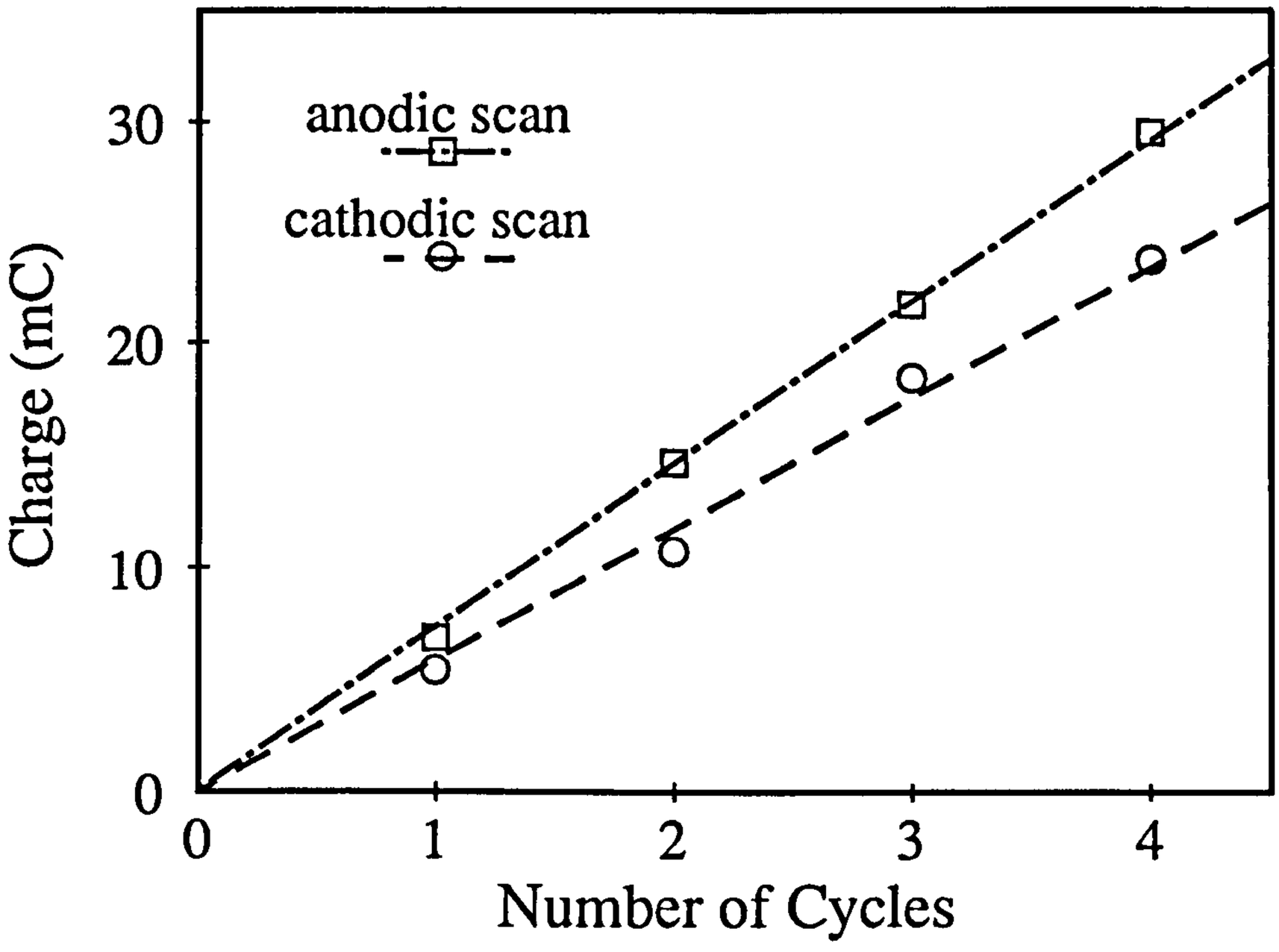

Fig. 39. Variation of the charge cycled by a 1 μm thick GC-$PPy^{+}(SO_4^{2-})$ electrode after successive scans in 0.01 M $CuSO_4$ solution.

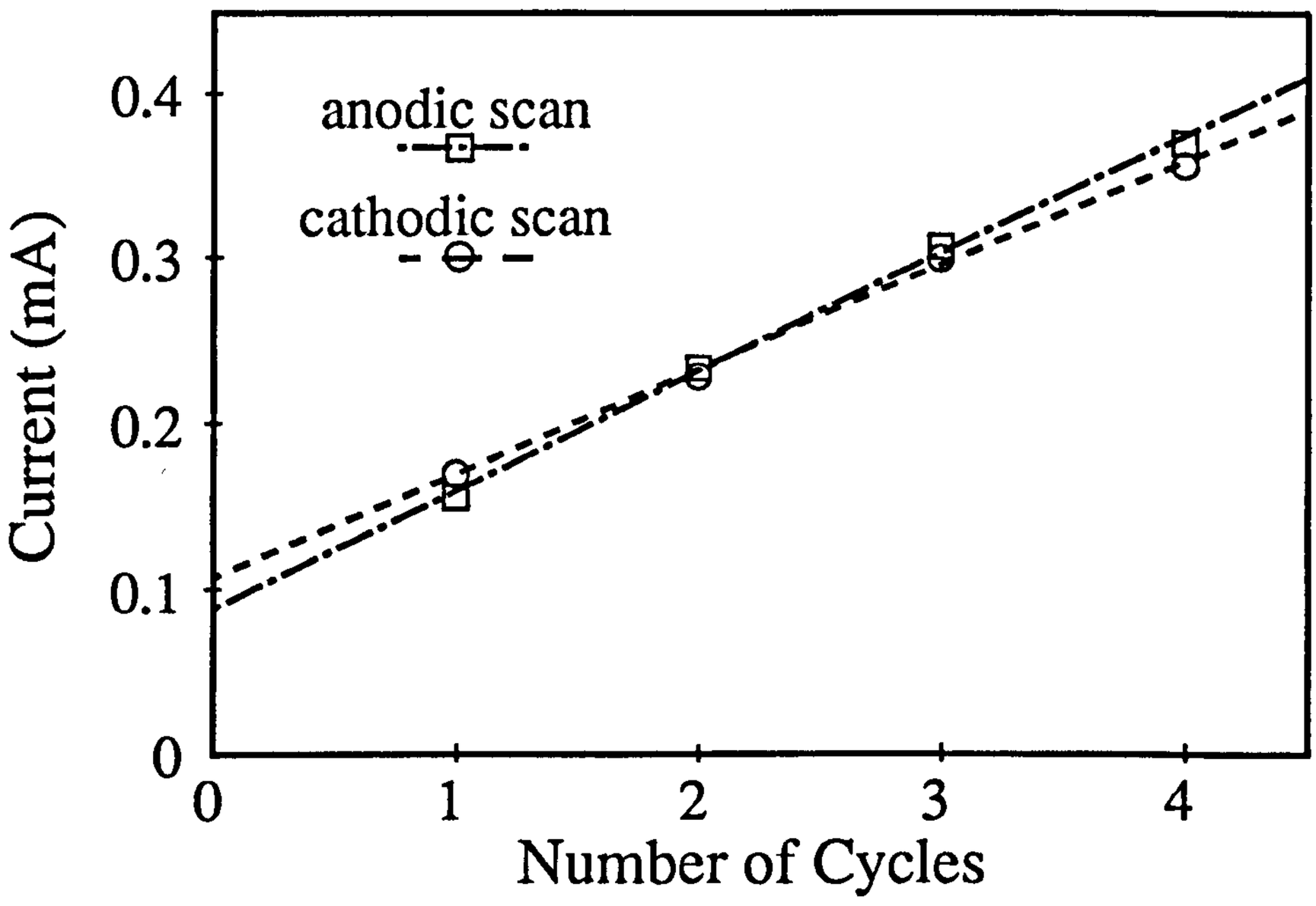

Fig. 40. Variation of the peak anodic and cathodic current values for a 1 μm thick GC-$PPy^{+}(SO_4^{2-})$ electrode after successive scans in 0.01 M $CuSO_4$ solution.

This is approximately equivalent to one Cu^{2+} per every 2.66 unit positive charges on polypyrrole, or one Cu^{2+} per 8 to 10.6 pyrrole units, (based on typical dopant ratios of between 0.24 to 0.33 univalent dopant anions per unit positive charge on polypyrrole; (see Table 1). Although this ratio of Cu^{2+} to PPy^{+} is slightly less than that which is typically exhibited for the incorporation of univalent anions, the linear increase in the amount of Cu^{2+} incorporated during each cycle, suggests that Cu^{2+} is incorporated to compensate for charge imbalances that arise in the polymer during the cathodic cycle. Indeed, similar observations have also been made for polypyrrole in the presence of H^{+} and Li^{+}, and Na^{+}[118,191-193]. A possible mechanism which explains this incorporation of Cu^{2+} is proposed in section 5.8.

Fig. 41 shows the electrochemical response of same GC-$PPy^{+}(SO_4^{2-})$ electrode after leaving to soak in distilled water for ~15 hours. Voltammograms of the initial scan in H_2SO_4 solution (Fig. 41a) and that obtained after cycling four times in copper solution (Fig. 41b) are included for comparison.

As shown, the effect of immersing in water is to cause a reduction in the electroactivity of the film to a level comparable to that exhibited after the first scan in copper solution. Since the shoulder at -0.30 V for the reduction of polypyrrole (Fig. 41c) remains unchanged in height, this decrease in electroactivity must therefore arise from a loss of Cu^{2+} from within the film, rather than through hydrolysis of polypyrrole. This latter explanation has previously been proposed in order to explain decreases in electroactivity of polypyrrole in aqueous solutions[86]. Another confirmation that the decrease in the electroactivity of the GC-$PPy^{+}(SO_4^{2-})$ electrode was due to the loss of Cu^{2+}, and not caused by degradation of polypyrrole, was that the original electroactivity of the film was restored by recycling in $CuSO_4/H_2SO_4$ solution, as shown in Fig. 41(d). This loss and regain of electroactivity caused by soaking in water, followed by immersion in $CuSO_4$ solution, indicates that any Cu^{2+} ions incorporated in the film are not permanently bound, but are free to diffuse from the film into bulk solution and vice-versa.

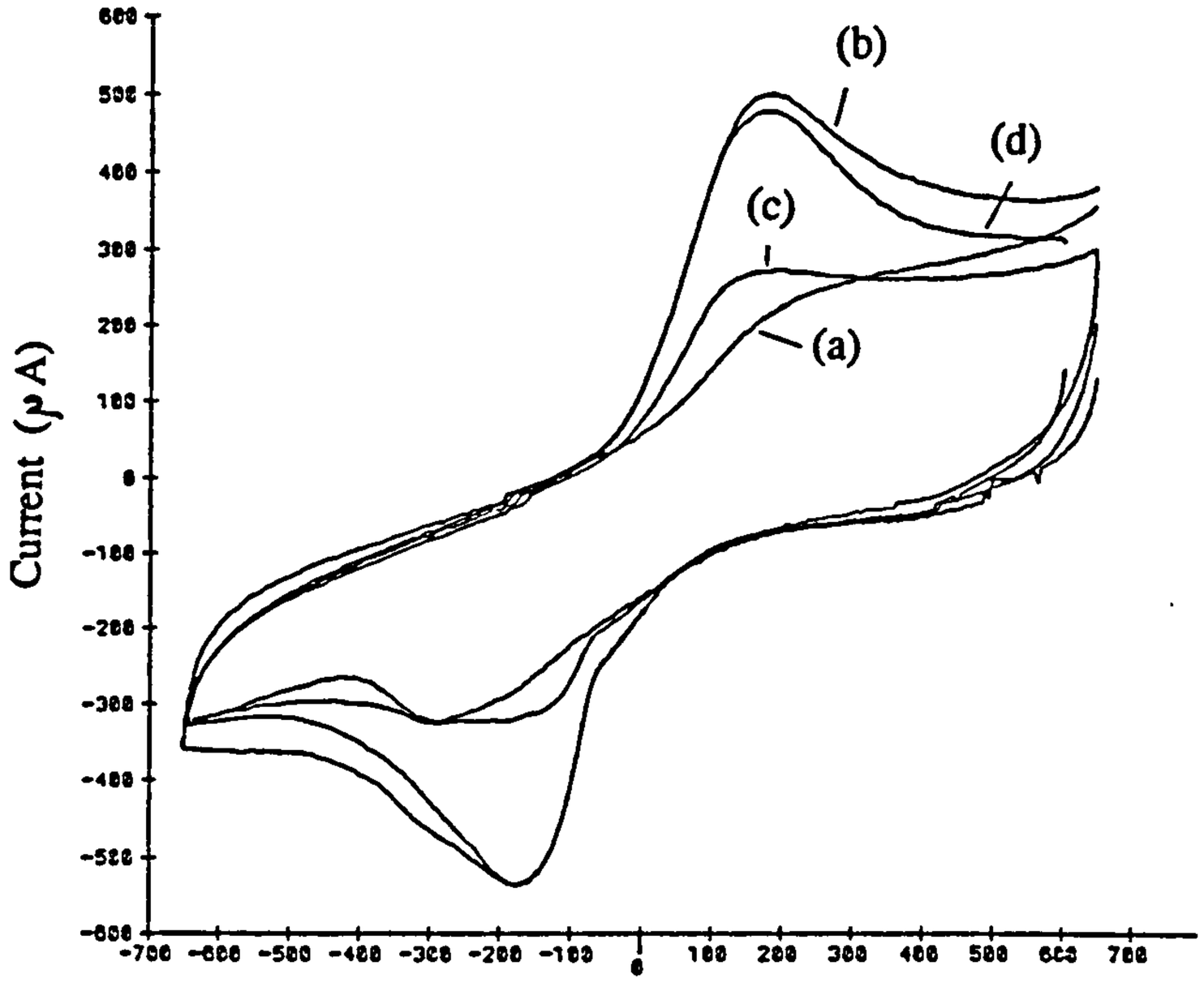

Fig. 41. (a) Original scan prior to immersion in Cu^{2+}, (b) response after cycling four times in $CuSO_4$ solution, (c) response after standing for 15 hours in de-ionised water, (d) response after re-cycling in $CuSO_4$ solution.

5.6.2 The Effects of $CuSO_4$ Solution on the Deposition and Stripping of Copper.

As discussed in section 5.6.1, Cu^{2+} is readily incorporated into polypyrrole by cycling in aqueous $CuSO_4$ at potentials which are sufficient to cause reduction/oxidation of the film. This section investigates the cyclic voltammetry of GC-$PPy^{+}(SO_4^{2-})$ electrodes following immersion in 0.01 M $CuSO_4$ with 0.1 M H_2SO_4 supporting electrolyte solution.

Fig. 42(a) displays voltammograms for the reduction and stripping of copper from these electrodes in 0.01 M $CuSO_4$ and 0.1 M H_2SO_4 supporting electrolyte, and that obtained after leaving the electrode to stand in the same solution for ~15 hours (Fig. 42b). Voltammograms were recorded at scan rates of 1.67 mVs^{-1} and 5 mVs^{-1}.

As shown in Fig. 42(b) there is an approximate doubling of the reduction current following immersion, with i_{pc} values (measured from the baseline of the charging current) of 0.62 and 1.13 mA, compared with 0.32 and 0.61 mA for the immediate response. The anodic stripping peaks are also distorted from their symmetrical shape and exhibit "tailing" at potentials greater than E_p.

(a)

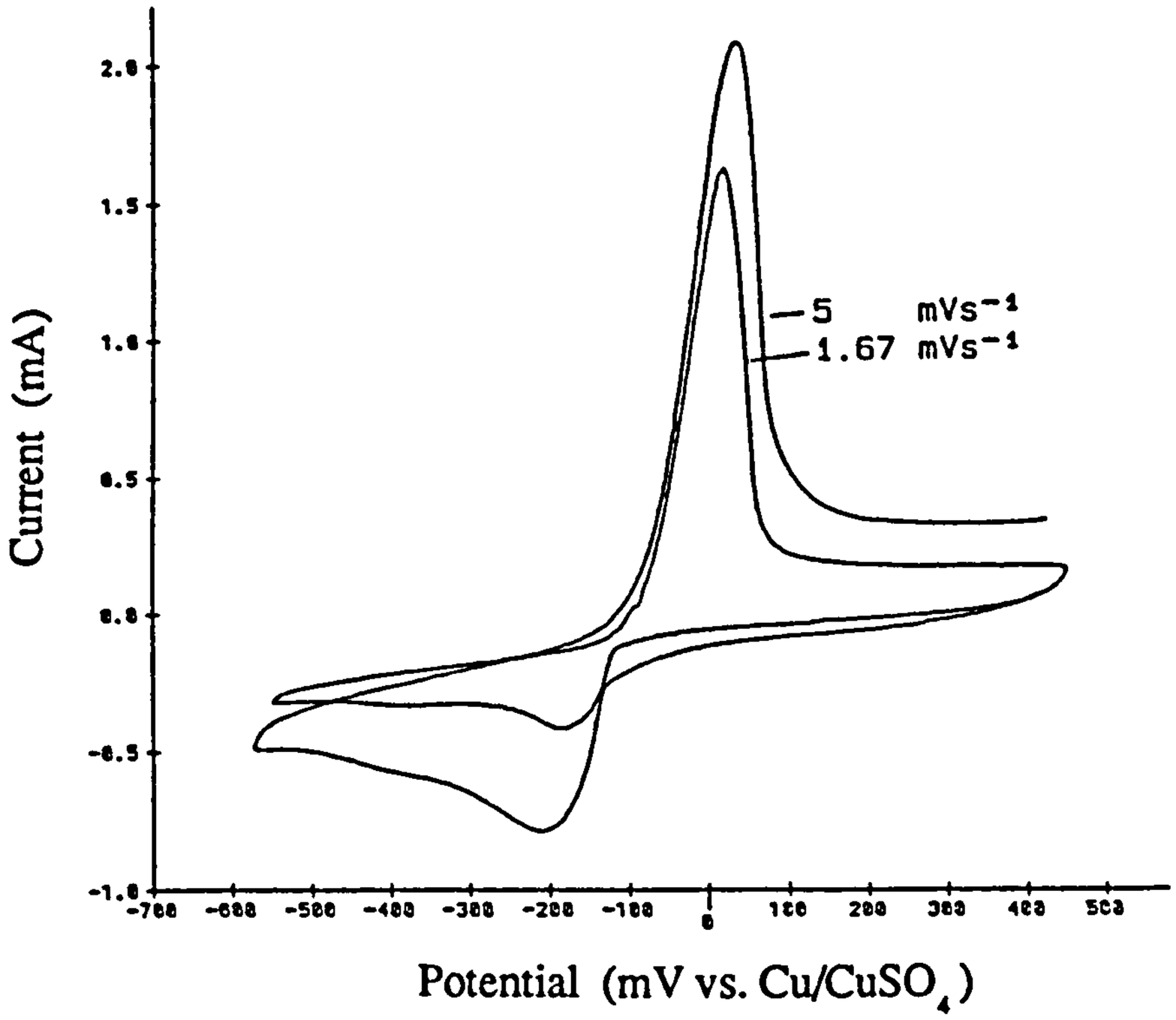

(b)

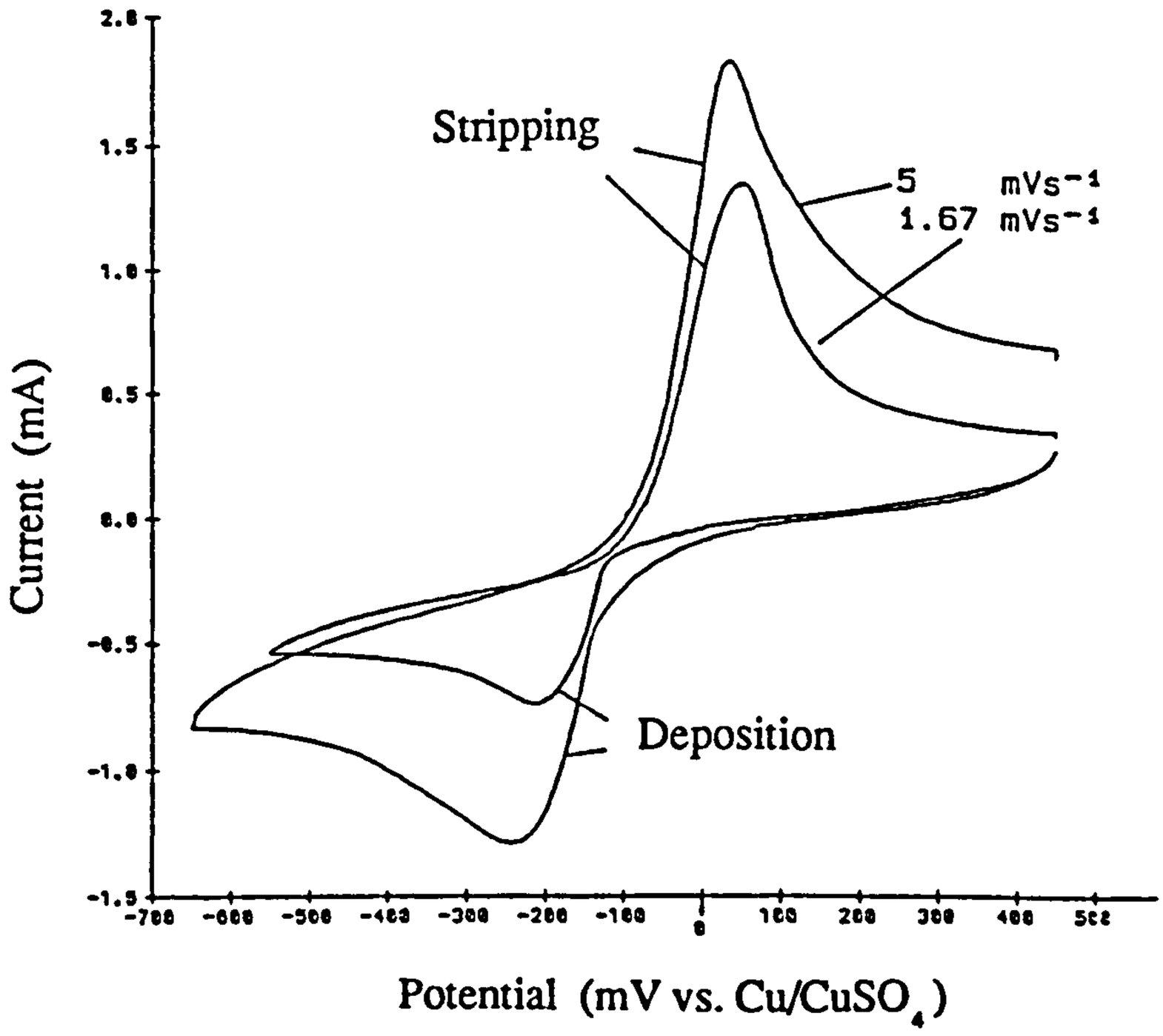

Fig. 42. Cyclic voltammograms for a 1 μm thick GC-$PPy^{+}(SO_4^{2-})$ electrode in 0.01 M $CuSO_4$ and 0.1 M H_2SO_4 supporting electrolyte; (a) immediate response, (b) response after immersion in the same solution for ~15 hours.

This tailing is indicative of an additional electrode process other than that associated with the stripping of copper from the electrode surface. Logarithmic analysis of this *i-E* response at potentials beyond the stripping peak is shown in Fig. 43. For a diffusion controlled reaction, the *i-E* response at potentials greater than E_p can be assumed to be the same as that for a large amplitude potential step and will decay according to $t^{-1/2}$ [19]. Linear regression analysis gives a slope of -0.496 ± 0.005, with a correlation coefficient = -0.996. This value of 0.5 is consistent with the diffusion of Cu^{2+} into bulk solution from within the polypyrrole film.

The similarity of the *i-E* response for GC-$PPy^{+}(SO_4^{2-})$ electrodes at potentials less anodic than the stripping peak, would also suggest that Cu^{2+} is lost from the film on the anodic cycle only after the surface stripping reaction is almost completed. This seems plausible, since a surface copper deposit would be expected to form an impermeable barrier to the diffusion of ions from within the film.

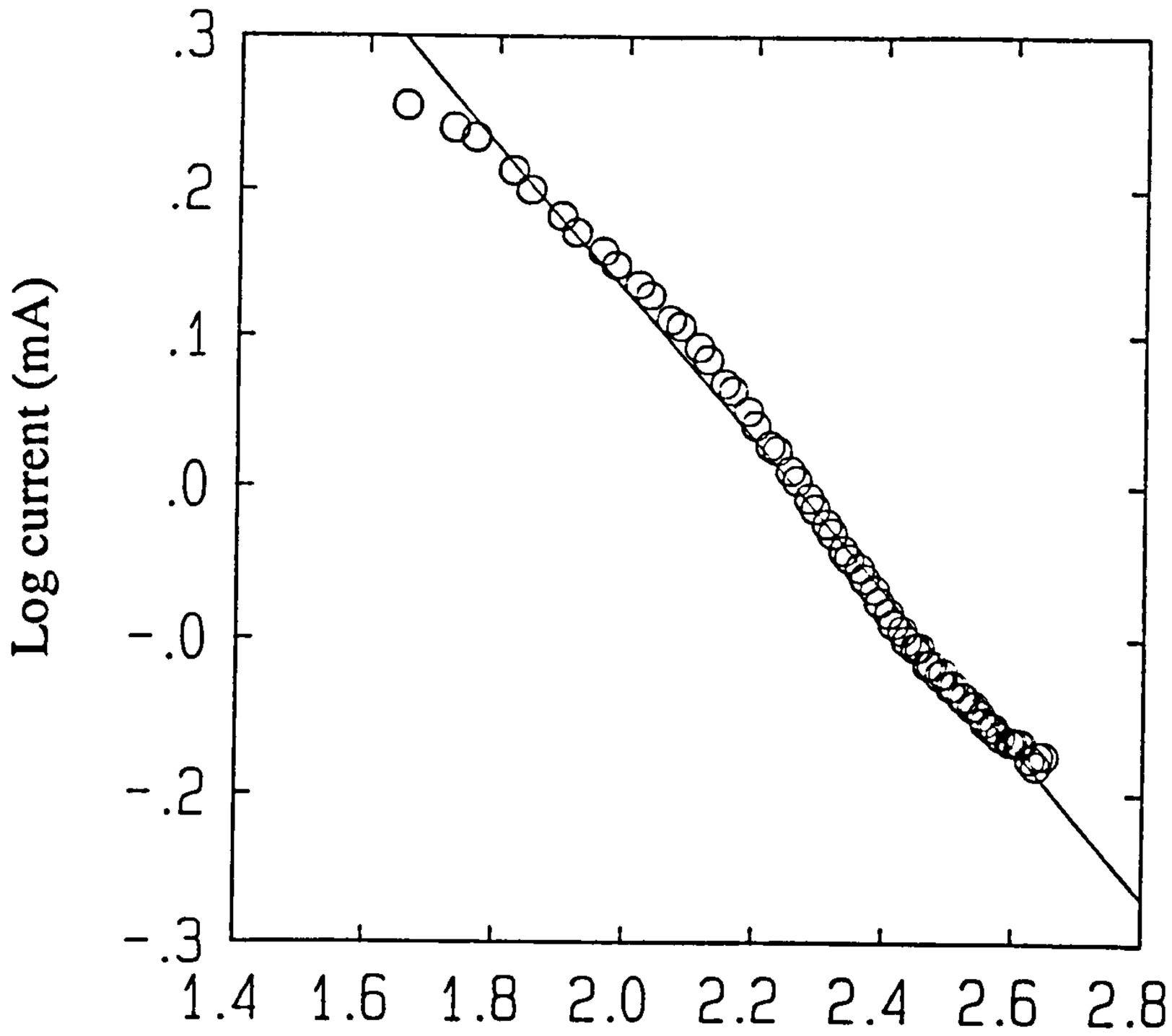

Fig. 43. Logarithmic analysis of the current-voltage response of Fig. 42b (5 mVs^{-1}) for electrode potentials in between 0.05 and 0.45 V.

The small reduction in anodic peak height values after standing in electrolyte solution, indicates that the stripping efficiency is reduced. This was confirmed by the fact that traces of copper were still visible on the electrode surface after the anodic scan was completed. However, since the i_{pa} values are only slightly reduced in magnitude, it can be argued that the amount of copper which is deposited onto the electrode surface remains approximately the same as that prior to immersion. Consequently, the increased cathodic currents which were obtained after immersion must originate from the reduction of Cu^{2+} to Cu^{o} incorporated within the film matrix, and are not due to a greater deposition of copper at the electrode surface.

5.7 Summary.

The results obtained in sections 5.6.1 and 5.6.2 clearly demonstrate the porosity of polypyrrole to solution based electrolyte when in the oxidised state, via the incorporation of Cu^{2+} which is electroactive in the potential range over which was scanned (± 0.65 V). Electrolyte from solution may incorporated by polypyrrole during cyclic voltammetry, when the film is cycled between its oxidised and reduced states, or by simply leaving to stand in solution.

This demonstration of the porosity of polypyrrole to ions in solution, is in accord with the recent consensus forwarded in references[98,191-193] which also shows that polypyrrole films are permeable to electrolyte from solution, but in disagreement with the earlier conclusions of Diaz *et al*[183], which suggested that polypyrrole formed an impermeable layer to electrolyte.

The following section describes possible mechanisms for the incorporation of electrolyte from solution.

5.8 Mechanisms for the Incorporation of Electrolyte from Solution.

As described in sections 5.6.1 and 5.6.2, Cu^{2+} has been shown to readily incorporated by polypyrrole from solution during cyclic voltammetry studies, and when immersed in solutions containing Cu^{2+}.

The current accepted view of the redox behaviour of polypyrrole, is that on the application of an external potential of sufficient magnitude to effect reduction, the oxidised polymer $PPy^{+}(A^{-})$ is reduced to the neutral non-conducting PPy° state, with concomitant expulsion of anions in order to preserve overall charge neutrality[183,119]. This reaction is shown in equation 5.7:

$$PPy^{+}(A^{-}) + e^{-} \rightleftharpoons PPy^{\circ} + A^{-} \qquad (5.7)$$

This process has been shown to be "quasi-reversible", with reversal of the electrode potential to a value sufficient to re-oxidise the film causing the converse process to occur. When this occurs, solvent based anions, which need not necessarily be the same as those originally accommodated within the film, are re-incorporated into the polymer[115,118,119,174].

However, more recent studies of the redox process in aqueous conditions, suggest in some instances, the redox process is more accurately described in terms of a competitive process between cation insertion and anion expulsion. For example, the degree of electrochemical reversibility which is exhibited when polypyrrole is cycled between the oxidised and reduced states, and the extent of exchange of the original film counteranion with solution based anions has been shown to be dependent on a number of parameters. These include solvent properties[95], solution pH[116,118], and the anion size coupled with diffusional mobility in the polypyrrole matrix[116,192,193]. For relatively small counteranions such as ClO_4^{-}, Cl^{-} and NO_3^{-}, the loss and regain process has been demonstrated to be both physically and electrochemically reversible[116]. Whereas for larger anions such as SO_4^{2-}, TsO^{-} or AsF_6^{-} [116], or polymeric polyanions such as sodium poly(styrene-sulphonate), PSSNa, ($MW = 1.0x10^5$) and potassium (polyvinylsulphate), PVSK, ($MW = 2.5x10^5$)[193], this process is either only partly reversible, or in some instances almost totally irreversible. This is considered to be due to lower rates of diffusion of these larger anions.

In this situation, the redox process has been shown to be a combination of both cation insertion and anion expulsion, with the incorporation of low molecular weight cations such as Li^+, Na^+, and K^+ from the electrolyte solution, in order to compensate for the charge imbalance that results from the incomplete expulsion of the original film counteranion[117,118,191,192].

Moreover, this competitive mechanism of ion exchange is able to account for several aspects of the electrochemical behaviour of polypyrrole in the presence of Cu^{2+} ions. These are now discussed.

Copper deposition at a polypyrrole electrode may occur by means of a combination of several steps, such as those illustrated in Fig. 44. These include the reduction of ions at the polymer surface via mass transfer from solution (i), the reduction of ions which permeate a certain extent into polypyrrole during the cathodic scan but which do not deposit on the electrode surface (ii), the reduction of ions at the GC electrode surface (iii), and (iv) the reduction of Cu^{2+} previously incorporated into polypyrrole by diffusion from bulk electrolyte.

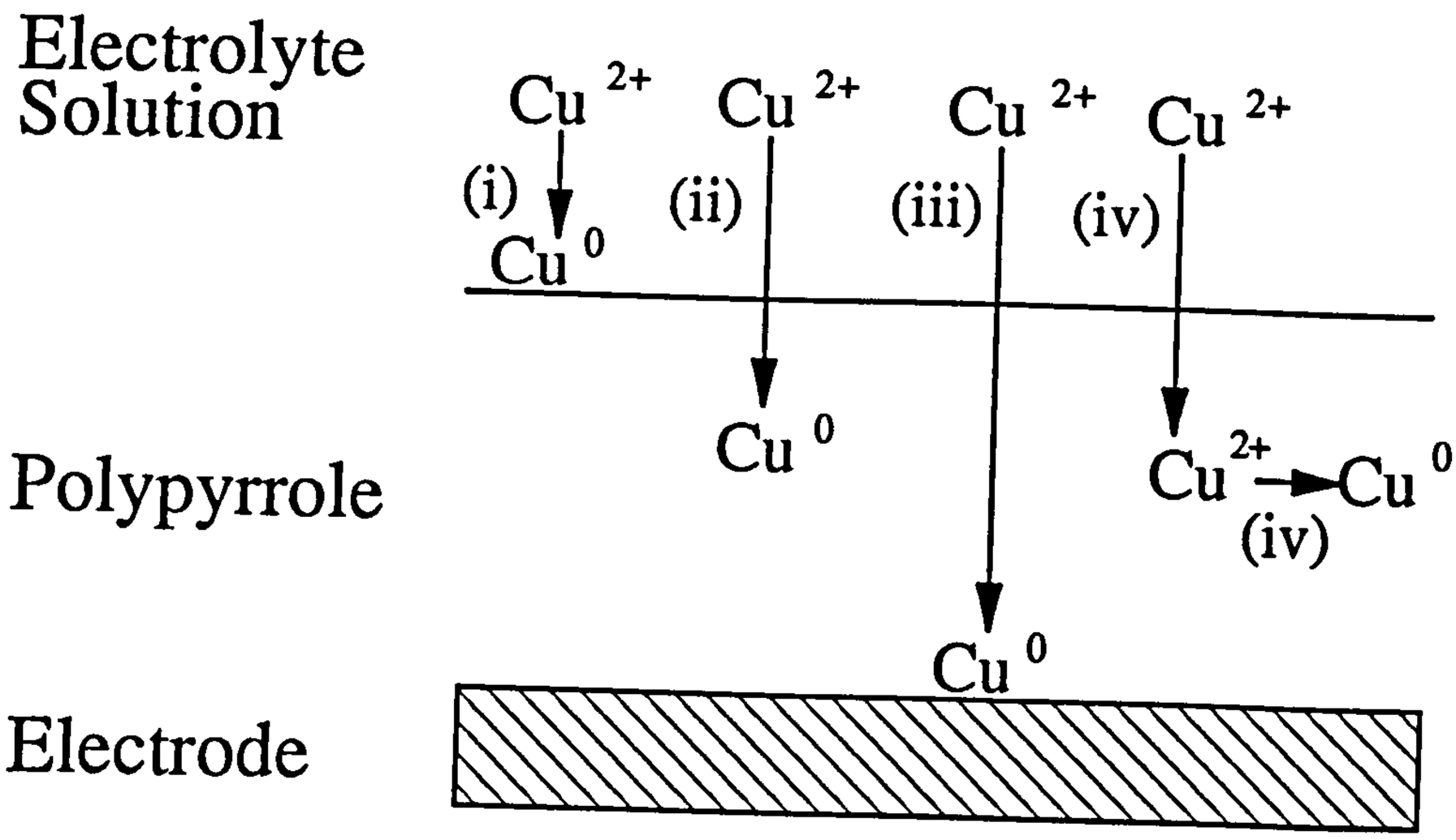

Fig. 44. Schematic representation showing possible mechanisms of metal deposition for a polypyrrole substrate.

When a fresh (previously unexposed to copper solution) polypyrrole substrate is cycled in the presence of Cu^{2+}, the predominant modes of deposition are a combination of steps (i) and (ii). This view is supported by sharp symmetrical shaped anodic stripping peaks (see Fig. 32) and the absence of correlation of i_p values with film thickness. If the predominant deposition mechanism was the reduction of copper ions at the electrode surface (step iii), peak currents would be severely depressed and would decrease with increasing film thickness[37,38]. This was not observed. After exposure to Cu^{2+}, deposition may also occur by the reduction of Cu^{2+} previously incorporated within the polymer matrix, step (iv). This gives rise to an increased cathodic current and "diffusional tailing" in the anodic region, such as that displayed in Fig. 42(b).

One interesting aspect of the electrochemistry of polypyrrole after cycling in copper solution, was that while metallic copper was readily stripped from the polymer surface, Cu^{2+} incorporated internally within the polymer matrix was much less readily expelled by cycling polypyrrole between its oxidised and reduced states. Indeed, in acidic conditions, and at low levels of incorporation, the level of Cu^{2+} remained unaffected by this cycling process as shown in Fig. 38. This behaviour is contrary to that expected from Eqn. 5.7 which predicts total anion expulsion from the film at electrode potentials for which polypyrrole is reduced. However, the seemingly anomalous behaviour of polypyrrole in Cu^{2+} is readily explained in terms of a competitive process between cation insertion and anion expulsion (see Fig. 45).

On the initial cathodic cycle, the charge imbalance resulting from the reduction of PPy^{+} to PPy^{o} is compensated for by expulsion of the original film counteranion, plus ingress of Cu^{2+} from solution. This is shown in Eqn. 5.8.

$$x/2Cu^{2+}_{(aq)} + PPy^{(n+)}(A^{-})_n + ne^{-} \rightleftharpoons PPy^{o}(A^{-})_{(n-x)}(Cu^{2+})_{x/2} + x\cdot A^{-} \qquad (5.8)$$

The amount of Cu^{2+} incorporated will depend on the relative mobilities of A^{-} and Cu^{2+} in the polypyrrole matrix. If mobility of the original film counteranion is low, or if the mobility of Cu^{2+} is significantly greater than A^{-}, then the charge imbalance resulting from reduction will primarily be compensated for by the

incorporation of Cu^{2+} from bulk solution. Since cyclic voltammetry was performed in the presence of H_2SO_4 supporting electrolyte, charge compensation by H^+ needs also to be considered.

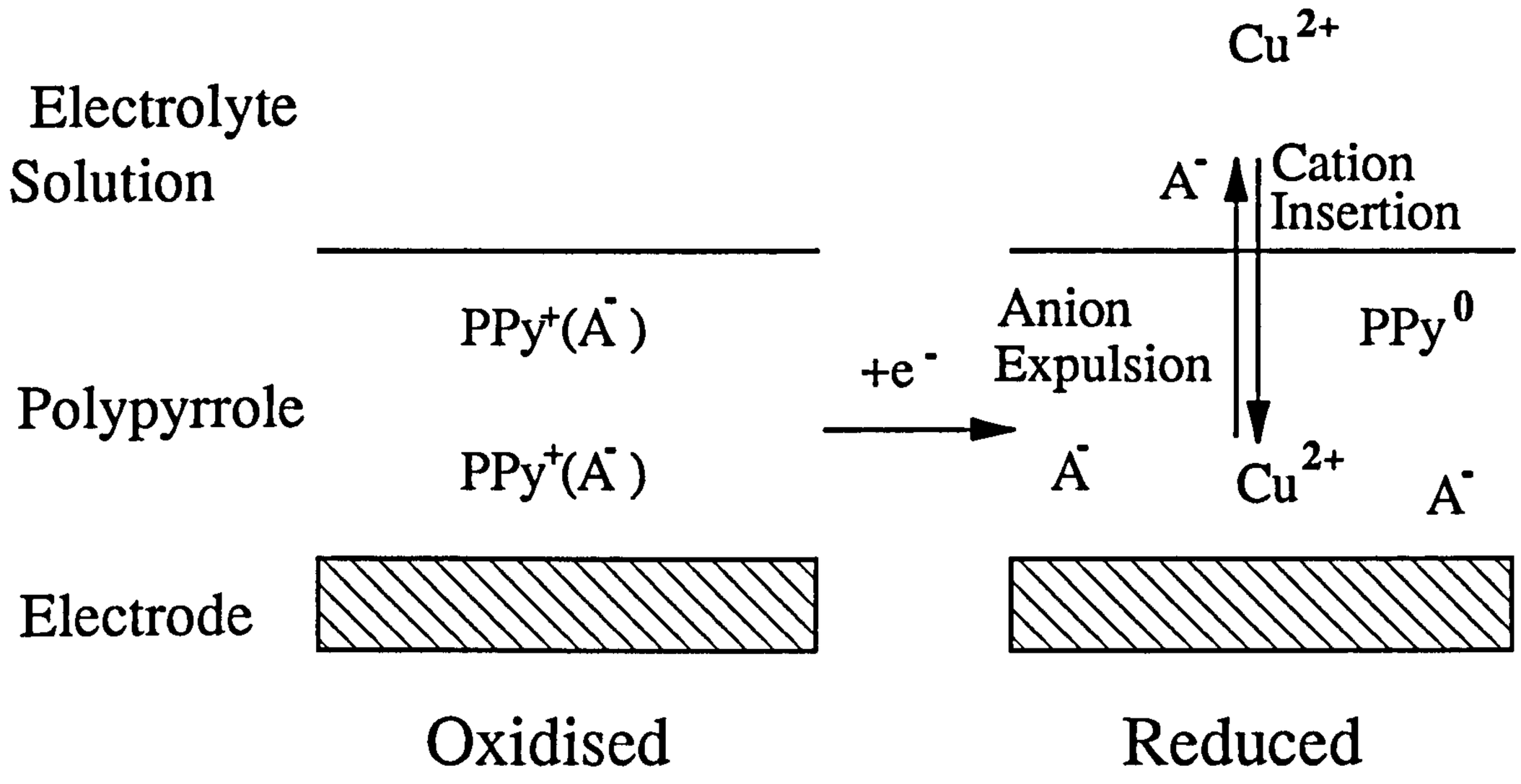

Fig. 45. Proposed mechanism for the incorporation of Cu^{2+} by polypyrrole during reduction. Overall film neutrality is maintained by anion expulsion coupled with cation insertion.

As the electrode potential is increased to more cathodic values, Cu^{2+} incorporated by polypyrrole during the initial stages of film reduction (Eqn. 5.8) is reduced to Cu°. This shown by the increased cathodic current at potentials between -0.05 to -0.45 V in Figs. 38 and 42(b). The charge imbalance resulting from the reduction of Cu^{2+} to Cu° is readdressed by the simultaneous expulsion of SO_4^{2-}, coupled with ingress of H^+ from solution.

On the anodic cycle, the charge imbalance resulting from oxidation of PPy° and Cu° is accounted for by a competitive process involving concurrent expulsion of Cu^{2+} and H^+, coupled with ingress of SO_4^{2-}. At low levels of Cu^{2+} incorporation, results obtained in section 5.6.1 suggest that overall film neutrality is restored primarily by the diffusion of SO_4^{2-} and H^+. However, at higher concentrations of Cu^{2+}, and at

anodic potentials, it is conceivable that Cu^{2+} will be expelled due to differences in concentration of copper ions in polypyrrole and in bulk solution, plus some electrostatic interactions between Cu^{2+}/Cu^{2+} and Cu^{2+}/PPy^{+}.

5.9 Morphology of Copper Deposits.

The morphology of copper electrodeposited on to the surface of polypyrrole substrates was examined using scanning electron microscopy (SEM). $PPy^{+}(SO_4^{2-})$ films adhered strongly to the GC substrate and could not easily be removed intact for analysis. To overcome this problem, several parameters were altered to improve the mechanical properties of the film and reduce adhesion. The polypyrrole coat thickness was increased to ~20 μm, the sulphate anion was exchanged for *p*-TsO^{-} to improve the mechanical strength[80], and the GC electrode was replaced with a stainless steel electrode polished to a 1 μm finish. The resultant films were easily removed and possessed good mechanical properties, as evidenced by the ability to be flexed without damage.

Following preparation, free-standing films were then rinsed thourghly in de-ionised water, before plating from a $CuSO_4/H_2SO_4$ solution. This was carried out according to the procedure described in section 3.16.1.

Copper deposition was observed immediately the potential was stepped to -0.9 V (*vs.* $Cu/CuSO_4$ ref.). By varying the current density, highly reflective and cohesive deposits were formed on the smooth surface of the polypyrrole film. These possessed good adherence, and were not easily removed by abrasion. Furthermore, the reflective appearance of the deposit was retained over a period of several months, and did not appear to tarnish any more rapidly than copper which was deposited onto metallic substrates. Copper was also readily deposited on the reverse side of the polypyrrole substrate facing away from the counter electrode, although the rough surface of the film did not permit the formation of reflective deposits.

Following deposition, the surfaces of coated polypyrrole substrates were characterised using SEM, using the procedure previously described in section 3.9. The

copper coated substrates were found to be sufficiently conducting, that further preparation in the form of an additional conductive surface coat was not necessary.

The surface morphology of the polypyrrole film which was in contact with the electrolyte solution was rough, and exhibited dendrite like growth which is similar to that previously reported for polypyrrole grown both in anhydrous[76] and aqueous[101] electrolytes. This type of growth is reminiscent of dendritic growth in metal deposition (see chapter 8), and is likely to be caused by the same phenomenon, namely, enhanced deposition rates at protrusions on the electrode surface[194].

In contrast, the surface of the film that directly contacted the electrode was smooth, and revealed little detail when examined by SEM.

Plates. 1(a-b) show micrographs of copper deposited on the rough side of the polypyrrole substrate at various magnifications. The large roundish features are the dendritic type structure of the underlying polypyrrole substrate. The smaller more uniform features are copper aggregates. From these micrographs, it may be seen that most of the particles have sizes that range between one and two microns in diameter. Closer inspection of some of these nuclei, show them to be composed of aggregations of a number of smaller nuclei with diameters less than 0.5 μm. However, the precise dimensions were not measurable due to the limits of resolution of the SEM. The aggregations of copper particulates show that once copper nuclei are formed, successive deposition then occurs preferentially at existing growth centres, rather than by further nucleation at other sites on the polypyrrole substrate. This observation is consistent with previous cyclic voltammetry results in section 5.4, which show a decrease in the potential needed for deposition once nucleation has taken place.

In contrast with metal deposition on the rough surface of polypyrrole, SEM observations of copper deposited onto the smooth surface of the polypyrrole substrate revealed an almost continuous and uniform copper layer, formed by the coalescence of similarly sized copper aggregates, with sizes much less than on the rough side of the film. It is considered that this is a result of the greater current density at the smooth surface of the polypyrrole film, due to the fact that this surface was facing the counter electrode.

(a)

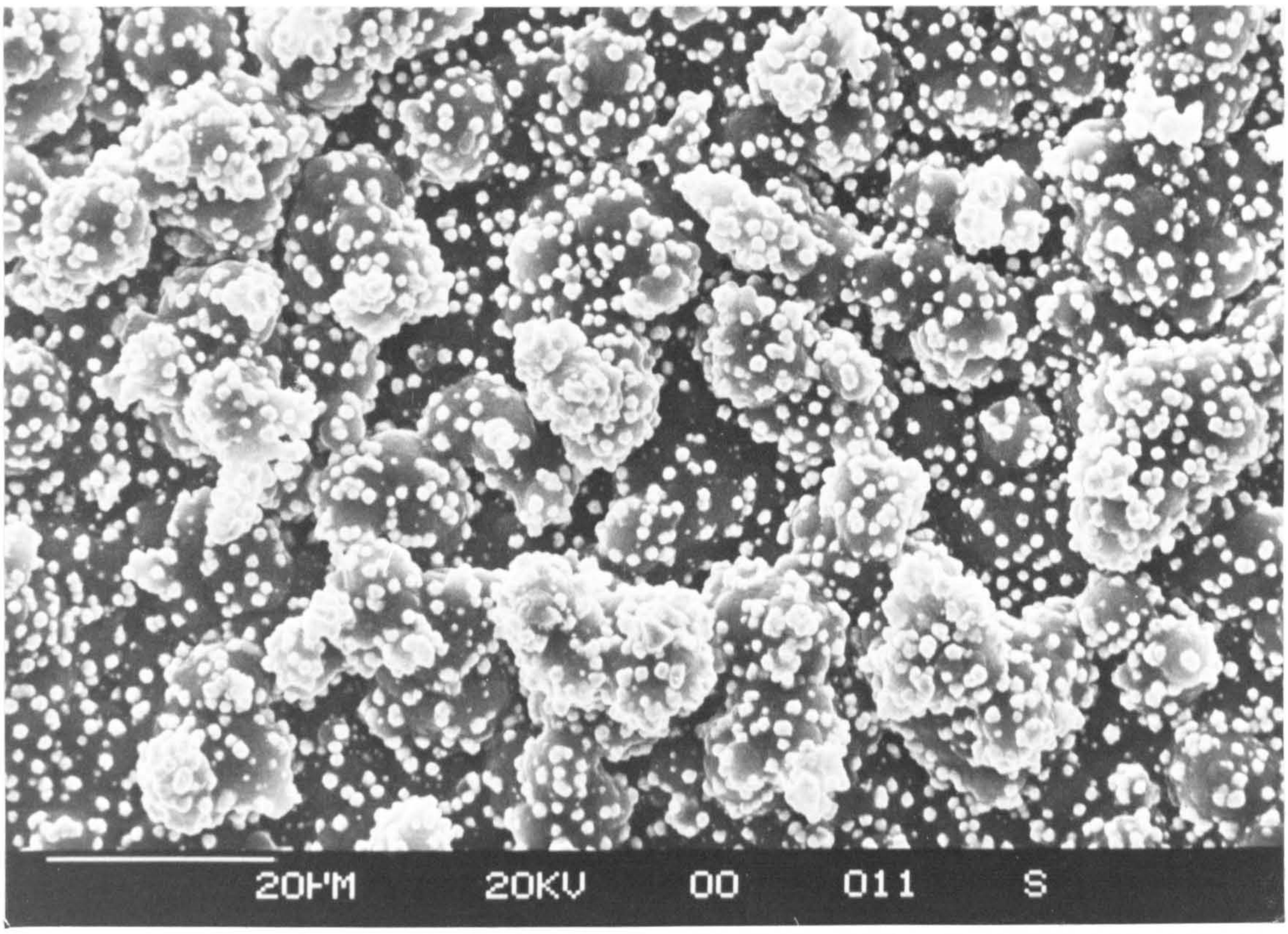

(b)

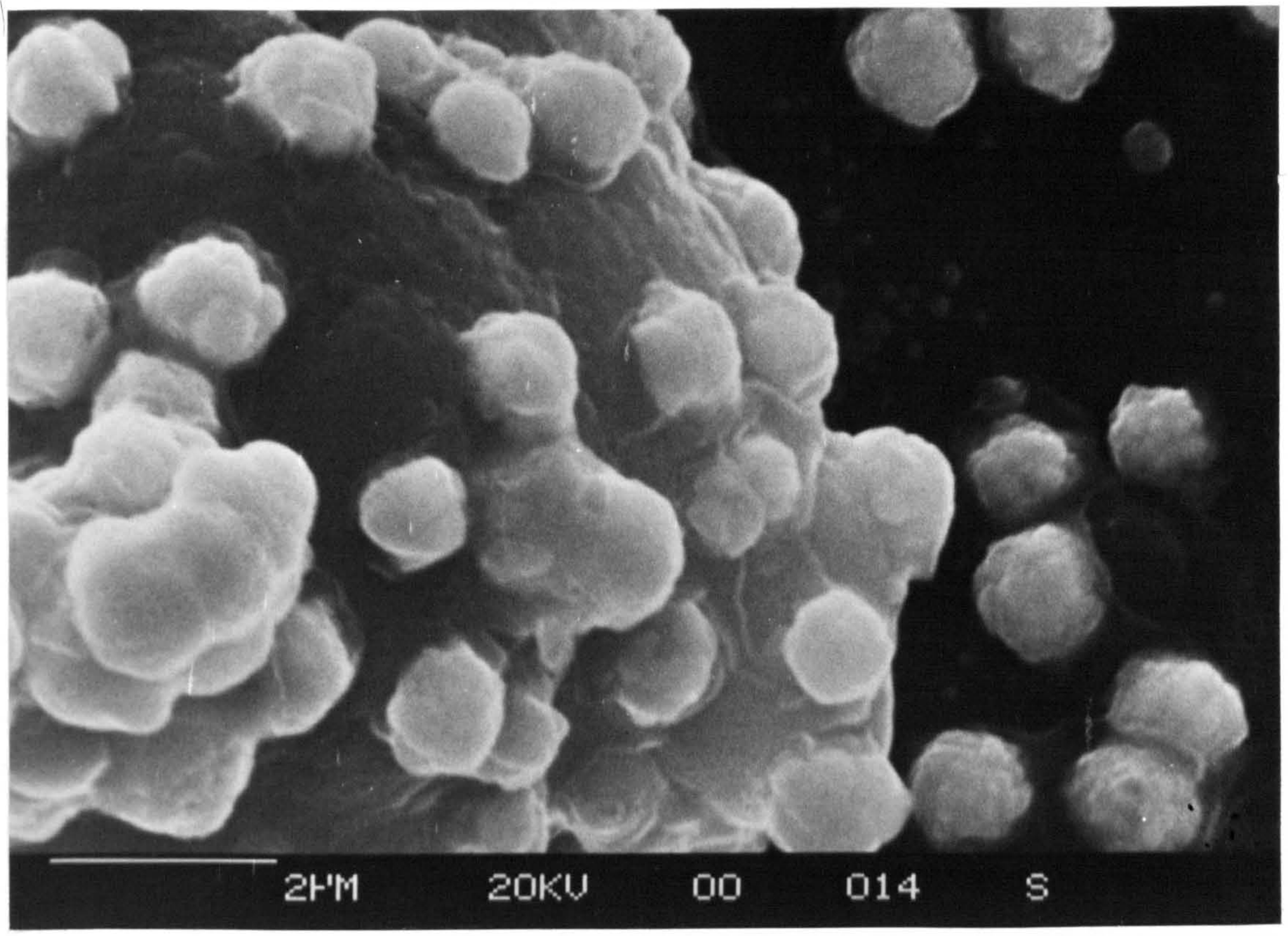

Plates 1(a-b), Copper aggregates deposited onto free-standing $PPy^{+}(p\text{-}TsO^{-})$ from 0.32 M $CuSO_4$ and 2 M H_2SO_4 solution at -0.9 V vs. $Cu/CuSO_4$ reference electrode.

The similar size of the copper aggregates deposited on the polypyrrole substrate, suggest that copper deposition occurs by a mechanism of instantaneous nucleation followed by growth. This deposition mechanism is frequently observed for electrocrystallization on metal surfaces when the deposition overpotential is small, and when the nucleation kinetics are rapid. This results in the formation of many nuclei at approximately the same time, which then continue to grow similarly in size thereafter. In contrast, progressive nucleation, the other common type of nucleation in electrocrystallization, occurs over a period of time and produces a variety of different sized growth centres[37].

The morphology of the copper deposit at polypyrrole shows instantaneous nucleation and growth, and concurs with previous results in Table 5, which show that only a small nucleation overpotential is required for the deposition of copper at GC-$PPy^{+}(SO_4^{2-})$ electrodes compared to deposition at bare graphite.

The deposition of metal aggregates (Ag. Pt), has also been reported on poly-(3-methylthiophene), a polyheterocyclic conducting polymer analogue of polypyrrole[41], and also on poly-$[Ru(bpy)_2(vpy)_2]^{2+}$ (Ag, Cu, Co, and Ni)[37], a mixed redox state conducting polymer [bpy=2,2'-bipyridine; vpy=4-vinylpyridine]. A comparison of the different morphologies of metal deposit, shows that copper deposited onto polypyrrole was similar to that obtained for the deposition of silver and platinum at poly-(3-methylthiophene), as might be expected in view of the similar nature of these materials, but in contrast to the "spongy, non-uniform, porous and dendritic" surface coats produced at poly-$[Ru(bpy)_2(vpy)_2]^{2+}$. These differences in morphology of metal deposit are thought likely to arise from the different types of electron transfer mechanism which operate in both these polymers. In polypyrrole and poly-(3-methylthiophene), charge transport is electronic, and is thus expected to be rapid and favour instantaneous nucleation, whereas charge transport in poly-$[Ru(bpy)_2(vpy)_2]^{2+}$ is diffusion controlled and occurs via mixed redox states in the polymer (see section 1.5.2). The slower rate of charge transport that is possible via mixed redox states, is thus more likely to promote progressive nucleation.

5.10 Cyclic Voltammetry of GC-PPy$^+$(NO_3^-) Electrodes in Silver Nitrate.

The deposition of silver from aqueous 0.01 M silver nitrate in 0.1 M KNO_3 supporting electrolyte, was studied by cyclic voltammetry, on GC-PPy$^+$(NO_3^-) substrates with thicknesses of 0.05, 0.5 and 5 µm. The method is detailed in section 3.11.

Silver deposition readily occurred on all GC-PPy$^+$(NO_3^-) substrates as was evidenced by the rapid formation of a silver deposit at potentials more cathodic than the reduction potential of Ag^+. Fig. 46 shows voltammograms obtained for the deposition of silver on a bare GC electrode, and on GC-PPy$^+$(NO_3^-) electrodes with polypyrrole coat thicknesses of 0.05 µm, 0.5 µm and 5 µm. Voltammograms of GC-PPy$^+$(NO_3^-) electrodes in 0.1 M KNO_3 electrolyte are included for comparison.

The cathodic limit on the potential scan is not sufficiently negative to completely reduce the PPy$^+$(NO_3^-) substrate to the neutral state, and only the initial portion of the reduction wave is observed. This occurred at around +0.20 V for the 0.05 µm film, +0.35 V for the 0.5 µm film and +0.40 V for the 5 µm film.

On the reverse scan, a slight anodic wave corresponding to the re-oxidation of the polypyrrole film is visible, and extends between +0.35 to +0.6 V. This becomes more apparent with increasing film thickness due to the increased charge associated with the redox process of the polypyrrole substrate.

The deposition of silver resembles that previously obtained for the deposition of copper. The deposition/stripping reaction of silver on bare GC displays a reduction peak at E_{pc} = 0.29 V, coupled to an anodic stripping peak at E_{pa} = +0.57 V. This has a broad and asymmetrical shape which indicates that the stripping reaction is not fully reversible[195].

When deposition is carried out on coated substrates, the E_{pc} values, with the exception of the 0.05 µm thick coat, are shifted to slightly more cathodic potentials, indicating an overpotential for nucleation. With the 0.05 µm thick layer, the peak potential value at E_{pc} = +0.31 V is similar to that obtained on bare graphite, and a comparison with other electrochemical data obtained at the un-coated electrode (see Table 6) reveals only minor differences.

(a)

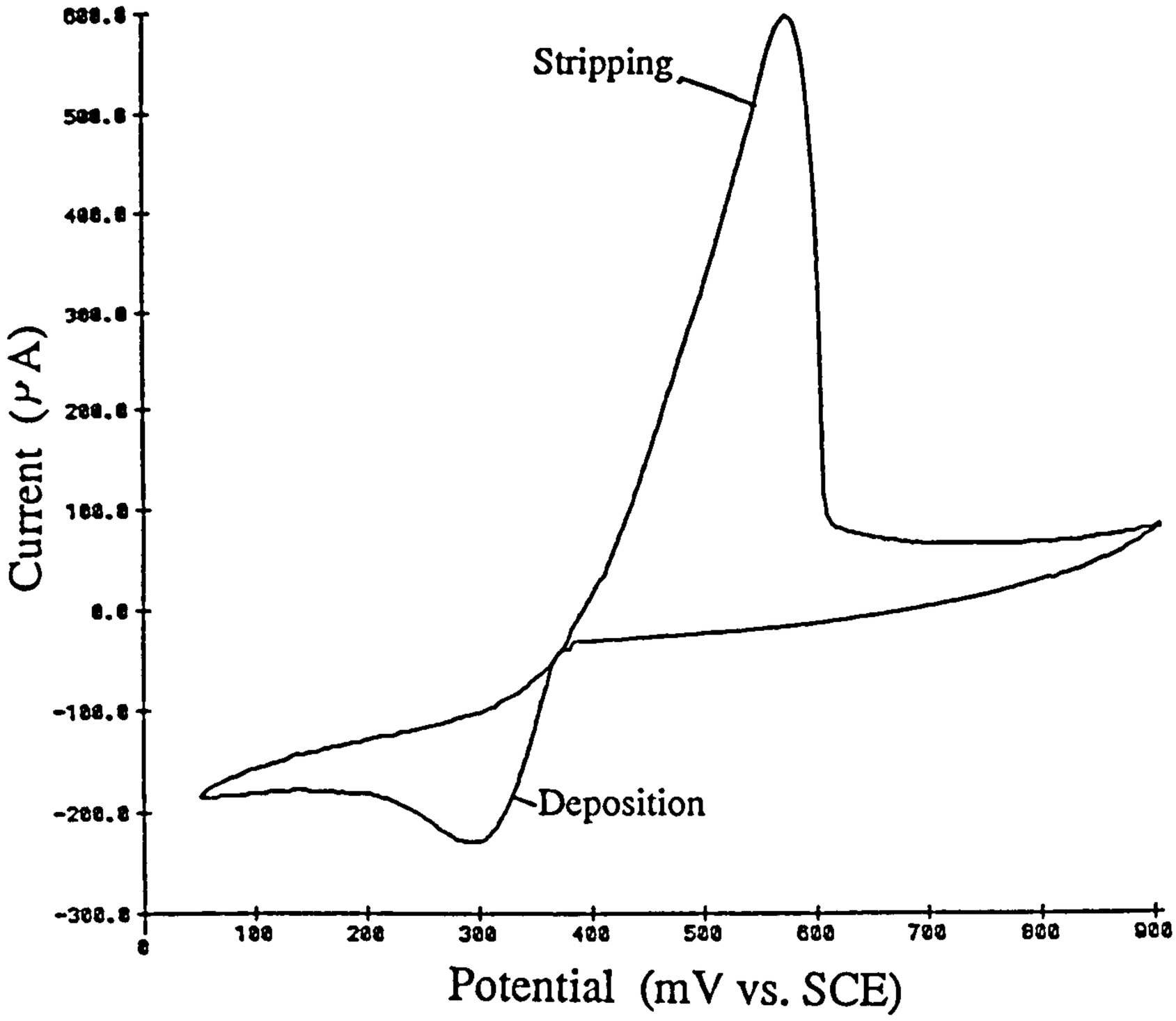

(b)

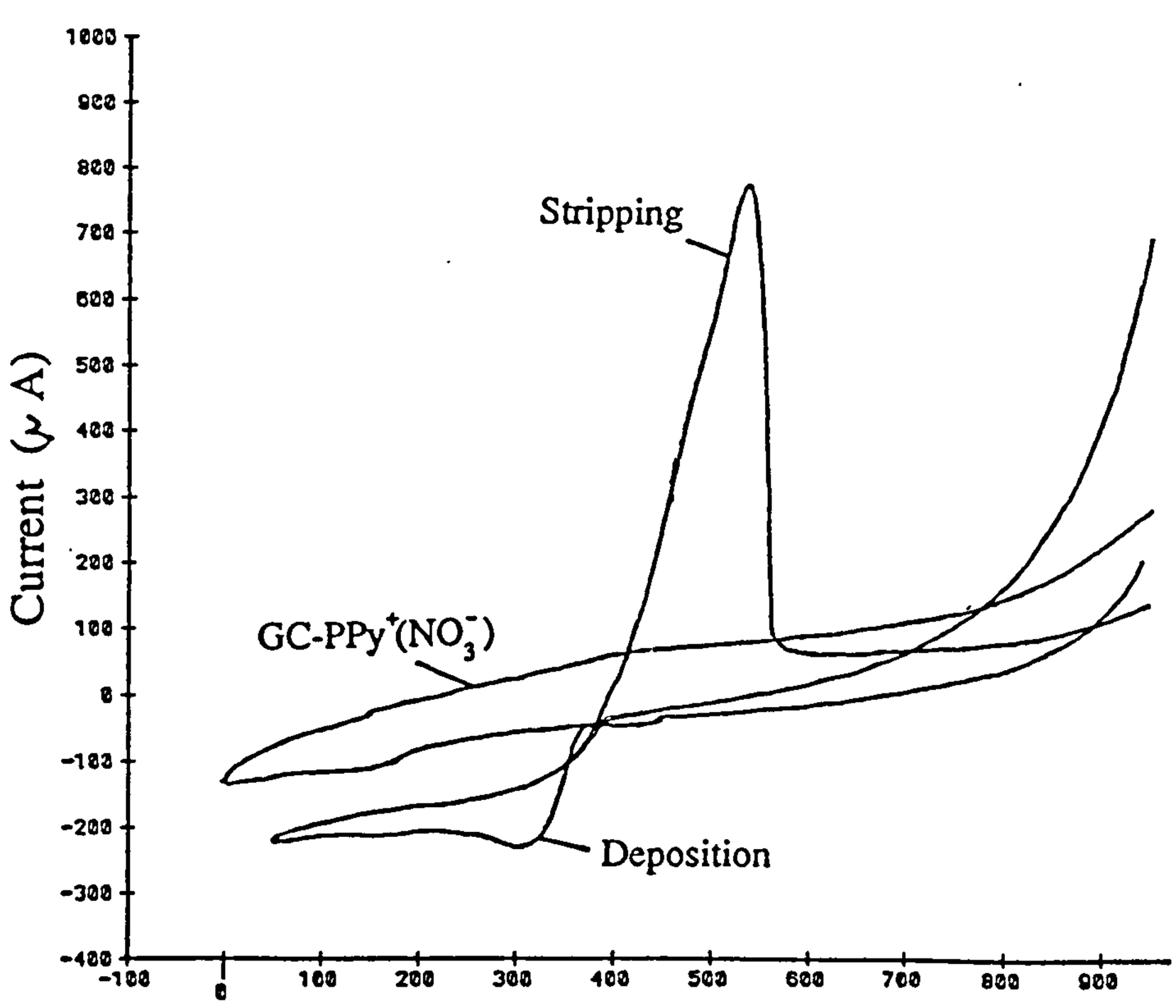

Fig. 46(a-b). Cyclic voltammograms showing silver deposition on (a) bare GC, and (b) GC with a 0.05 μm thick GC-$PPy^{+}(NO_3^{-})$ coat.

(c)

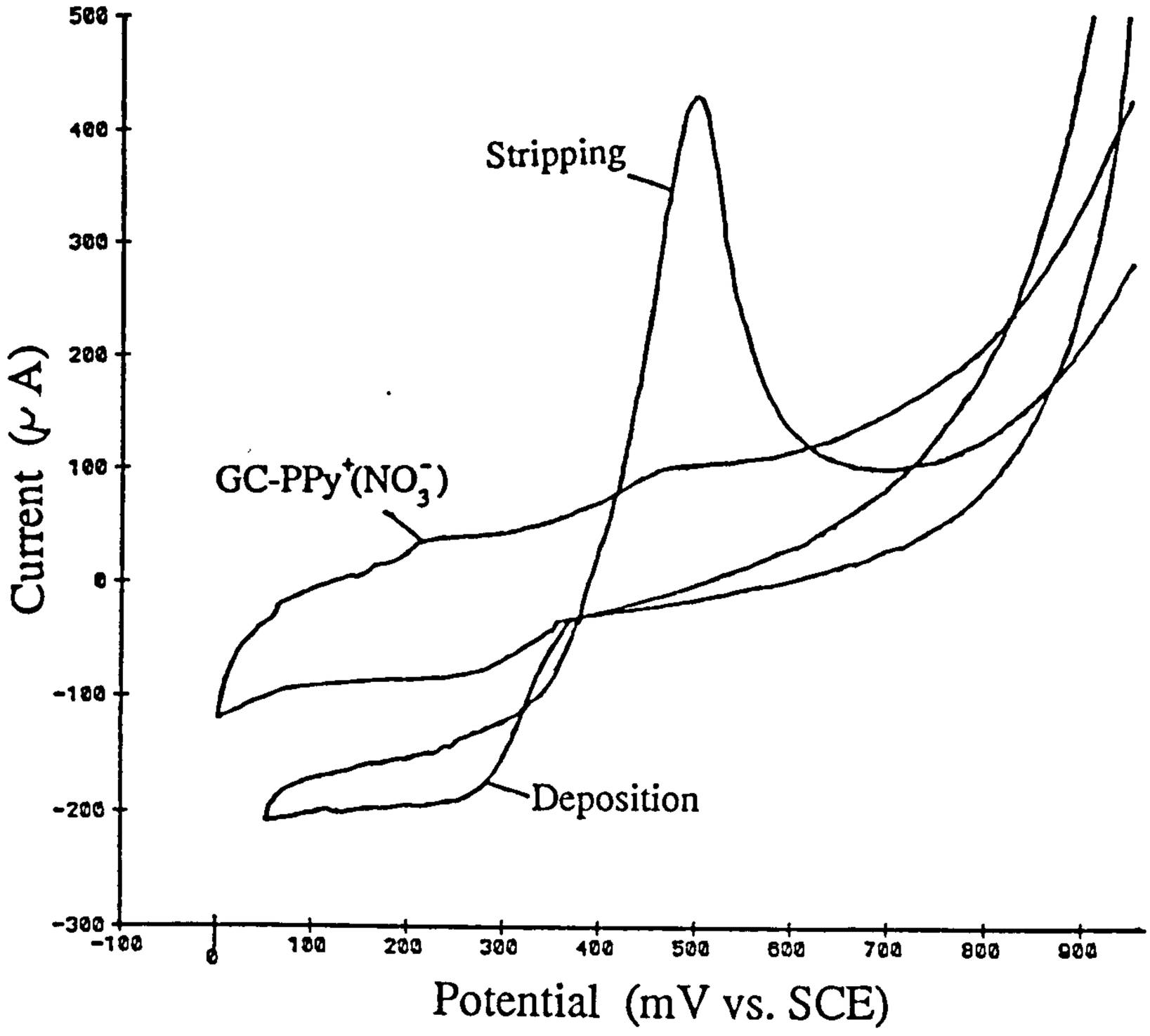

(d)

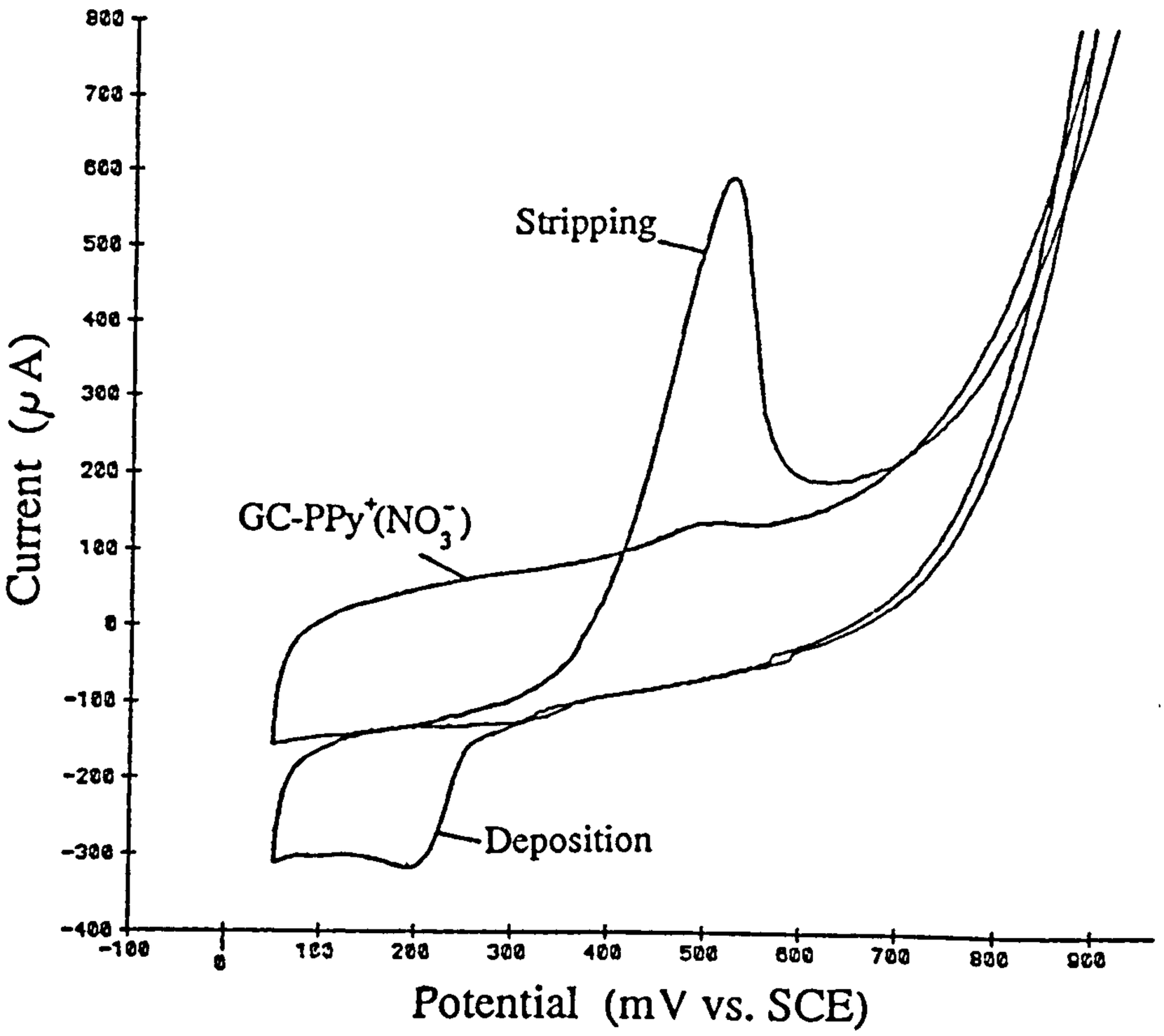

Fig. 46(c-d). Cyclic voltammograms showing silver deposition on GC-PPy^{+}(NO_3^{-}) electrodes with polypyrrole coat thicknesses of; (c) 0.5 μm and (d) 5 μm.

This could be due to the fact that silver deposition occurs before the onset of the reduction of polypyrrole at this coat thickness, as indicated in Fig 46(a). However, in view of the asymmetric anodic stripping peak (which is similar in shape to that obtained with bare GC) and the large i_{pa} value, it is also conceivable that the electrode surface is not completely covered with polypyrrole. This would also account for the similarity in the observed electrochemical response at both these electrodes.

Table 6. Electrochemical parameters for the deposition and stripping of silver at GC and GC-PPy$^+$(NO_3^-) electrodes of various thicknesses.

Electrode	E_{pc} (V)	i_{pc} (μA)	E_{pa} (V)	i_{pa} (μA)	ΔE_p (V)	PWHH (mV)
Bare GC	+0.29	193	+0.57	537	0.28	102
GC-PPy (0.05 μm)	+0.31	180	+0.53	705	0.22	80
GC-PPy (0.5 μm)	+0.26	114	+0.50	330	0.24	85.3
GC-PPy (5 μm)	+0.19	184	+0.52	461	0.33	80

Key: PWHH=Peak width at half height.

As the thickness of the polypyrrole substrate is increased, the effects of the substrate on the deposition process becomes more pronounced, so that for the 5 μm substrate, the overpotential for silver deposition has increased to E_{pc} = +0.19 V. The cathodic peak shapes also become more rounded in appearance, and the current plateau which is observed after the deposition peak in Fig. 46(c), suggests that the deposition process is kinetically controlled[196]. The increase in the overpotential for deposition which accompanies the increasing film thickness is also consistent with the higher current on the reverse scan (anodic direction), at potentials prior to the stripping peak for both the 0.05 and 0.5 μm thick GC-PPy$^+$(NO_3^-) electrodes. The absence of this overlap with the 5 μm film is presumably due to the larger background current of this electrode, rather than differences caused by the thicker polypyrrole coat.

The increase in overpotential for deposition, coupled with the current overlap at potentials prior to the metal stripping reaction, indicates that the nucleation of silver

is retarded by the presence of the polypyrrole coat, and is in accord with previous results obtained for the deposition of copper at polypyrrole. The substantial difference in nature between polypyrrole and silver is considered a likely explanation for both these nucleation effects[37,38].

When the i_{pc} values are corrected for the effects of the background current by subtracting the current contribution from the underlying polypyrrole substrate, the values for the deposition process are within less than 7% of that obtained on the uncovered graphite electrode, with the exception of the 0.5 µm coat. This similarity suggests that the deposition of silver occurs primarily at the polypyrrole substrate surface in a similar fashion to that obtained with copper deposition, and not on the underlying graphite electrode.

Although silver deposition appears to be retarded by the increased thickness of the polypyrrole coat, the anodic stripping process remains largely unaffected. Peak shapes of the 0.5 and 5 µm films are well defined and are symmetrical about the peak position at E_{pa} ~0.52 V. Peak width at half-height (*PWHH*) values are also close to the value of 90 mV (n=1) expected from Eqn. 5.9 for a surface reaction with Nernstian behaviour[197].

$$\Delta E_{p.\left(\frac{1}{2}\right)} = \frac{3.53\ RT}{nF} \qquad (5.9)$$

Where F is Faraday's constant.

5.11 Summary.

The results of cyclic voltammetry studies at GC-PPy electrodes show that thin films of polypyrrole (0.05-20 µm), are sufficiently conductive to be used as substrates for the deposition of copper and silver from aqueous electrolytes.

The nucleation of these metals was retarded by the presence of the polypyrrole layer, even for very thin polypyrrole coat thicknesses (0.05 µm). This result is in accord with that obtained by Pletcher *et al*[38] for the deposition Pt, Pb and Pd at

polypyrrole electrodes. However, once an initial seed layer of metal had been deposited, growth occurred rapidly for the deposition of copper, and was diffusion controlled at scan rates up to 70 mVs^{-1}. In contrast, the growth of silver was limited by the polypyrrole substrate even at slow scan rates (1.16 mVs^{-1}).

The locus of metal deposition occurred mainly at the polypyrrole surface, by a mechanism of instantaneous nucleation and growth. Under optimised plating conditions, highly reflecting and coherent copper deposits were obtained.

Polypyrrole was demonstrated to be porous to electroactive species in solution, via the incorporation of Cu^{2+} ions. This result is in consensus with recent opinion[98,191-193] for the porous nature of polypyrrole. Cyclic voltammetry studies of polypyrrole electrodes in the presence of Cu^{2+}, suggests that the redox behaviour of polypyrrole is more complex than was originally assumed in the literature, and is more accurately described in terms of a competitive process of cation insertion and anion expulsion, rather than just by anion expulsion. Indeed, in solutions containing highly mobile cations such as H^+, Li^+ and Na^+, or with polypyrrole films containing large immobile counteranions, it is suggested that this mechanism might form the predominant mode for the restoration of charge imbalances that arise when polypyrrole is cycled between redox states.

CHAPTER 6

CHEMICAL METALLIZATION OF POLYPYRROLE

6.1 Introduction.

In conventional autocatalytic (electroless) plating, the surfaces of plastics and other non conductors are coated with the nuclei of precious metals in order to render them catalytic to electroless plating solutions. Palladium is the most commonly used metal to activate non-conducting surfaces, since, in general it is un-reactive to the formation of surface oxides and other passive layers. In principle, however, any conductor could be considered as a suitable conducting surface for deposition[4,16]. Following surface pretreatment, the subsequent stage is electroless deposition as previously described in section 1.3.1.3.

An accepted mechanism for the electroless deposition of copper (from a formaldehyde based plating solution) is shown in Fig. 47. Copper reduction is facilitated via electron transfer at the catalytic surface through adsorbed reactive chemical intermediates.

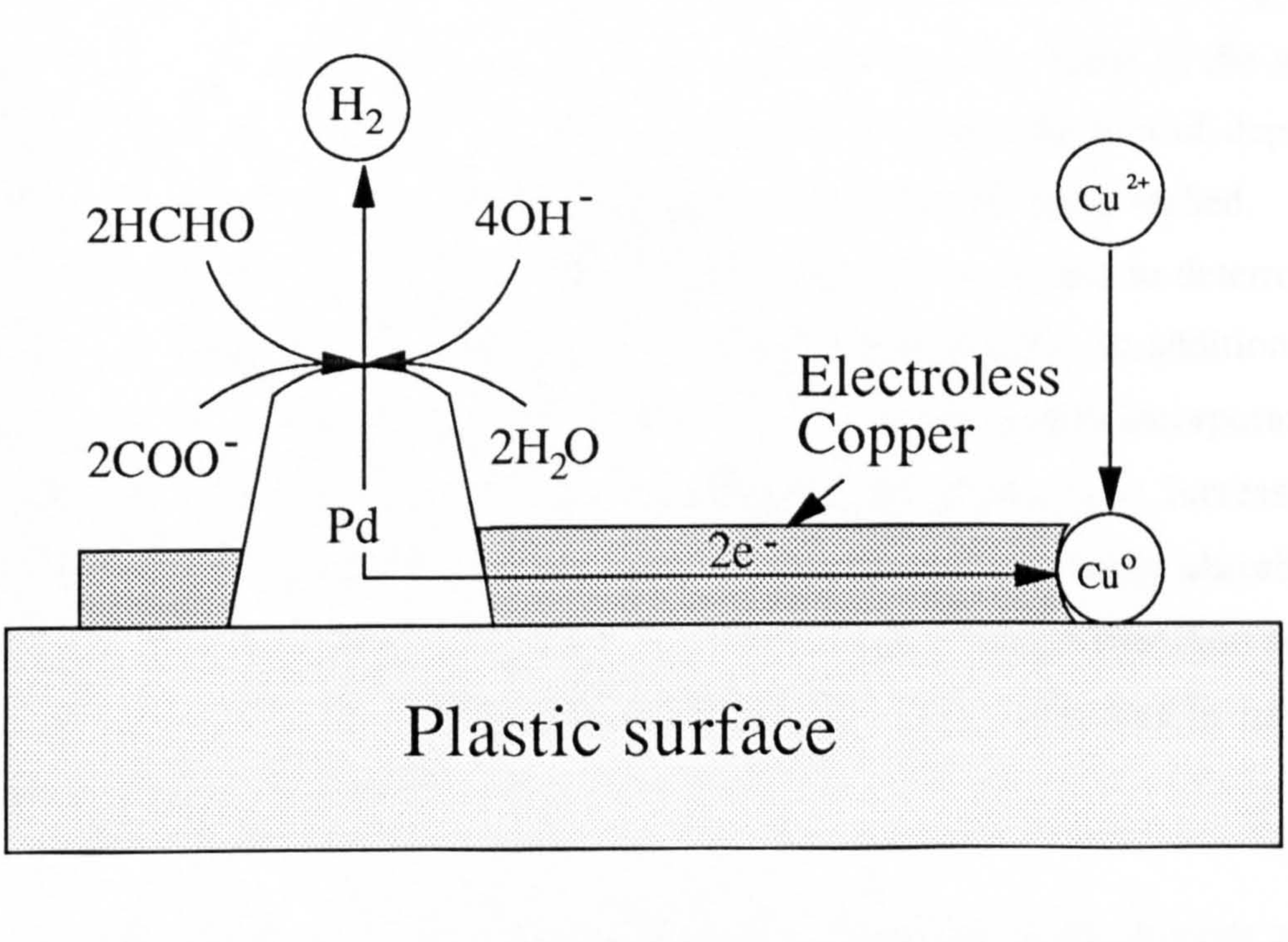

Fig. 47. Mechanism of electroless copper deposition at a plastic surface activated with palladium nuclei.

The electroactive form of formaldehyde responsible for the reduction of copper (II) ions can be either created in bulk solution by general base catalysis (Eqn. 6.1), or at the electrode surface by reaction with adsorbed OH^- (Eqn. 6.2), and is described by the following pair of equations.

$$H_2C(OH)_2 + (OH^-)_{ads} \rightleftharpoons [H_2C(OH)O^-]_{ads} + H_2O \qquad (6.1)$$

or

$$HCHO + (OH^-)_{ads} = [H_2C(OH)O^-]_{ads} \qquad (6.2)$$

The overall reaction can then be represented by the following half reactions;

Oxid^n. $$H_2C(OH)O^- = HCOOH + 1/2H_2 + e^- \qquad (6.3)$$

Red^n. $$[Cu(EDTA)]^{2-} + e^- = [Cu(EDTA)]^{3-} + e^- = Cu^\circ + EDTA^{4-} \qquad (6.4)$$

Whilst this technique has been utilized successfully since development in 1946[20,21], it has a number of disadvantages. It is expensive by virtue of the need for precious metal compounds, and in order to provide suitable adhesion of deposits, it can only be applied to plastics whose surfaces are capable of being etched.

This chapter describes investigations which were conducted to determine the suitability of polypyrrole as a substrate for electroless deposition. In addition to low cost, polypyrrole offers a number of other benefits. It can be readily incorporated into the surface of a wide variety of different polymer substrates, thus increasing the number of materials that might be plated. Since polypyrrole is actually absorbed into the surface of the host substrate, this method is also expected to provide firm adhesion of the surface coat, a problem still encountered with many substrates in traditional electroless plating technology.

Investigations were conducted on polypyrrole substrates which were prepared by both electrochemical and chemical methods. Although several metals are capable of electroless deposition, copper is most significant from a commercial point of view. Therefore, this chapter is restricted primarily to the electroless deposition of copper

from formaldehyde plating solution. Following this, section 6.4 considers the electrochemistry of polypyrrole in sodium hydroxide solution, a major component of the electroless plating solution. The interaction of base treated polypyrrole with oxygen is discussed in section 6.5. Finally, the chemical oxidation of base treated polypyrrole with copper and silver ions is covered in section 6.8.

6.2 Preparation of Substrates for Autocatalytic Copper Deposition.

As previously described in chapter 2, polypyrrole can be prepared by both electrochemical and chemical methods. Both of these procedures were utilized for the preparation of polypyrrole substrates for autocatalytic (electroless) deposition studies.

6.2.1 Electrochemically Prepared Substrates.

Electroless deposition was carried out on preformed $PPy^{+}(p\text{-}TsO^{-})$ substrates with thicknesses of approximately 25 μm. These were prepared according to the procedure previously described in section 3.10.

6.2.2 Chemically Prepared Substrates.

The synthesis of polypyrrole by chemical oxidative techniques leads to the formation of a powdery dispersion in the bulk of the oxidising solution. As such, this form of polypyrrole is unsuitable as a material for autocatalytic deposition. To overcome this problem, stripped polyethylene coaxial cable and filter paper were used as supports on which chemically oxidised polypyrrole was formed. Materials prepared by this procedure had the advantage of being easy to prepare and handle. Procedures used for the preparation of polyethylene and filter paper substrates are detailed in section 3.12.2.

The motivation for using coaxial cable was to find a technique suitable for replacing the copper wire braiding which is currently used to shield the inner copper core from electromagnetic interference.

6.3 Autocatalytic (Electroless) Copper Deposition.

After preparation, autocatalytic copper deposition studies were carried out using a simple formaldehyde based plating solution, according to the procedure previously detailed in section 3.16.2.1.

On immersion in the plating solution, chemically prepared paper composites and electrochemically prepared polypyrrole substrates immediately assume a copper/bronze colour. This colour change is similar to that previously reported for polypyrrole films that have been electrochemically reduced[99,114,198]. It was therefore considered likely, that the formaldehyde solution, which is a strong reducing agent at high pH, was causing the reduction of polypyrrole. However, after a period of about eight minutes, copper deposition was observed on the surface of the substrates. This extended to approximately one quarter of the substrate surface (total substrate area ~9.8cm^2) after leaving to stand for a further ten minutes.

This copper deposition was initially attributed to the catalytic activity of polypyrrole. However, further investigation showed that metal deposition did not occur until the onset of bulk decomposition of the plating solution.

The spontaneous decomposition of copper/formaldehyde plating solution is a common phenomenon in electroless plating[199] unless special preemptive procedures are taken. These include the filtering of solutions and the use of additives which retard metal deposition. The cause of instability arises from the formation of copper(I) oxide particles in the bulk plating solution (Eqn. 6.5), which can either undergo disproportionation (Eqn. 6.6), or react directly with HCHO (Eqn. 6.7). In both instances, copper powder is formed which subsequently catalyses the decomposition of the plating solution.

$$2Cu^{2+} + HCHO + 5OH^- \rightarrow Cu_2O + HCOO^- + 3H_2O \qquad (6.5)$$

$$Cu_2O + H_2O \rightarrow Cu^\circ + Cu^{2+} + 2OH^- \qquad (6.6)$$

$$Cu_2O + 2HCHO + 2OH^- \rightarrow 2Cu^\circ + H_2 + 2HCOO^- + H_2O \qquad (6.7)$$

Hence, it was concluded that the copper deposition on the polypyrrole coated substrates was caused by the indirect catalytic activity of either H_2 or copper particles adsorbed onto the surface of polypyrrole from bulk solution. Once catalytic nuclei become adsorbed in this way, they are then able to catalyse further electroless copper deposition, and the overall result is then difficult to distinguish from direct catalytic deposition.

Since polypyrrole is non-catalytic towards electroless copper deposition, further plating studies were concentrated on cathodic polarization as a method of activating autocatalytic deposition.

6.3.1 Initiation by Cathodic Polarization.

An alternative method of initiating electroless deposition on conducting substrates is by cathodic polarization[200]. This produces an initial metal deposit by electrodeposition which then catalyses electroless deposition. GC-PPy^+(p-TsO^-) substrates (~25 μm thick) were cathodically polarized for up to 3 minutes at potentials between -0.5 and -1.6 V (*vs.* SCE). The negative limit of the cathodic potential was determined by electrolysis of the electrolyte solution, with H_2 evolution at potentials more cathodic than this.

Consistent results from polarization studies were difficult to obtain, since polypyrrole films tended to shrink on immersion in the plating solution and detach from the electrode surface. However, even with films that did not detach, no evidence of copper deposition was observed for polarizations within the above potential range.

The shrinkage of polypyrrole on exposure to base solution has been reported previously[169,171], and is attributed to the exchange of the original film counteranion with OH^- from solution. Another effect of the interaction of OH^- with polypyrrole, which may also be related to the lack of deposition, is a decrease in conductivity of polypyrrole by up to 5 orders of magnitude[169,171,172]. This loss of conductivity would mean that electronic conduction through polypyrrole, which is an essential step in the catalysis of electroless deposition, would be difficult. The lack of catalytic activity of polypyrrole may also arise from interaction with formaldehyde solution. At pH > 10,

this is a sufficiently strong reducing agent to be able to effect the reduction of oxidised polypyrrole to the neutral non-conducting state.

The combination of these effects are considered likely explanations of why the attempts to electroless plate polypyrrole proved unsuccessful.

In order to investigate these points further, the electrochemistry of polypyrrole in basic solution was investigated using cyclic voltammetry. This is discussed in the following section.

6.4 Cyclic Voltammetry of Sodium Hydroxide Solution.

The electrochemistry of oxygenated and deoxygenated sodium hydroxide solution was examined at GC-PPy^{+}(*p*-TsO^{-}) electrodes and also at bare graphite for comparison. Cyclic voltammetry studies at both these electrodes were conducted according to the procedures previously described in section 3.11.

6.4.1 Response of Sodium Hydroxide at Uncovered Graphite Carbon Electrodes.

Cyclic voltammograms of 1.25 M NaOH solution at a bare graphite electrode are shown in Fig. 48, both before (scan b) and after (scan a) purging with O_2 free nitrogen (BOC white spot grade).

In the solution which had not been purged, a broad cathodic wave corresponding to the reduction of O_2, was observed at potentials more negative than 0.0 V (*vs.* SCE), with E_{pc} centred at ~ -0.5 V. This is coupled with a broad anodic oxidation wave at potentials more positive than ~0.0 V. The large potential separation for each of the redox processes, coupled with the much smaller limiting current on the anodic scan indicates that the reduction of O_2 is largely irreversible on graphite. Similar observations for the reduction of O_2 in base have been reported in other studies[201-203]. In the purged solution, only background current is observed.

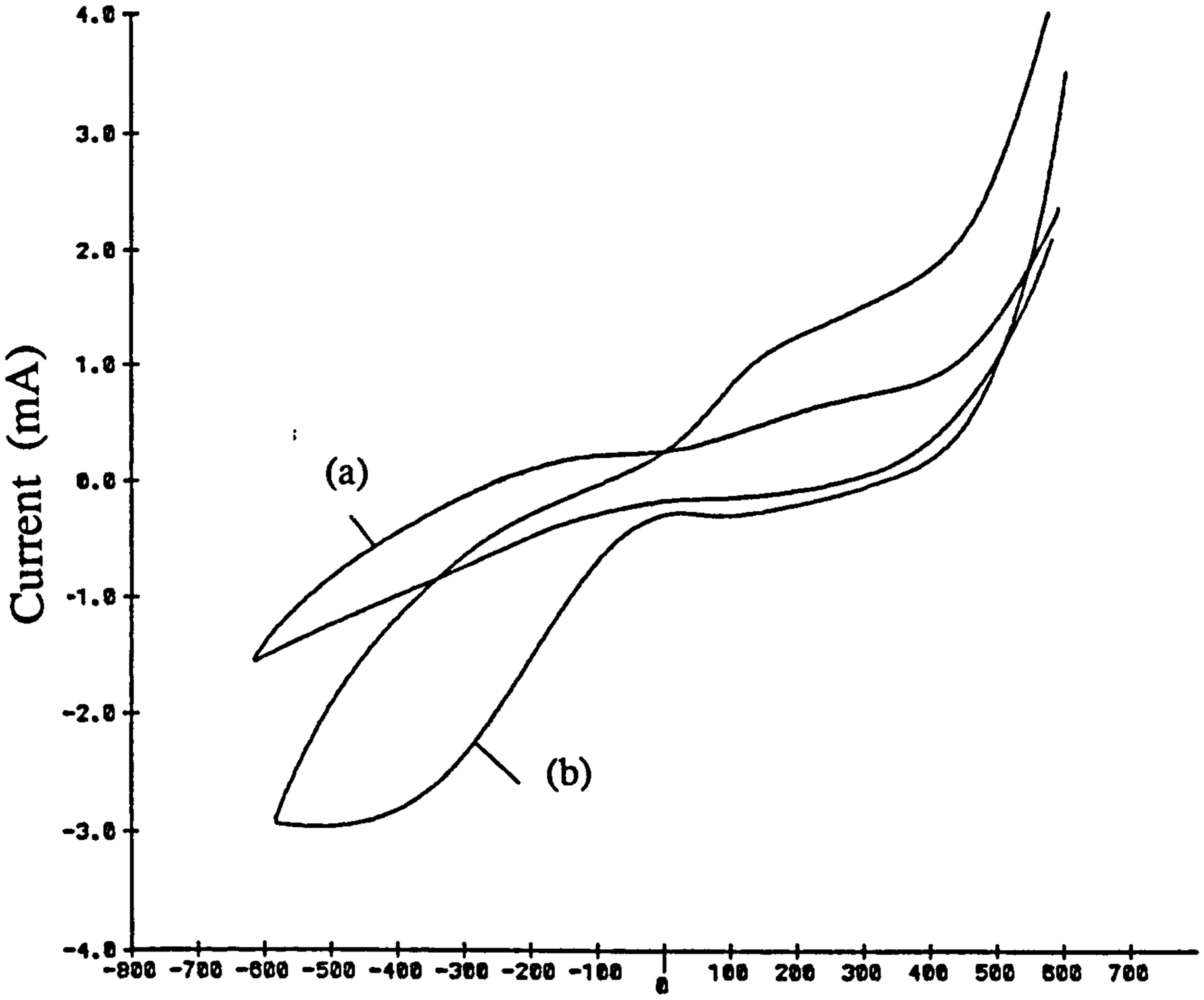

Fig. 48. Cyclic voltammograms of 1.25 M NaOH solution at bare graphite carbon; Scan (a), oxygen free solution, scan (b), oxygenated. Scan rate =10 mVs^{-1}.

Oxygen reduction at graphite carbon in alkaline solution has been studied by several investigators. The proposed mechanism for the electrochemical response of OH^- at bare graphite carbon enables the interpretation of the electrochemistry of GC-PPy^+(p-TsO^-) electrodes under analogous conditions.

The reduction of O_2 has been reported to occur by two two-electron transfer steps[201,204] in what is called the "sequential path". These may be represented by the following equations. Eqn. 6.8 describes the formation of a peroxide intermediate which then undergoes further reduction to OH^- at more cathodic potentials (Eqn. 6.9).

$$O_2 + H_2O + 2e^- \xrightarrow{E_p=-0.5V} HO_2^- + OH^- \qquad (6.8)$$

$$HO_2^- + H_2O + 2e^- \xrightarrow{E_p=-1.5V} 3\ OH^- \qquad (6.9)$$

Since reaction 6.9 occurs at E_p = -1.5 V, the reduction wave observed in Fig. 48 is attributed to step 6.8. This is composed of a number of more elementary steps which may be represented by Eqns. 6.10(a)-(d). The initial step (a) is the adsorption of O_2 at the graphite electrode surface to produce GC···O_2. This is then followed by electron transfer (b), proton transfer from a water molecule (c), and finally, a second electron transfer step to produce peroxide. The peroxide then undergoes a further two-electron reduction to OH^- as described in Eqn. 6.9.

$$O_2 + GC \rightleftharpoons GC\cdots O_2 \quad (6.10a)$$

$$GC\cdots O_2 + e^- \rightleftharpoons GC\cdots O_2^- \quad (6.10b)$$

$$GC\cdots O_2^- + H_2O \rightleftharpoons GC\cdots HO_2 + OH^- \quad (6.10c)$$

$$GC\cdots HO_2 + e^- \rightleftharpoons HO_2^- + GC \quad (6.10d)$$

6.4.2 Response of Sodium Hydroxide at Graphite Carbon-Polypyrrole/*para*-Toluene Sulphonate Electrodes.

GC-PPy$^+$(*p*-TsO$^-$) electrodes with thicknesses in the range 0.5 to 1 μm were prepared according to the procedure described in section 3.10. Cyclic voltammetry studies were performed in 1.25 M NaOH solution which had been thoroughly purged with oxygen free nitrogen.

The electrochemical behaviour of a GC-PPy$^+$(*p*-TsO$^-$) electrode in oxygen free NaOH solution is shown in Fig. 49. Scan a is the immediate response and scans b and c were obtained after standing the electrode in the same electrolyte solution for 15 and 60 minutes, with continuous purging of N_2 between successive scans.

The electrochemical response of the GC-PPy$^+$(*p*-TsO$^-$) electrode is comparable to the that obtained at a bare GC electrode under identical conditions (see Fig. 48), ie, the GC-PPy$^+$(*p*-TsO$^-$) electrode is not electroactive. Moreover, the similarity between Figs. (49a-c) indicates that any interaction of OH^- with polypyrrole occurs before the first scan is completed and implies that the interaction of OH^- with polypyrrole is rapid.

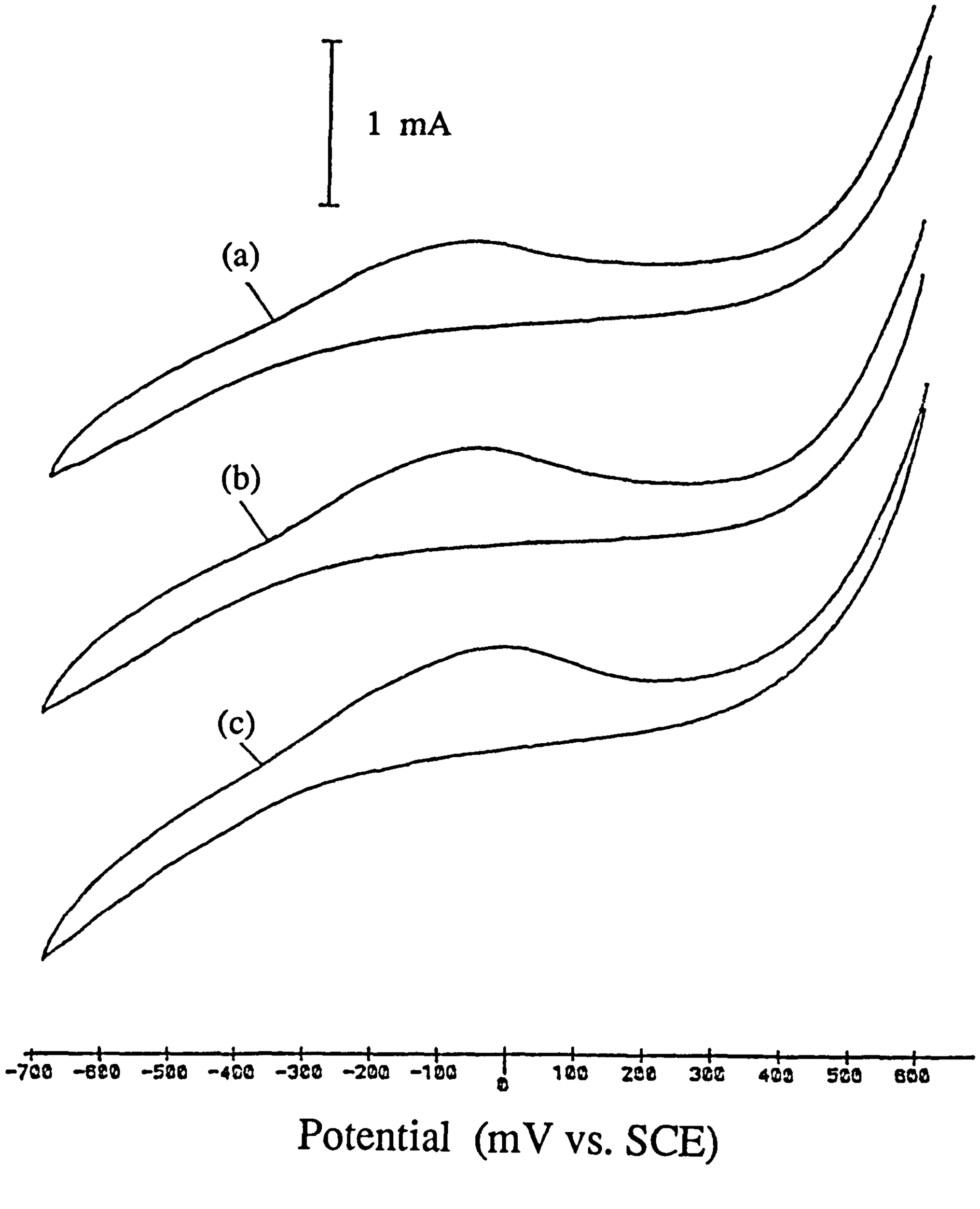

Fig. 49. Successive cyclic voltammograms of a 0.5 μm thick GC-PPy^{+}(*p*-TsO^{-}) electrode in deoxygenated NaOH (1.25 M) solution, (v=10mVs^{-1}). Scan (a) is the immediate response, scans (b) and (c) taken after 15 and 60 minutes respectively.

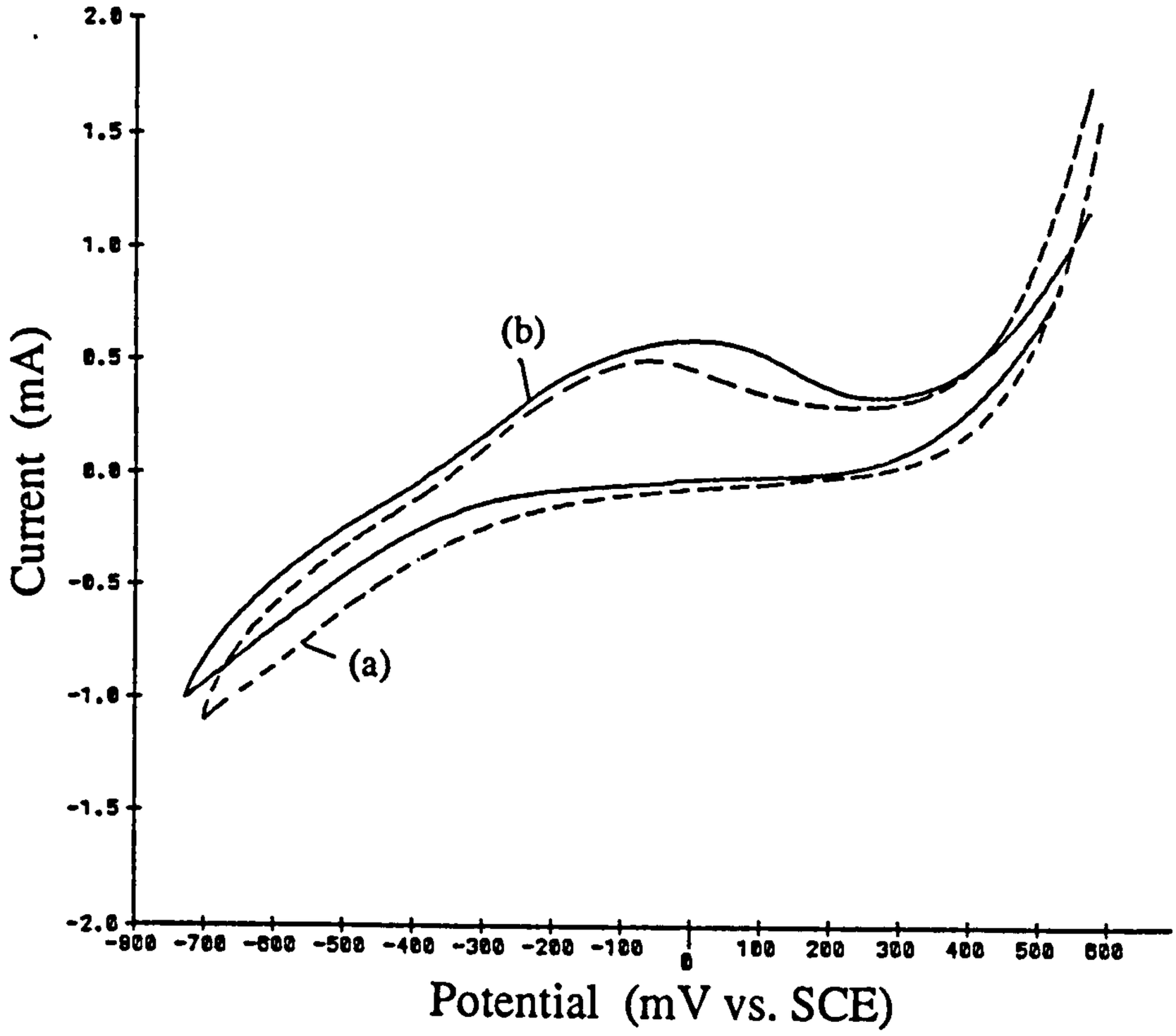

Fig. 50. Comparison of the electrochemical response of a GC-PPy$^+$(*p*-TsO$^-$) electrode in deoxygenated NaOH solution scan (a) with that made after purging the electrolyte solution with O_2 for ~45 minutes scan (b); scan rate =10 mVs^{-1}.

Fig. (50) shows a comparison of the electrochemical response made after purging the electrolyte solution with O_2 for ~45 minutes (scan b), with scan c of Fig. 49. Except for the slight increase in the peak height of the anodic wave, both voltammograms are similar to each other and also to that obtained on bare graphite in the absence of O_2.

The apparent lack of electroactivity of these base treated films is in agreement with Brajter-Toth *et al*[94] who also used solutions that were purged with nitrogen prior to recording voltammograms, but contrary to the findings of others[106,172,175] for voltammograms obtained in oxygenated solutions.

In the studies by Qian[172] it was reported that PPy$^+$(*p*-TsO$^-$) exhibits reproducible cathodic/anodic redox peaks centred at -0.63 V and -0.50 to -0.56 V (*vs.* SCE). Furthermore, these peaks were shown to be reproducible over numerous cycles in the potential range -0.2 to -1.0 V if the scan rate was kept below 20 mVs^{-1}.

A possible mechanism of interaction of polypyrrole with base which was proposed to explain this electroactivity is shown in Eqns. 6.11. The first step involves the exchange of the original film counteranion with OH^- to produce $PPy^+(OH^-)$ (Eqn. 6.11a). The redox behaviour in the potential range -0.2 to -0.8 V was then attributed to the reduction and oxidation of $PPy^+(OH^-)$ according to Eqn. 6.11b. This mechanism of the redox behaviour of polypyrrole in base is analogous to that described previously in Eqn. 5.7, for polypyrrole incorporating counteranions other than OH^- when cycled in non-basic media.

$$PPy^+(A^-) \xrightarrow{NaOH} PPy^+(OH^-) + NaA \qquad (6.11a)$$

$$PPy^+(OH^-) + e^- \rightleftharpoons PPy^\circ + OH^- \qquad (6.11b)$$

Although this explanation of the electroactivity of base treated polypyrrole is a reasonable interpretation of the results presented by Qian, if correct, it also raises several further questions which need to be addressed. For example, it does not explain the different potentiodynamic response of polypyrrole in base compared to that obtained in the presence of other anions.

As described in section 5.3.1, the redox process of polypyrrole in aqueous conditions is quasi-reversible, and manifests characteristic broad redox waves which extend between +0.6 to -0.5 V, and from -0.1 to +0.6 V in the anodic and cathodic potential scan directions respectively. In contrast, voltammograms recorded by Qian in base solution are approximately symmetrical about E_p values (-0.6 V, ΔE_p ~70 mV), and anodic and cathodic peak currents scale linearly with scan rates up to 20 mVs^{-1}, with the ratio of i_{pa}/i_{pc} approximately equal to unity[172]. This behaviour is more typical of behaviour expected from a surface localised electroactive species with quasi-reversible electrode kinetics.

Since the voltammograms shown in Fig. 49 were all initiated at around +0.65 V, it could be argued that this accounts for the absence of any redox behaviour in the potential range (+0.65 to -0.65 V). Indeed, Qian[172] showed that if $PPy^+(OH^-)$ was cycled at potentials more anodic than +0.35 V (*vs.* SCE), the electrode underwent irreversible oxidation and the electroactivity of the film was destroyed. In order to

determine whether the absence of redox behaviour could be explained in this way, the electrochemical behaviour of a 0.5 μm thick GC-PPy$^+$(*p*-TsO$^-$) electrode was examined at potentials between 0.0 to -0.75 V.

Fig. 51 shows voltammograms obtained after an electrode had been left to stand for 15 minutes in a thoroughly deoxygenated solution of NaOH (1.25 M), (scan b), and for comparison, the response of an identical film cycled under the same conditions, except with O_2 initially present (scan a).

The response of the GC-PPy$^+$(OH$^-$) electrode cycled between 0 and -0.75 V in the absence of O_2 resembles previous scans in between 0.6 and -0.65 V. However, voltammograms recorded in oxygenated solution show pronounced oxidation and reduction peaks, with peak positions centred at E_p = -0.54 and -0.65 V. This redox behaviour of PPy$^+$(p-TsO$^-$) in oxygenated NaOH solution resembles that obtained by other workers[106,172,175] and demonstrates that the lack of electroactivity of GC-PPy$^+$(*p*-TsO$^-$) in the potential range 0 to -0.75 V in deoxygenated solution, is due to the absence of O_2.

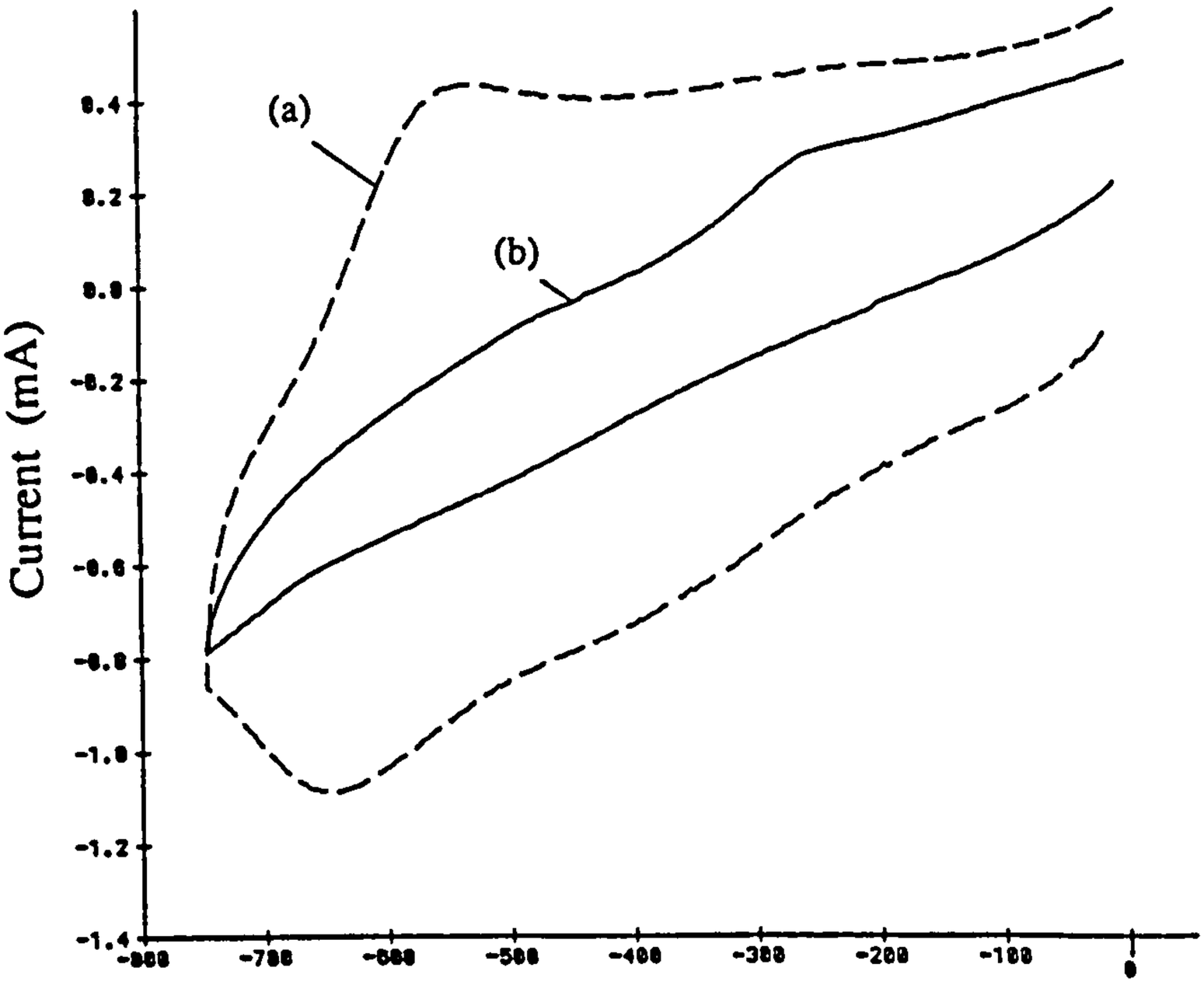

Fig. 51. Comparison of the response of 0.5 μm thick GC-PPy$^+$(*p*-TsO$^-$) electrodes in NaOH solution; scan (a), oxygenated solution; scan (b), oxygen free solution. Scan rate =10 mVs^{-1}.

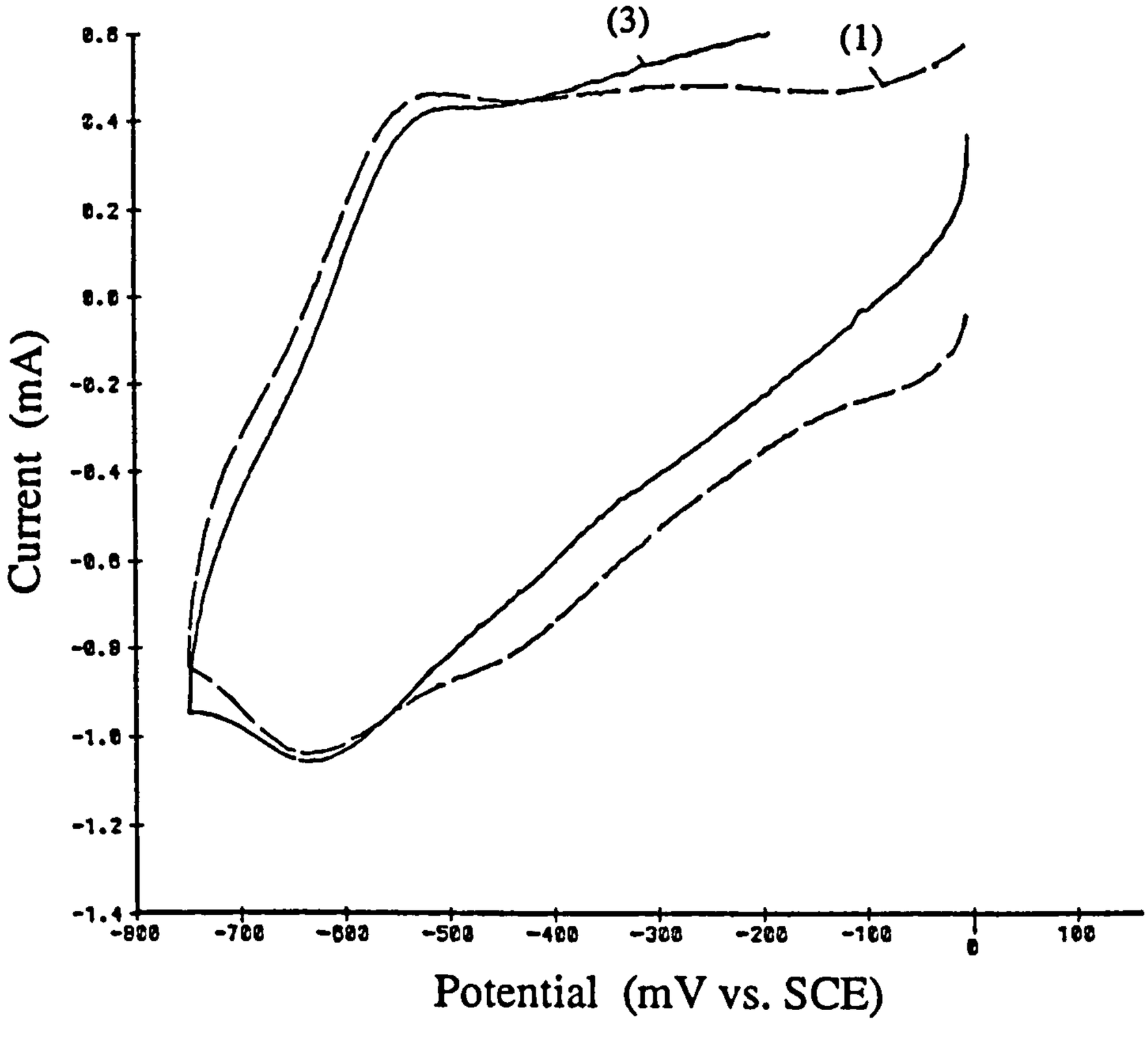

Fig. 52. Comparison of Fig. 51(a), scan (1), made with oxygen initially present in solution, with third scan made after purging with oxygen free nitrogen. Scan rate =10 mVs^{-1}.

Figs. 52 shows the first and third scans of the electrode used to record the scans shown in Fig. 51(a), after thoroughly purging the above oxygenated solution with oxygen free nitrogen. Surprisingly, the GC-$PPy^{+}(p\text{-}TsO^{-})$ electrode remains electroactive, and broad oxidation and reduction waves are observed which are similar to those obtained in the presence of O_2. Since the voltammograms were recorded after purging with nitrogen, this response must originate from O_2 which was incorporated by polypyrrole film when cycled in oxygenated solution.

The incorporation of electroactive species from bulk solution by polypyrrole has already been demonstrated in section 5.6.1 with Cu^{2+} ions. Thus, this result supports the evidence previously presented, that polypyrrole is porous to electroactive species in solution when in the oxidised state, or when cycled between redox states.

Analysis of data from recent papers which also suggests the inclusion of O_2 by polypyrrole when immersed in oxygenated base solution is discussed below;

In an elemental analysis of polypyrrole after treatment with base, it has been shown that the original film counteranions are removed, and that up to one molecule of O_2 is incorporated for every 2.58 to 3.1 pyrrole units (normalised to the nitrogen content in the sample)[172,173]. Comparison of this value to the various ratios of pyrrole monomer units per univalent dopant anions reported for electrochemically prepared polypyrrole films (see Table 1), leads to the conclusion that approximately one mole of O_2 is incorporated into polypyrrole for every positive charge on the polymer backbone.

Infra-red spectra of base treated polypyrrole are inconsistent with the formation of $PPy^+(OH^-)$[169], but are identical to that reported for O_2 absorbing neutral polypyrrole which has been electrochemically reduced (de-doped) and then exposed to air[127].

As a result of the cyclic voltammetry data presented in this section, and from other workers[94], and also from a consideration of elemental analysis data[172,173], infra-red and dispersive X-ray spectroscopies[169], it is concluded that the redox behaviour of polypyrrole immersed in oxygenated NaOH solution is due to the presence of O_2 incorporated within polypyrrole and is not due the reduction/oxidation of $PPy^+(OH^-)$ as proposed by Qian[172] in Eqn. 6.11. The nature of this interaction is discussed in the following section.

6.5 Interaction of Base Treated Polypyrrole with Oxygen.

As described in section 6.4, cyclic voltammetry studies carried out in this thesis, and experimental data presented by other workers, suggests the incorporation of oxygen by polypyrrole on immersion in oxygenated base solution.

In this section, a mechanism for the interaction of polypyrrole with oxygenated NaOH solution is proposed. This mechanism is based on a model suggested by Inganas *et al*[171,173], for reversible proton transfer between the acidic pyrrolylium hydrogen (>N-H) and OH^-; on proposed mechanisms of reduction of O_2 adsorbed at graphite carbon[201,204] and on graphite carbon modified with hemine[203]; and finally,

on suggested mechanisms of interaction of deprotonated polypyrrole with organic electron acceptors[206].

The mechanism proposed by Inganas *et al*[171,173], for proton abstraction from polypyrrole in NaOH solution is shown in Eqn. 6.12.

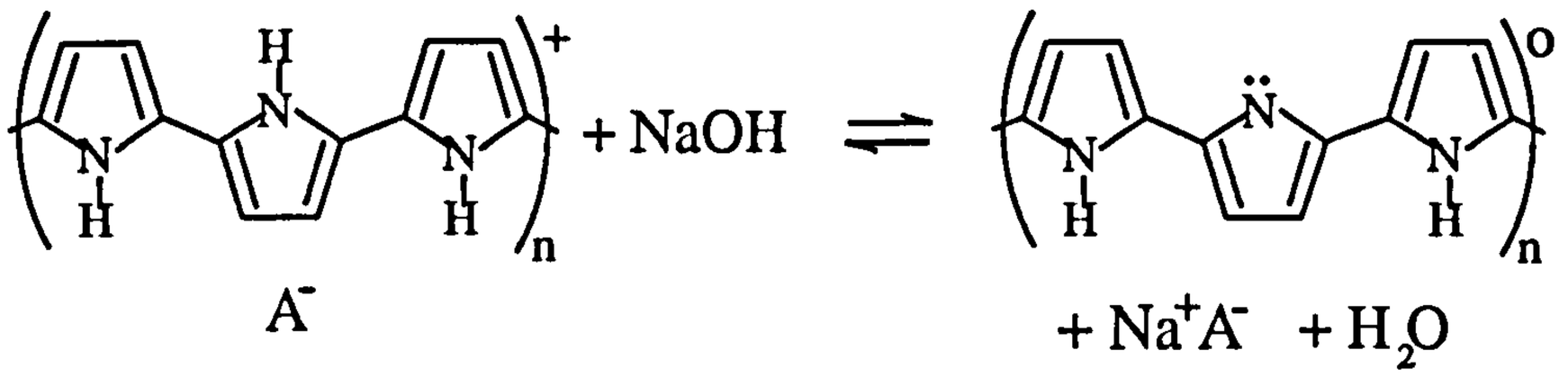

(6.12)

The pyrrolylium (>N-H) proton has an estimated pK_a of less than 14 and is abstracted by OH^- to form water. The electron which is left behind is then free to combine with the positive charge on the polymer backbone, leading to a reduction in the number of overall charge carriers and consequently a decrease the conductivity of the polymer. This reaction is also simultaneously accompanied by the loss of the anion from the film so that overall charge neutrality is maintained. Subsequent exposure of the polymer to acid solution readily reverses the above process, reforming the cleaved pyrrolylium (>N-H) bond.

Evidence for this mechanism was obtained from electrical conductivity versus pH measurements, optical absorption and X-ray photoelectron spectroscopy. Other X-ray photoelectron studies by Kang *et al*[206] are also in support of this mechanism.

It has been shown in studies conducted by Pfluger *et al*[198] and Scott *et al*[99,207], that electrochemically reduced polypyrrole (PPy°) is irreversibly oxidised on exposure to O_2, forming oxygen to nitrogen bonds with as many as one third of the nitrogen atoms on polypyrrole. The interaction of base treated polypyrrole PPy(-H)° with O_2 is expected to be closely analogous to that of PPy°, due to the similarity of the chemical structures, and also because the equilibrium potential of base treated polypyrrole in 1 M NaOH solution is -0.49 V (*vs.* NHE)[172]. On this basis, a possible mechanism for the reaction of PPy(-H)° with O_2 is proposed in Eqn. 6.13.

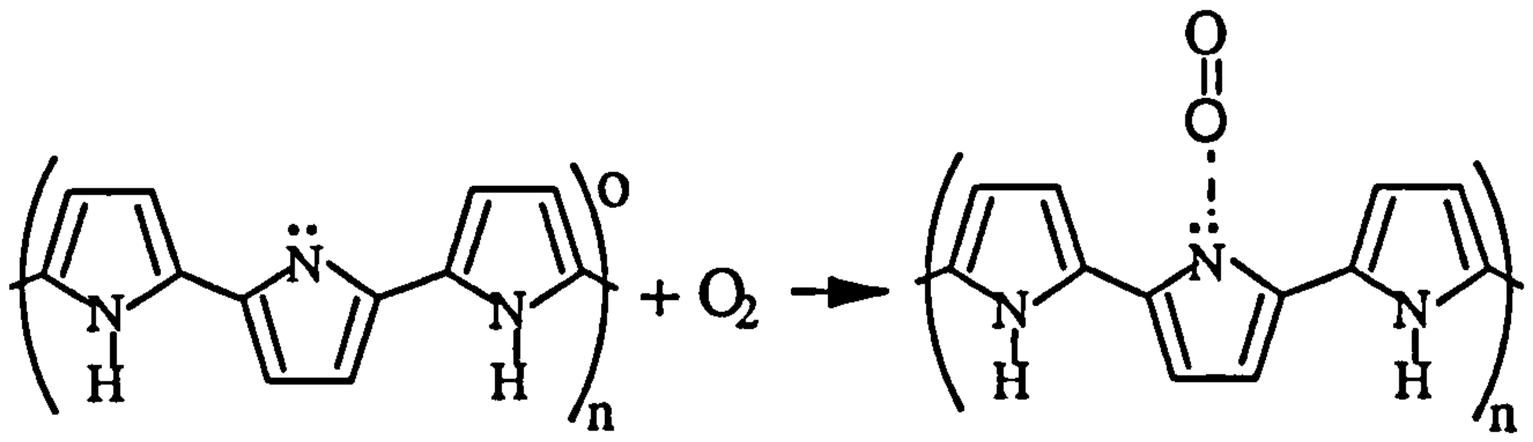

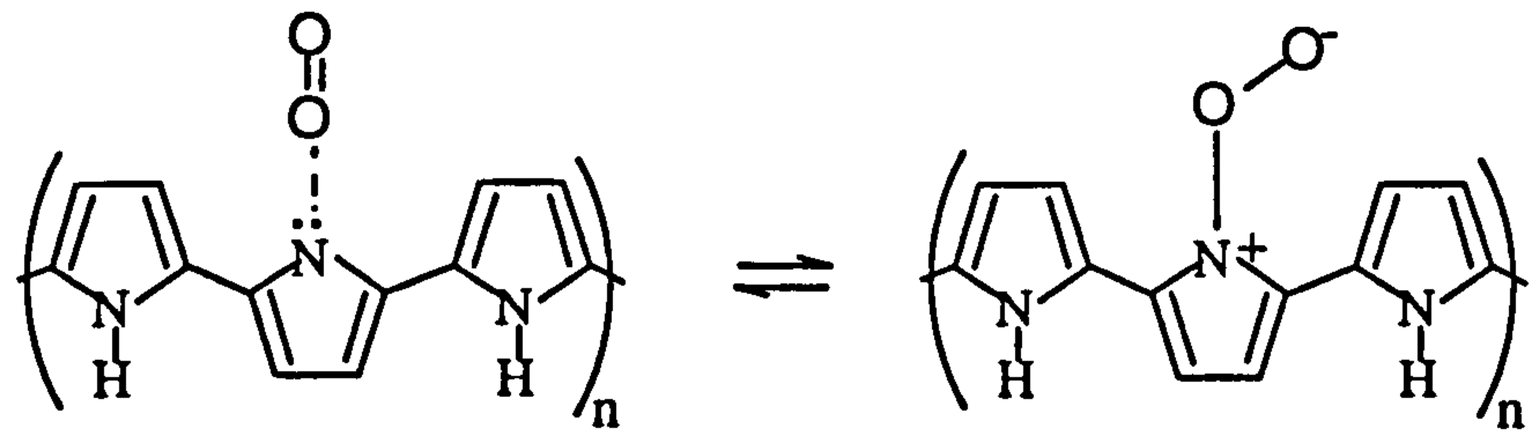

(6.13)

The first step is the complexation of deprotonated polypyrrole (PPy(-H)°) with O_2 to form a charge transfer complex. This step is analogous to that reported by Kang *et al*[206], for the interactions of organic electron acceptors such as *o*-chloroanil and halobenzoquinone with deprotonated base treated polypyrrole. Eqn. 6.13 is also similar to that proposed for the interaction of O_2 with monomeric hemine adsorbed onto carbon fibres[203,208]. In this, O_2 is bound to Fe(II) which exists in a resonance between $Fe(II)\cdot O_2$ and $Fe(III)\cdot O_2^-$ states. From a consideration of the similarity of redox potentials[172,202] in alkaline conditions for the reactions;

$$O_2 + e^- \rightleftharpoons O_2^- \quad = -0.56 \text{ V } (vs. \text{ NHE}) \tag{6.14}$$

$$PPy^+ + e^- \rightleftharpoons PPy^\circ \quad = -0.49 \text{ V } (vs. \text{ NHE}) \tag{6.15}$$

a resonance between $PPy(-H)^\circ\cdot O_2$ and $PPy(-H)^+O_2^-$ states is also considered likely.

The reduction/oxidation of base treated polypyrrole may then be represented by the following Eqns 6.16(a-b).

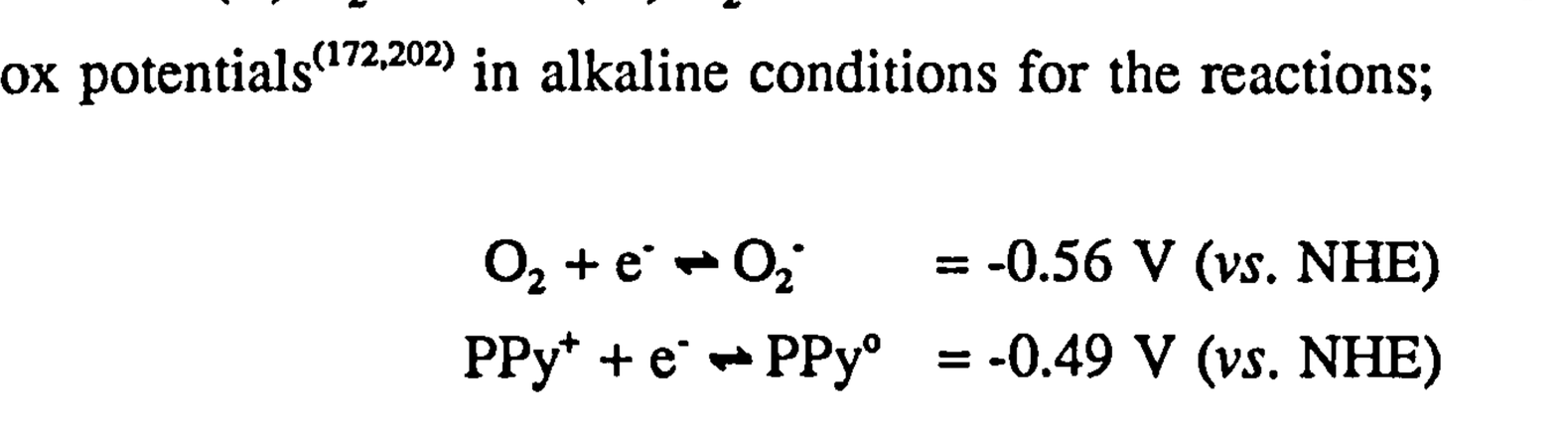

(6.16a)

or

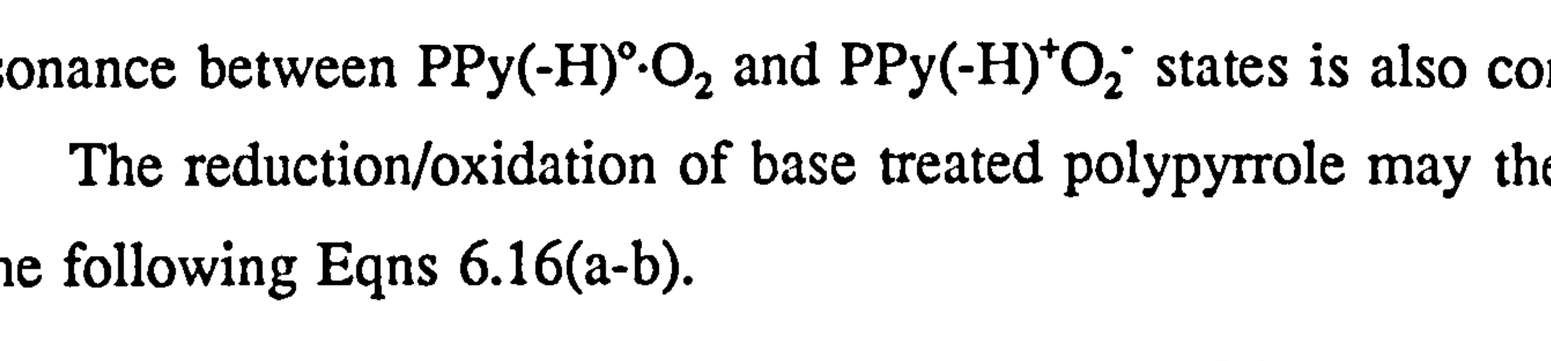

(6.16b)

The reduction of O_2 adsorbed at graphite carbon and on graphite carbon modified by hemine adsorption occurs at $E_p \simeq$ -0.5 V. Hence, the proposed mechanism for reduction/oxidation of oxygenated base treated polypyrrole is consistent with the observed redox behaviour shown in Fig. 51(a) and with that reported in the literature[46,106,172,175]. This is in contrast to the anomalous redox behaviour observed with $PPy^+(OH^-)$ as proposed by Qian[172].

6.6 Irreversible Oxidation of GC-PPy^+(*p*-TsO^-) by OH^-.

In section 6.4.2 the electroactivity of base treated polypyrrole in the potential range -0.2 to -0.8 V was demonstrated to be due to the presence of O_2, either in solution or else incorporated by polypyrrole from solution.

As previously mentioned in section 6.4.2, studies by Qian *et al*[172] and Wernet[106] have shown that the electroactivity of base treated polypyrrole is destroyed by cycling at electrode potentials more positive than +0.30 V (*vs.* SCE). This section describes the cyclic voltammetry of oxygenated base treated polypyrrole at potentials more anodic than this, followed by a discussion of mechanisms which have been proposed to account for this loss of electroactivity. This loss of electroactivity/conductivity is considered to be the principal reason for the failure of electroless deposition at polypyrrole substrates, (section 6.3).

Fig. 53 shows successive voltammograms of a GC-PPy^+(*p*-TsO^-) electrode, recorded under identical conditions in oxygenated solution, except that scan (b) was initiated at +0.50 V. The lack of electroactivity on the second scan is consistent with previous studies by Qian *et al*[172] who have demonstrated the irreversible oxidation of $PPy^+(NO_3^-)$ in NaOH solution at potentials more anodic than +0.35 V *vs.* SCE.

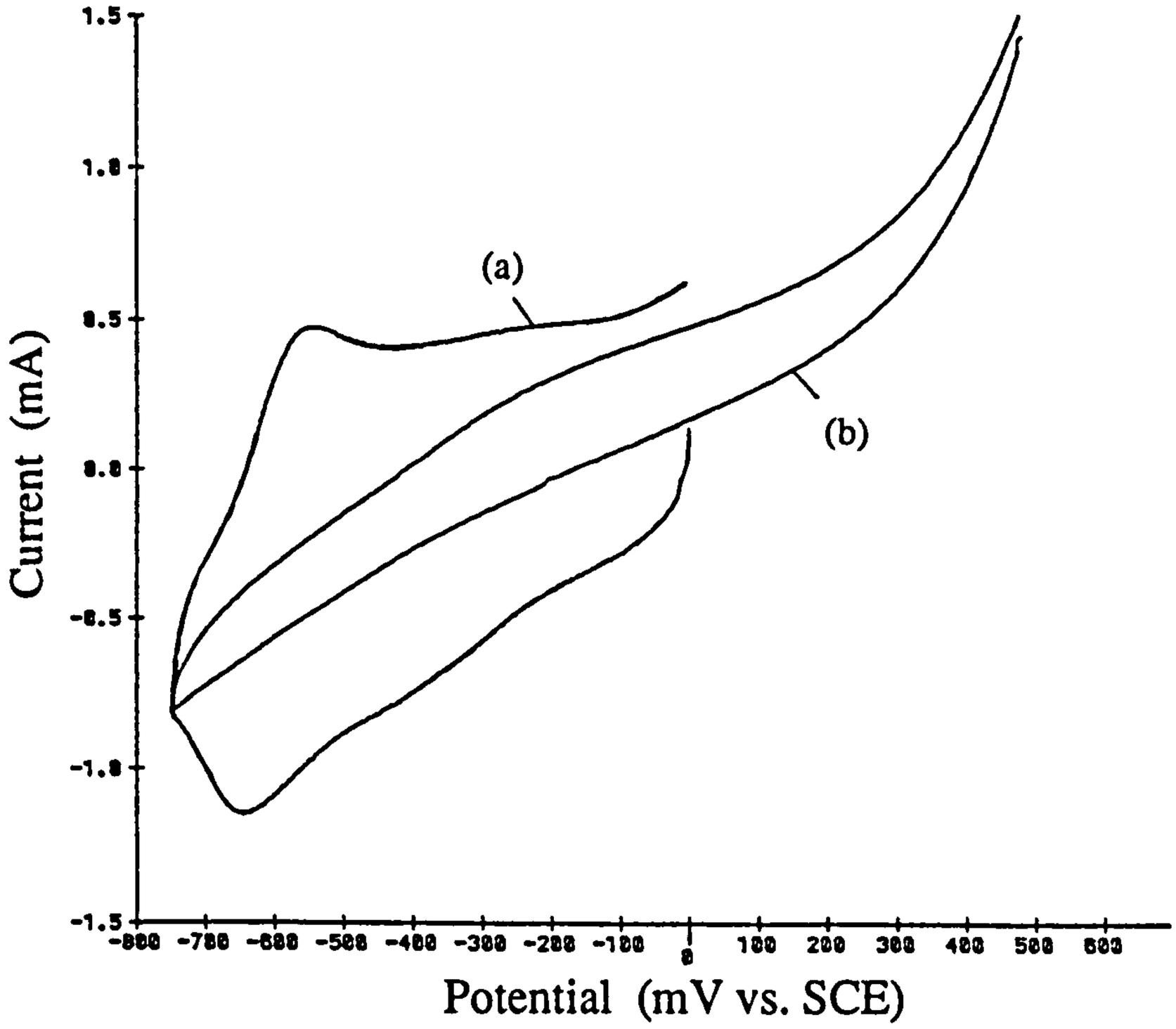

Fig. 53. The effect of the anodic potential limit on the redox behaviour of GC-PPy^{+}(*p*-TsO^{-}) electrodes in oxygenated NaOH solution (1.25 M). Scan (a) initiated at 0.0 V; scan (b) initiated at 0.5 V. Scan rate =10mVs^{-1}.

Explanations which have been suggested for this loss of electroactivity, include nucleophilic attack of OH^- at sites along the polymer backbone[103,106,169-171]. The mechanism proposed by Wernet[106] is shown in Fig. 54.

Nucleophilic attack of OH^- at oxidised pyrrole units leads to enamine like structure elements in which the nitrogen atom is more electron-rich and the π-system of the polymer backbone is partially interrupted. Hydroxyl groups which are not removed during the reduction process then react to form keto groups on the subsequent oxidation cycle and destroy the π-conjugation of polypyrrole. The effects of the loss of conjugation are a decrease in the conductivity of the polymer, which is in accordance with experimental observations.

Nucleophilic attack by OH^- leading to ring opening has also been proposed[173], a possible mechanism is shown in Fig. 55.

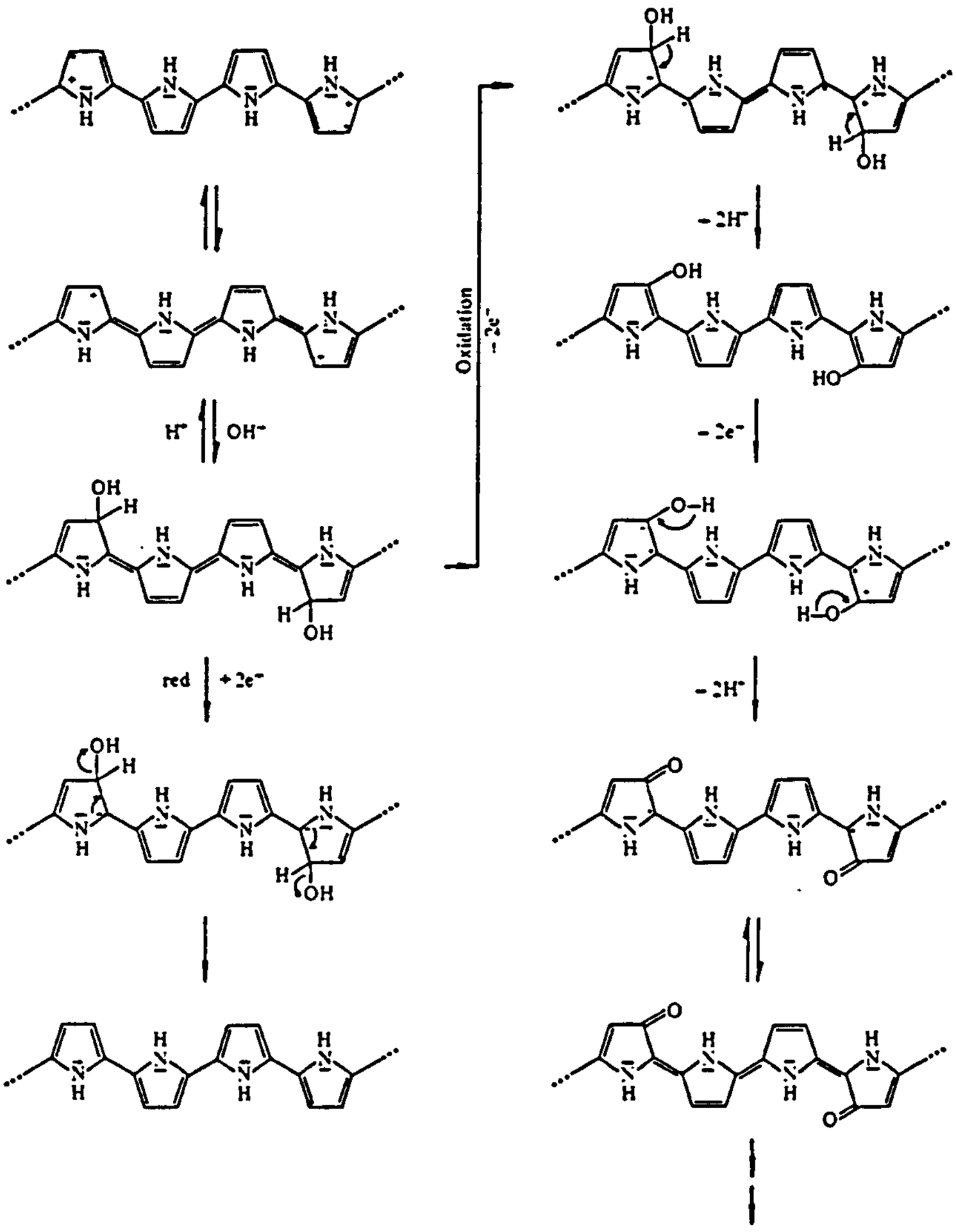

Fig. 54. Proposed mechanism of nucleophilic attack at polypyrrole by OH^- resulting in loss of electroactivity, after ref.[106].

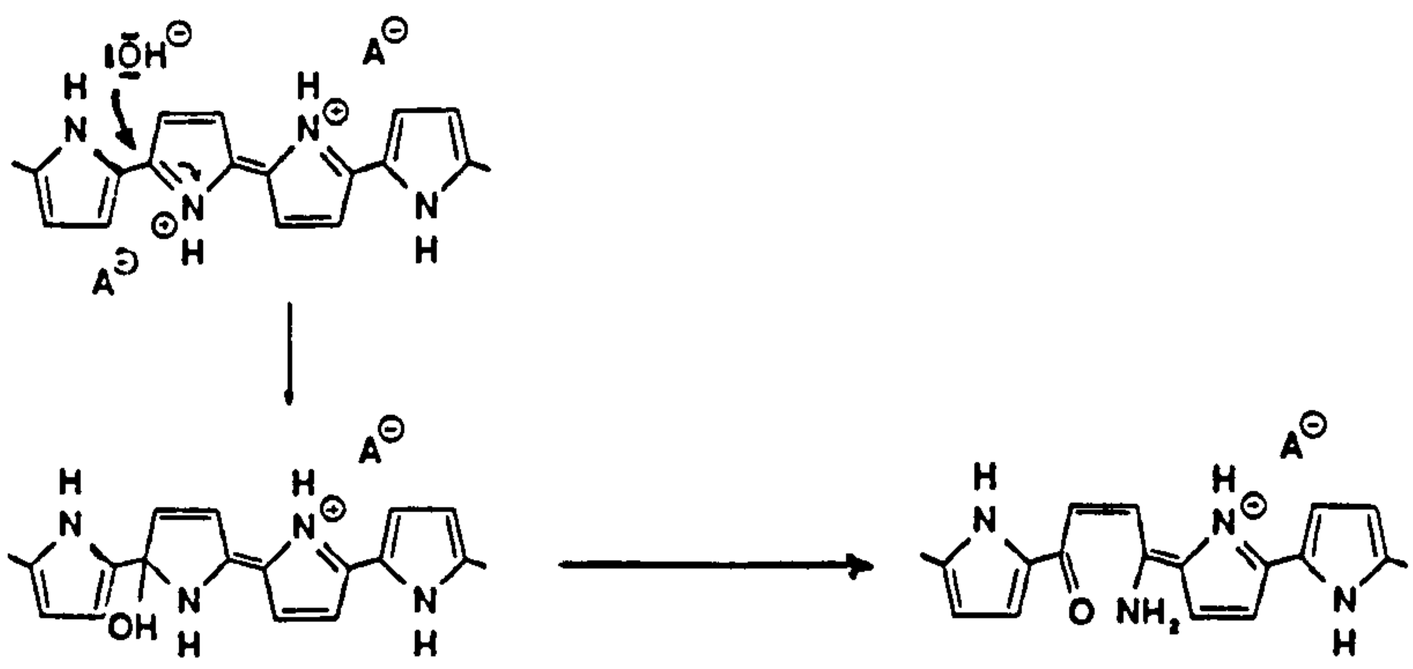

Fig. 55. Nucleophilic attack at polypyrrole backbone leading to ring opening and degradation of electroactivity, after ref.[173].

Similar mechanisms have also been used to explain the degradation that occurs by over-oxidation of polypyrrole in aqueous electrolytes[86,92]. However, in the present study it is expected that the principal reaction will be with OH^-, since OH^- is the more powerful nucleophile.

The mechanisms shown in Figs. 54 and 55 for the nucleophilic attack of polypyrrole by OH^- lead to a disruption of the π-character of polypyrrole and cause an irreversible degradation of electroactivity. This behaviour, however, is in contrast to short-term investigations by Munstedt[169], which show that the decrease in conductivity and weight loss of base treated polypyrrole can be almost restored by subsequent treatment with Bronstead acids.

To determine whether or not the mechanisms shown in Figs. 54 and 55 fully account for the loss of electroactivity of base treated polypyrrole when cycled at potentials more anodic than 0.30 V, cyclic voltammetry was performed on GC-PPy^+(*p*-TsO^-) electrodes in *p*-TsOH after cycling in NaOH solution.

Fig. 56 shows successive cyclic voltammograms of a 3 μm thick GC-PPy^+(*p*-TsO^-) substrate cycled between -0.75 V and +0.70 V (ν= 10 mVs^{-1}). Scan a is in de-oxygenated NaOH solution, and scans b-d were recorded after transferring to de-oxygenated 0.1 M *p*-TsOH solution. The amount of charge that cycled by polypyrrole increases on each successive scan which indicates that much of the polymer backbone must remain unaffected by nucleophilic attack. Hence, the loss of electroactivity caused by cycling oxygenated base treated polypyrrole at potentials more anodic than +0.35 V cannot be described exclusively by mechanisms which involve the disruption of π-conjugation as shown in Figs. 55 and 56, although some degradation of polypyrrole by the above mechanisms is considered likely.

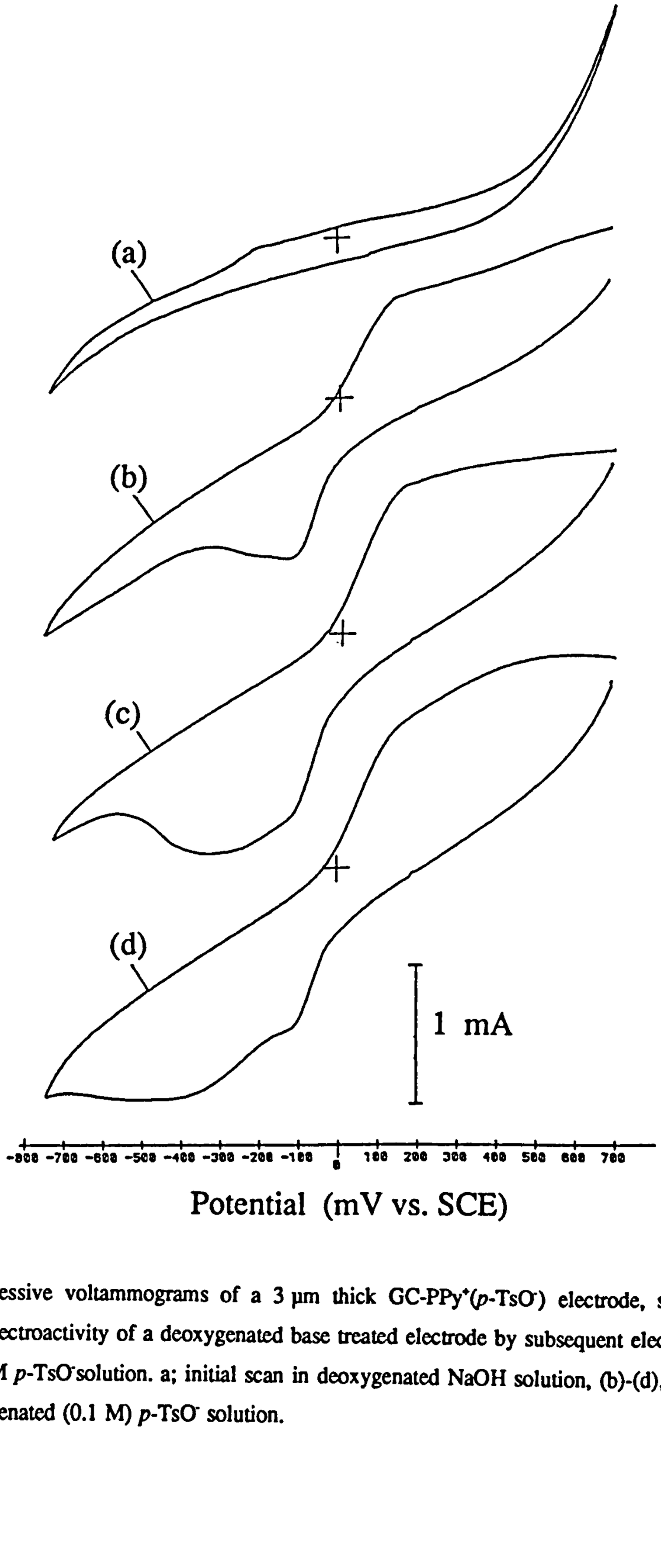

Fig. 56. Successive voltammograms of a 3 μm thick GC-PPy^{+}(*p*-TsO^{-}) electrode, showing the restoration of electroactivity of a deoxygenated base treated electrode by subsequent electrochemical cycling in 0.1 M *p*-TsO^{-}solution. a; initial scan in deoxygenated NaOH solution, (b)-(d), subsequent scans in deoxygenated (0.1 M) *p*-TsO^{-} solution.

In order to account for the loss of electroactivity observed in Fig. 53, an alternative mechanism based on the oxidation of $PPy(-H)^{+}\cdots O_2$ is proposed. This is shown in Fig. 57. Oxygen which is released by the oxidation of polypyrrole is lost by diffusion into bulk solution. This state of polypyrrole $PPy(-H)^{+}/PPy(-H)^{\circ}$, has previously been demonstrated to be inert to reduction in the potential range 0.0 to -0.75 V (*vs.* SCE) and explains the lack of electroactivity which is observed on subsequent scans.

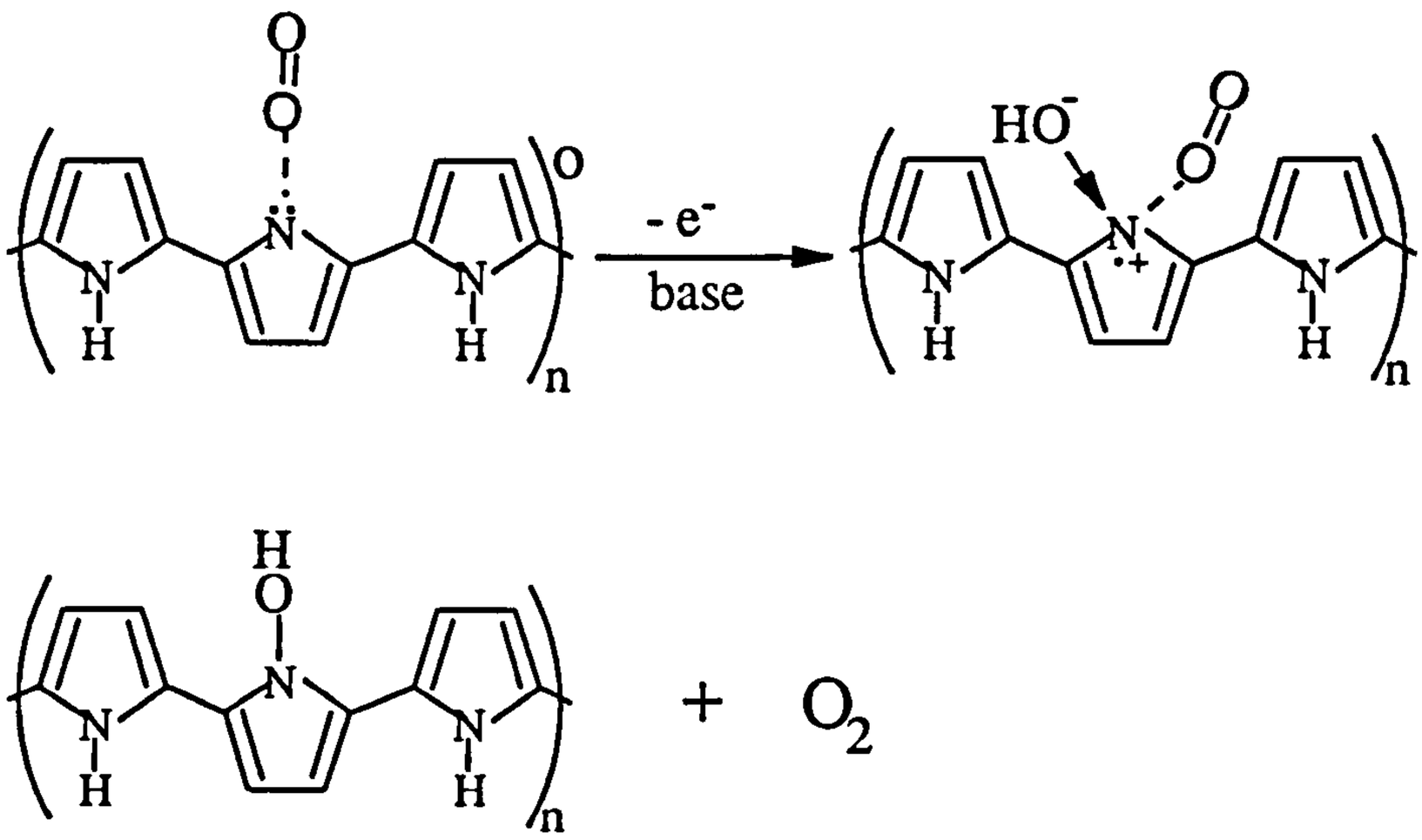

Fig. 57. Proposed mechanism to explain the loss of electroactivity of oxygenated base treated polypyrrole.

An explanation of the restoration of electroactivity of deoxygenated base treated polypyrrole ($PPy(-H)^{\circ}$) has been given by Inganas *et al*[171] and involves re-protonation of the deprotonated nitrogen on pyrrole, coupled with the simultaneous incorporation of the anion of the acid into polypyrrole so as to maintain overall charge neutrality. The gradual as opposed to instantaneous restoration of the electroactivity which is displayed in Figs. 56 is attributed to the low diffusional mobility of p-TsO^{-} in the polypyrrole matrix. Apparently p-TsO^{-} is not a good dopant in the presence of H^{+}[118].

6.7 Summary.

The electrochemistry of oxygenated and de-oxygenated NaOH solution was studied by cyclic voltammetry at graphite carbon (GC) and GC-$PPy^+(p\text{-}TsO^-)$ electrodes. The redox of behaviour polypyrrole in the range 0.0 to -0.75 V (*vs.* SCE) which is observed in oxygenated base solution, is consistent with the formation of $PPy(\text{-}H)^\circ\cdots O_2$ or $PPy(\text{-}H)^+O_2^-$ and is not due to the PPy^+/PPy° redox couple as proposed in refs.[106,172,175]. When polypyrrole is immersed in de-oxygenated base solution, the pyrrolylium (>N-H) bond is rapidly cleaved forming $PPy(\text{-}H)^\circ$. This form of polypyrrole is not electroactive in the range 0.0 to -0.75 V (*vs.* SCE). However, the original electroactivity can be almost restored by subsequent treatment with protonic acids. This restoration of electroactivity demonstrates that the π-conjugation of polypyrrole is not significantly degraded by short term exposure to OH^-.

6.8 Chemical Oxidation of Base Treated Polypyrrole.

Electrochemically reduced neutral polypyrrole (PPy°) has been shown to be readily oxidised by a variety of chemical oxidants, including metal salt solutions of Ag^+, Cu^{2+} and Fe^{3+}[99]. This reactivity can be readily explained in terms of the more negative electrode potential of the PPy^+/PPy° redox couple which is 0.09 V (*vs.* NHE)[71,114]. The chemical oxidation of base treated polypyrrole is expected to be closely analogous to that of PPy°, due to the similarity of chemical structures, and also because the equilibrium potential of base treated polypyrrole in 1 M NaOH solution is -0.49 V (*vs.* NHE)[172]. Thus, the chemical oxidation of $PPy(\text{-}H)^\circ\cdots O_2$ with solutions of Ag^+ and Cu^{2+} ions should effect the reduction of these ions to the zero valence state, whilst simultaneously forming a metal surface layer. Although previous oxidative studies of electrochemically reduced polypyrrole with Cu^{2+} and Ag^+ have been made[99], there have been no reports of the deposition of metallic deposits.

This section describes the chemical oxidation of base treated polypyrrole with solutions containing Cu^{2+} and Ag^+ ions. The morphology of the treated samples are described in sections 6.8.1.1 and 6.8.2.2 respectively.

Preformed free standing films of $PPy^{+}(p\text{-}TsO^{-})$ (~25 μm thick) were prepared by the electrochemical oxidation of pyrrole, according to the procedures described in section 3.10. After removing from the electrode surface, films were rinsed in distilled water and immersed in 1.25M NaOH solution. Films were then transferred to metal salt solutions containing either $AgNO_3$ or $CuSO_4$. No attempts were made to outgas any of the solutions unless otherwise indicated.

6.8.1 Oxidation with Cu^{2+}.

The oxidation of base treated polypyrrole was carried out with Cu^{2+} ions in both the "free state" and also complexed with ammonia, and ethylenediaminetetraacetic acid (EDTA). The preparation and compositions of these solutions are detailed in section 3.16.4.2.

Films which were transferred directly from the NaOH solution to $[Cu(II)(H_2O)_6]^{2+}$ were coated in a gelatinous precipitate of $Cu(OH)_2$. This was easily removed by rinsing in distilled water. The surface of the polypyrrole substrate beneath this was coated with a shiny dark blue copper deposit which rapidly tarnished on exposure to air. Smaller areas of the film were also coated with a metallic 'pink' deposit which proved more resistant to oxidation. However, in general this procedure did not produce good metallic copper deposits. Pickup and Murray[37] have also reported similar blue coloured deposits for the reduction of copper at reduced poly-$[Ru(bpy)_2(vpy)_2]^{2+}$, an electroactive polymer. In this example the blue colour was attributed to the formation of a very thin copper deposit of the order of 40-100 nm thick.

In order to overcome the problems associated with the formation of $Cu(OH)_2$, three different methods of deposition were tried. In the first method, excess OH^{-} was rinsed from the surface of the substrates prior to immersion in $[Cu(II)(H_2O)_6]^{2+}$. However, films treated in this way showed no evidence of copper deposition. It was thought that this was due to the rapid oxidation of $PPy(-H)^{\circ}\cdots O_2$, either by atmospheric oxygen whilst the film was transferred between solutions, or else by oxygen dissolved in the copper solution. Since a similar negative result was obtained after purging

solutions with O_2 free nitrogen, it was considered that the lack of deposit was caused by contact of the film with air. In view of this, NaOH solution was not rinsed from film surfaces in subsequent experiments, so as to maintain a barrier to atmospheric oxidation.

The second method involved the addition of concentrated sulphuric acid to the Cu^{2+} solution (~10 drops/50 cm^3 solution). This proved successful in the elimination of $Cu(OH)_2$, resulting in the formation of bright metallic copper deposits on both surfaces of polypyrrole substrates. The deposition of copper was found to be critically dependent on the amount of acid added to the plating solution. At too high a pH, $Cu(OH)_2$ formation was not entirely eliminated, whereas if excess acid was added, the initial copper deposit rapidly redissolved.

The rate of deposition of copper, the degree of surface coverage, and the uniformity of metal coat were all found to be dependent on the copper ion concentration in solution. Generally, more highly uniform deposits with a greater overall surface coverage were obtained by exposing $PPy(-H)^{\circ}\cdots O_2$ to dilute solutions of copper ions ($< 10^{-3}$ M). However, the improvement in film quality was offset by an increase in deposition time.

A third method of avoiding the formation of copper hydroxide was the use of complexing agents. These combine with Cu^{2+}, thereby reducing the amount of free copper present in solution. Since only a small amount of copper is free to react with OH^- and form copper hydroxide, the solubility product is not exceeded and precipitation does not occur.

Using this method, excellent highly reflective deposits with high surface coverage and good uniformity of deposit were obtained with the copper sodium potassium tartrate solution. These metallic deposits were superior to those obtained with acidified Cu^{2+} solution.

In contrast to the excellent metal deposition obtained from copper sodium potassium tartrate solution, no evidence of copper deposition was observed with either the $[Cu(II)(NH_3)_4]^{2+}$ or $[Cu(II)(EDTA)]^{2-}$ complexes. This lack of deposition can be explained by a comparison of the redox potentials of polypyrrole (PPy^+/PPy° = +0.09 V *vs.* NHE, neutral or acid conditions)[71,114] with the standard

electrode potentials of the various copper complexes that were used (See Eqns. 6.17-6.20). From thermodynamic considerations, copper deposition would be expected to occur with any complex having a redox potential more positive than +0.09 V. This behaviour was confirmed by the lack of deposition with $[Cu(II)(NH_3)_4]^{2+}$ and $[Cu(II)(EDTA)]^{2-}$ complexes which both have redox potentials more negative than that of the PPy^+/PPy^o redox couple.

$$Cu(H_2O)_6^{2+} + 2e^- \rightleftharpoons Cu^{2+} + 6H_2O \qquad E^o = +0.337\ V \qquad (6.17)$$

$$Cu(SPT)_3^{4-} + 2e^- \rightleftharpoons Cu^{2+} + 3\ SPT^{2-} \qquad E^o = +0.154\ V \qquad (6.18)$$

$$Cu(NH_3)_4^{2+} + 2e^- \rightleftharpoons Cu^{2+} + 4\ NH_3 \qquad E^o = -0.070\ V \qquad (6.19)$$

$$Cu(EDTA)^{2-} + 2e^- \rightleftharpoons Cu^{2+} + EDTA^{4-} \qquad E^o = -0.203\ V \qquad (6.20)$$

6.8.1.1 Morphology of Copper Deposits.

The surface morphology of the copper coated polypyrrole substrates prepared via the oxidation of base treated polypyrrole with $[Cu(II)(H_2O)_6]^{2+}$ and $[Cu(II)(SPT)_3]^{4-}$, was examined using SEM as described in section 3.9. All the samples proved sufficiently conducting for use in the SEM without the need to apply a further conducting surface coat.

Plates 2(a-b) show micrographs of copper deposited from acidified (0.16 M) $CuSO_4$ solution, onto the smooth surface of the polypyrrole substrate. Magnifications are at 5 and 10k. Plates 3(a-b) show micrographs for copper deposited onto the reverse (rough) side of the substrate using the same solution. Plates 4(a-b) show micrographs of copper deposited onto both the rough and smooth sides of the polypyrrole from copper tartrate solution.

The morphology of copper deposited from both the acid copper and copper tartrate solutions is composed of clusters of submicron copper particulates, and resembles that shown in Plates 1(a-b) for copper deposited on polypyrrole by electrodeposition. This similarity suggests that a mechanism of simultaneous nucleation and growth occurs in both types of deposition.

(a)

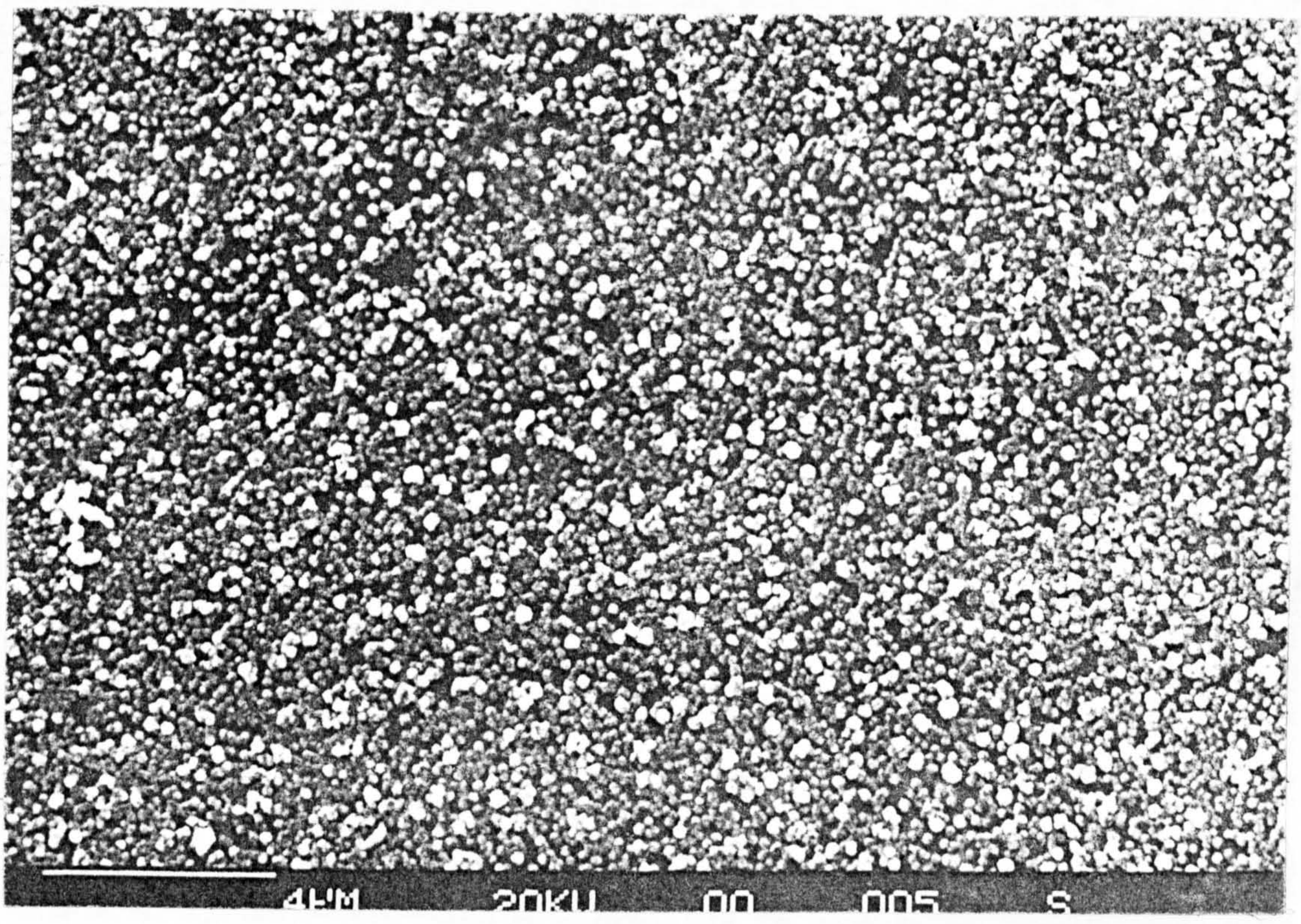

(b)

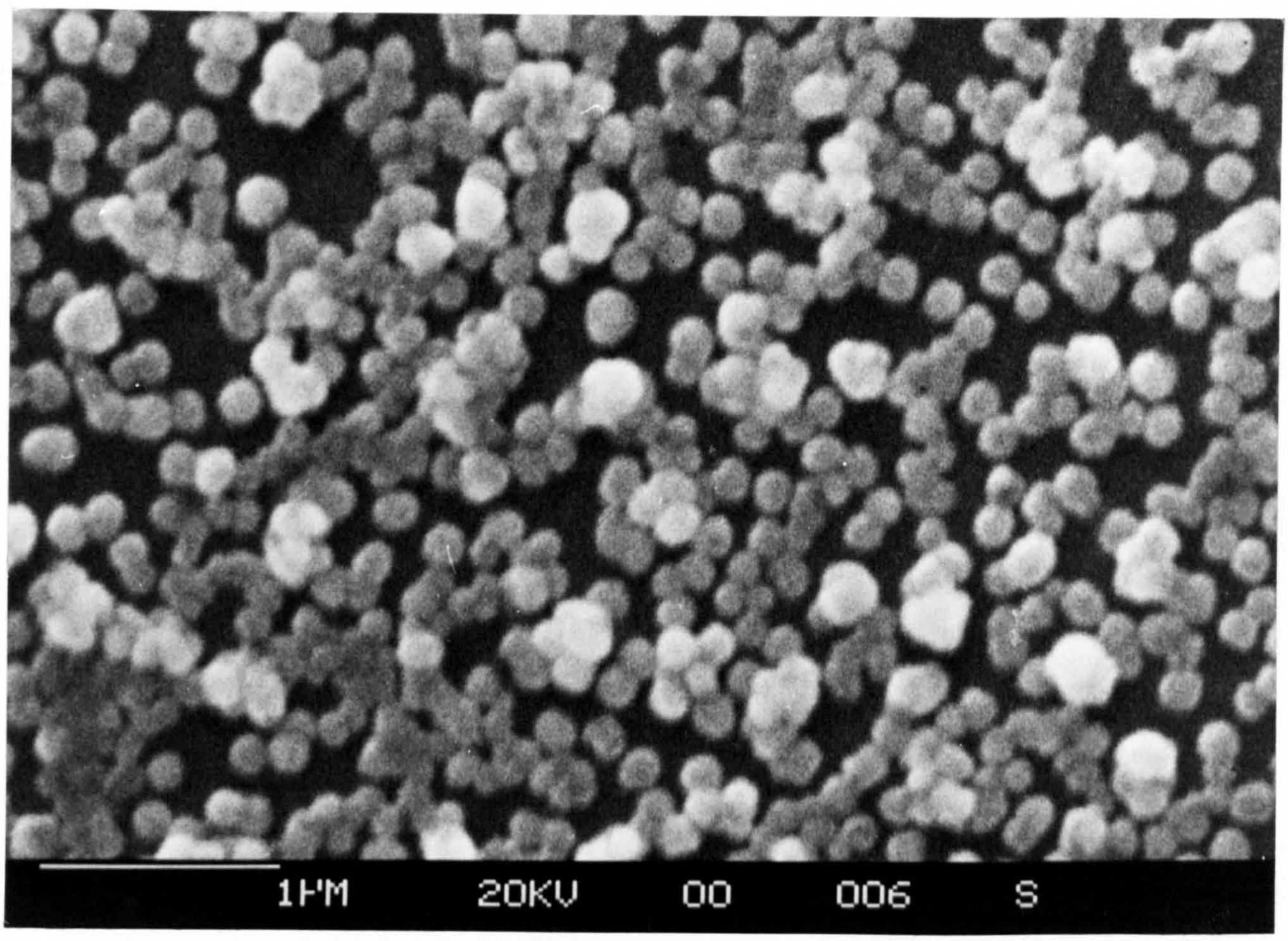

Plates 2(a-b). Copper aggregates deposited on smooth surface of base treated PPy^{+}(*p*-TsO^{-}) from acidified copper sulphate solution (0.16 M).

(a)

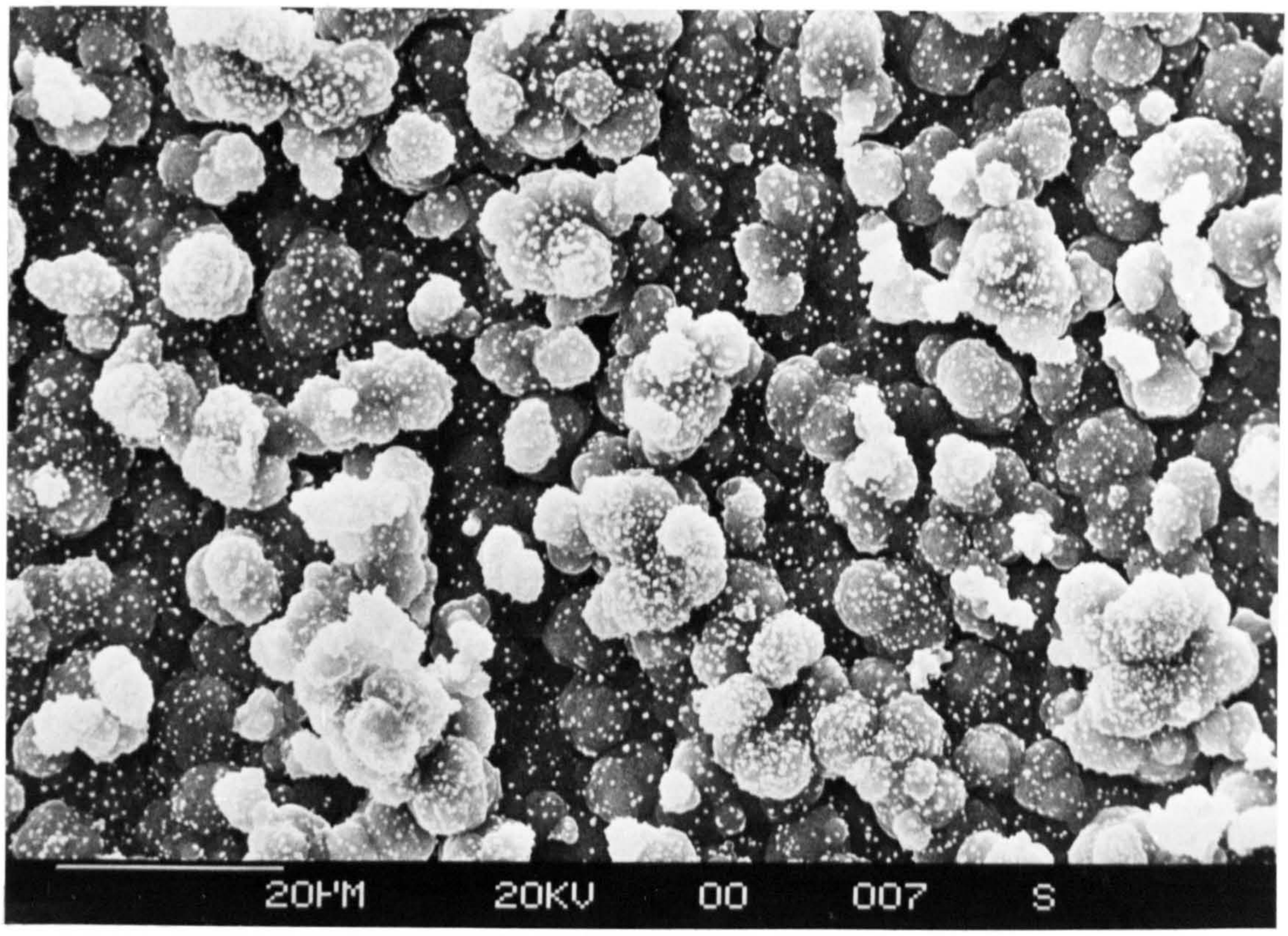

(b)

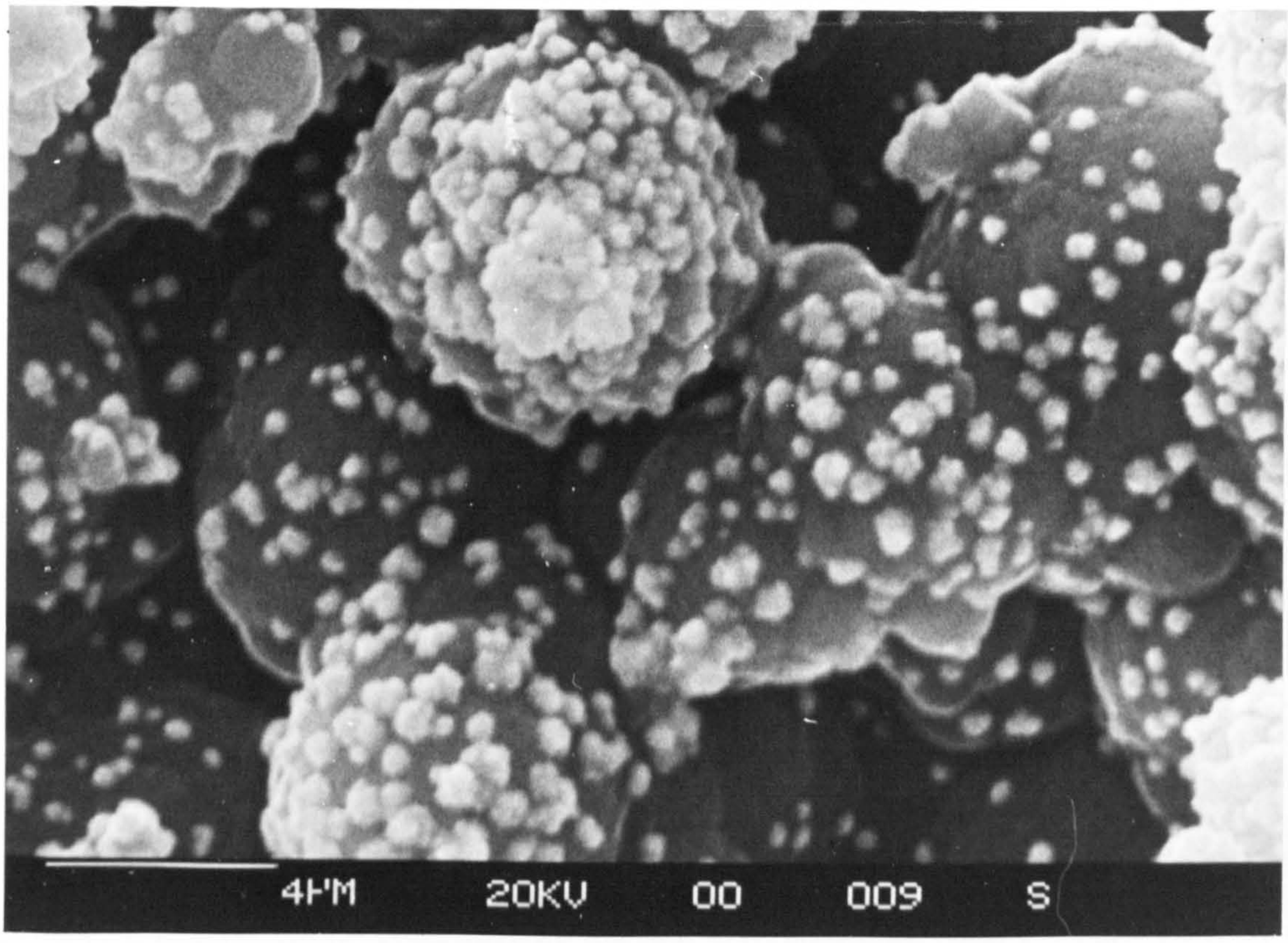

Plates 3(a-b). Copper aggregates deposited on rough surface of base treated PPy^{+}(*p*-TsO^{-}) from acidified copper sulphate solution (0.16 M).

(a)

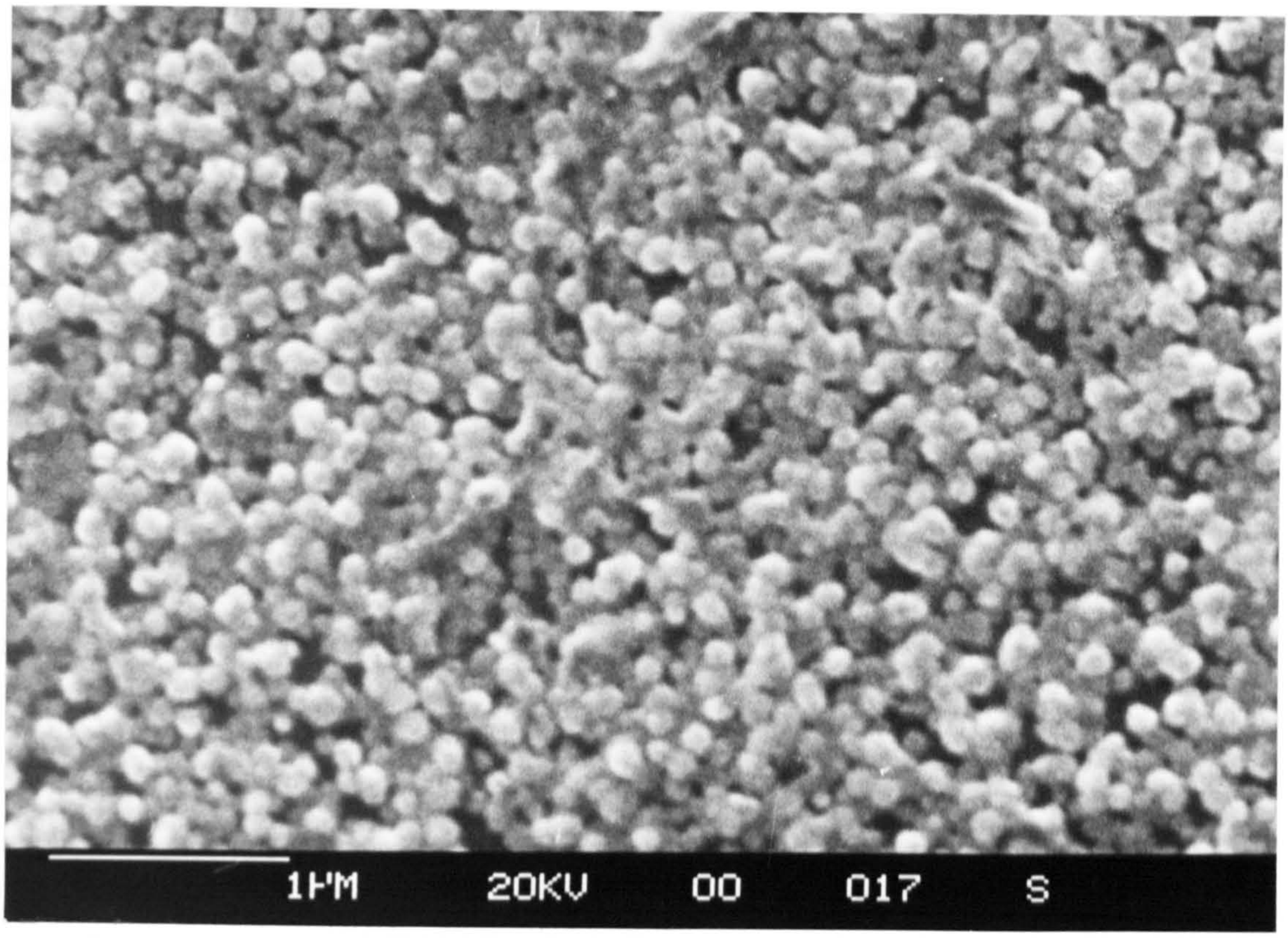

(b)

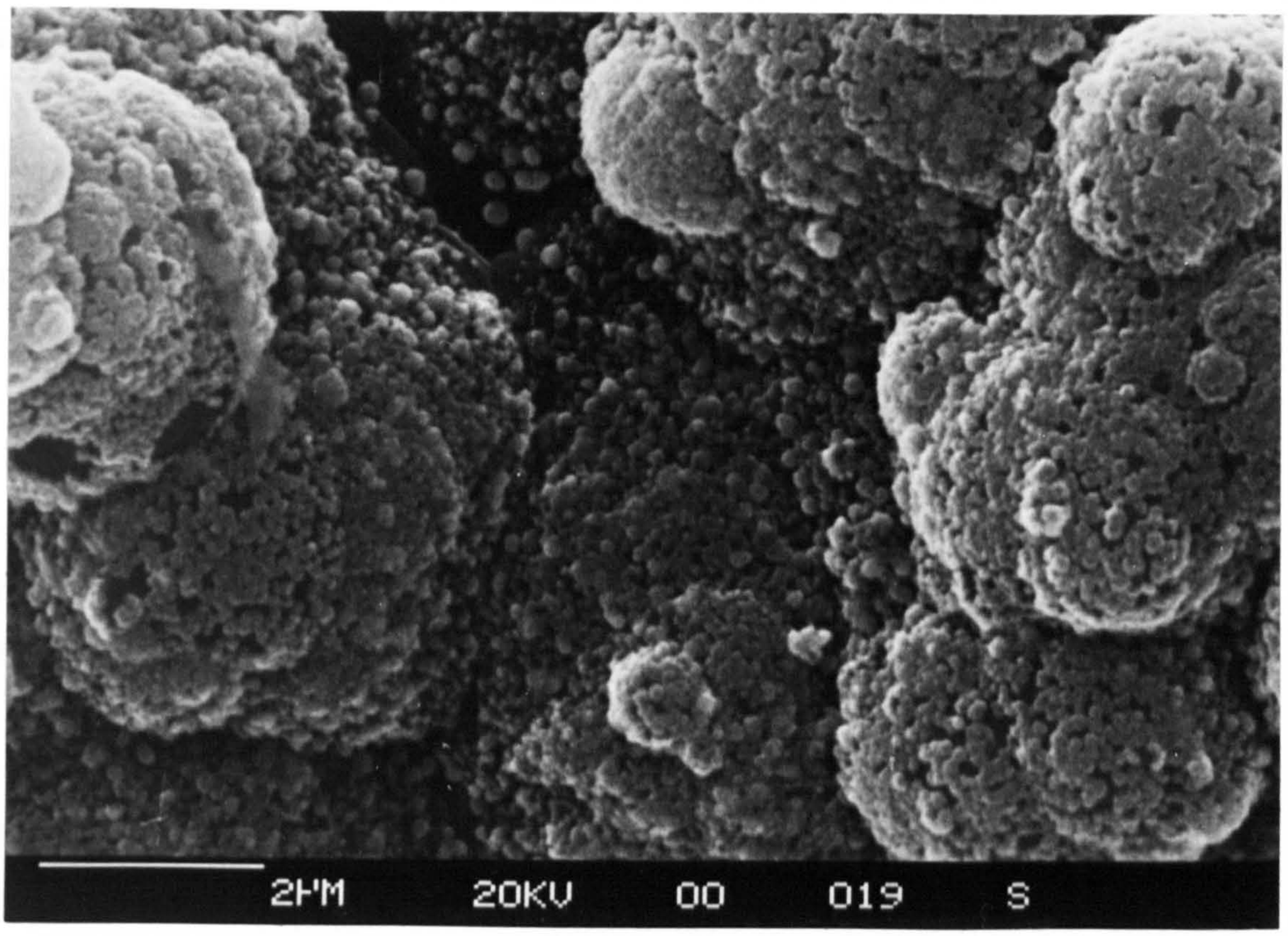

Plates 4(a-b). Copper aggregates deposited on smooth and rough surfaces of base treated PPy^{+}(*p*-TsO^{-}) from copper tartrate solution.

In the case of the copper tartrate solution, many of the individual particles coalesce to form an almost continuous metallic layer, although the deposit is still somewhat porous in nature. The higher surface coverage and more uniform deposit obtained with this solution also accounts for the superior visual appearance which is obtained using this solution. The average size of the copper particulates deposited from the tartrate solution varies from about 0.08 to 0.16 μm, compared to ~0.12 to 0.2 μm for copper aggregates deposited from the copper sulphate solution.

The deposition on the reverse (rough) side of the film, shows that copper is not randomly dispersed over the surface, but appears to be preferentially deposited on the round dendrite like features which protrude from the surface of the film. This uneven deposit is considered to be due to diffusion effects, resulting from a greater access of Cu(II) to the raised surface protrusions.

6.8.2 Oxidation with Ag^+.

The oxidation of $PPy(-H)^{\circ}\cdots O_2$ by Ag^+ was carried out using ammoniacal silver nitrate solution according to the procedure described in section 3.16.2.2.

The standard electrode potential of the Ag^+/Ag^0 redox couple in the presence of NH_3 is +0.0373 V. Hence, exposure of base treated polypyrrole to ammoniacal silver nitrate solution is expected to reduce $[Ag(NH_3)_2]^+$ to Ag°, according to the following half reaction.

$$Ag(NH_3)_2^+ + e^- \rightharpoonup Ag^{\circ} + 2\ NH_3 \qquad E^{\circ} = +0.373\ V \qquad (6.21)$$

The immersion of base treated polypyrrole in ammoniacal silver nitrate solution produced excellent highly reflective silver coats at the surface of polypyrrole substrates. The morphology is discussed in the following section.

6.8.2.1 Morphology of Silver Deposits

Plates 5(a-b) show micrographs of silver which is deposited on the smooth surface of the polypyrrole substrate taken at magnifications of 10 and 25k.

(a)

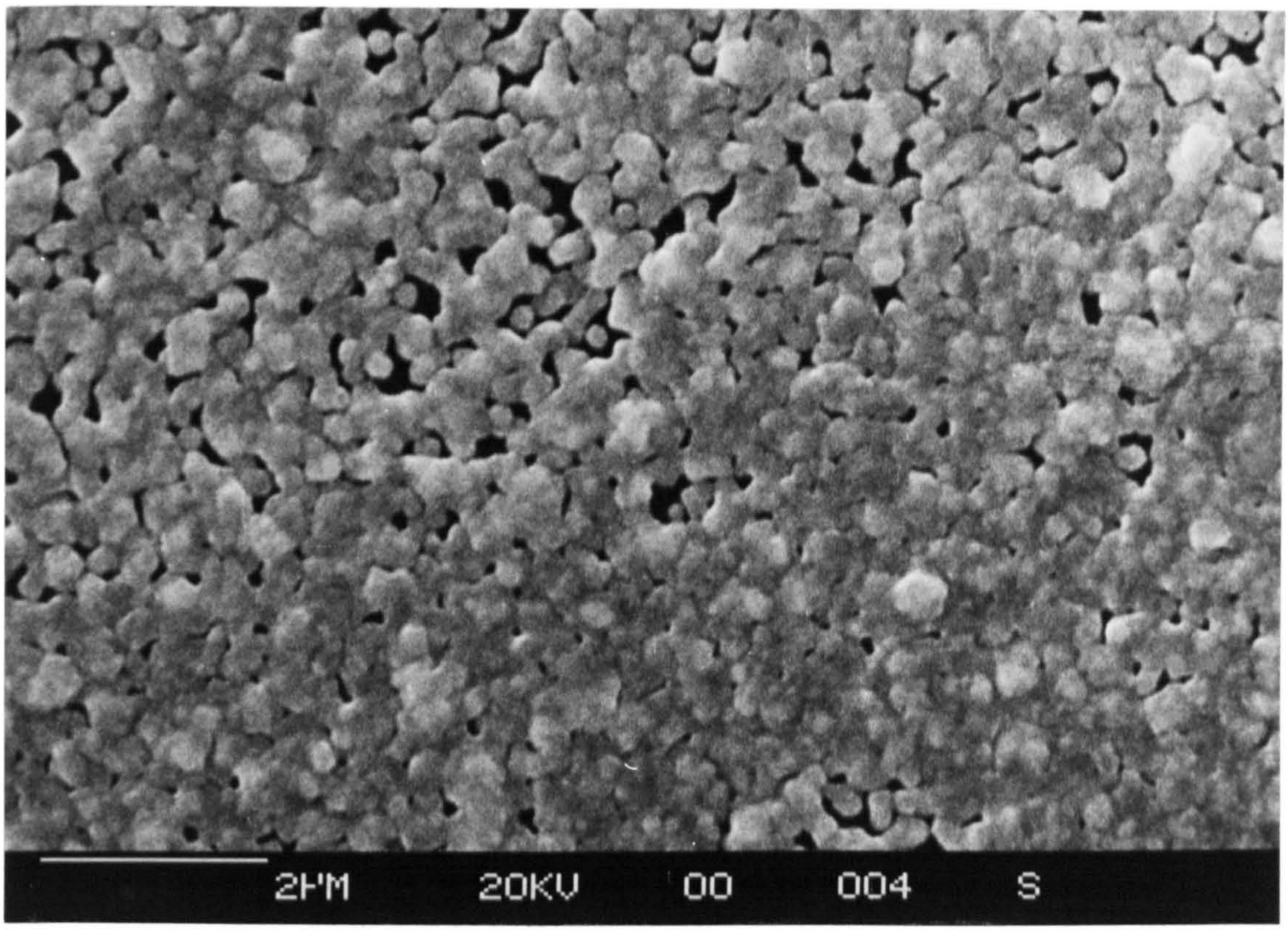

(b)

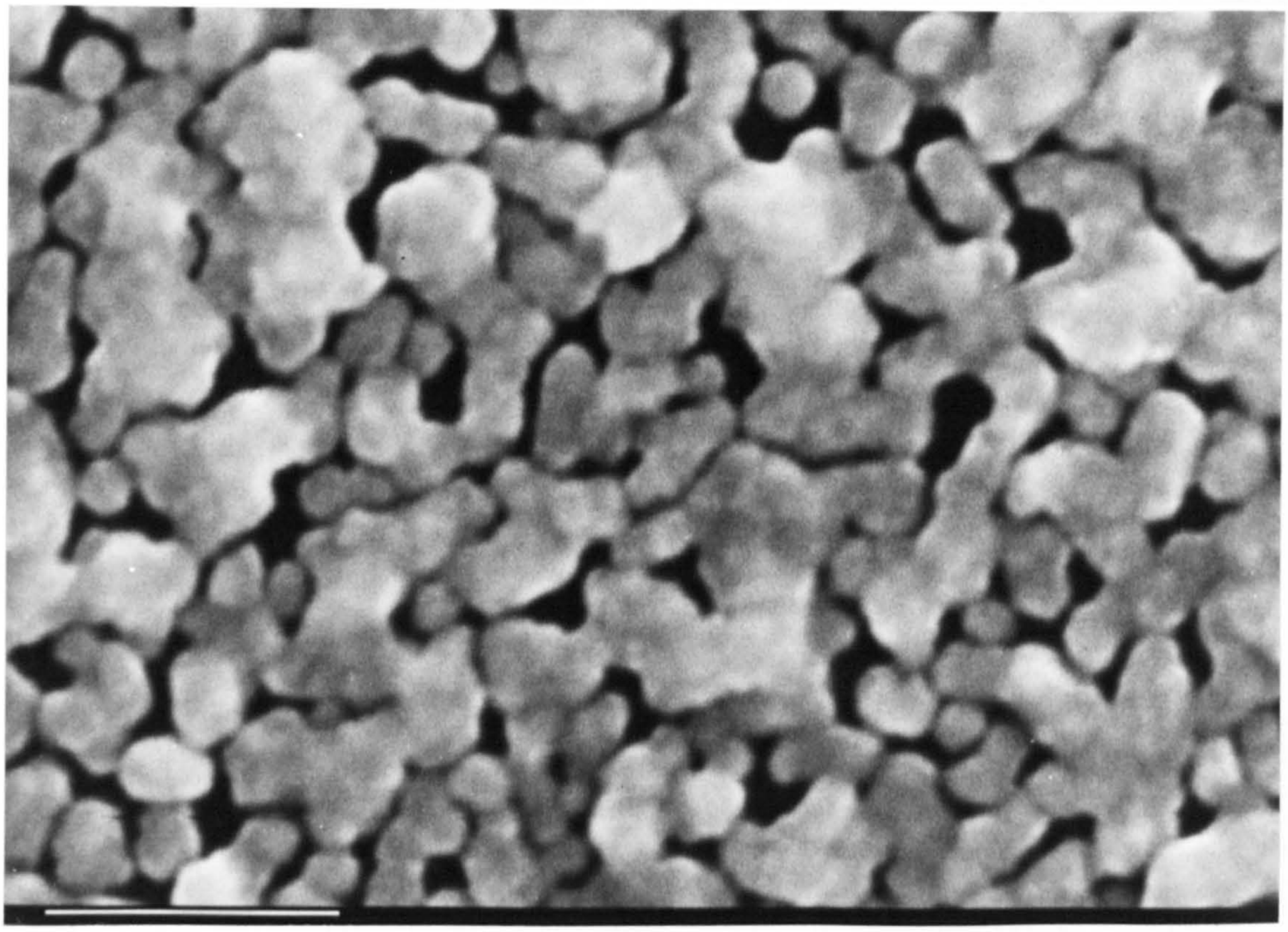

Plates 5(a-b). Silver aggregates deposited onto smooth surface of base treated $PPy^{+}(p\text{-}TsO^{-})$ film from ammoniacal silver nitrate solution.

(a)

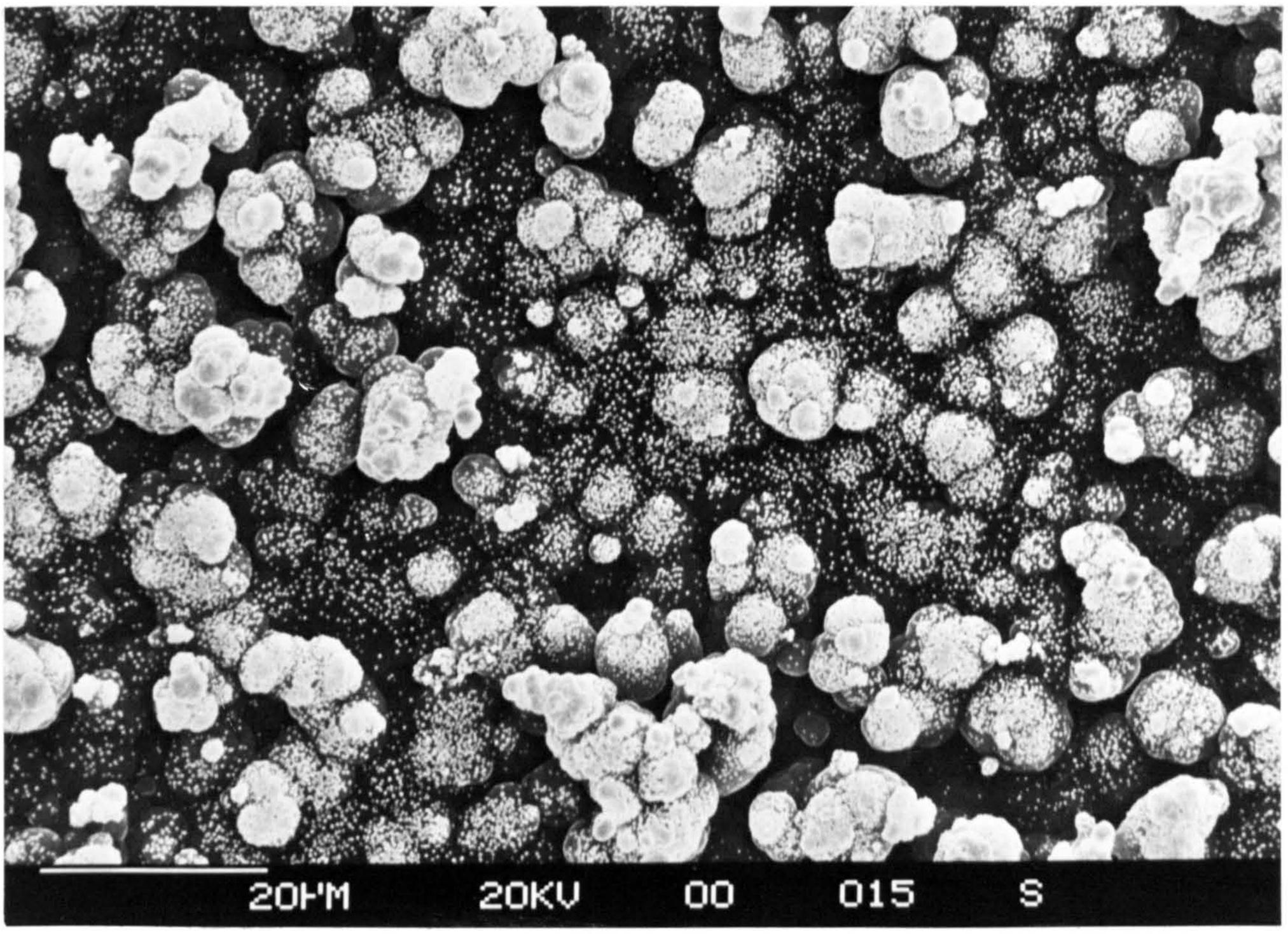

(b)

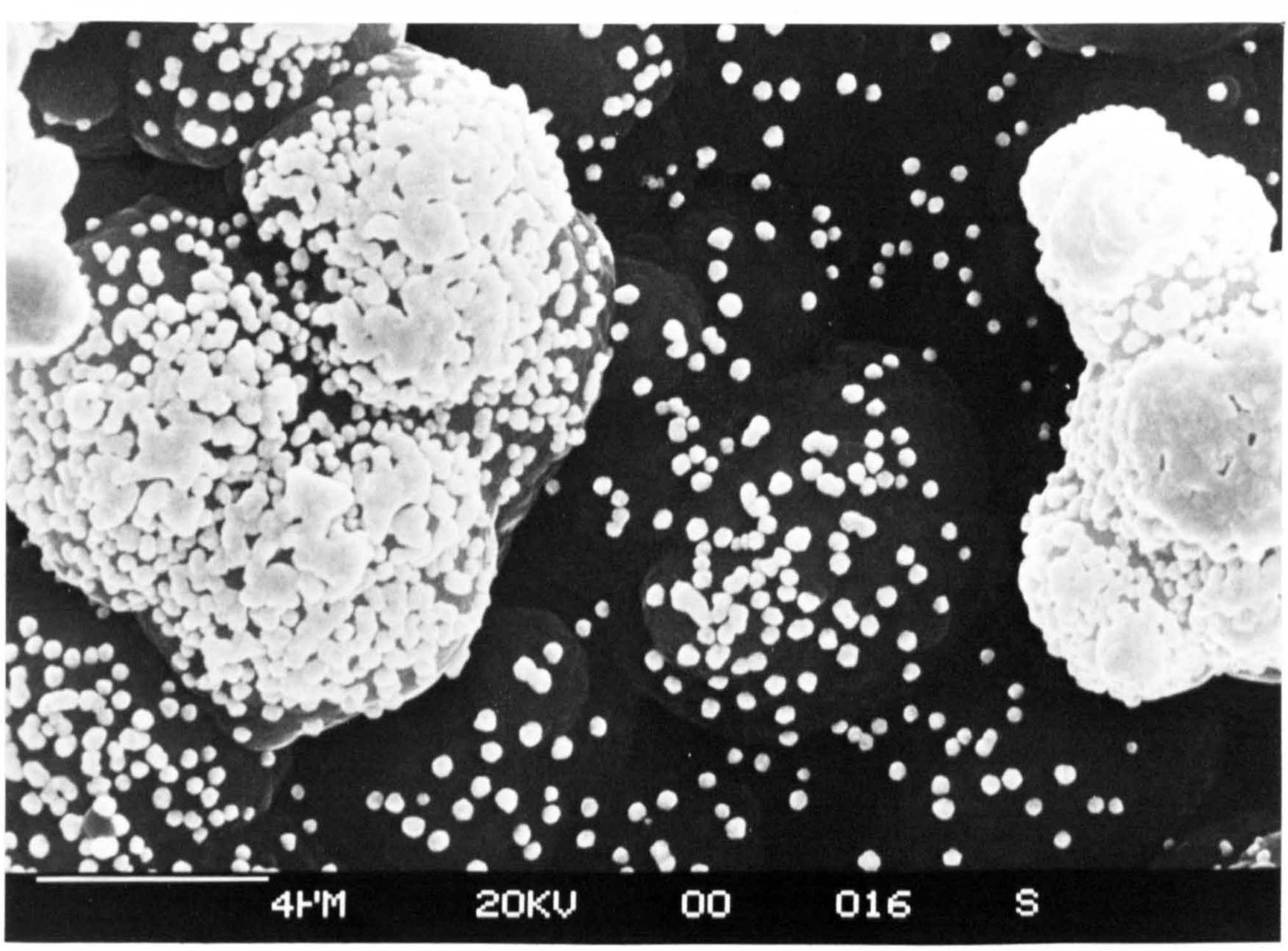

Plates 6(a-b). Silver aggregates deposited onto rough surface of base treated $PPy^{+}(p\text{-}TsO^{-})$ film from ammoniacal silver nitrate solution. Magnifications are 1 and 10k respectively.

The morphology of the silver deposit shows a number of similarities to that observed in the deposition of copper. In common with copper deposits, the silver layer appears to be composed of many individual particulates which have coalesced to form larger aggregate structures of irregular size and shape. The deposition of silver also occurs preferentially on the surface protrusions of the polypyrrole substrate. Silver deposited from ammoniacal silver nitrate solution exhibits a greater continuity and less porosity than either of the deposits obtained from copper solution. If the oxidation polypyrrole by salts of metal ions is stoichiometric, this would be explained by the fact that two moles of silver are deposited for every mole of copper. Gentle abrasion of the silver coat did not remove the metal layer, implying good adhesion of the surface coat to the polypyrrole substrate.

6.9 Summary.

The chemical oxidation of base treated polypyrrole with solutions of copper and silver ions, has been shown to effect the deposition of metallic surface deposits. These deposits are composed of clusters of metal aggregates with sizes in the range 0.08 to 0.20 μm. Under optimized conditions, continuous and reflective surface coats with good adhesion to the polypyrrole substrate can be obtained.

CHAPTER 7

THE APPLICATION OF CONDUCTING POLYMER COMPOSITES TO THE METALLIZATION OF PLASTICS

7.1 Introduction.

Although conducting polymeric materials have been known for some time, the practical application of these materials has been limited. Undoubtedly, this has been due in part to the poor mechanical properties of these materials, coupled with their poor environmental stability. The insoluble and infusible nature of these materials is another major drawback, and precludes conventional processing and material fabrication techniques. Because of this, attention has focused on the preparation of preformed conducting polymer-plastic composites which combine the relatively high conductivity of these materials (σ= 1-100 Scm^{-1}) with the superior mechanical properties of the host polymer.

Polypyrrole and polyaniline are two of the most commonly used conducting polymers, since they are relatively environmentally stable in comparison with other conducting polymers[73,139,141,152], and are easily synthesised by both chemical and electrochemical techniques. Therefore, it is not surprising to find that both these polymers have been utilized in the preparation of conducting polymer composite materials. Indeed, such materials might have potential application in antistatic packaging and electromagnetic shielding (EMI).

Following chapters 5 and 6 which described the electrochemical and chemical metallization of polypyrrole, this chapter deals with preliminary experiments which were conducted to determine the optimum conditions for the preparation of polypyrrole and polyaniline composite materials for metallization. The need to be able to control experimentally the parameters which affect the nature of the conducting polymer coat is vital, since this layer provides the interface between the host substrate material and the subsequent metallic layer. Section 7.2 investigates the preparation of polypyrrole-plastic composite films by electrochemical and chemical methods, and the advantages in each of these approaches is discussed in section 7.3. For thicker sectioned objects, chemical preparative methods must be used to prepare composite materials, and these are described in section 7.4, with particular reference to nylon and

polyethylene substrate materials. After assessment of the surface and cross-sectional morphologies of chemically prepared substrates in section 7.5, a mechanism for the formation of the conducting polymer layer is proposed in section 7.6. Experimental conditions required for the optimization of chemically prepared conducting composite materials are then discussed in terms of the proposed mechanism in section 7.7.

7.2 Composite Film Substrates.

Conducting polymer composite films can be prepared by both electrochemical and chemical techniques as described previously in section 2.4. The electrochemical method has been most commonly used, as this is able to produce conducting polymer composite films which possess high conductivities (σ= 50 Scm^{-1}) combined with good mechanical properties (see Table 2). More recently, chemical methods of preparing conducting polymer films have also been developed. These methods can also produce highly conducting polymer composites, and have the advantage of being suited to the preparation of large area conducting films using low cost reagents[140].

This section describes the preparation of conducting polypyrrole composite films via both electrochemical and chemical methods, and a comparison is made between both routes.

7.2.1 Electrochemical Preparation.

The electrochemical polymerization of pyrrole was carried out at poly(vinylidene fluoride-trifluoroethylene) 60-40 copolymer; P(VF_2/VF_3) 60-40, coated stainless steel electrodes, with film thicknesses in the range 30-50 μm. The experimental procedure has been described previously in section 3.6. This combination was selected as a system to investigate, since the author has previously demonstrated the preparation of composite materials with excellent mechanical properties, and uniform polypyrrole content[93].

Polymerization was initiated across the whole of the electrode surface as soon as the electrode potential was stepped to +1.2 V (*vs.* silver wire) as evidenced by the formation of a black deposit at the electrode/P(VF_2/VF_3) 60-40 copolymer interface. The immediate formation of polypyrrole implies that the copolymer film is highly permeable to the electroactive species in solution. Films which are not as highly swelled by solvent require an induction period to allow for ingress of monomer and electrolyte to the electrode surface before polymerization commences. This is usually of the order of several minutes for solution cast films, but can be much longer, depending on the porosity of the substrate (see Table 2).

Initial current densities varied depending on film thickness, but were of the order of 0.8 $mAcm^{-2}$ for a 40 μm thick film. As polymerization progressed, this gradually increased to a limiting current density of approximately ~1.6 $mAcm^{-2}$, and thereafter remained at about this level until the thickness of the polypyrrole deposit exceeded the thickness of the P(VF_2/VF_3) 60-40 copolymer coat. This was usually between 200-300 minutes after deposition had commenced, and is comparable in duration to polymerization times reported at other solution cast polymer coated electrodes[151,152,158].

Polypyrrole impregnated copolymer films possessed excellent mechanical properties, as was demonstrated by their ability to be flexed without damage. In contrast, polypyrrole films produced using similar conditions were brittle. During electrodeposition, polypyrrole was incorporated uniformly within the bulk of the host film, and not at the electrode surface/polymer film interface as has been reported for other electrochemically prepared polymer substrate materials[157,158]. Evidence for this uniformity was the absence of polypyrrole on the electrode surface after deposition, coupled with the fact that polypyrrole could not be delaminated from the surface of the polymer substrate (electrode side) by abrasion. Conversely, polypyrrole which had exceeded the thickness of the host film grew laterally across the surface of the P(VF_2/VF_3) 60-40 copolymer film and was easily removed.

7.2.2 Chemical Preparation.

Composite films were prepared using variations of the method described in the work of Bocchi and Gardini[139,140], since this was reported capable of forming highly conductive (10-30 Scm^{-1}) materials. As described in section 2.4.2, three different procedures were used.

Using the first procedure, in which samples were immersed in neat pyrrole followed by oxidation with $Fe(III)Cl_3$ solution, only PVC films showed signs of deposition having occurred. However, the poor quality of deposit precluded conductivity measurements. The lack of success of this method was attributed to the inability of pyrrole to significantly permeate into the films that were used.

In the second procedure, tetrahydrofuran (THF), a solvent for PVC, was added to swell the film. Using this method, PVC substrates were successfully coated with dark coloured surface deposits of polypyrrole after ~7 minutes contact with ferric(III) chloride solution. These continued to darken in colour, so that after ~24 hours, much more extensive, uniform deposits were obtained.

The third method of preparing composite films is illustrated in Fig. 24, and used the polymer film to seal one end of a glass tube, thus forming the interface between neat pyrrole and the aqueous ferric(III) chloride solution. Polymerization then occurs on contact of pyrrole with the aqueous phase, following diffusion through the polymer film. This method proved more successful.

To assess the quality of deposition, coated films were backlit with a 1000W tungsten lamp. PVC, polyethylene, and polyester films were all coated with polypyrrole with varying degrees of success, although in general, deposits were poor and speckled in appearance. None of the films formed what can be described as a "true composite material" in which polypyrrole permeated throughout the whole thickness of the sample. The analogous method as described in ref.[140] makes no mention of the homogeneity of composite films prepared using this method. The inhomogeneous nature of deposition probably arises from differences in permeability

of pyrrole/Fe(III)Cl_3 in the film, caused by areas of differing crystallinity. Highly crystalline areas would tend to impede permeation, giving rise to regions with lower polypyrrole content, and vice versa. Indeed, similar effects have been reported for crystalline nylon-66 substrate materials impregnated with pyrrole[164].

One other point of note, was the formation of a fine dispersion of polypyrrole in bulk solution. This suggests that the rate of oxidation of pyrrole at 0°C is significantly slower than at room temperature, where oxidation is located primarily at the substrate surface. This rate effect was investigated in further detail with solid nylon and polyethylene substrates, and is discussed in section 7.6.

7.2.3 Conductivity Measurements.

The effectiveness of both electrochemical and chemical polymerization procedures was evaluated by measuring the conductivity of the resultant composites films. Using electrochemical polymerization, polypyrrole was grown throughout the entire thickness of the substrate film, thus permitting the bulk (through film) conductivity of the composites to be determined using the photoconductance apparatus and procedure described in section 3.13.

The conductivities of composites varied in the range $\sigma = 10^{-4}$ to 3 Scm^{-1}. These values are low in comparison to that reported in the literature for polypyrrole (σ= 10 to 100 Scm^{-1}), but are comparable to other similarly prepared composite materials (see Table 2). The lower values are probably due to incomplete growth of polypyrrole through the thickness of the material, which results in a highly resistive electrode-film contact.

Using chemical methods of preparing composite films, the conducting polymer deposit formed at the surface of the film only, thus precluding the use of the photoconductance cell. Instead, an approximate measure of the conductivity of the conductivity of the samples was obtained by contacting the surface of the oxidised film with the terminals of an Avometer. Although these results were not of optimum

accuracy, they were sufficient to indicate the effectiveness of the oxidation procedure. The conductivity of the coated films varied in the order polyester > polyethylene >> PVC > P(VF_2/VF_3) 60-40 copolymer (where coated). With the exception of the polyester film, this roughly paralleled the visual appearance of the composites, with the most highly coated films producing the highest conductivities. The relatively high conductivity of the polyester film was attributed to the fact that polypyrrole was formed largely on the surface of the sample, and therefore was probably more representative of polypyrrole, rather than of the PPy/polyester composite.

7.3 Comparison of Electrochemical and Chemical Methods of Forming Composite Materials.

In order to be successfully electroplated, a polypyrrole-plastic film composite must exhibit both uniform surface coverage of polypyrrole, and good conductivity to allow the facile electrodeposition of metal. It is also desirable that the polypyrrole surface coat is smooth and adheres strongly to the plastic substrate. The requirements of the overall technique are that it should be: (i) versatile, so that it can be readily adapted to suit different substrate materials, (ii) simple and quick to perform, and (iii) comparable in cost to alternative methods of fabricating conductive composite materials. Neither the electrochemical or chemical techniques adequately satisfy all these criteria, and neither method produced a composite film which was readily platable, although some copper was deposited on electrochemically prepared materials.

The advantages of electrochemical insertion as a method of producing composites, arise from the superior uniformity and homogeneity of the polypyrrole coat, and the greater degree of control over the thickness and conductivity of the polypyrrole layer, compared to chemical methods[76]. On the whole, the electrochemical method of synthesis came closest to achieving the first two requirements. Indeed, optimization of the preparative conditions with respect to

deposition potential, film counteranion, and solvent, etc., might, in future, enable the preparation of good quality platable substrates.

The major disadvantages of this approach are the need of a power source, the fact that composites are limited in size and shape by the use of electrodes, and long polymerization times. The latter drawback arises from the fact that both monomer and supporting electrolyte must diffuse through the substrate to the electrode surface before polymerization can occur. Ideally, the host substrate would be highly porous to enable rapid impregnation by pyrrole and electrolyte, and preformed rather than a film cast on the electrode surface. In practice, these requirements are inclined to be mutually exclusive, and studies by Penner and Martin[158] and Buttery and Anson[209] have shown that solution cast films possess a more porous structure than commercially available preformed films. This observation was also confirmed in previous studies, during the preparation of PPy/PVDF composite films[93].

Attempts at overcoming long polymerisation times have focused on the use of porous membranes such as Gortex[158], and the inclusion of ionic species, such as the addition of supporting electrolyte into film substrates[157]. Both of these approaches reduce deposition times by increasing the rate of ingress of electrolyte through the film. However, the number of substrates which possess porous type structures, or which are suited to impregnation by ionic centres is small, and therefore the use of this technique as a method of preparing substrates for metallization is limited.

Whilst the quality of chemically prepared composites is inferior to those produced electrochemically, chemical methods of impregnating plastic films offer several advantages; (i) monomer needs only to diffuse into the surface of the substrate, so that in principle, reaction times should be much less than that of electrochemical methods, (ii) the technique affords the possibility of preparing large area conducting films, and (iii) the use of aqueous based solvents for chemical oxidants is attractive from an industrial applications viewpoint, and might be cheaper than using electrochemical methods.

However, the major drawback of chemical methods of coating plastic substrates, was the impregnation of the film substrate with sufficient pyrrole to be able to achieve a homogeneous conducting deposit. Generally, deposits were also less adherent, and were rough in comparison with electrochemically prepared samples. Further work would be needed to overcome these problems before chemically prepared composites could be considered as suitable substrates for metal deposition.

7.4 Chemical Impregnation of Solid Plastic Substrates.

The thicker bulk of solid plastic objects precludes the use of electrochemical methods of preparation, as polymerization times will be prohibitively long. This necessitates the use of chemical methods of preparation. As mentioned in section 2.4.2, there are three different types of chemical procedure that are commonly used to prepare conducting plastic composite materials (see Table 3). These are emulsion polymerization, "in-situ" polymerization and impregnation methods. Of these methods, only "in-situ" polymerization and impregnation methods are considered as possible options for the preparation of composite substrates for metal deposition.

Emulsion polymerization techniques produce composites which are highly non-uniform with respect to both surface morphology and conducting polymer content[160,161]. They are also highly porous, and limited by poor mechanical properties. In contrast, in-situ polymerization techniques offer the advantage of being able to deposit smooth, uniform and coherent coats of conducting polymer onto a variety of different polymer surfaces[142,162,163]. However, this technique also possesses several drawbacks. Firstly, conducting polymer is formed on the substrate surface, with little penetration of the host, consequently adhesion is expected to be poor. Secondly, conducting polymer coat thicknesses are very thin (0.07 to < 5 μm)[142,163], and thirdly, lengthy reaction times (up to 6 hours) are required to coat substrates. The low rate of polymerization presumably being limited by the low concentrations of solutions (10^{-2} - 10^{-1} M) with respect to monomer and oxidant, that are necessary to prevent polymerization from occurring in bulk solution.

Some improvement in adhesion of conducting polymer surface coats has been achieved with in-situ polymerization techniques, through the chemical derivation of substrate surfaces with carboxylic and sulphonic groups. These groups function as dopants for the conducting layer, and because they are also chemically bonded to the substrate surface, improved adhesion is obtained. However, this benefit is partly offset by the increase in the time required for the preparation of substrates prior to deposition (up to 24 hours), and the increased complexity of the procedure. Moreover, this procedure also produces a slight increase in surface roughness of the substrate surface[162].

Chemical impregnation techniques offer several advantages over both emulsion and in-situ methods of preparing conducting polymer composites. These include the ability to be able to prepare thick conducting polymer coats, with conductivities of the order of 100 Scm^{-1}, which is comparable to that obtained using electrochemical methods of polymerization. Reaction times needed to complete polymerization at room temperature can be of the order of minutes, depending on the porosity of the substrate material. This is significantly shorter than that required for in-situ polymerization. Furthermore, since monomer or oxidant is incorporated in the matrix of the substrate, highly adhesive surface coats are also obtained.

In this section the formation of solid conducting polymer composites by the impregnation method is studied. The substrates chosen for study were both hydrophobic and hydrophilic, and included polyethylene co-axial cable, polyethylene and nylon. The objective behind using co-axial cable was to investigate the feasibility of replacing the copper wire braid which is currently used to screen electromagnetic radiation, via a conducting polymer/metal coat combination. Nylon substrates were also used to investigate the versatility of this procedure with other materials.

7.4.1 Polyethylene Co-axial Cable.

Polyethylene co-axial cable substrates were impregnated with polypyrrole and polyaniline according to the method previously described in section 3.14.1.

No appreciable uptake of either monomer occurred below the temperature at which polyethylene softened ~95°C. Whereas at temperatures higher than this, pyrrole and aniline were both readily absorbed.

Polymerization was carried out at 20°C using ferric(III) chloride (25% wt.). The rate of oxidation of the absorbed pyrrole was rapid, and complete surface coverage was achieved after about six minutes. At this stage, the polypyrrole surface coat did not permeate the co-axial substrate and could be easily removed by scraping with a sharp edge. This was not the case for samples which had been immersed in oxidant for several hours. With these, the conducting coat permeated the thickness of the cable, giving rise to highly adherent matt black surface coats.

Following impregnation with aniline, samples were immersed in either ferric(III) chloride, or ammonium persulphate solution at 0° and 20°C. Treatment with ferric(III) chloride at 20°C yielded polyaniline coats, but not at 0°C. In contrast, ammonium persulphate solution effected oxidation at both 0°C and 20°C, which is consistent with the fact that this is the stronger of the two oxidants. In all instances, oxidation produced adherent matt black coats of polyaniline which permeated into the surface of the co-axial cable.

It was not possible to obtain quantitative measurements of the amount of polymer formed during oxidation, due to the fact that ferric(III) chloride etched and dissolved the inner copper core. In fact, all ferric(III) chloride treated substrates displayed a net weight decrease compared to the original untreated cable. Another problem that precluded accurate measurements, was the ingress of monomer between the copper core and the inner part of the cable. For these reasons, quantitative measurements were carried out on solid substrates only.

7.4.2 Nylon-6, Nylon-12; Polypyrrole Composites.

Nylon-6 and Nylon-12 substrates were both readily impregnated with pyrrole, and uniformly coated polypyrrole composite materials were obtained by using the procedure which is described in section 3.14.2.

Fig. 58 shows the weight uptake of pyrrole monomer by nylon-6, and the yield of polypyrrole following oxidation with ferric(III) chloride solution (25% wt. for 24 hours) as a function of temperature. All samples were immersed in monomer for 15 minutes. The rate of ingress of pyrrole into the substrate increased linearly with temperature up to 60°C and then more rapidly as the glass transition temperature of the nylon substrate was reached.

The rate of formation of polypyrrole at 0°C was much slower than that for co-axial cable at room temperature, and samples needed to be immersed for several hours to achieve an all over uniform coat. The slow rate of oxidation at 0°C produced a low yield of polypyrrole as illustrated in Fig. 58. This decrease in weight subsequent to immersion in ferric(III) chloride solution implies that some pyrrole was leached out of the substrate during oxidation.

Also plotted on the same axes for comparison, are the theoretical yields of polypyrrole that might be expected from the reaction of pyrrole with aqueous $FeCl_3$. These were calculated from the following equation,

$$\text{T.Y.} = N_{(py)} \cdot (\text{M.wt. of pyrrole moiety } -2) + (\text{M.wt. per dopant anion}) \cdot f \qquad (7.1)$$

where $N_{(py)}$ is the number of moles of pyrrole adsorbed by the substrate, and f is the dopant ratio. Since different workers are in disagreement over the nature of the dopant anion and levels of doping which are achieved via chemical oxidation, values are plotted for both $Cl^{-(143,145)}$ and $FeCl_4^{-(128,141,143)}$ anions, at dopant ratios of between 0.25 and 0.33. These levels of oxidation are typical of that reported for the electrochemical oxidation of pyrrole with other univalent anions (see Table 1).

Fig. 59 shows the weight uptake of pyrrole by nylon-6 at 60°C as a function of time. Due to the poor yield of polypyrrole obtained with ferric(III) chloride at 0°C, the oxidation of pyrrole impregnated nylon-6 was carried out at 20°C only. This resulted in a much more rapid oxidation, and visible deposits of polypyrrole were formed on substrate surfaces after only a few minutes. The higher oxidation temperature also increased the yield of polypyrrole for a given time of exposure to oxidant, as shown.

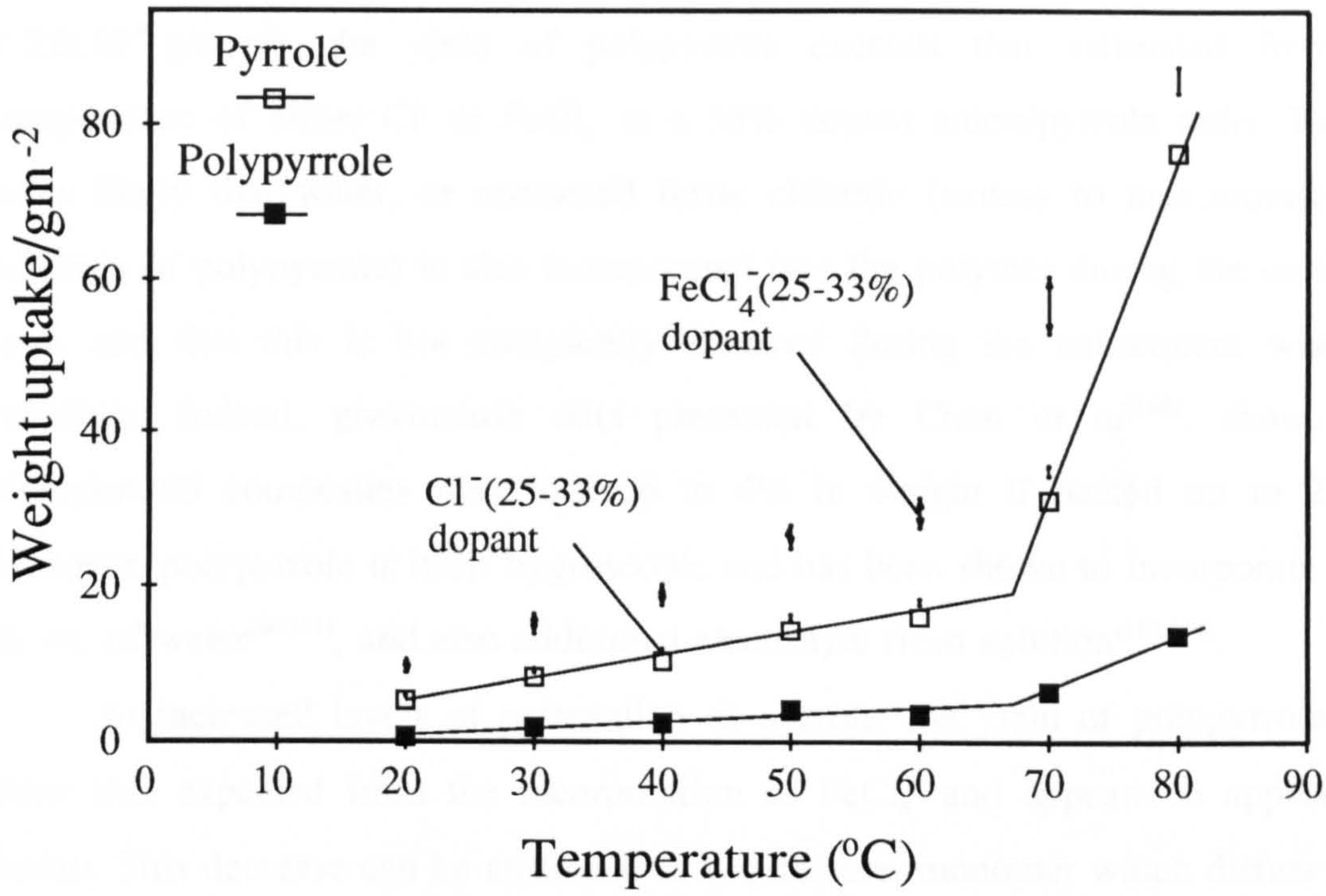

Fig. 58. The weight uptake of pyrrole monomer by nylon-6 as a function of temperature, and the yield of polypyrrole following oxidation with ferric(III) chloride solution (25% wt. for 24 hours at 0°C). Samples were immersed in pyrrole 15 minutes.

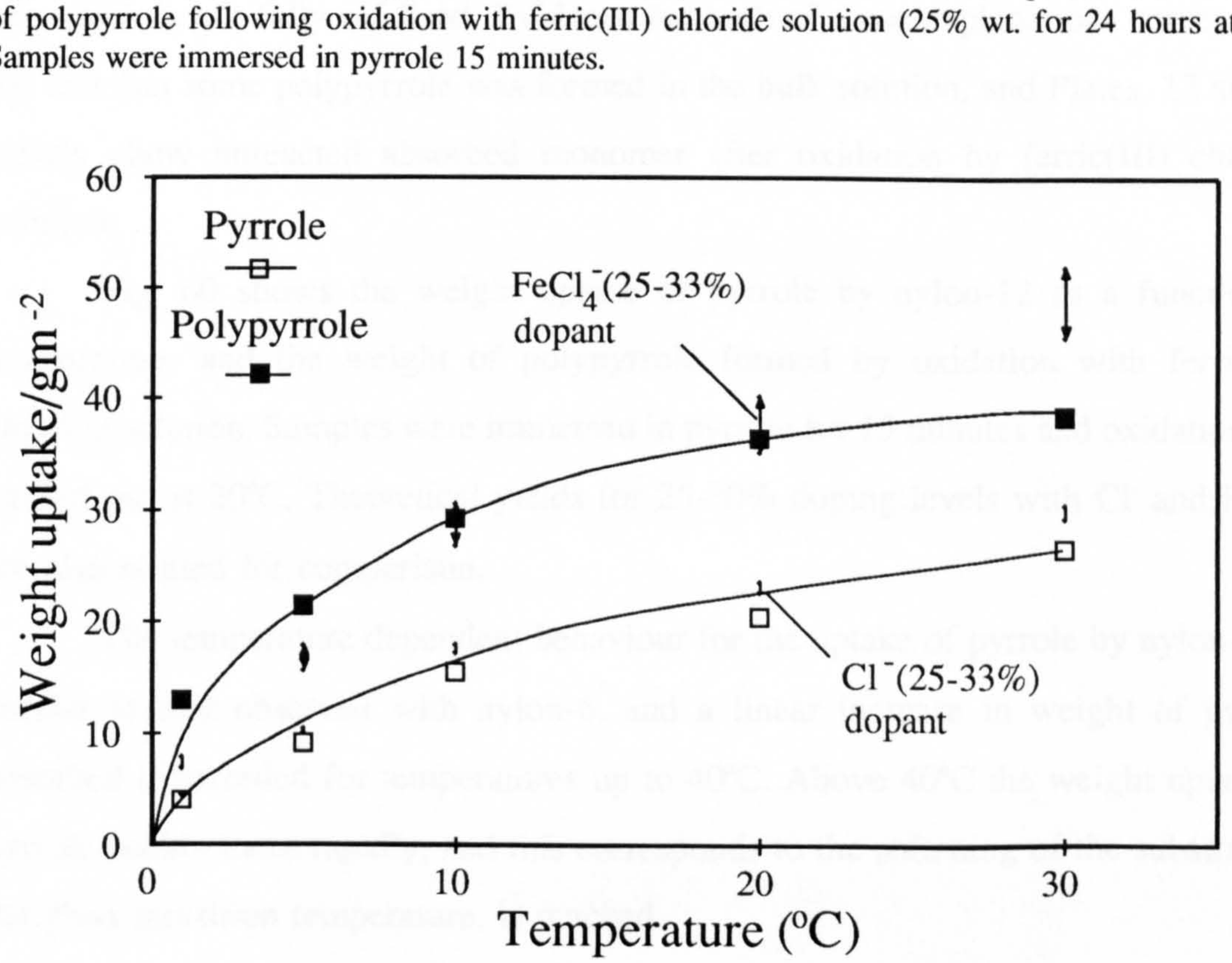

Fig. 59. The weight uptake of pyrrole by nylon-6 at 60°C as a function of time, and the yield of polypyrrole after oxidation with ferric(III) chloride solution (25% wt. for 24 hours at 20°C).

At low levels of ingress of pyrrole into the nylon-6 substrate ($< 22x10^{-6}$ g/mm^2), the yield of polypyrrole exceeds that estimated from the incorporation of either Cl^- or $FeCl_4^-$ at a 33% dopant anion/pyrrole ratio. Thus, it seems likely that water, or unreacted ferric chloride (excess to that required for oxidation of polypyrrole) is also incorporated into the polymer during the oxidation stage, and that this is not completely removed during the subsequent work up procedure. Indeed, gravimetric data presented by Chen *et al*[164], shows that PPy/nylon-66 composites may lose up to 4% in weight if heated up to 230°C. Moreover, polypyrrole is itself hygroscopic and has been shown to incorporate up to 7% wt. of water[80,131], and also additional electrolyte from solution[119,121].

At increased levels of permeation of pyrrole, the yield of polypyrrole falls below that expected from the incorporation of $FeCl_4^-$ and appears to approach a plateau. This decrease can be attributed to two factors, monomer which diffuses into bulk solution before undergoing oxidation, and monomer which is absorbed by nylon, but which is not fully oxidised. Evidence for both of these explanations comes from the fact that some polypyrrole was formed in the bulk solution, and Plates. 12 and 13 clearly show unreacted absorbed monomer after oxidation by ferric(III) chloride solution.

Fig. 60 shows the weight uptake of pyrrole by nylon-12 as a function of temperature, and the weight of polypyrrole formed by oxidation with ferric(III) chloride solution. Samples were immersed in pyrrole for 15 minutes and oxidation was carried out at 20°C. Theoretical yields for 25-30% doping levels with Cl^- and $FeCl_4^-$ are also plotted for comparison.

The temperature dependent behaviour for the uptake of pyrrole by nylon-12 is similar to that observed with nylon-6, and a linear increase in weight of pyrrole adsorbed is recorded for temperatures up to 40°C. Above 40°C the weight uptake of pyrrole occurs more rapidly, and this corresponds to the softening of the substrate as the glass transition temperature, is reached.

7.4.3 Nylon-6, Nylon-12; Polyaniline Composites.

Nylon-6 samples were prepared according to the procedure described in section 3.14.2, and then heated at 50°C for 15 minutes in aniline. Oxidation was carried out with $FeCl_3$ (25% wt./vol.), at 0°C and 20°C for 24 hours. Nylon-6 substrates were not readily impregnated with aniline, and samples which were oxidised at 0°C did not form a polyaniline coat. Samples which were immersed in aqueous ferric(III) chloride solution at 20°C did show surface oxidation, but insufficient aniline was oxidised to produce an overall surface coat, and in general surface deposits were unsatisfactory.

In contrast, nylon-12 substrates were much more readily impregnated by aniline, and formed shiny black polyaniline coats on oxidation. Fig. 61 shows the weight increase of nylon-12 samples after 15 minutes immersion in aniline as a function of temperature. Oxidation was performed at 20°C in $FeCl_3$ for 24 hours.

The rate of permeation of aniline into nylon-12 below 40°C is only 0.15 times that of pyrrole under analogous conditions (measured from the gradients in Figs. 60 and 61), and indicates that nylon-12 was more highly swelled by pyrrole than aniline. The rate of chemical oxidation of aniline in aqueous ferric(III) chloride was also significantly lower than that of pyrrole, and samples were only uniformly coated after being immersed in oxidant for several hours. This observation was borne out by the poor yields of polyaniline that were obtained. In fact, samples that were impregnated with aniline at temperatures less than 40°C, all weighed less than samples impregnated with aniline only. This weight loss for the oxidised samples indicates that a significant amount of aniline must have diffused from the sample into bulk solution, and this was confirmed by the presence of a powdery dispersion of polyaniline in the bulk solution after oxidation.

Fig. 61: The weight increase of nylon-12 samples after 15 minutes immersion in aniline as a function of temperature, and the yield of polyaniline following oxidation with ferric(III) chloride solution at 20°C.

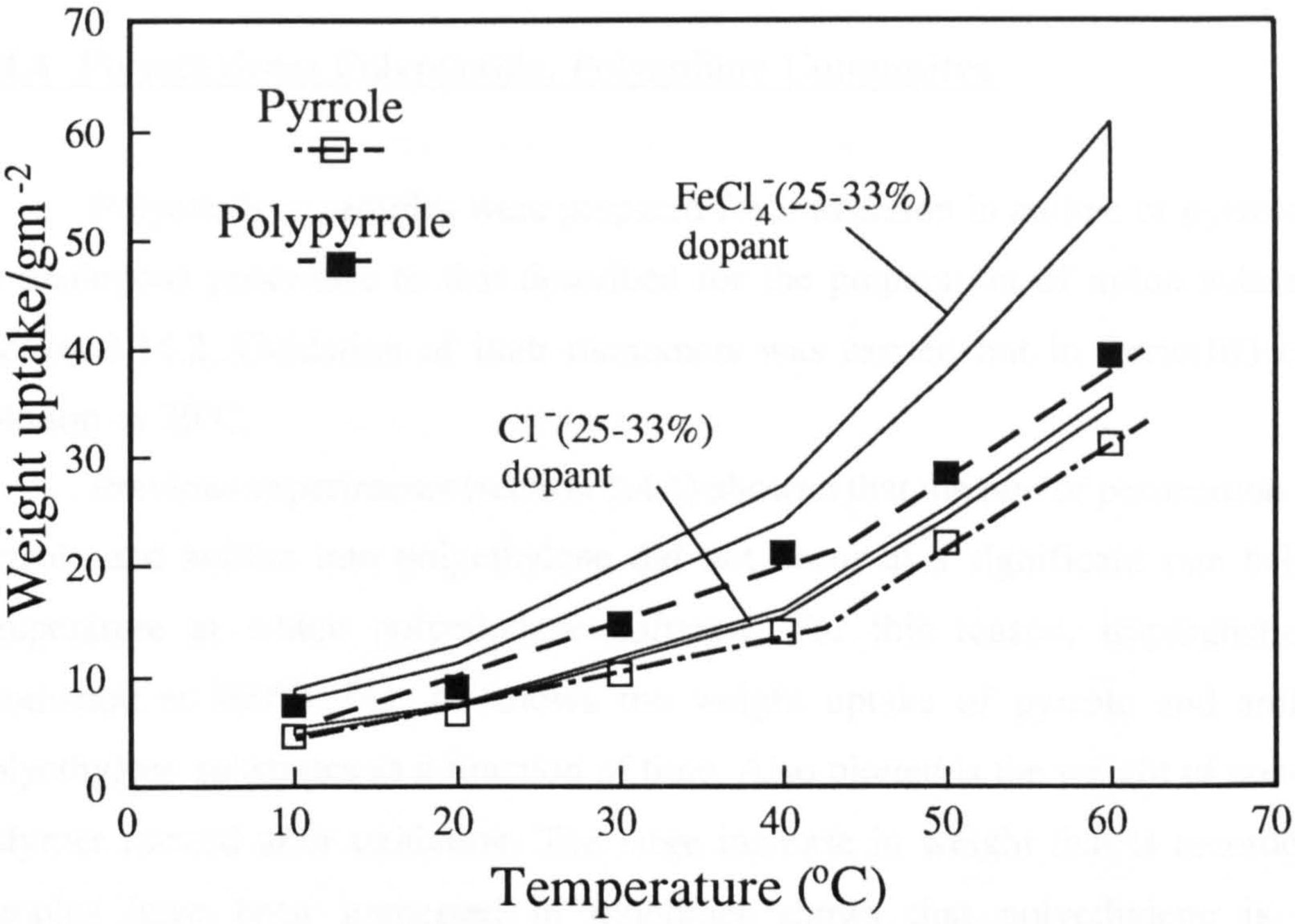

Fig. 60. The weight uptake of pyrrole by nylon-12 as a function of temperature, and the weight of polypyrrole formed by oxidation with ferric(III) chloride solution at 20°C.

Fig. 61. The weight increase of nylon-12 samples after 15 minutes immersion in aniline as a function of temperature, and the yield of polyaniline following oxidation with ferric(III) chloride solution at 20°C.

7.4.4 Polyethylene; Polypyrrole, Polyaniline Composites.

Polyethylene samples were prepared for immersion in aniline or pyrrole, using an analogous procedure to that described for the preparation of nylon substrates in section 3.14.2. Oxidation of both monomers was carried out in ferric(III) chloride solution at 20°C.

Previous experiments (section 7.4.1) showed that the rate of permeation of both pyrrole and aniline into polyethylene did not occur at a significant rate below the temperature at which polyethylene softened. For this reason, impregnation was conducted at 100°C. Fig. 62 shows the weight uptake of pyrrole and aniline by polyethylene substrates as a function of time. Also plotted is the weight of conducting polymer formed after oxidation. The large increase in weight that is recorded after samples have been immersed in monomer shows that polyethylene is readily impregnated by both pyrrole and aniline. However, in contrast to experiments conducted on nylon substrates, the rate of ingress of aniline in polyethylene was higher than that of pyrrole.

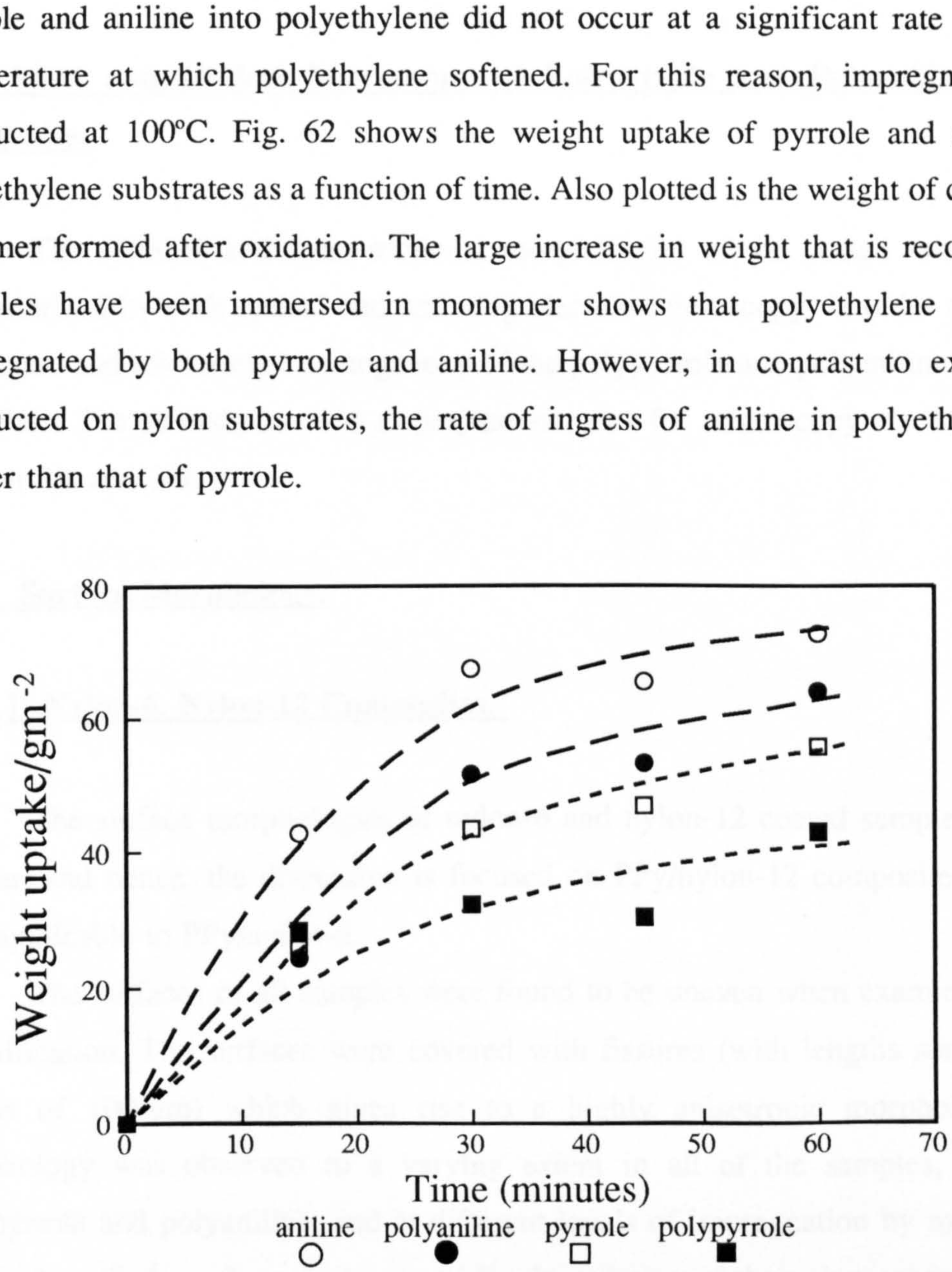

Fig. 62. The weight uptake of pyrrole and aniline by polyethylene substrates as a function of time. Also plotted is the weight of conducting polymer formed after oxidation with $FeCl_3$, (25% wt., 24 hours at 20°C).

The surfaces of polyaniline and polypyrrole coated polyethylene substrates were much rougher in comparison to nylon coated samples. This was probably due to the harsh conditions that were required to effect monomer impregnation, necessitated by the fact that monomer was not significantly absorbed at temperatures below that at which polyethylene softened. Under these conditions the amount of impregnation of monomer in to the substrate is difficult to control, and can easily result in excessive degradation of the polymer substrate materials.

7.5 SEM and Optical Microscopy of Polypyrrole and Polyaniline Coated Substrates.

The surfaces and cross-sectional morphologies of the coated samples were characterized by both optical and scanning electron microscopy, in order to evaluate the macro and micro-level homogeneity of the polypyrrole and polyaniline composite materials. The procedures used to prepare samples for microscopy are described in section 3.8 and 3.9.

7.5.1 Surface Morphology.

7.5.1.1 Nylon-6, Nylon-12 Composites.

The surface morphologies of nylon-6 and nylon-12 coated samples are very similar, and hence, the discussion is focused on PPy/nylon-12 composites, but it is also applicable to PPy/nylon-6.

The surfaces of all samples were found to be uneven when examined at high magnification. The surfaces were covered with fissures (with lengths sometimes in excess of 100 μm) which gives rise to a highly anisotropic morphology. This morphology was observed to a varying extent in all of the samples, both with polypyrrole and polyaniline, and at different levels of impregnation by monomer. It is therefore likely to have been caused by degradation of the nylon substrate during the chemical pre-treatment stage, rather than by fibrillar type growth of polypyrrole or polyaniline.

The extent of surface degradation appears to be almost independent of the level of pyrrole incorporation, and more affected by the difference in monomer. Aniline produced the greatest degradation of the nylon surfaces, as shown by the comparison of plates 7 and 8, which show samples impregnated with polypyrrole and polyaniline. PPy/nylon-6 composites were also slightly more affected by the chemical oxidation procedure compared to PPy/nylon-12 samples.

The degree of surface roughness exhibited by these samples is comparable to that of substrates which are used in electroless deposition, in which samples are normally etched to depth of 1-2 μm[2-4]. Plastics which are electroplated typically have metal deposits with thickness of up to ~40 μm, depending on the envisaged application[4,16]. Since metal plating solutions usually contain levellers which smooth out irregularities[8,16], roughness of scale of a few microns is not significant unless thin metal deposits are required. Hence, this procedure of preparing polypyrrole and polyaniline coated nylon substrates displays potential for further investigation, if the conditions of chemical impregnation and oxidation were optimized.

7.5.1.2 Polyethylene Composites.

Plates (9-11) show the typical surface morphology exhibited by PE samples following impregnation with polyaniline and polypyrrole. The surfaces of all PPy/PE and PA/PE composites were highly degraded during preparation. Plates 9 and 11 of PPy/PE and PA/PE composites, show that crack lengths of several tens of microns completely cover the surface, and also penetrate into the bulk polymer. The fact that the fracture surfaces are not sharply cleaved suggests that this degradation occurs during the impregnation and oxidation steps rather than during the subsequent drying stage.

Plates 10 and 11 shows the surface morphology of PA/PE composites which were impregnated with aniline for durations of 30 and 60 minutes respectively. The surfaces of samples which were immersed for the shortest time are much smoother than that obtained after 60 minutes, although both samples would be considered to be too rough for electroplating. Since both samples were oxidised under similar

(7)

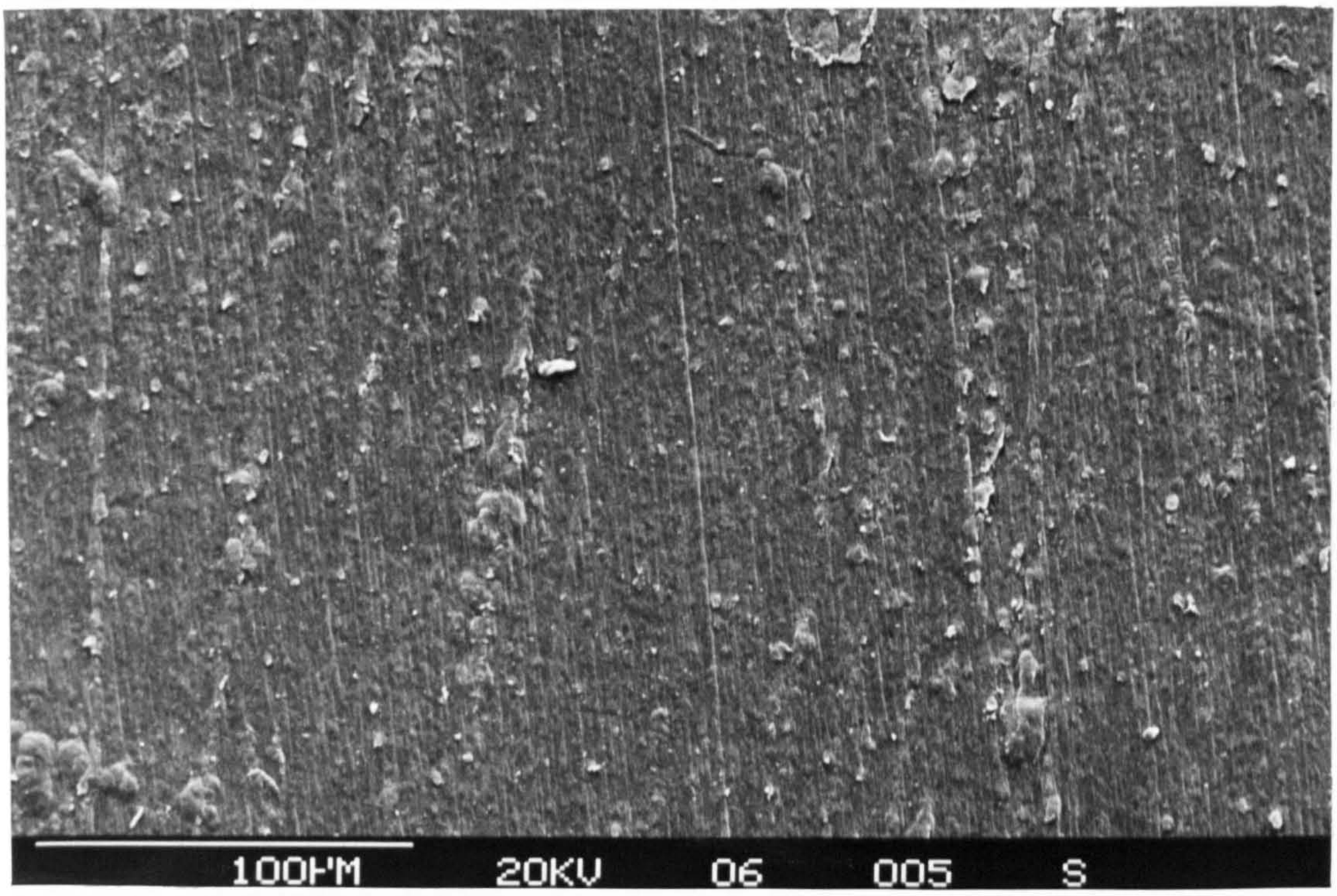

(8)

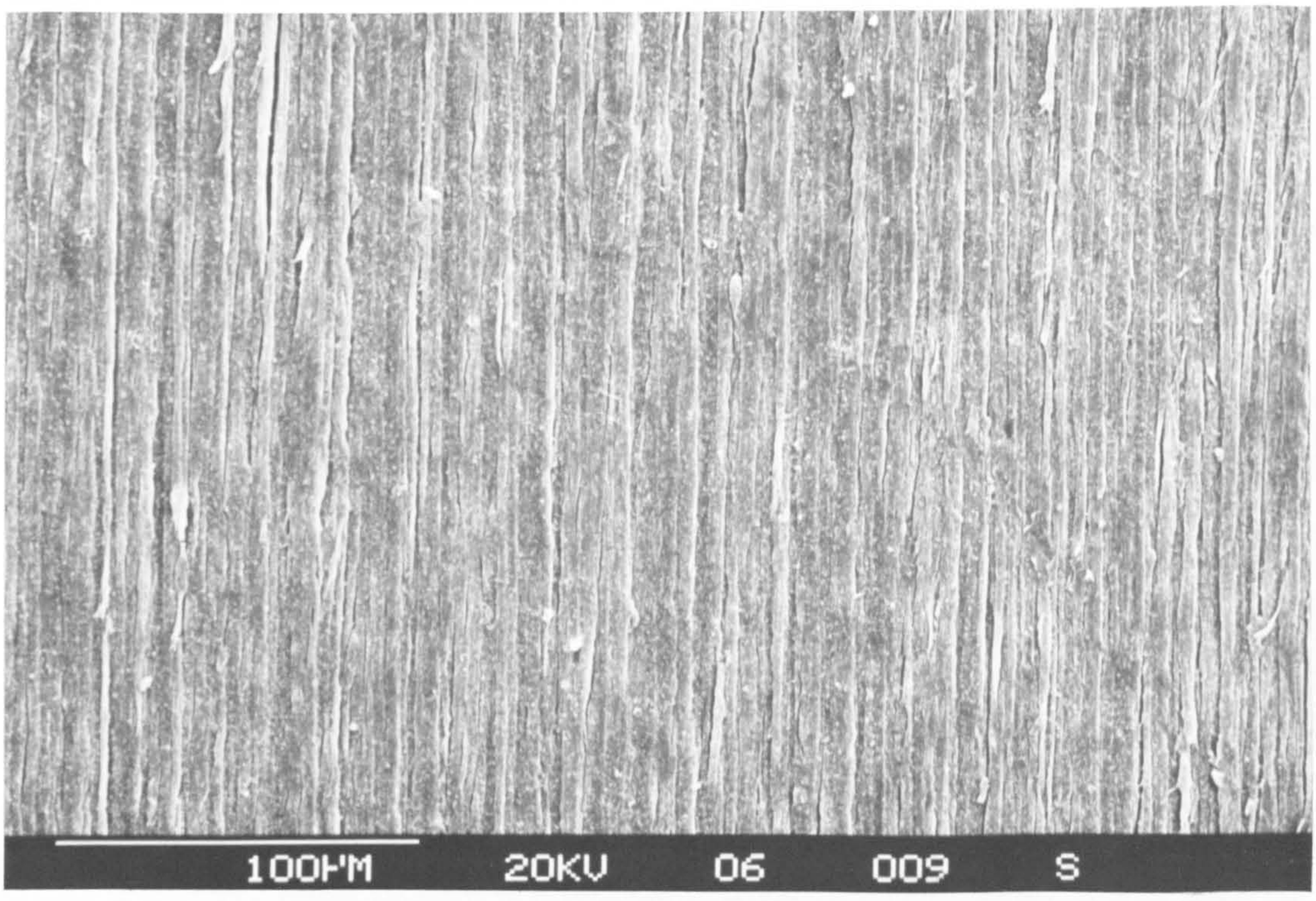

Plates 7 and 8. Surface morphology of polypyrrole/nylon-12 (7), and polyaniline/nylon-12 (8) composites; prepared by immersion in monomer (15 minutes at 60°C) followed by oxidation with ferric(III) chloride solution (25% wt. at 20°C).

(a)

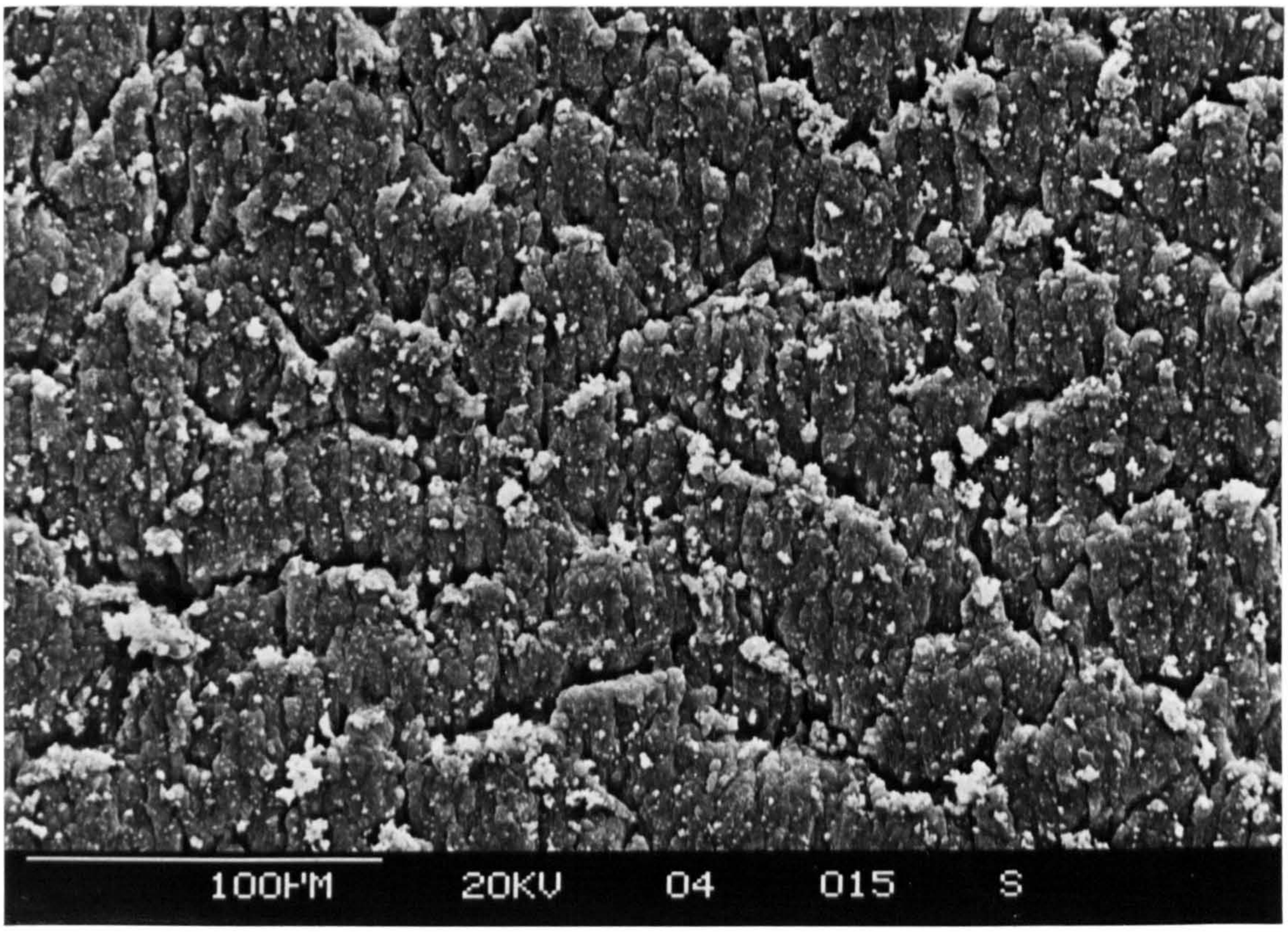

(b)

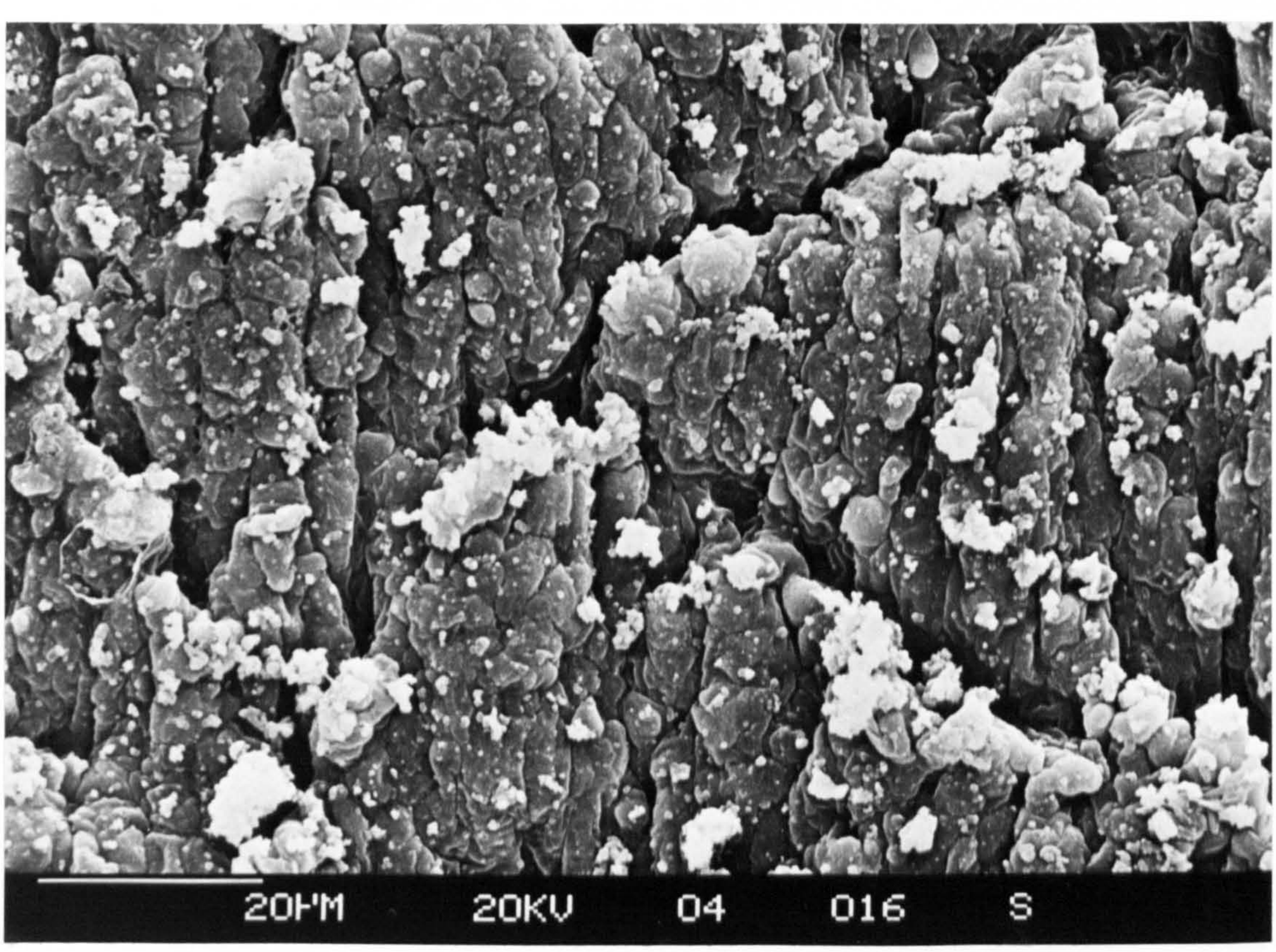

Plates 9(a-b). Surface morphology of a polypyrrole/polyethylene composite; prepared by immersion in pyrrole (30 minutes at ~100°C) followed by oxidation with ferric(III) chloride solution (25% wt. at 20°C).

(a)

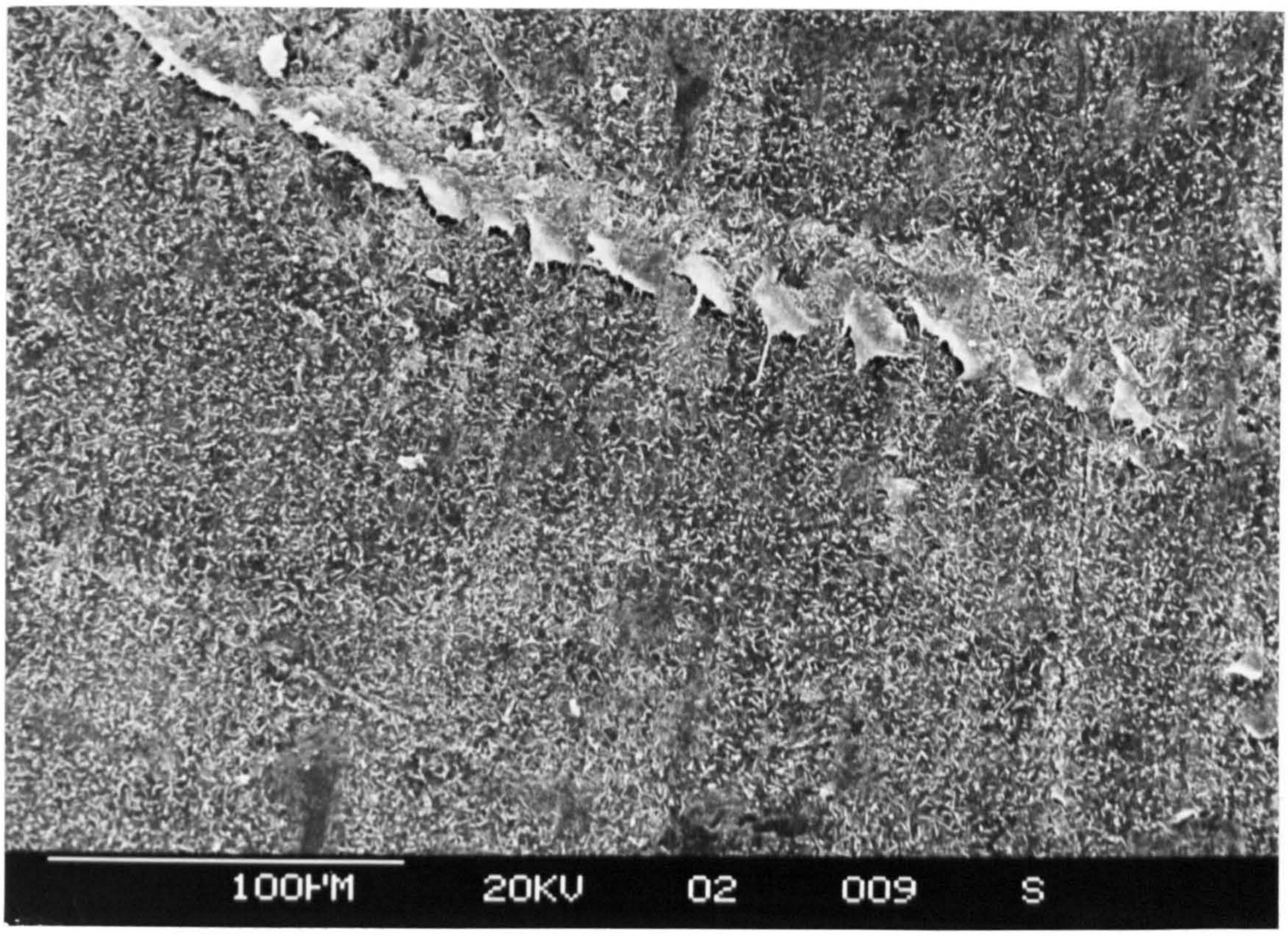

(b)

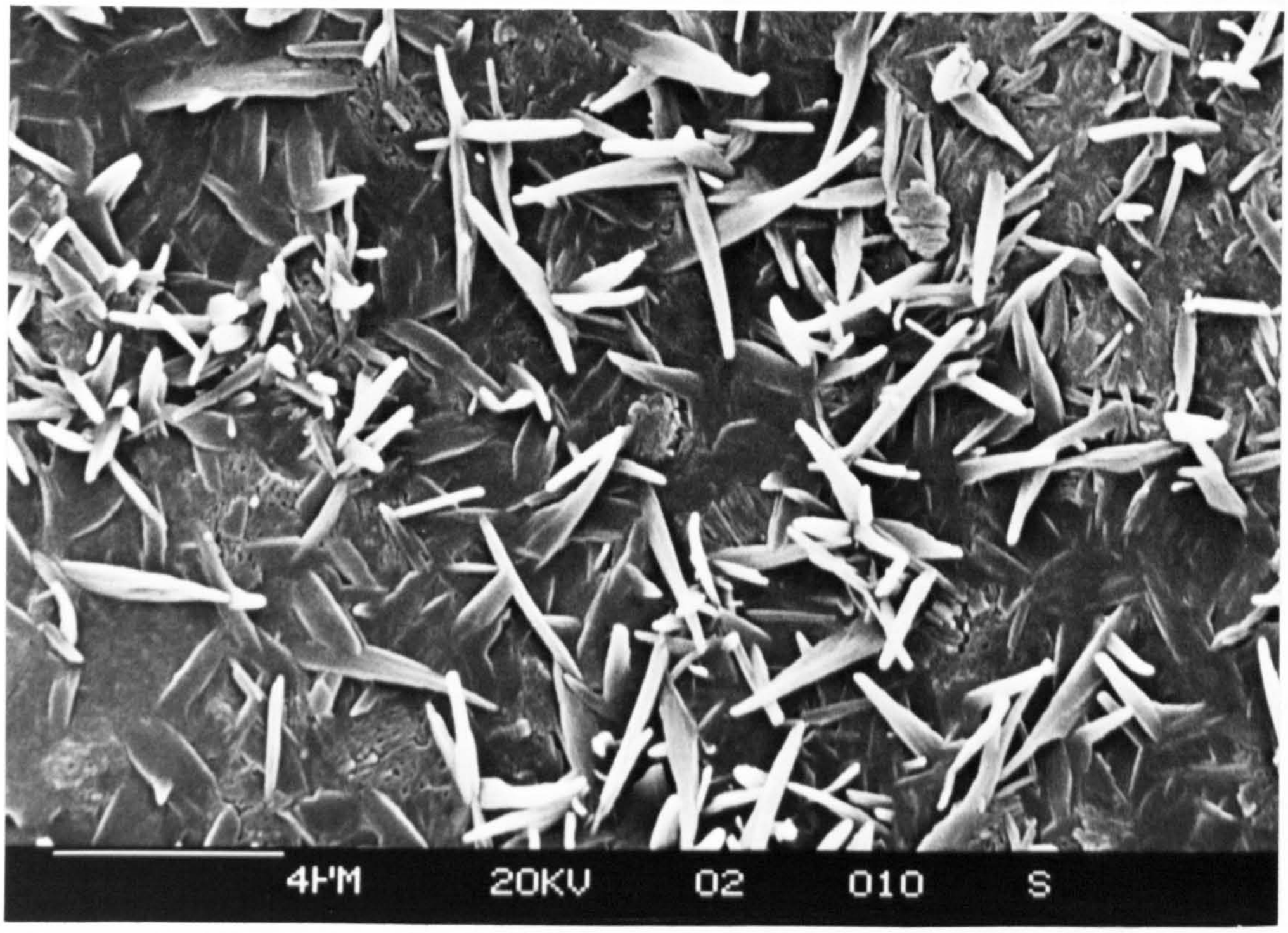

Plates 10(a-b). Surface morphology of a polyaniline/polyethylene composite; prepared by immersion in aniline (30 minutes at ~100°C) followed by oxidation with ferric(III) chloride solution (25% wt. at 20°C).

(a)

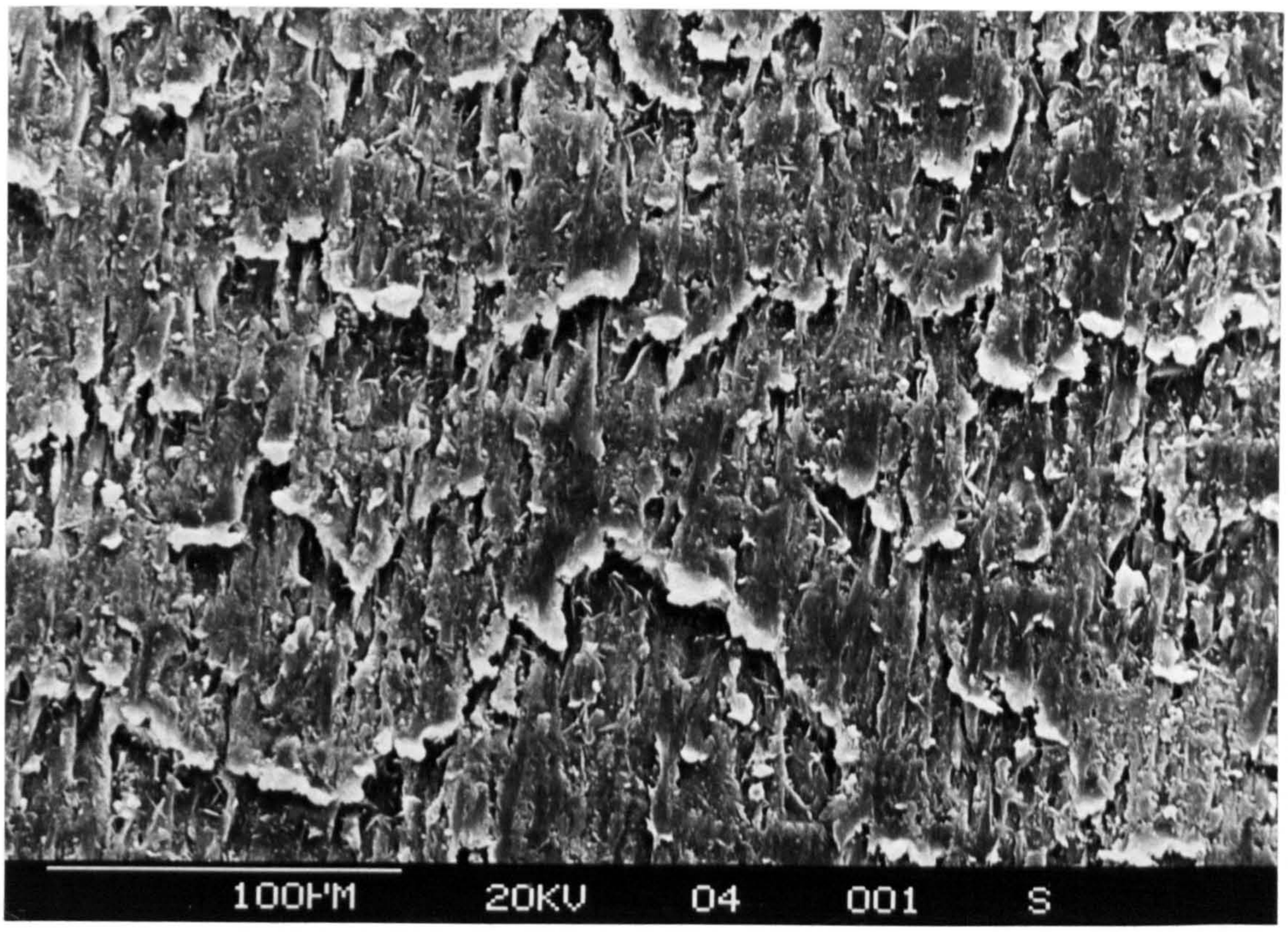

(b)

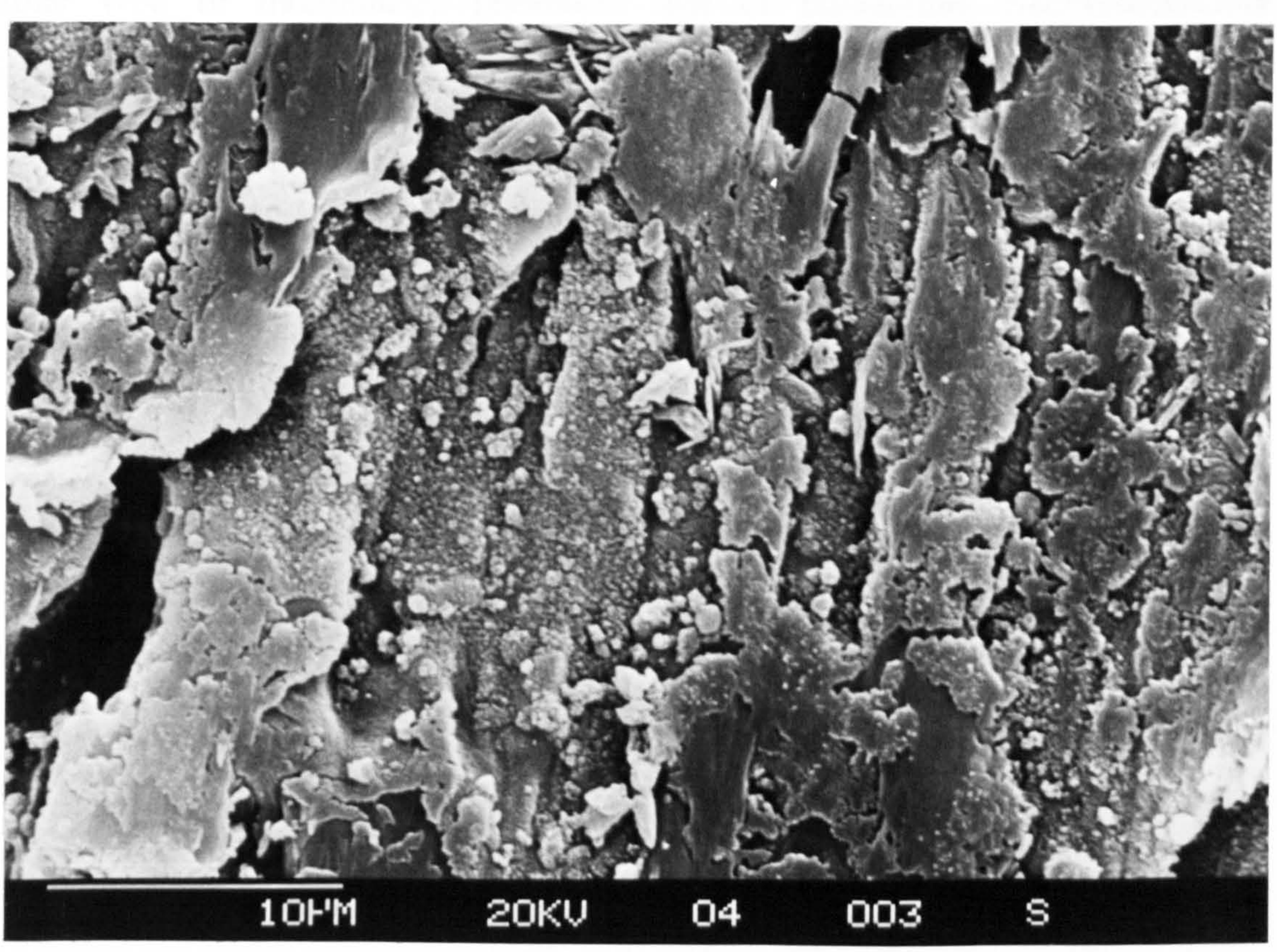

Plates 11(a-b). Surface morphology of a polyaniline/polyethylene composite; prepared by immersion in aniline (60 minutes at ~100°C) followed by oxidation with ferric(III) chloride solution (25% wt. at 20°C).

conditions, the major degradation of the surface is likely to have occurred during the monomer impregnation stage, rather than during the subsequent oxidation stage. Other PA/PE samples which were impregnated for 45 minutes (not shown), display intermediate levels of surface degradation, and confirm that the monomer impregnation stage is the major cause of surface degradation.

One interesting phenomenon of the polyaniline coated samples in Plate 10(b) is the needle like morphology of the surface layer. This was unique to PA/PE composites, and is unusual, since chemical oxidation generally produces amorphous deposits. However, it is difficult to determine from these micrographs, whether this type of morphology is due to polyaniline, or whether it is an artefact of the underlying poly(ethylene) surface. Comparison with other micrographs of polyaniline in the literature is hindered by the fact that there has been no thorough morphological study. Moreover, in the reports that do contain micrographs, polyaniline has been prepared by electrochemical synthesis, thus precluding a direct comparison. In spite of this, the fibrillar type of morphology resembles that of polyaniline electrochemically polymerized in the presence of perchlorate anions[210], and the more powdery type of morphology shown in Plate 11(b) is reminiscent of that electrochemically deposited onto graphite fibres with chloride anions[211]. These comparisons suggest that the observed surface morphology may be due to polyaniline.

The dependence of surface morphology on reaction conditions would need to be investigated more thoroughly if polyaniline or polypyrrole coated polyethylene substrates were to be considered as substrates for electroless/electrochemical deposition. Certainly, the present level of surface roughness produced using this impregnation and oxidation procedure would preclude the use of these composites as substrates.

7.5.2 Cross-Sectional Morphology.

In addition to the surface analysis of morphology by SEM, the cross-sectional morphology of chemically prepared nylon and polyethylene composites was also examined using optical microscopy.

7.5.2.1 Nylon-6 Composites.

Plates 12 and 13 are typical optical micrographs of cross-sections of nylon-6 coated with polypyrrole. The sample shown in plate 12 was impregnated with pyrrole for 15 minutes at 60°C, followed by oxidation with ferric(III) chloride solution at 0°C. The sample shown in plate 13 was prepared under identical conditions, except that oxidation was carried out at 20°C.

Two distinct regions of polypyrrole deposit can be identified from the micrographs. These are designated as:

(i) An inner region of "polypyrrole" in which the degree of oxidation of the absorbed pyrrole varies from that of essentially unreacted monomer (yellow), through to that of almost fully oxidised polypyrrole (black). The extent of oxidation is conveniently shown by the gradual change in colour across this region, which varies through yellow, orange, brown, and black.

(ii) An outer region of more heavily oxidised polypyrrole which is darker in colour than the adjacent region. The thickness of this layer is of the order of 0.01 to 0.02 mm thick, and is considerably less than that of region (i) (~0.1 mm), which is defined by the depth of permeation of pyrrole into the substrate. It is possible that this outer layer consists almost entirely of polypyrrole formed on the surface of the substrate. This view is supported by comparison with micrographs of cross-sections of other PPy/nylon composite materials in the literature, prepared by impregnation methods, which also show regions of polypyrrole formed on the surfaces of substrates[164].

The extent of formation of regions (i) and (ii) was dependent on the conditions of synthesis, such as the time of immersion in monomer, impregnation temperature, oxidation temperature. Plate 13 shows that oxidation at 0°C produced polypyrrole coat thicknesses much thinner than that formed by oxidation at 20°C, which is in accord with the gravimetric data presented in Fig. 58. However, as a result of the complexities of the interaction between the various parameters, no quantitative relationship between the thickness of the conducting polymer layer and each of these parameters could be determined.

(12)

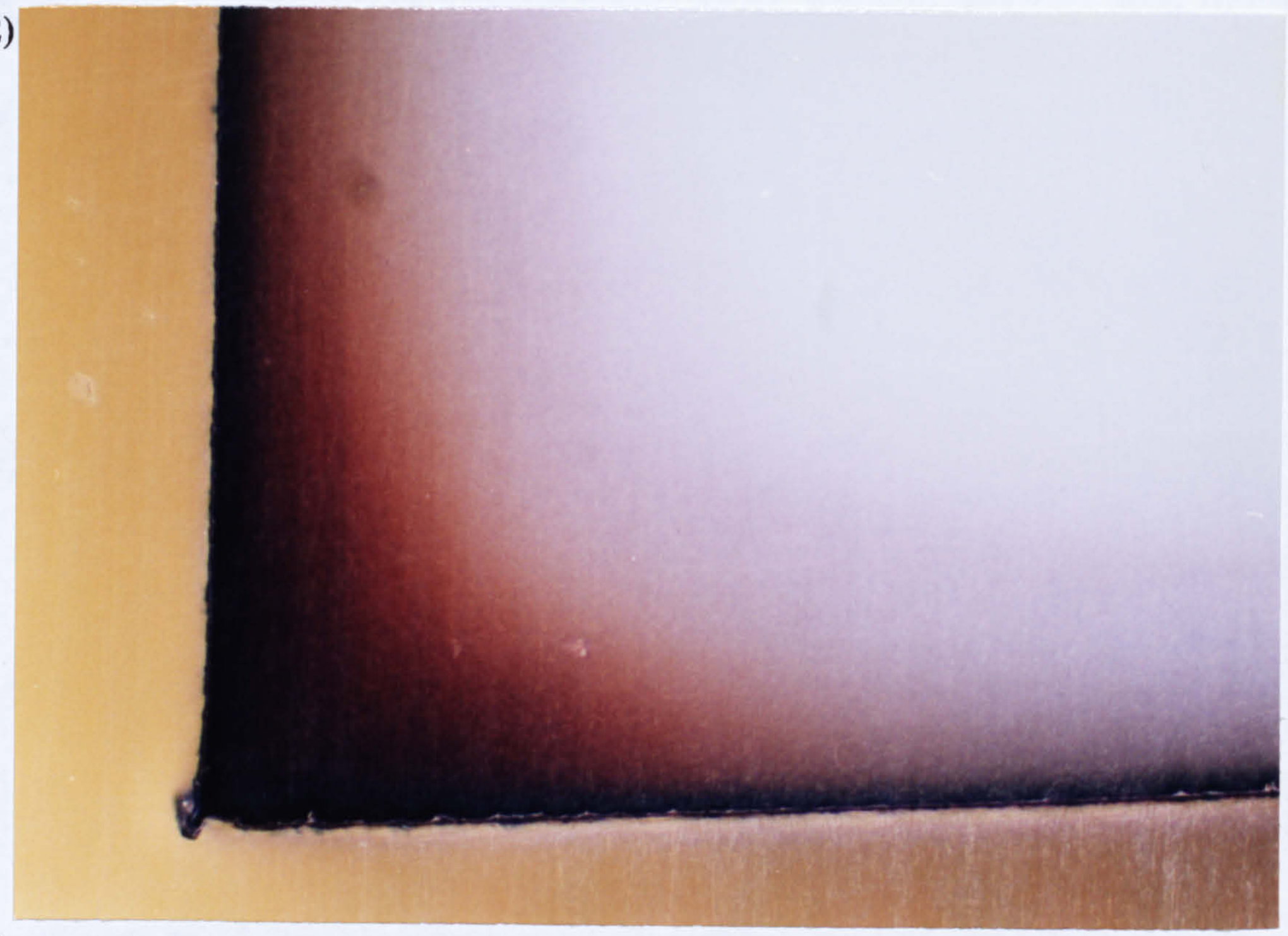

(13)

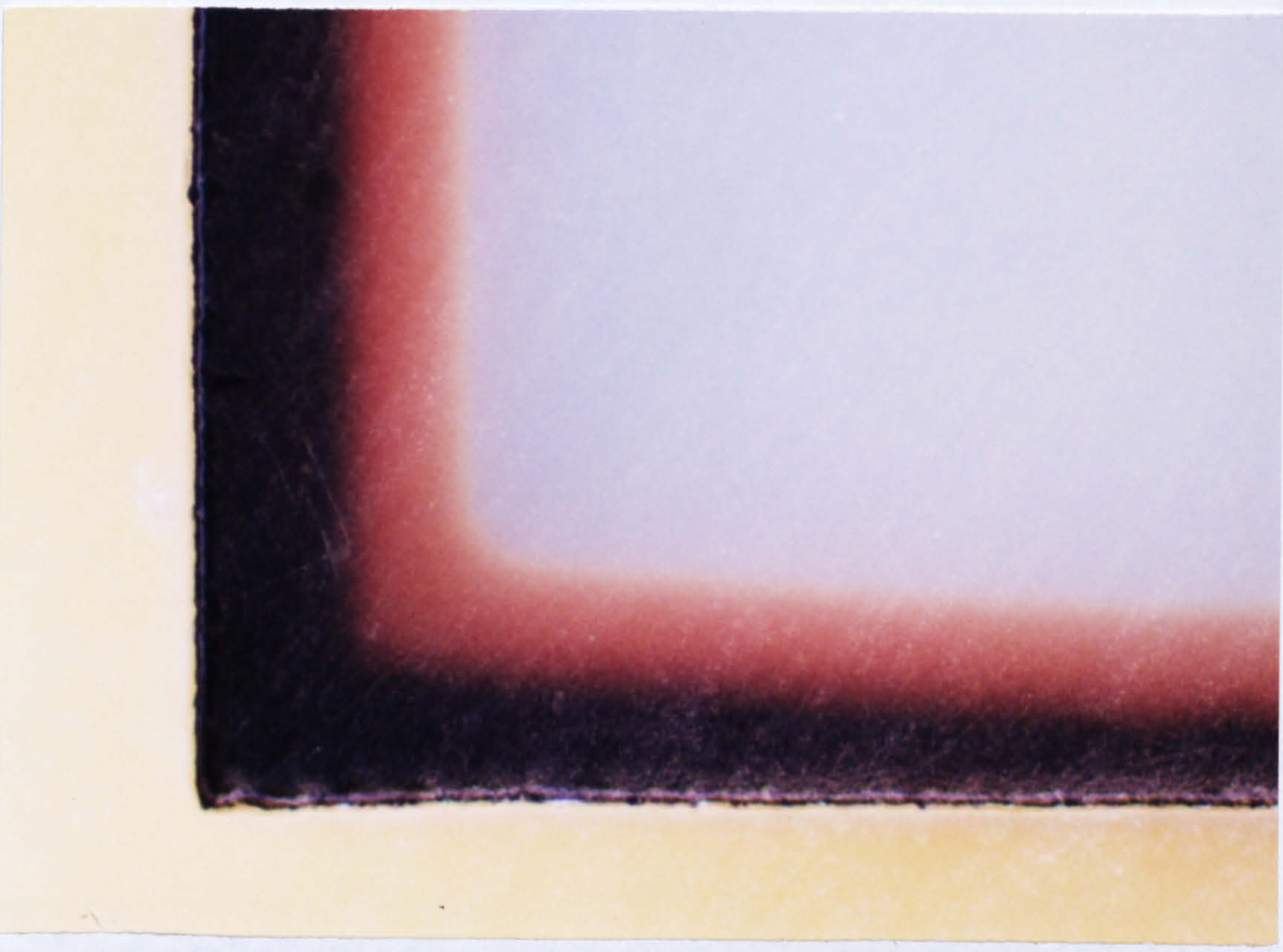

Plates 12 and 13. Optical micrographs of cross sections of nylon-6 coated with polypyrrole. Samples were impregnated with pyrrole for 15 minutes at 60°C, followed by oxidation with ferric(III) chloride solution (25% wt.). Plate 12, oxidation carried out at 0°C, Plate 13, oxidation carried out at 20°C.

7.5.2.2 Nylon-12 Composites.

A wide variety of different cross-sectional morphology was observed for nylon-12 samples, with the variations showing approximate correlation with the conditions of synthesis. Unreacted and/or only partly oxidised monomer was evident with polypyrrole coated substrates, indicating incomplete oxidation (c.f. nylon-6 coated samples in Plates. 12 and 13, but is not apparent with samples that were impregnated with aniline. This can probably be explained by the much lower level of incorporation of aniline by nylon-12 during synthesis, as shown in Fig. 61.

Plates 14(a-b) shows a comparison of PPy/nylon-12 composites that were immersed in pyrrole at 30°C and 60°C. Substrates impregnated with monomer at the lower temperature exhibit uniform coats of polypyrrole, ~0.01-0.015 mm thick, with few obvious defects. On the other hand, the outer layer of substrates impregnated with pyrrole at 60°C are extensively degraded, and contain cracks or fissures that penetrate the surface to a depth of up to 0.08 mm. These fissures produce areas of non-uniformity in the thickness of the surface coat, by allowing ferric(III) chloride solution to permeate into the bulk more easily. Consequently, such areas are highly non-uniform and display a higher level of oxidation than the surrounding regions. Defects of this nature are undesirable and are expected to seriously affect the bulk mechanical properties of composite materials. The implications of this are discussed in relation to the application of a subsequent metallic surface coat at the end of this section.

The fissure type of defect exhibited by PPy/nylon-12 substrates is typical of that caused by solvent permeation of semi-crystalline substrate materials, and has previously been reported to occur in plastics that are solvent etched during electroless plating procedures[212,213]. Similar examples are also contained in the literature for solvent etched polyethylene[212] and polyetherimide[213].

The origin of these defects has been attributed to differing levels of stress in the plastic substrate material[212]. This produces non-uniform rates of etch by solvent, giving rise to the formation of surface irregularities, and eventually results in disintegration of the plastic. It is thus considered likely, that intrinsic stress

(a)

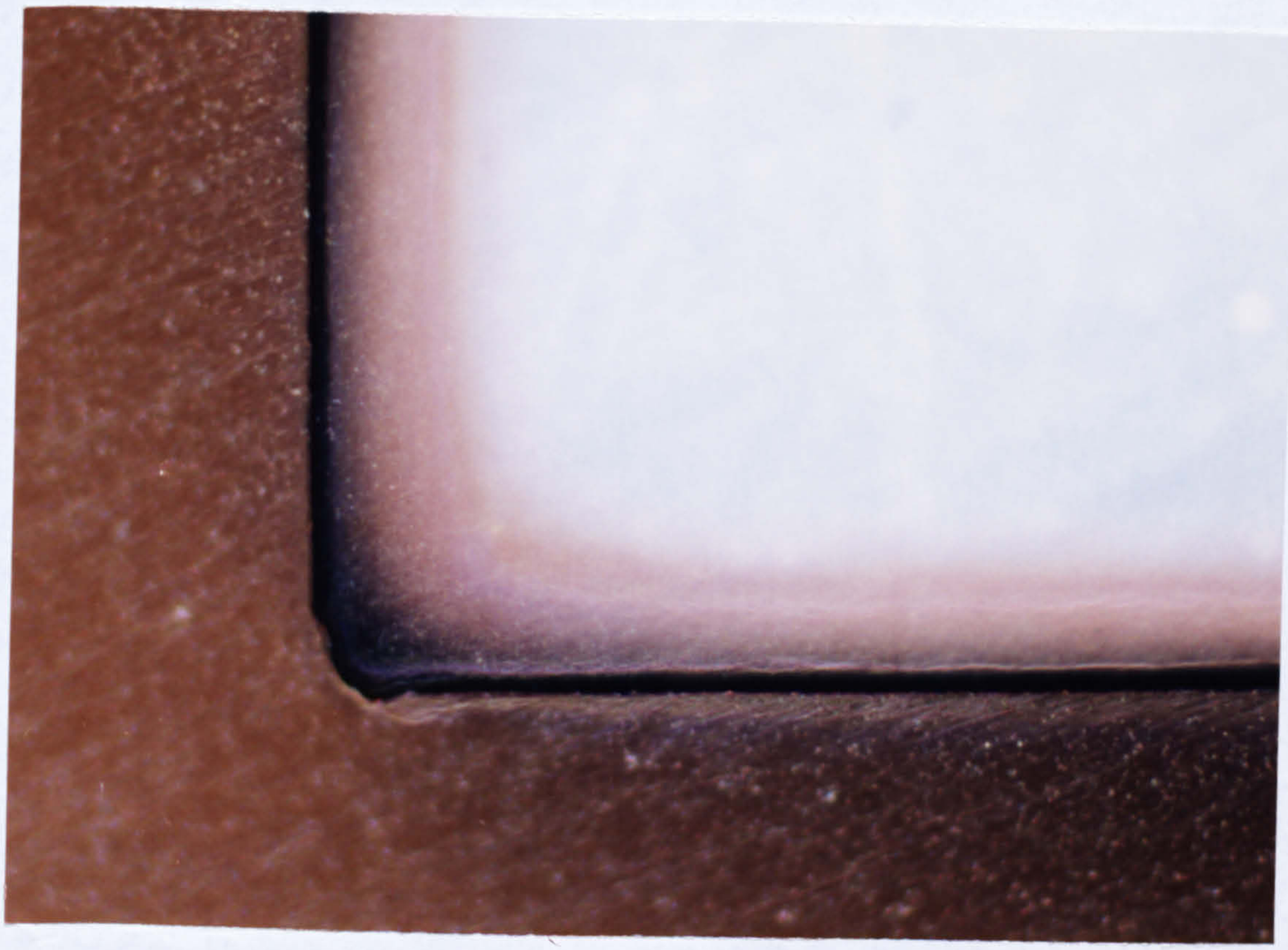

(b)

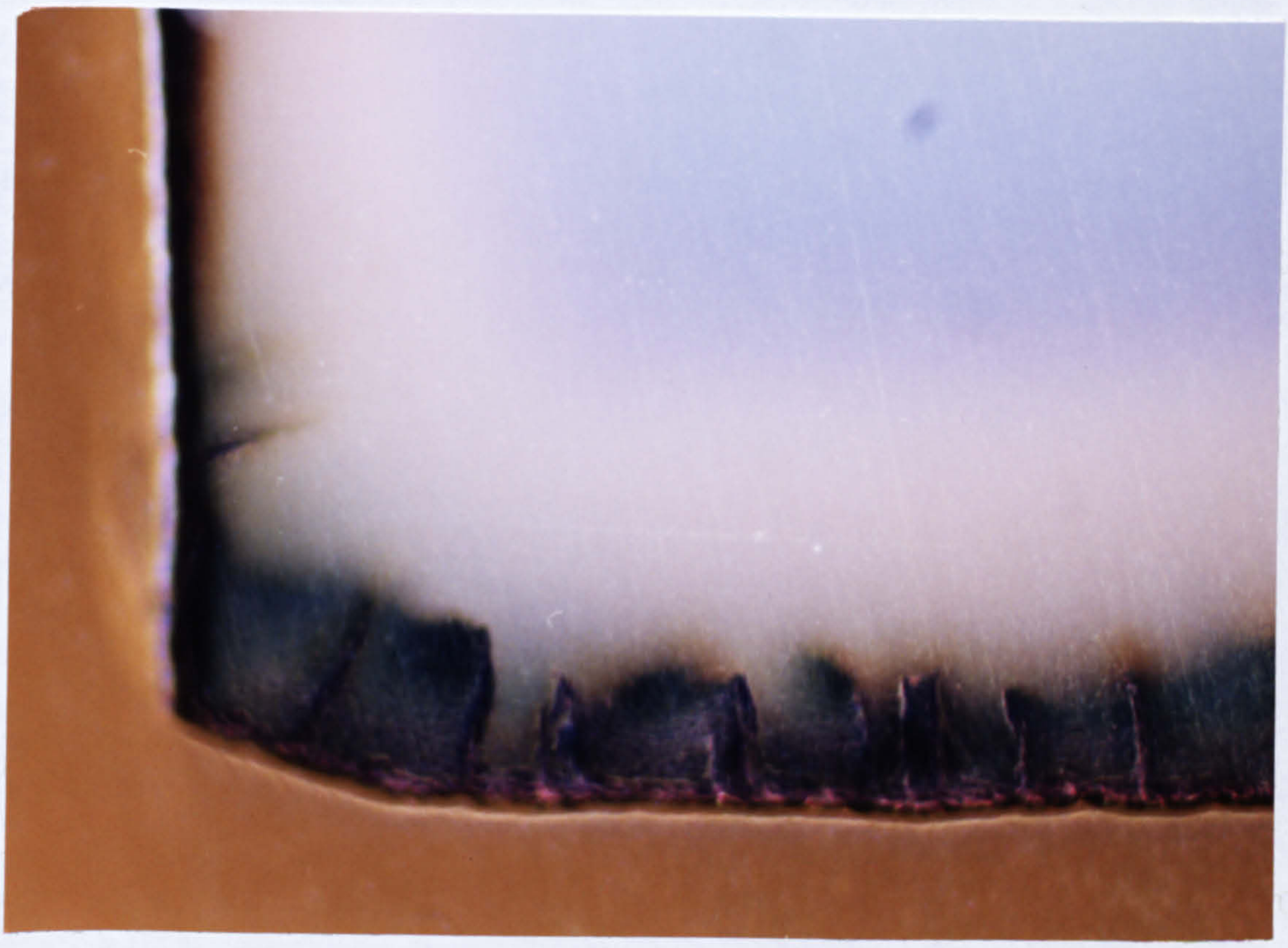

Plates 14(a-b). Polypyrrole/nylon-12 composites, showing the effect of the monomer impregnation temperature on the cross-sectional morphology of coated samples. Plate 14a, impregnated with pyrrole at 30°C; Plate 14b, impregnated at 60°C. Both samples oxidised with ferric(III) chloride solution at 20°C.

incorporated during the manufacture of the nylon substrate is a cause of the uni-directional nature of the defects exhibited by PPy/nylon-12 composites.

Another type of defect that was common to nylon composites, was areas of non-uniform dendrite-like growth of polypyrrole and polyaniline. An example of this is shown in Plate 15. Unlike the crack type defects shown in Plate 14(b) the surfaces of these defects are not as sharply cleaved and consequently are not expected to degrade the bulk properties of the substrate to the same extent. The dendritic nature of the growth in these regions suggests that oxidation is probably initiated at defects or fissures in the surface, which then enables ferric(III) chloride to ingress further into the bulk, causing oxidation at deeper levels.

From the point of view of subsequent metal deposition, both of these types of defect are undesirable, since the affected regions possess a non-uniform polymer content, giving rise to uneven surfaces. This unevenness is not likely to be masked by subsequent electroless and/or electroplating, and is expected to translate into an uneven metallized surface layer.

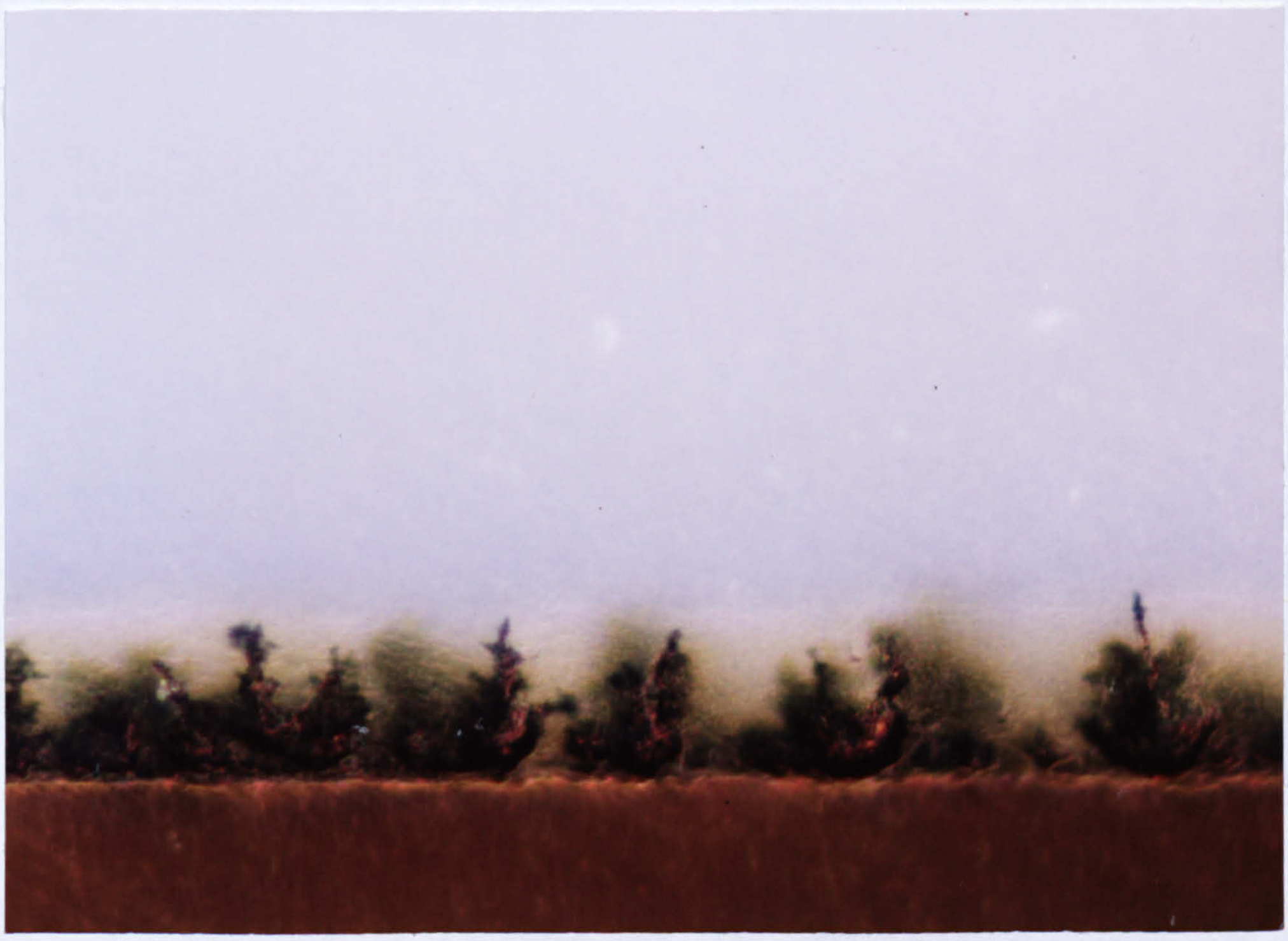

Plate 15. Example of dendrite type defect, exhibited by polypyrrole and polyaniline nylon composites.

However, a potentially more serious problem is the adverse affect that these defects are likely to have on the bulk properties of the polymer, causing a reduction the mechanical strength of the substrate material, and thus, a reduction of the strength of adhesion of the surface coat. This is an important consideration in the electroplating of plastics with metals, since in order to be accepted by industry, the strength of adhesion of the surface coat needs to conform to several procedures devised by the industry standards committee of the American Society of Electroplated Plastics. (ASEP TP-200, ASEP TB-201, and ASTM B533[214]). However, it should be noted that these tests measure the strength of the weakest layer in the metal-substrate combination, which is not necessarily the same as the strength of adhesion of the metal layer to the surface, as failure can occur in the bulk of the substrate.

7.5.2.3 Polyethylene Composites.

Plates 16 and 17 shows typical optical micrographs of cross sections through PPy/PE and PA/PE composites.

Both the polypyrrole and polyaniline layers are highly non-uniform, which is consistent with previous SEM observations of the surface morphology (see Plates 9-11). Optical and SEM micrographs of PA/PE composites show that in common with nylon coated materials, the surface coat is comprised of two regions, an outer layer of conducting polymer (~12 μm thick) and an inner region consisting of conducting polymer impregnated into polyethylene. The combined thickness of this layer, for both polyaniline and polypyrrole coated materials is the order of 0.1 mm, which is similar to that obtained with PPy/nylon-6 composites oxidised under similar conditions. The coat thicknesses of other polyethylene composites impregnated with different amounts of monomer are also about the same. This would suggest that the coat thickness is determined primarily by the ingress of ferric(III) chloride or chloride ions into the polymer, rather than by the amount of absorbed monomer.

Plate 16 (PPy/PE prepared by immersion in pyrrole for 15 minutes at 100°C followed by oxidation with ferric(III) chloride at 20°C) illustrates two types of defect which were commonly observed with polyethylene coated samples, namely, fissures,

which penetrated into the bulk to depths of up to 0.27 mm, and the highly non-uniform and irregular surface. Both of these effects, as previously stated, are due to solvent penetration of the surface, which permits the relaxation of internal stresses, via the reorientation of molecular segments[212].

The extensive degradation of the polyethylene surfaces which is caused during the chemical pre-treatment steps, precludes the use of this material as a substrate for metal deposition in the present state. However, the use of less harsh conditions might enable the formation of smooth surfaces with good adhesion. This aspect of research would need to be considered in further detail in future work.

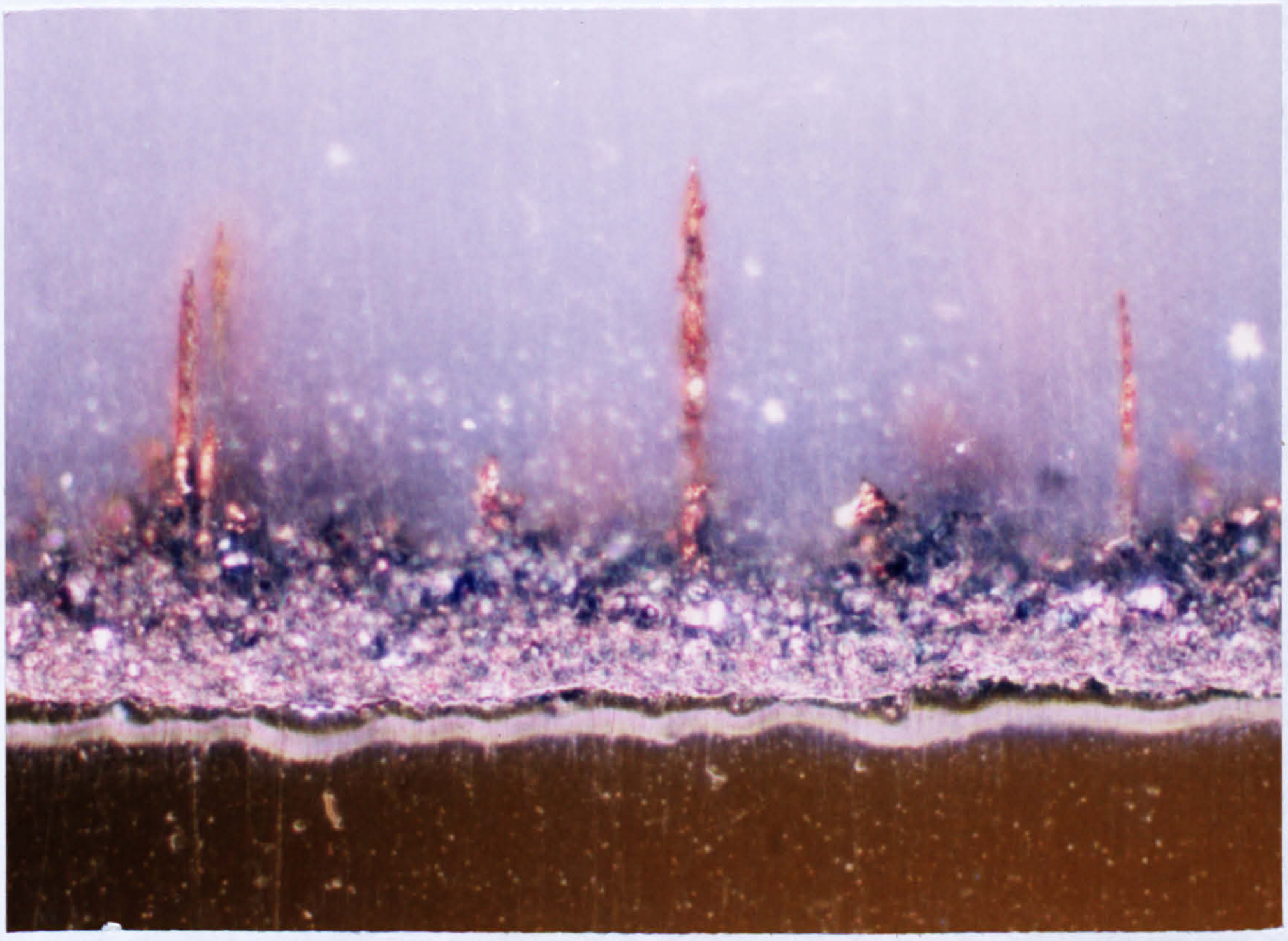

Plate 16. Cross-section of polyethylene coated with polypyrrole. Prepared by immersion in pyrrole for 15 minutes at 100°C, followed by oxidation with ferric(III) chloride solution (24 hours at 20°C.)

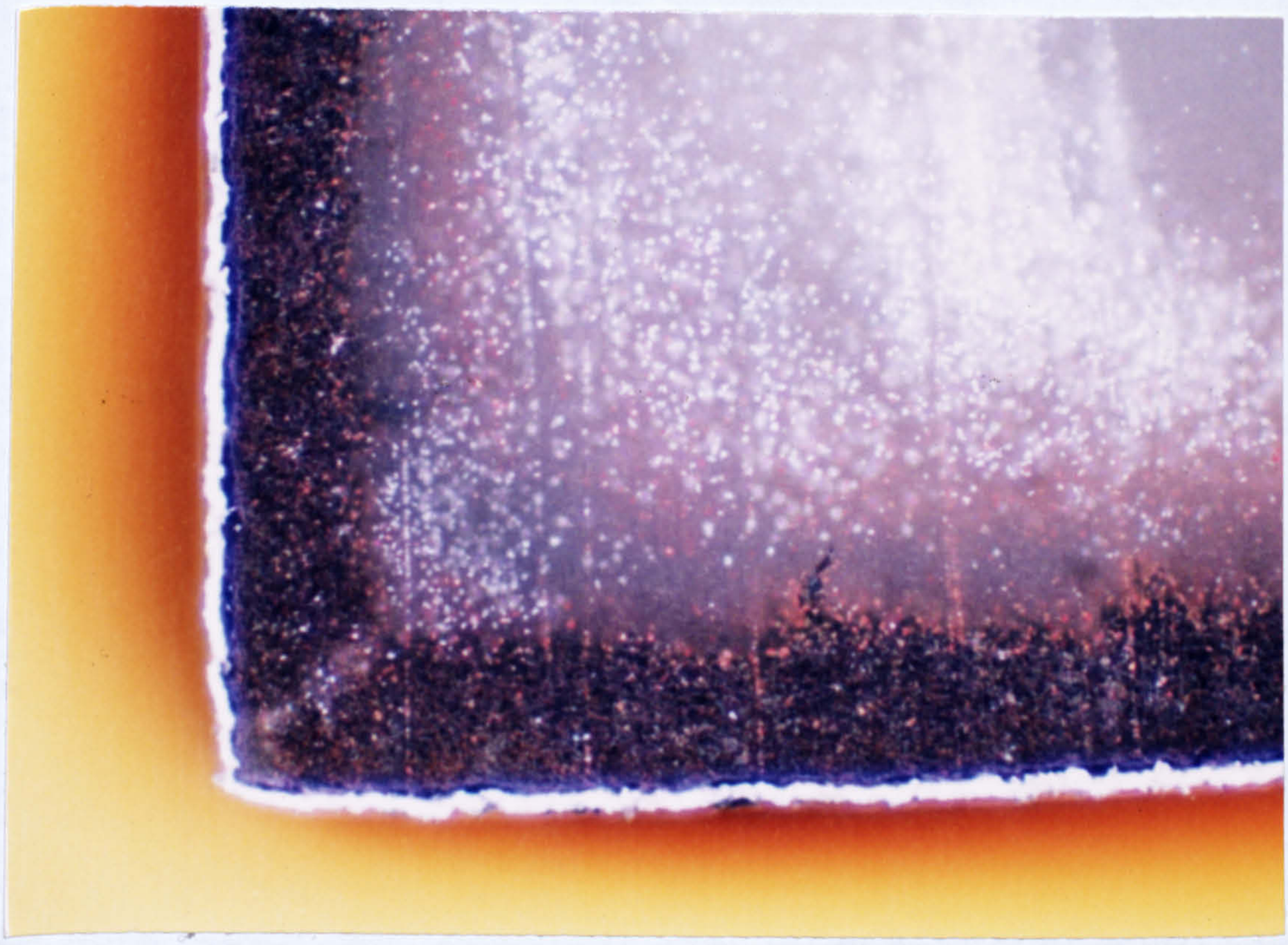

Plate 17. Cross-section of polyethylene coated with polyaniline. Prepared by immersion in aniline for 15 minutes at 100°C, followed by oxidation with ferric(III) chloride solution (24 hours at 20°C.)

Polyethylene coated substrates exhibit two unusual phenomena that were not observed with nylon. These are the band of white specks that forms behind the outer surface coats of the polyaniline and polypyrrole layers, and the reddish/orange deposit which is visible primarily in polyaniline coated samples. Plates 18(a-b) show optical and electron micrographs of PA/PE composites which illustrate these features at higher magnification.

The origin of the white specks is uncertain. It was initially thought that these were due to fillers such as zinc oxide or titanium dioxide which are commonly added to polyethylene during processing[212,215]. However, the fact that the specks are not distributed homogeneously throughout the polymer, as would be expected in the case of filler, coupled with the failure to detect any extraneous material using surface analysis, makes this explanation unlikely.

The reddish/orange deposit is probably due to oligomers of aniline, and is analogous to the brown-yellow colouration observed in Plates 12 and 13 with pyrrole impregnated samples. Unreacted ferric(III) chloride can be discounted, since elemental analysis revealed the presence of chloride anions only.

(a)

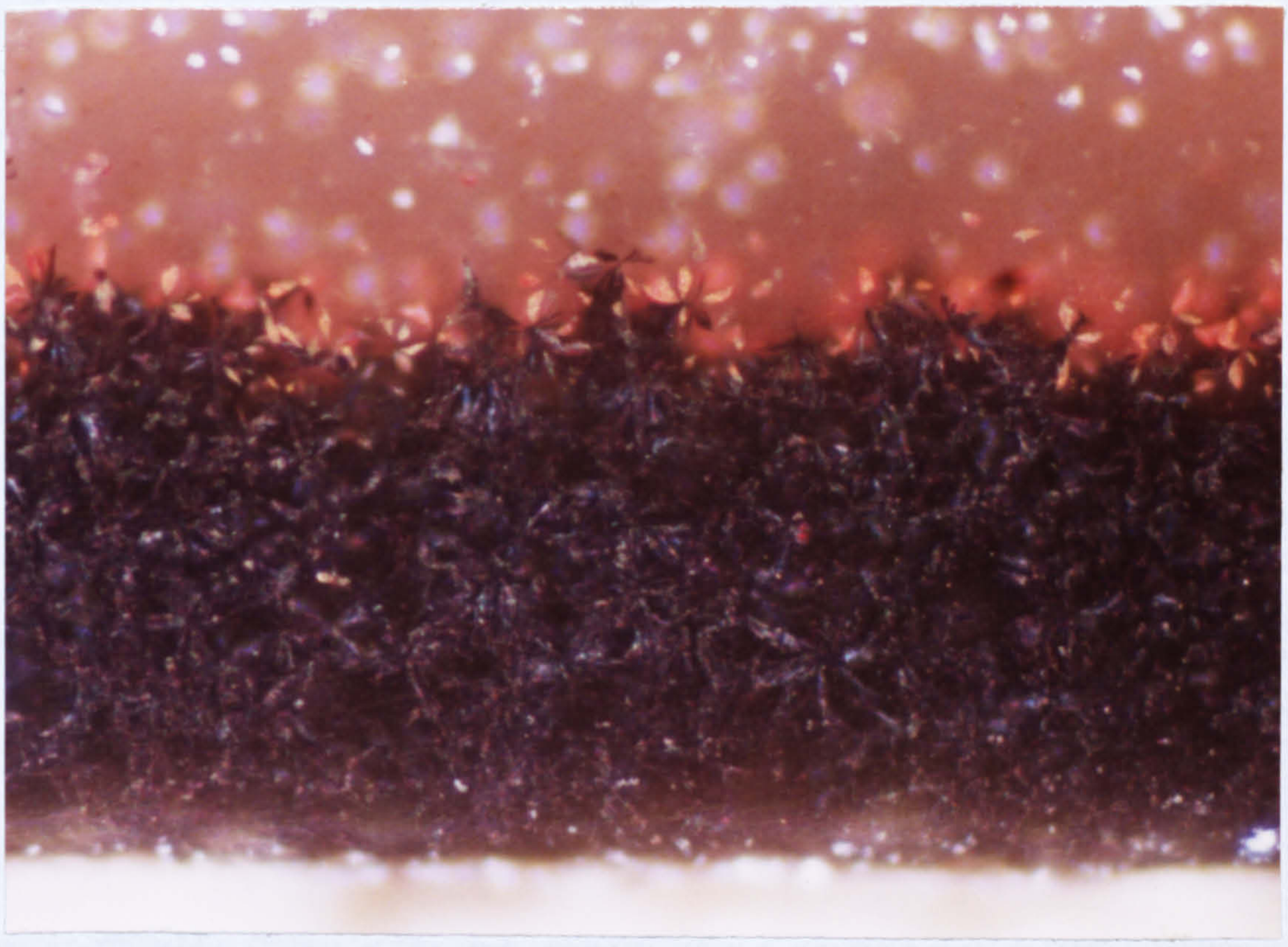

(b)

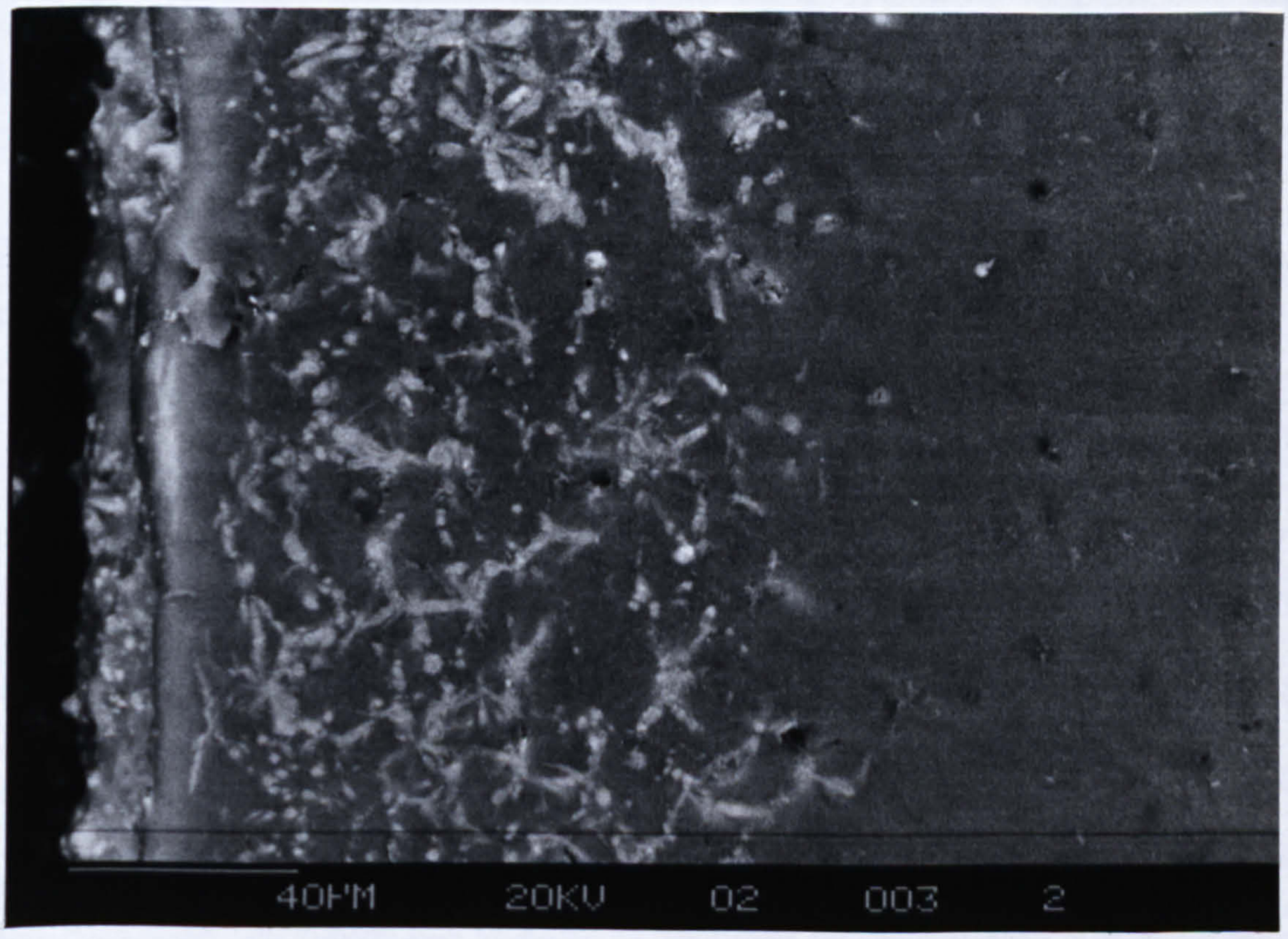

Plates 18(a-b). Cross-section of polyethylene coated with polyaniline showing white specks and red/orange deposit that was observed with polyaniline coated polyethylene substrates. (a) optical micrograph; (b), scanning electron micrograph.

7.5.2.4 Summary.

In conclusion, these results show that both aniline and pyrrole can be chemically polymerized within matrix of nylon and polyethylene substrates, producing conductive surface coats with thicknesses up to 0.1 mm. Furthermore, these techniques have been demonstrated to be applicable to a wide variety of polymer substrates, of both hydrophobic and hydrophilic nature, which can be in the form of a solid or film.

7.6 Mechanism of Formation of Conducting Polymer Layer.

In this section, a mechanism for the formation of a conducting polymer coat at a substrate surface is described. A mechanism previously proposed for the "in-situ" polymerization method[113], as described in section 2.4.2, involves the physical absorption of radical cations or oligomers of polymer, followed by polymerization in the plane of the liquid/solid interface. Because this mechanism is specific to in-situ polymerization, i.e, where reactants are mixed in bulk solution, it is not applicable to the present study, which involves chemical impregnation as one of the steps.

By considering the rate determining step in the reaction of monomer with oxidant, it is possible to explain the form of the data displayed in Figs. 58-62, and the different types of cross-sectional morphology that are exhibited by nylon and polyethylene substrate materials. In order to maintain simplicity, the present approach assumes that the conducting polymer layer which is formed at the substrate surface/solution interface does not alter the rates of diffusion of the reacting species in this layer, ie that it is porous to the reactants. This assumption is considered justified on the basis that polypyrrole has shown to be porous when in the oxidised state[119,121], and it is likely that polyaniline will be also.

Also implicit to this mechanism, is the assumption that oxidation occurs via a series of reaction steps analogous to that previously discussed in section 2.2.3 for electrochemical oxidation, and not by a free radical chain reaction. Evidence that this assumption is valid for chemical oxidation has been previously discussed in section 2.3.3.

The proposed mechanism is limited to a qualitative treatment for two reasons.

(i) The outer surfaces of samples were deformed during the chemical impregnation and oxidation stages, giving rise to irregular and non-uniform surface coats which did not permit accurate measurement of coat thicknesses.

(ii) Boundaries between adjacent regions of deposit were diffuse and not easily distinguished by optical or SEM examination.

The different types of cross-sectional morphology that are exhibited in Plates 12-18 can be explained by considering the relative rates of the steps (i-v) which are listed below.

(i) Diffusion of oxidant to the polymer substrate surface.

(ii) Diffusion of oxidant through polymer to the reaction interface.

(iii) Diffusion of monomer through polymer to the reaction interface.

(iv) Rate of oxidation of monomer by oxidant.

(v) Rate of diffusion of oligomer through bulk polymer.

With highly concentrated solutions of ferric(III) chloride (10-30% wt./vol.) such as those typically employed in the preparation of composite materials (see Table 3), it is assumed that the rate of oxidation of monomer was not limited by mass transport of $FeCl_3$ to the polymer surface, ie. step (i) is not rate determining in the oxidation of monomer. The locus of deposition will then depend on the relative rates of steps (ii-iv), as depicted in Fig. 63.

If the rate determining step for polymerization is the rate of diffusion of oxidant through the substrate (step ii), polymerization will occur predominately at the substrate surface. The extent of compactness of the conducting polymer coat will then be governed by the rate of diffusion of oligomers through the bulk polymer (step v). This, in turn, is expected to be dependent on the degree of polymerization of oligomers, with low molecular weight oligomers being able to permeate the bulk polymer more effectively. Chen *et al*[164] has reported that a distribution of oligomers with conjugation lengths of up to six, are formed by reaction of pyrrole with ferric(III)

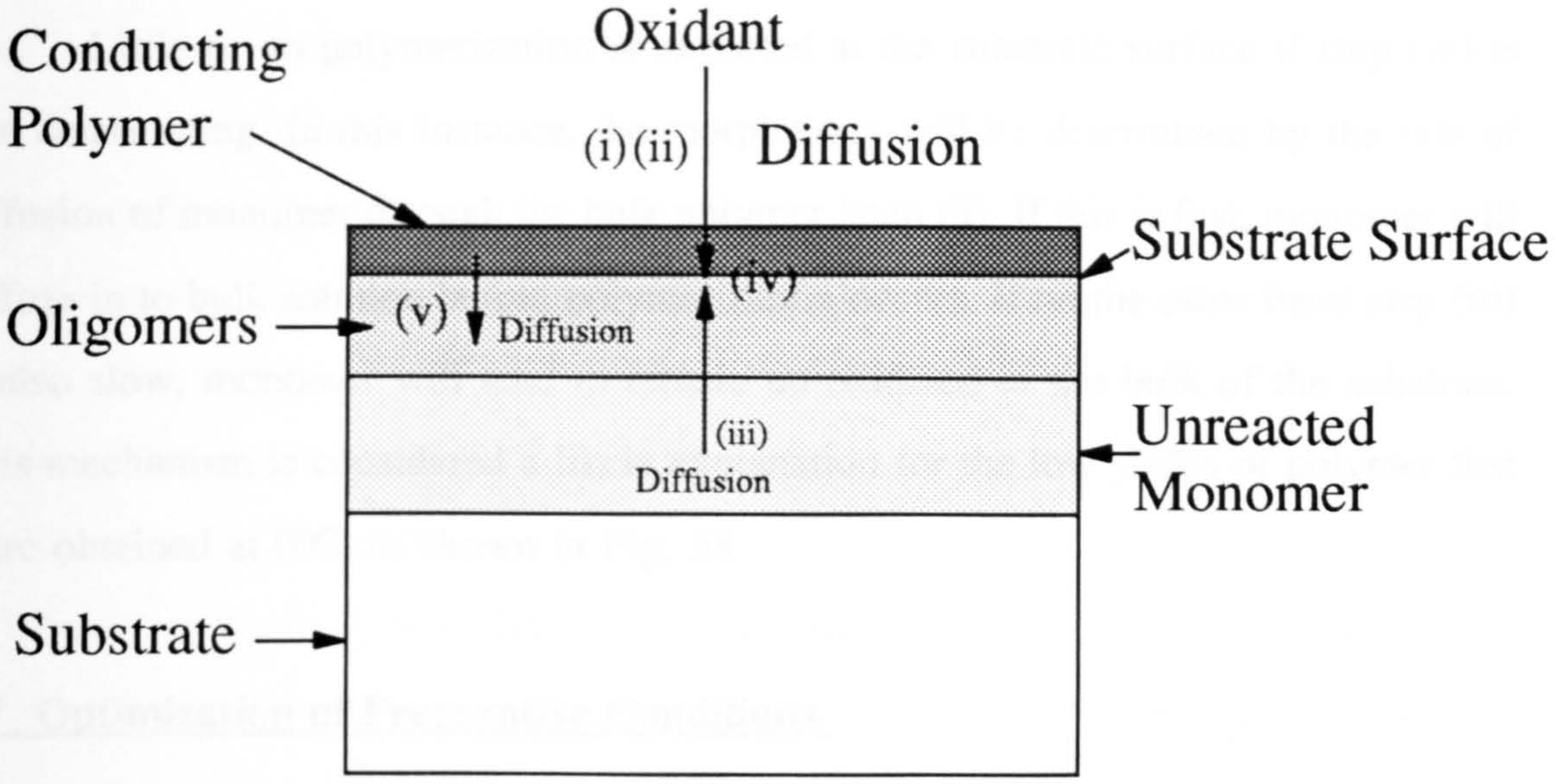

Fig. 63. Schematic representation of the steps involved in the formation of a conducting polymer composite material. Steps (i and ii), diffusion of oxidant to the reaction interface; Step (iii), diffusion of monomer through the polymer to the reaction interface; Step (v); diffusion of oligomers through bulk polymer.

chloride solution. Thus, a diffuse band of oligomers may be expected to form beneath the outer surface conducting polymer layer, with colours ranging from yellow (low molecular weight oligomers) furthest from the outer surface, to dark brown/black (higher oligomers) nearest the outer conducting polymer layer. This is what is observed in Plates 12 and 13 and is typical of cross-sectional morphology exhibited by nylon substrates.

If the rate of diffusion of monomer to the reaction interface is slow (step iii), the cross-sectional morphology which will be dependent on the relative rates of diffusion of oxidant and oligomers in the bulk polymer (steps ii and v). If both these steps are also slow, the time needed for monomer to diffuse to the reaction interface will be long, and may well exceed the duration of oxidation. This combination of reaction steps is thus expected to give rise to thin conducting polymer coats, and regions of unreacted monomer. In contrast, a slow step (iii) in combination with rapid

steps (ii and v), is expected to produce a cross-sectional morphology similar to that predicted previously corresponding to the case in which step (ii) is slow.

Little or no polymerization is expected at the substrate surface if step (iv) is rate determining. In this instance, the morphology will be determined by the rate of diffusion of monomer through the bulk polymer (step iii). If this is fast, monomer will diffuse in to bulk solution before polymerization occurs. If on the other hand step (iii) is also slow, monomer will tend to remain un-oxidized in the bulk of the substrate. This mechanism is considered a likely explanation for the low yields of polymer that were obtained at 0°C, as shown in Fig. 58.

7.7 Optimization of Preparative Conditions.

In order to be considered as substrates for metal deposition, conducting polymer coated materials need to meet several specifications. These include: (i) smooth and uniformly coated surfaces, and (ii) good adhesion of the surface coat to the substrate. Inclusive in both these requirements is that the external conducting polymer coat should permeate the outer surface layer of the host substrate to a sufficient depth to furnish suitable adhesion, but not too deep so as to degrade the bulk properties of the polymer. Moreover, it is also desirable that there should be no unreacted monomer left within the substrate once oxidation is completed. Finally, the outer conducting surface coat needs to be sufficiently conductive to permit direct electrodeposition, or thick enough to reduce sufficient metal ions from solution in electroless deposition, so as to deposit an outer metallic coat. From the point of view of manufacture it is also desirable that: (i) the coating procedure can be carried out rapidly, (ii) is simple to perform, and (iii) is low cost.

By considering the relative rates of the steps (i)-(v) of the mechanism of formation of the conducting polymer layer discussed in section 7.6, it should be possible to determine an ideal set of conditions that fulfils the majority of these requirements.

In principle, the combination of a high rate of diffusion of monomer through the polymer substrate, to facilitate a rapid uptake of monomer during the impregnation stage, and rapid diffusion of monomer to the reaction interface during oxidation (fast step iii), coupled with a slow rate of diffusion of oxidant through the polymer (slow step ii), and a slow rate of diffusion of oligomers in the bulk polymer (slow step v) is considered likely to achieve these objectives. Ideally, each of these steps should be optimised with respect to achieving the requirements discussed at the beginning of this section. However, because there is no one set of reaction conditions that is applicable to all substrate materials, reaction conditions need also to be optimised to suit individual substrates. This point was illustrated in the preparation of PA/nylon composites. It was observed that nylon-6 was not appreciably swelled by aniline at temperatures below 65°C and did not form conducting polymer surface coats, whereas nylon-12 did swell, and was readily coated with a surface layer of polyaniline.

In practice, this would require careful optimization of both the chemical impregnation and oxidation stages, precise control of experimental parameters such as temperature, reactant concentrations, and the duration of impregnation and oxidation, and thus, may be difficult to achieve. Moreover, reaction conditions which favour high yields of polymer (high permeation of substrate with monomer and polymerization at room temperature), also produce substrates with a non-uniform surface morphology and cause bulk degradation of polymer. In contrast, it is reported for polypyrrole composites, that low concentrations of pyrrole and oxidant (the conditions favoured for producing smooth surface morphology with no bulk degradation) produces poorly conducting deposits[141]. Hence, some measure of compromise is necessary.

7.8 Comparison with other Chemical Methods of Preparing Composite Materials.

As discussed in section 2.4.2, in-situ polymerization, chemical impregnation, and emulsion polymerization are the three most common methods of preparing conducting polymer composite materials (see Table 3). The preparation of conducting

polymer composites via chemical impregnation was considered the most suitable method of preparation for the reasons discussed in section 7.4.

The impregnation of substrates with monomer, followed by chemical oxidation, according to the procedure described in section 3.14, successfully demonstrates the impregnation method of coating non-porous substrates, for both hydrophilic (nylon-6, nylon-12) and hydrophobic (polyethylene) solid polymer substrates. This is in contrast to previous applications of the chemical impregnation method of effecting polymerization, which has been limited to the preparation of highly porous substrate materials, such as cellulose paper[136], wood, cloth[140] or films cast from water soluble polymers, such as poly(vinylalcohol)[154], and poly(4-vinylpyridine)[167]. Moreover, subsequent treatment with ferric(III) chloride solution, rapidly effected polymerization, producing conducting polymer coat thicknesses of up to 0.02 mm for PPy/nylon-6 composites and up to 1 mm in the case of PPy/PE and PA/PE composites. This is much thicker than that previously obtained using other techniques, where thicknesses of the order of a few microns are obtained[164].

The conducting surfaces have excellent adhesion, due to the formation of conducting polymer within the outer surface layer of the host substrate, and were not delaminated by gentle abrasion. Moreover, the adhesion of this layer is expected to be significantly higher than that produced by in-situ polymerization techniques, where the conducting polymer layer is formed on the substrate surface, with little or no penetration of the polymer host[142].

A comparison of micrographs in the literature for conducting polymer coated materials, shows that the surface morphology of PPy/nylon-6, PPy/nylon-12 and PA/nylon-12 composites are rougher than that exhibited by in-situ polymerization techniques, smoother than that obtained by emulsion polymerization methods, and comparable with that obtained with other chemical impregnation techniques. Optimization of the preparative conditions, such as that described in section 7.7, would be expected to increase the smoothness of the substrate surface to a level comparable

with that obtained with in-situ techniques, whilst still retaining the benefits of thick conducting coats.

Another major advantage of the composites prepared in this thesis, is the relatively short reaction times that are required to prepare conducting composites. For example, the time taken to prepare conducting polymer coats with nylon-6 substrates was of the order of a few minutes (c.f. nylon-6 substrates immersed in pyrrole for one minute, followed by oxidation in ferric(III) chloride solution at 20°C). This compares favourably with other chemical impregnation techniques, such as the "template polymerization" method employed by Mohammadi *et al*[167], which requires polymerization times in excess of 150 minutes. The method described by Qian *et al*[164] which takes up to 48 hours, and various in-situ techniques which require up to 30 hours.

The procedure is also easy to perform, requiring only monomer impregnation followed by oxidation, this latter stage having the advantage of requiring only water as a solvent. In contrast, other chemical techniques utilize non-aqueous solvents, or require vapour phase polymerization to achieve high conductivities, or alternatively, surface modification, such as the covalent attachment of anionic groups to produce adhesion[160,162]. All of these alternatives add extra complexity to the overall preparation procedure, and are incompatible with some of the desirable elements required for polymerization cited in section 7.7.

In conclusion, the advantages afforded by preparing conducting polymer composites according to the methods described in section 7.4, are: (i) thick surface coats (~0.1 mm) can be formed, (ii) conducting polymer is actually incorporated within the host substrate and is therefore highly adherent, (iii) the procedure is straightforward, being conducted in two simple stages, (iv) oxidation is carried out with aqueous based oxidants, and (v) only short reaction times are required to produce conducting coats.

7.9 Summary.

The chemical impregnation method of preparing conducting polymer composites, involving impregnation of the host substrate with either pyrrole or aniline, has been successfully applied to solid non-porous hydrophilic (nylon-6, nylon-12) substrates, and hydrophobic (polyethylene) substrates. The major advantages of this method of preparing conducting polymer composites compared to other methods described in the literature, are that it produced thick conducting polymer layers with good adhesion.

The depth of permeation of monomer into the substrate was determined by the nature of the substrate, and the temperature and duration of immersion in monomer. Polymerization was successfully accomplished using ferric(III) chloride (25% wt./wt.) at 0°C and 20°C with pyrrole, but only at 20°C with aniline. The temperature of oxidation was the principle experimental parameter in determining the yield, and hence, thickness of conducting polymer layer, with the highest yield of polymer being formed at room temperature.

The conducting polymer coats displayed two different regions of varying levels of oxidation of monomer. These were an outer region, comprised mainly of conducting polymer, and an inner region over which the extent of oxidation of monomer varied from that of essentially unreacted monomer, through to that of the fully oxidised polymer. The extent of formation of these different regions was governed by the reaction conditions employed during preparation, with oxidation by ferric(III) chloride at room temperature producing the thickest conducting polymer coats.

7.10 Metal Deposition on Composite Substrates.

The electrochemical and electroless deposition of copper and silver on polypyrrole substrates was discussed in chapters 5 and 6. In this section, the discussion will be extended to the electrochemical deposition of copper on polypyrrole

and polyaniline impregnated polyethylene co-axial cable and PPy/nylon-6. Further experiments were also conducted into the electroless deposition of copper and silver on PPy/nylon-6 composites.

7.10.1 Polyethylene Co-axial Cable.

Copper deposition was carried out via electrochemical deposition at polypyrrole and polyaniline coated co-axial cable, using an acidified aqueous copper sulphate bath, according to the procedure described in section 3.16.1.

Copper deposition was effected on both polypyrrole and polyaniline coated cable which had been oxidised with ferric(III) chloride solution, but not on samples which were oxidised with ammonium persulphate. This was attributed to the much higher electrical resistance of samples oxidised with ammonium persulphate solution.

The copper deposited onto the cable insulation was salmon pink in appearance, and similar to that deposited onto stainless steel electrodes from the same solution. The rate of deposition of copper was however, highly non-uniform along the length of the cable, occurring most rapidly at the point of closest contact to the external electrical connection. This was attributed to a potential drop along the length of the cable, caused by its electrical resistance. The problem of non uniformity of deposition was overcome to some extent by initiating deposition at the end of the cable furthest from the point of electrical connection. Then, as deposition proceeded, more cable was gradually exposed to the plating solution. Using this method, a reasonably thick and uniform copper deposit could be built up along the length of the cable. Whilst this technique would lend itself to a continuous coating process, it suffered from the disadvantage that the rate of deposition was slow, and deposition times in excess of 30 minutes were required to completely coat a 25 mm length of cable.

7.10.1.2 Surface Morphology.

The surface morphology of co-axial cable coated with polypyrrole and copper, was characterized using scanning electron microscopy. Plate 19 shows the surface morphology of co-axial cable coated with polypyrrole. The coat of polypyrrole was continuous, and completely covered the surface of the cable. However, further examination at higher magnification revealed a nodular morphology, interspersed with voids which penetrated into the thickness of the coat, (the depth of penetration was not apparent from micrographs). The uneven surface of the polyethylene co-axial cable is reminiscent of other conducting polymer coated polyethylene samples (section 7.5.2.3), and is attributed to the partial degradation of the polyethylene during the chemical impregnation and oxidation stages, as previously discussed. The fact that surface morphology is rough need not necessarily be detrimental if the cable is subsequently plated with a surface coat of metal. Indeed, surface irregularities such as these might provide suitable points of mechanical anchorage for any subsequent metal deposit, thus ensuring good adhesion.

Plate 20 shows copper deposited onto the surface of polypyrrole impregnated co-axial cable. The structure of the deposit was different from that obtained previously with electrochemical and chemical deposition, (see Plates 1-4). In this instance, the deposit consisted of highly irregular shaped spheres or growth centres, which have coalesced to produce a highly inhomogeneous and porous layer.

The porous and irregular nature of the deposit can probably be attributed to the crude plating conditions that were used to coat the sample. With suitable optimization with respect to the potential and current density, and utilization of commercial plating solutions which contain additives and levellers etc, it is considered that this composite does possess possibilities for commercial plating application.

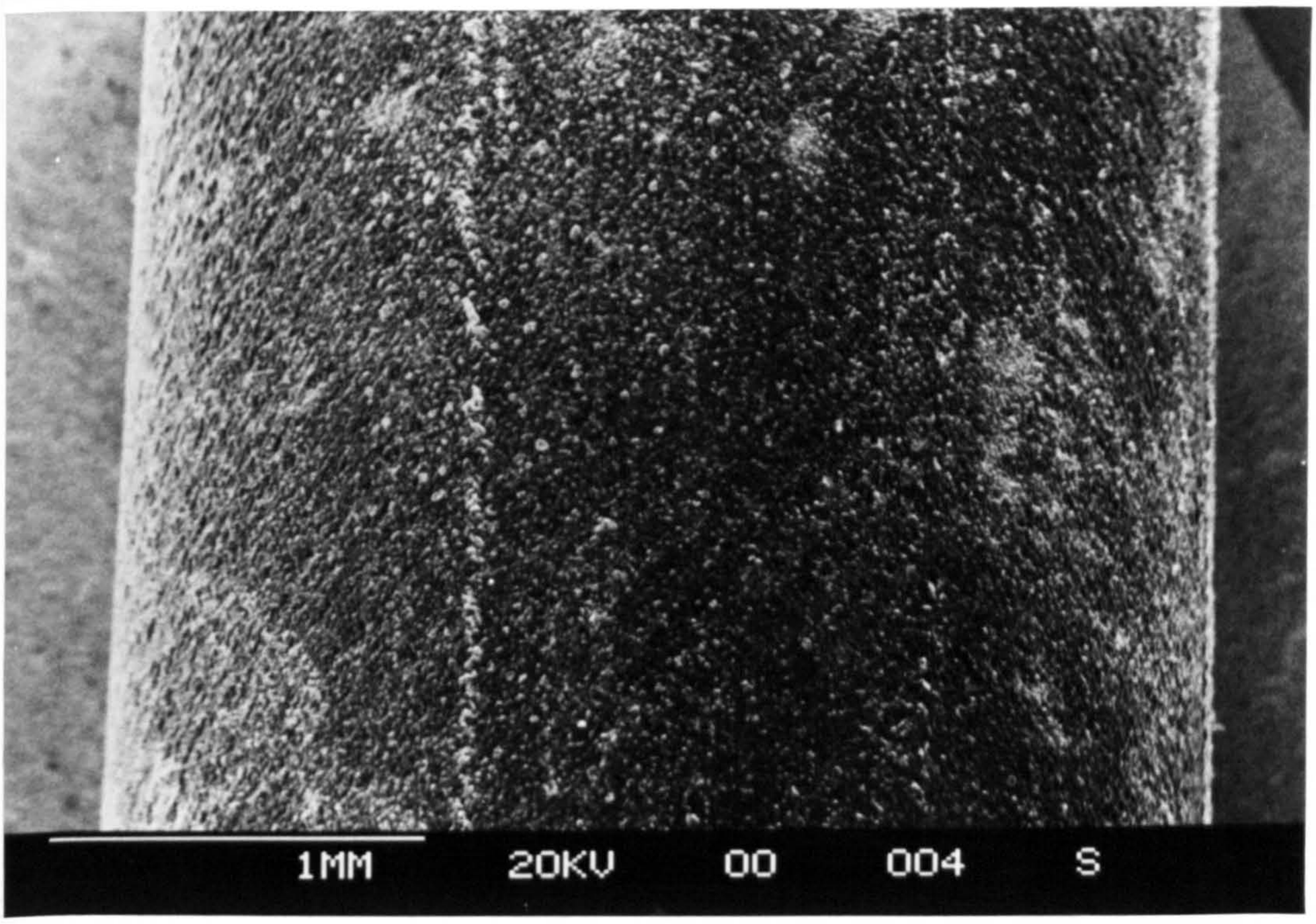

Plate 19. The surface morphology of co-axial cable coated with polypyrrole. Prepared by immersion in pyrrole for 15 minutes at 100°C, followed by oxidation with ferric(III) chloride solution (24 hours at 20°C.)

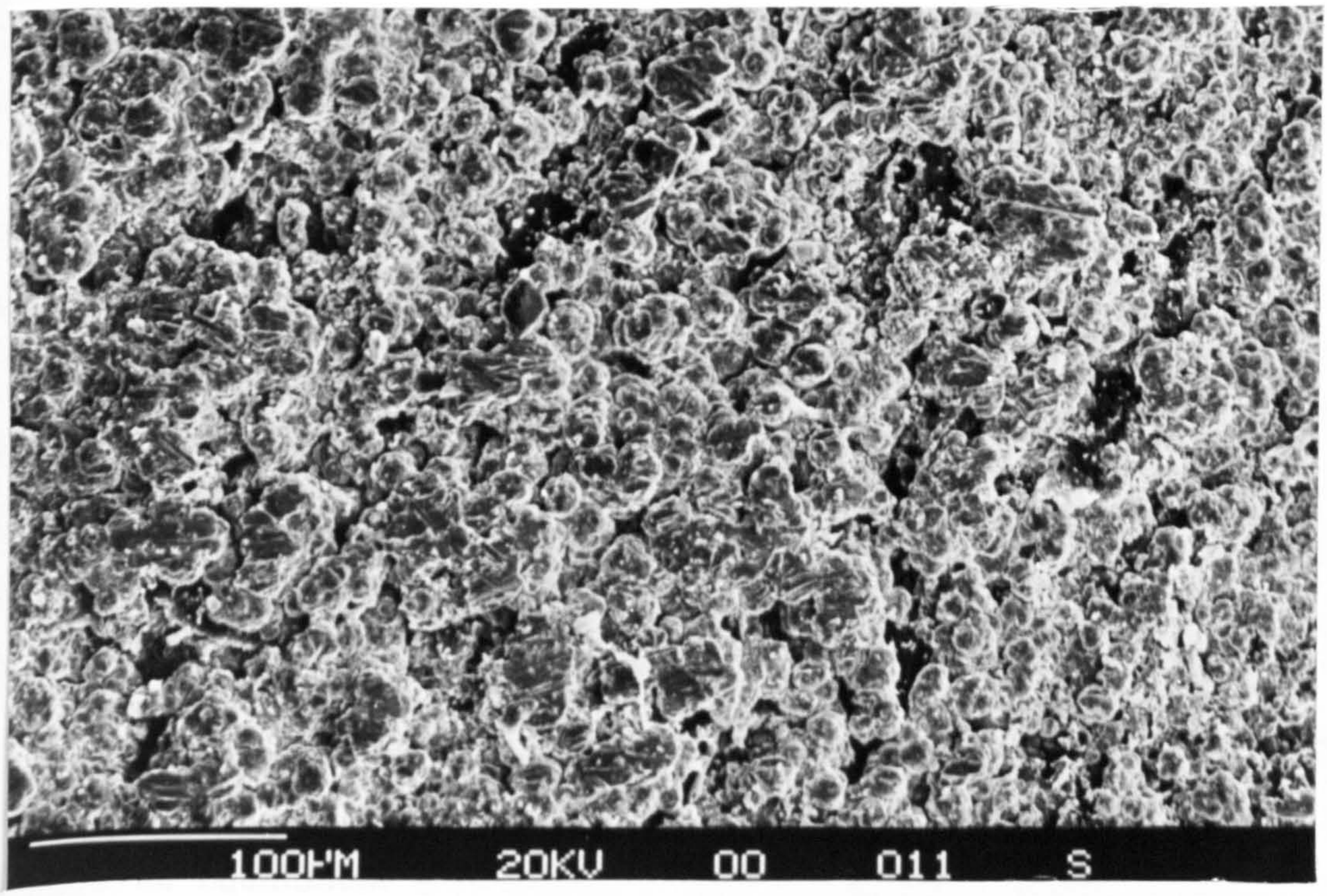

Plate 20. Copper deposited onto the surface of polypyrrole impregnated co-axial cable.

7.10.2 Polypyrrole/nylon-6 Composites.

The electroless deposition of copper and silver was carried out on PPy/nylon-6 composites according to the procedure described in section 3.16.2.

The immersion of composite substrates in sodium hydroxide solution caused a colour change in the surface polypyrrole coat from black to a copper bronze colour. This change is similar to that observed previously for free-standing polypyrrole films immersed in sodium hydroxide solution, as discussed in section 6.3, and is interpreted in an analogous manner, ie. deprotonation of the acidic pyrrolylium hydrogen, coupled with loss of the accompanying counteranion. However, with the composite substrates, the time taken to change colour was significantly longer in comparison to that observed with free-standing films, requiring several minutes as opposed to less than a second with free-standing films. This difference is attributed to a reduction in the porosity of polypyrrole in the conducting polymer composite substrate, caused by the fact that the conducting polymer layer is interspersed to some extent within the matrix of the host nylon substrate, as illustrated in plates 14(a-b).

Plate 21 shows PPy/nylon-6 substrates electrolessly coated with copper from slightly acidified copper sulphate solution, and silver from ammoniacal silver nitrate solutions.

The electroless deposition of copper on the PPy/nylon-6 substrate was very slow (of the order of several minutes), and resulted in a very poor surface coverage. Indeed, the base treatment/metallization process needed to be repeated several times in order to build up a copper deposit. In spite of this, large areas of uncoated substrate are still visible. In contrast, almost complete surface coverage was obtained with silver. The difference in extent of surface coverage is much greater than that expected purely on the basis of the difference in charges on the copper and silver ions, from which it would be predicted that the extent of surface coverage by silver would be approximately twice that of copper. The reasons for this are not entirely obvious, but one explanation could be dissolution of Cu° in the presence of Cu^{2+}, in order to maintain an equilibrium concentration of Cu^{+}, as was discussed previously in section 5.5.

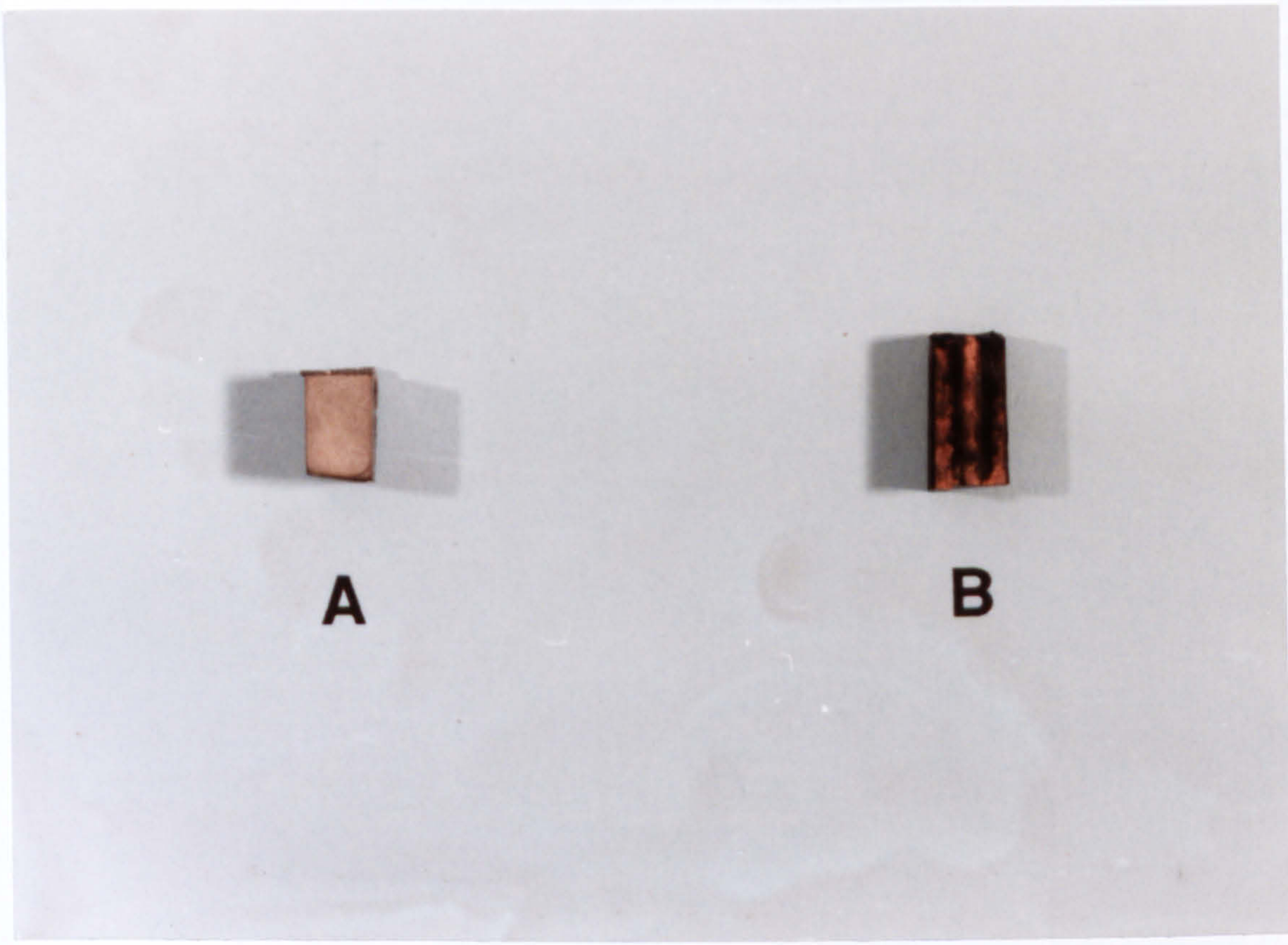

Plate 21. PPy/nylon-6 substrates electrolessly coated with (a), silver from ammoniacal silver nitrate solution, and (b), copper from slightly acidified copper sulphate solution.

7.11 Summary.

In conclusion, a combination of chemical and electrochemical techniques was used to metallize polyethylene and nylon-6 non-conducting plastics using polypyrrole as a mediator. Polypyrrole is not unique in this respect, and polyaniline can be used as an alternative where deposition is carried out electrochemically. Under optimum conditions, the technique produces very adherent and cohesive metal surfaces, and could be applied to plastic articles where shape or volume render in-vacuo metal coating methods difficult, or as an alternative to traditional tin/palladium based electroless methods such as that described in chapter 1.

CHAPTER 8

THE ELECTRODEPOSITION OF SILVER INTO POLYMER FILMS.

8.1 Introduction.

A number of procedures have been recently reported in the literature, which describe the metallization of polymer films using alternative approaches to traditional tin/palladium based electroless procedures, such as that previously described in section 1.3.

These recent developments include the deposition of metals by both electrochemical and chemical techniques, and may be divided into several categories, including; (i) electroless (counter-current) deposition, (ii) polymer-mediated electrodeposition, (iii) the doping of neutral polymer films with metal salts followed by chemical reduction, (iv) polymer-mediated chemical deposition, (v) carrier-mediated electrodeposition, and (vi) direct electrochemical deposition. The latter category includes the electrodeposition of metals into non-electroactive polymer films, which is analogous to the method described in this chapter, and also onto conducting polymers. Each of these methods (i) to (vi) is described in detail in chapter 1.

The work described in this chapter is concerned with the development of a novel method for electroplating plastics, based on the direct electrodeposition of silver into polymer films. As previously described in section 1.6, this method was considered as having potential for application to a wide variety of polymer film substrates, and was considered to be superior to the other methods which are listed at the start of this section.

This chapter describes the electrodeposition of silver into P(VF_2/VF_3) 60-40 copolymer, PVC and polyacrylate films. These materials were chosen for their industrial importance, and to demonstrate the versatility of electroreduction as a general procedure for electroplating polymer films.

8.2 The Electrodeposition of Silver into Polymer Films.

In order to successfully deposit metals into polymer films, it is essential that the film being plated should be permeable to the electroactive constituents in solution.

This enables metal ions to diffuse through the polymer film to the electrode surface, where deposition can occur. The mechanism of deposition is illustrated in Fig. 9.

The polymer film substrates that are used in this present study are hydrophobic in character, which precludes the use of traditional aqueous based electroplating systems. Despite the disadvantage of having to develop non-aqueous solutions from which to electrodeposit silver, hydrophobic polymer materials were chosen as substrates, since these are expected to exhibit a greater environmental stability compared to polymers that are swelled by water (hydrogels). These latter types of polymer contain water as an integral part of the film structure[216], and shrink or become brittle if left to dehydrate. Thus, these materials are expected to be unsuitable for use in anhydrous environments, and as a consequence, are likely to be restricted to few applications.

Preliminary work was concerned with the development of non-aqueous based plating solutions from which to deposit silver into polymer films. This required the study of electrolyte/solvent, and polymer film/solvent combinations. Following this, deposition studies were carried out to determine the optimum conditions for the preparation of highly reflective and coherent metal coated polymer films.

8.2.1 Electrolyte/Solvent Combinations for the Electrodeposition of Silver into $P(VF_2/VF_3)$ Copolymer Films.

The literature contains a number of reports of the deposition of metals from non-aqueous solutions[217-220], however, the majority of these are concerned with the deposition of metals, such as aluminium, magnesium, tungsten and titanium, that cannot be deposited from aqueous solutions. In contrast, there are no reports involving the deposition of silver from non-aqueous solutions after 1924[220].

Several physical properties have been identified as being important in the deposition of metals from non-aqueous solvents[217,218], including; (i) the dielectric constant, (ii) the dipole moment and (iii) the strength of the bond formed between the metal ion and solvent. The dielectric constant and dipole moments of solvents that were used in this study are listed in Table 7.

Table 7. Physical properties of selected organic solvents.

Solvent	Liquid range (°C)	Dielectric constant	Dipole moment
Ethyl acetate	-83.9 to 77.1	6.02	1.88
Methanol	-97.6 to 64.7	32.7	2.87
Acetonitrile	-43.8 to 81.6	37.5	3.44
1-2 Dichloroethane	-35.6 to 83.4	10.36	1.86
Propylene carbonate	-49.2 to 241.7	64.4	----
N,N-Dimethylacetamide	-20.0 to 166.1	37.78	3.72
N,N-Dimethylformamide	-60.4 to 153.0	36.71	3.86

In general, solvents with high dielectric constants and high dipole moments have a greater tendency to dissolve ionic solutes and form conducting solutions in which the metal salt is dissociated. This would suggest the use of solvents such as N,N-dimethylacetamide, N,N-dimethylformamide, acetonitrile and methanol. A conducting solution however, is not a sufficient criterion to determine whether or not metal deposition will occur[217], the strength of the bond between solvent and metal ion is also an important consideration[217,218]. If the complex formed between the metal ion and solvent is too stable, electrolysis does not yield metallic deposits, and the discharge of the solvent or other electroactive species is likely to occur.

In order to determine suitable solvent/electrolyte combinations from which to deposit silver, preliminary solubility and electrolysis studies were carried out using commercially available silver salts, in solvents that are commonly used for non-aqueous electrochemistry[177,221].

The choice of electrolyte/solvent combination was determined principally by the solubility of the silver salt in the solvent, and whether or not metal deposition was

effected by the application of a cathodic deposition potential. A secondary consideration was the convenience of use of the electrolyte/solvent combination. In this respect, $AgNO_3$ was considered the most preferable choice of silver salt since this does not require special conditions of storage. In contrast, it is recommended that $AgBF_4$ and $AgCH3C_6H_5SO_3$ be stored under nitrogen, and $AgClO_4$ at 0°C.

The solubilities of $AgNO_3$, $AgBF_4$, $AgCH_3C_6H_5SO_3$ and $AgClO_4$, as determined from experiment, are listed in Table 8. Of the solvents that were tested, acetonitrile was regarded the best option for further study, as this dissolved all of the silver salts that were considered. In addition, acetonitrile has a convenient liquid range (see table 7), a large potential window (limited by the discharge of the supporting electrolyte rather than reduction or oxidation of the solvent[177], and a relatively high dielectric constant, which facilitates the dissolution of a large number of commonly used electrolytes to the extent of 0.1 M concentrations[177]. Furthermore, preliminary electrolysis studies carried out at bare stainless steel electrodes with 1% wt./vol. solutions of $AgBF_4$, $AgNO_3$, $AgClO_4$, and $AgCH_3C_6H_5SO_3$ devoid of other supporting electrolyte, yielded metallic silver deposits.

8.2.2 Solvent-Polymer Film Combinations.

As previously stated in section 8.2, it is essential that the film being plated should be permeable to the electroactive constituents in solution. Therefore, a pre-requisite of the solvent system is that it should partly swell the film. Preliminary studies were carried out in order to determine the effects of various solvents on $P(VF_2/VF_3)$ 60-40 copolymer, polyacrylate and PVC polymer films that were used in this study.

Strips of solution cast polymer films (~80 µm thick) were prepared according to the general procedure as described in section 3.6. The effects of solvent on the polymer were then monitored for up to one hour. This is approximately the duration of the longest times which were required for electrodeposition (see Tables 12-15). The results are summarized in Table 9.

Table 8. Solubilities silver salts in various solvents.

Silver salt	1-2 dichloroethane	Methanol	Acetonitrile	Propylene carbonate
$AgNO_3$	IS	IS	S	IS
$AgBF_4$	--	S	S	--
$AgClO_4$	IS	S	S	S
$AgCH_3C_6H_4SO_3$	IS	--	S	IS

IS=Insoluble, S=Soluble

Table 9. Solubilities of polymer film in various solvents.

Polymer film	Ethyl acetate	THF	1-2 dichloroethane	Methanol	Acetone	DMA	DMF	Acetonitrile
$P(VF_2/VF_3)$ copolymer	D	D	N	N	D	D	D	D
Polyacrylate	DG	--	D	Sw	DG	DG	DG	DG
PVC	N	D	N	N	N	D	D	Sw

D=dissolves, DG=degrades, N=no significant affect, Sw=swells.

No single solvent was able to swell all the polymer films that were used. Consequently, the choice of solvent needed to be adjusted to suit individual polymer films. Therefore, rather than develop numerous individual plating solution/polymer combinations, the work was primarily focused on the deposition of silver into $P(VF_2/VF_3)$ 60-40 copolymer, since this polymer had previously been investigated in deposition studies with polypyrrole, and had facilitated the preparation of excellent polypyrrole composite films.

Although the use of acetonitrile was ideal as regards the electrolyte/solvent combination, a disadvantage of this system was the rapid dissolution of $P(VF_2/VF_3)$ copolymer (see Table 9). Thus, deposition from co-solvent systems proved necessary. The function of the other component of the co-solvent system was to reduce the concentration of acetonitrile to a level which did not cause film degradation over the duration of the experiment (~1 hour). Accordingly, any solvent which does not significantly swell $P(VF_2/VF_3)$ copolymer and which is miscible with acetonitrile can be used. Of the solvents that were tested, only 1-2 dichloroethane and methanol met these criteria (see Table 9). Therefore, further studies were concentrated on co-solvents systems based on acetonitrile/1-2 dichloroethane and acetonitrile/methanol.

A co-solvent system with a ratio of 85/15 vol./vol. acetonitrile, with either 1-2 dichloroethane or methanol was found to be suitable for the deposition of silver into $P(VF_2/VF_3)$ copolymer films. These co-solvent combinations contained sufficient acetonitrile to enable the rapid ingress of Ag^+ into the polymer, without causing degradation or loss of mechanical properties to the film. The permeability of the film to Ag^+ was demonstrated by the immediate electrodeposition of metallic silver at the electrode surface/polymer film interface, on the application of an electrode potential of sufficient magnitude to effect reduction. Results from both these systems are discussed in section 8.3 after a consideration of the effects of the electrode substrate on deposition.

8.2.3 The Effect of the Electrode Substrate on the Electrodeposition of Silver.

The nature of the electrode substrate is critical to the electrodeposition of metallic films. For instance, deposit epitaxy (the extent to which the structure of the new surface phase follows that of the underlying substrate), texture, grain size and stress, are all affected by the substrate material[186,222]. For this reason, different metal electrodes were examined as substrates for the deposition of silver into $P(VF_2/VF_3)$ 60-40 copolymer film.

Gold, silver, platinum, and type 316 stainless steel electrodes were prepared according to the procedure detailed in section 3.5.1. Silver was electrodeposited at -0.5 V *vs.* a silver wire reference electrode, from a 1% wt./vol. solution of silver nitrate dissolved in methanol/acetonitrile (90:10 vol./vol.). The homogeneity of the silver layer was determined after deposition by visual inspection of both the polymer film and electrode surfaces.

The uniformity of the silver coat was interpreted in terms of the lattice mismatch parameter (*P*). This is the principal factor in determining whether ad-atoms of the depositing metal are incorporated directly into the existing crystal lattice of the substrate (epitaxial growth), or whether deposition occurs by nucleation of new growth centres[186,223]. The lattice mismatch parameter is defined by:

$$P = \frac{a-b}{b} = \frac{\pi}{2}\left(\frac{\gamma a^2}{2W}\right)^{\frac{1}{2}} \qquad (8.1)$$

where a is the lattice constant of the substrate, b the lattice constant of the new phase, with a force constant γ, and a potential field $1/2W$. It has been calculated that the maximum lattice misfit above which epitaxial growth is no longer favourable is approximately 9%[186,223]. The magnitude of P also affects the strength of adhesion between the substrate and depositing phase. Generally, maximum adhesion is obtained when the crystal lattice of the base metal is continued by the structure of the deposit (i.e. epitaxial growth)[232]. Therefore, in order to obtain good adhesion, the lattice parameters of the substrate and electrodeposit should agree within the limits -2.4 to +12.5%[232].

Lattice constants for each of the substrates, and critical misfit values between silver and the electrode metal, calculated from Eqn. 8.1, are given in Table 10. No precise value for the lattice parameter of type 316 stainless steel may be determined, since it is an alloy with a composition given by 0.03% C, Max 2% Mn, 11% Ni, 16.5% Cr, 2.25% Mo, 0.15% N and 68.07% Fe[224]. However, from a consideration of the lattice parameters of the major constituents, it is anticipated that the lattice mismatch will be substantial.

Table 10. Lattice parameters of electrode substrates.

Metal	Lattice constant (Å)	Lattice misfit (%)
Silver	4.08	0
Platinum	3.92	-3.92
Gold	4.07	0.25
γ-Fe	3.56	-12.7
Nickel	3.52	-13.7
Chromium	2.89	-29.1

In the case of silver and gold substrates which have lattice misfit parameters lower than the critical value, deposition occurred at the electrode surface. As a consequence, little or no silver was deposited in the polymer film.

With platinum substrates, electrodeposition occurred both on the electrode surface and also in the polymer film, producing films with a non-uniform silver coat. For stainless steel, deposition occurred at the electrode surface/polymer film interface, via the nucleation of new growth centres. Indeed, of the different types of electrode substrate that were tested, only stainless steel provided silver deposits that were uniform.

An additional factor which affects the strength of adhesion between the substrate and depositing phase is the cleanliness of the electrode surface. For good

adhesion, the interface should be free of foreign substances, such as grease, or oxide layers which disrupt the continuity of the structure. The adhesion of electrodeposits to oxide layers is generally low since metallic bonding cannot be achieved, and surfaces generally require pre-treatment by etching in dilute acids to provide adhesion[225].

Silver coated polymer films were easily removed from stainless steel electrodes following deposition. This implies that the adhesion forces between the deposited silver layer and polymer film were greater than that between silver and the stainless steel substrate. The poor adhesion can probably be attributed to the existence of an oxide layer on the surface of stainless steel. At ambient temperature this layer is relatively thick, and is composed mainly of chromium oxides, and to some extent nickel oxides[226]. An additional benefit afforded by the oxide layer, is a high resistance to corrosion[93]. For these reasons, stainless steel supports were used in all subsequent metallization studies.

8.3 The Deposition of Silver into P(VF_2/VF_3) 60-40 Copolymer from Acetonitrile Based Co-Solvent Systems.

As described in section 8.2.2, acetonitrile based co-solvent systems were considered as providing ideal combinations from which to deposit silver into polymer films. This section describes the deposition of silver into P(VF_2/VF_3) 60-40 copolymer films using various silver salts.

8.3.1 Acetonitrile/1-2 Dichloroethane System.

For the reasons detailed in section 8.2.2, one of the systems which was chosen to study the electrodeposition of silver was acetonitrile/1-2 dichloroethane (85/15 vol./vol.). Electrolysis was performed at P(VF_2/VF_3) copolymer coated stainless steel electrodes, with silver perchlorate ($AgClO_4$) and silver paratoluene sulphonate ($AgCH_3C_6H_5SO_3$) electrolytes. The results are shown in Table 11.

Table 11. Electroreduction of silver from acetonitrile/1-2 dichloroethane co-solvent system.

Silver Salt	wt./vol. (%)	Potential (V)	Comment
$AgClO_4$	4	-0.30	Partial deposition, film discoloured.
		-0.45	No deposition.
	2	-0.50	Good deposition, film discoloured.
$AgCH_3C_6H_5SO_3$	2	-0.50	Good deposition, rapidly tarnished in air.

Consistent results for the deposition of silver from $AgClO_4$ were difficult to obtain. Reflective metallic deposits were obtained in some instances, although generally, deposits were matt or frosted in appearance. There was also a tendency for silver to deposit unevenly across the film surface, giving rise to non-uniform silver coats. This variability in the nature of silver deposit, suggests that this co-solvent/silver salt combination was sensitive to the conditions of deposition, and that optimization might be difficult to achieve. Silver perchlorate also caused a slight brown/black discolouration of the copolymer film, possibly caused by oxidation. For these reasons, further deposition studies were concentrated on the deposition from other silver salts.

Attempts to deposit silver from silver paratoluene sulphonate were partly successful, and electrolysis yielded homogeneous reflective metallic deposits. However, these rapidly tarnished on exposure to air, producing yellowish/brown surface coats. A likely cause of this tarnishing is considered to be the incorporation

of sulphur into the silver deposit during electrodeposition[227]. The inclusion of sulphur in metal deposits has been demonstrated with other metals when deposition is carried out in the presence of sulphur-containing compounds, such as aromatic sulphonates[227]. Furthermore, silver is known to rapidly tarnish in the presence of sulphur-containing media, giving rise to films of silver sulphide[227].

Because of the problems of tarnishing, an alternative co-solvent system based on methanol/acetonitrile with silver nitrate electrolyte was investigated.

8.3.2 Acetonitrile/Methanol/$AgNO_3$ System.

Highly reflective and adherent silver/P(VF_2/VF_3) copolymer films were obtained in preliminary electrolysis studies. These films were superior to those obtained using co-solvent systems with silver perchlorate and paratoluene sulphonate electrolytes as previously discussed in section 8.3.1.

In order to identify the optimum plating conditions for the acetonitrile/methanol/silver nitrate system, a comprehensive investigation of the effects of variations in the silver ion concentration, electrode potential, and co-solvent composition was undertaken. Electrolysis was carried out in solutions containing silver nitrate only, since the addition of 0.1 M additional supporting electrolyte (tetrabutylammonium tetrafluoroborate ($TBABF_4$), tetraethylammonium tetrafluoroborate ($TEABF_4$), or tetraethylammonium hexafluorophosphate ($TEAPF_6$)) decreased the reflectivity and homogeneity of the silver films. Likewise, care was taken to ensure anhydrous conditions throughout electrolysis, as contamination of the plating solution with water resulted in "frosty" deposits. Stainless steel substrates were polished prior to deposition to surface finishes smoother than 1 µm using the procedure detailed in section 3.5.1.

8.3.2.1 The Effect of the Deposition Potential and Silver Nitrate Concentration on the Nature of the Silver Deposit.

This section describes the effects of the electrode potential and silver ion concentrations on the reflectivity and continuity of silver coated P(VF_2/VF_3) copolymer films. These parameters were varied in order to find the optimum conditions for electrodepositing continuous reflective silver films.

Metallized polymer films were categorized by optical microscopy of cross-sections of film and by visual inspection, according to the reflectivity and homogeneity of the silver deposit at the surface of the polymer film (the surface in direct contact with the electrode substrate).

The apparent quality of a film is dependent on the amount of light which is reflected from its surface, and depends on the roughness of the surface at dimensions on the microscopic scale[227,228]. Surfaces appear reflective when light is reflected unidirectionally and matt when light is reflected diffusely. When the majority of incident light is reflected directionally with only a small proportion of scatter, surfaces appear semi-reflective, or what is commonly referred to in electroplating as "bright". In general, surfaces appear bright or reflective when surface roughness has dimensions smaller than the shortest wavelength of light (~0.4 μm).

Two types of brightness have been distinguished[227] depending on the origin, these are reproduced and intrinsic brightness. Silver coated polymer films in this study have reproduced brightness. This is where coatings replicate the surfaces of smooth substrates for thin coat thicknesses, but which decrease in reflectivity as the thickness of the deposited layer exceeds certain limits. Intrinsic brightness is where deposits remain bright as the thickness of the deposit is increased. This is usually only achieved for deposits which contain brightening additives, or which are deposited using current-reversal techniques (pulsed plating)[229,230].

The results for the electrodeposition of silver, for electrode potentials in the range -0.2 to -0.7 V (*vs.* silver wire quasi-reference) and silver ion concentrations between 0.1 and 4% wt.vol. are detailed in Table 12 together with comments on the quality of the films. These results are also illustrated schematically in Fig. 64. It can

be seen that both the deposition potential and silver ion concentration have a considerable effect on the nature of the silver film.

Several different regions corresponding to different categories of deposit may be identified, these are labelled A-D. The boundaries differentiating between these regions are only approximate, as a consequence of the difficulties in determining the exact nature of the deposit. This is because the transition between neighbouring regions is not sharp, but occurs over a potential range (*ca.* 50 mV). In order to determine the boundary positions with greater accuracy, it would be necessary to make a much larger number of depositions over the transition regions, and to couple this to a more quantitative method of determining the quality of the deposit. A suitable method could be based on a more accurate measurement of the reflectivity of the film such as that detailed in section 8.8. However, this was not undertaken since it was not expected to alter the general features of the diagram significantly.

Region A is where excellent, highly reflective, continuous silver coats are obtained. Films were easily removed from the electrode surface, and there was no indication of deposition having occurred on the electrode surface rather than in the film. The silver deposits generally had an excellent adherence to the polymer film, and were resistant to delamination, even by direct abrasion. Back illumination with a 1000 W light source revealed a continuous metal layer which was free from microscopic pores, or other defects.

Region B is where good ("bright") deposits are obtained. These films are similar in almost all respects to those in region A, except that they were not as highly reflecting.

Silver films in **region C** were matt in appearance and generally of a poor quality with respect to both the reflectivity and continuity of the metal deposit. Back illumination revealed many microscopic defects and the films were partly transparent. At deposition potentials less than -0.25 V (*vs.* silver wire reference), deposition occurred both in the polymer film and on the electrode surface. This gave rise to poorly adhering, thin silver coats. Plate 22 illustrates the partial delamination of a thin silver coat from the surface of a polymer film. It can be seen that the silver deposit did not penetrate the film, but formed a separate layer at the electrode surface/polymer film interface.

Table 12. $P(VF_2/VF_3)$ 60-40 copolymer, $AgNO_3$/methanol/acetonitrile (90/10 vol./vol.)

$AgNO_3$ (wt.%)	Potential V *vs.* Ag ref.	Duration (S)	Charge passed (mC)	Film thickness (μm)	wt. silver deposited (g)	Comment code
0.2	-0.50	3750	4826	21.1	5.16	E
0.2	-0.60	3462	5003	20.5	1.03	E
0.2	-0.70	2485	5013	18.8	2.69	E, B
0.4	-0.50	1308	5039	18.6	----	P, T
0.4	-0.55	1335	5010	16.7	1.48	E
0.4	-0.60	828	5389	15.7	1.60	E
0.4	-0.65	1083	5216	16.0	2.66	E
0.4	-0.70	744	5454	17.6	1.36	E
1.0	-0.20	2667	5099	29.1	4.81	M, T
1.0	-0.25	1452	5102	21.0	3.64	E, T
1.0	-0.30	1425	4949	23.8	----	E
1.0	-0.40	852	5410	19.1	----	G
1.0	-0.45	894	5368	18.8	1.29	E,
1.0	-0.55	1335	5010	16.7	1.48	E
1.0	-0.60	1215	5098	22.31	2.99	E, D
1.0	-0.65	1014	5244	25.4	3.66	E, D

$AgNO_3$ (wt.%)	Potential V *vs.* Ag ref.	Duration (S)	Charge passed (mC)	Film thickness (µm)	wt. silver deposited (g)	Comment code
2.0	-0.20	2100	~5200	36.9	----	P, T
2.0	-0.30	1074	5215	19.2	4.11	G
2.0	-0.40	600	5606	19.9	4.15	E, D
2.0	-0.50	561	5618	22.8	4.71	G
2.0	-0.60	912	5334	29.1	5.80	E, D
3.0	-0.30	360	5006	19.1	2.76	G, T
3.0	-0.40	357	5068	19.0	2.73	G
3.0	-0.50	216	5011	18.2	2.73	G, D
3.0	-0.60	285	5024	23.6	2.34	G, D
3.0	-0.70	350	5027	25.5	4.68	E, D
4.0	-0.25	564	5037	13.9	3.38	M/G
4.0	-0.40	185	5044	15.7	2.66	M/G
4.0	-0.50	336	5061	25.5	3.05	G, D
4.0	-0.60	298	5051	21.8	2.87	E, D
4.0	-0.70	254	5038	25.5	5.72	M/G, D
4.0	-0.75	216	5091	25.4	9.14	P, T, D

Comment Code: P=poor deposit, M=matt deposit, G=good deposit, E=excellent deposit,
T=thin deposit, D=dendritic deposit, B=burnt deposit

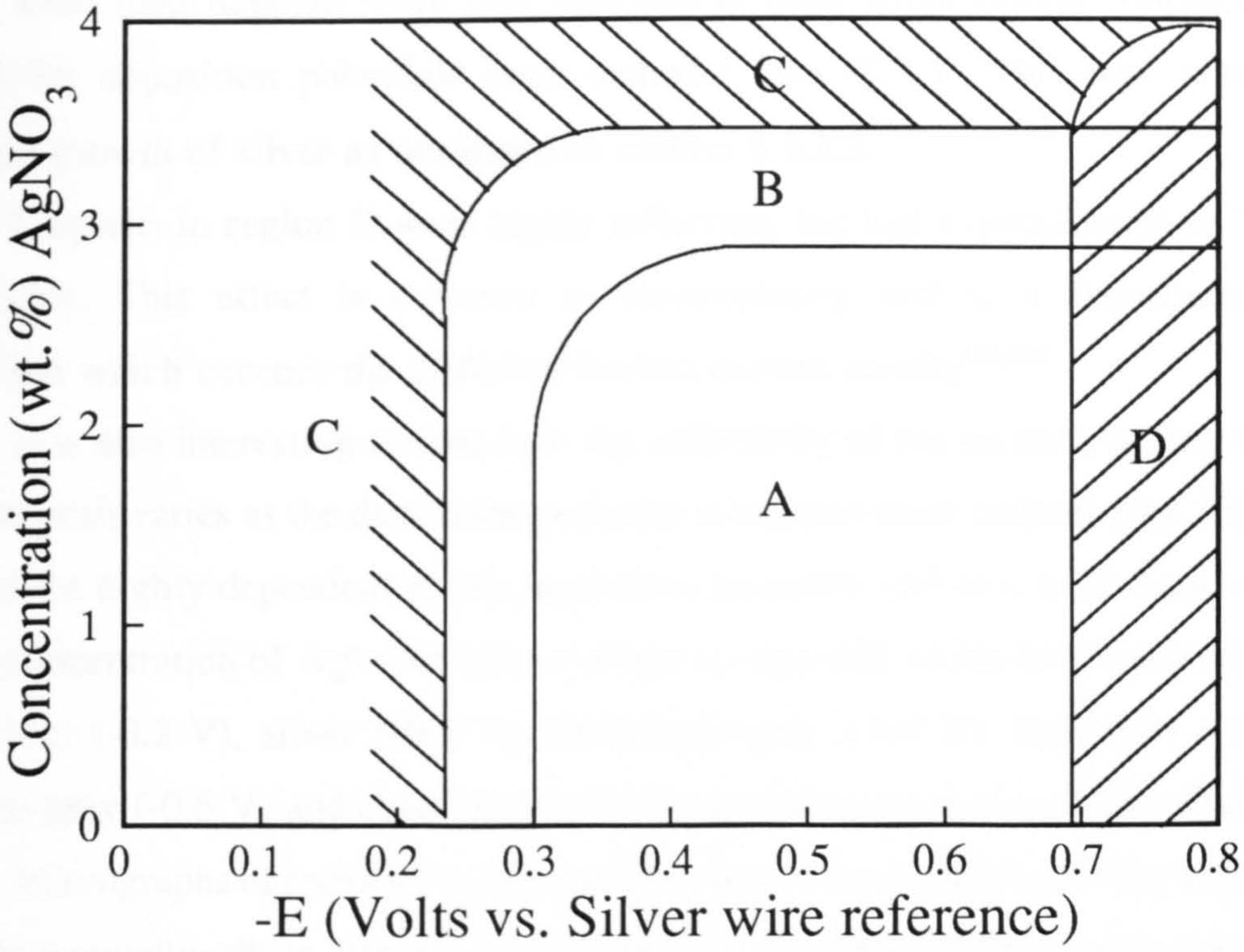

Fig. 64. Schematic representation of the results obtained for deposition with the acetonitrile/methanol/$AgNO_3$ (90/10 vol./vol.) co-solvent system.

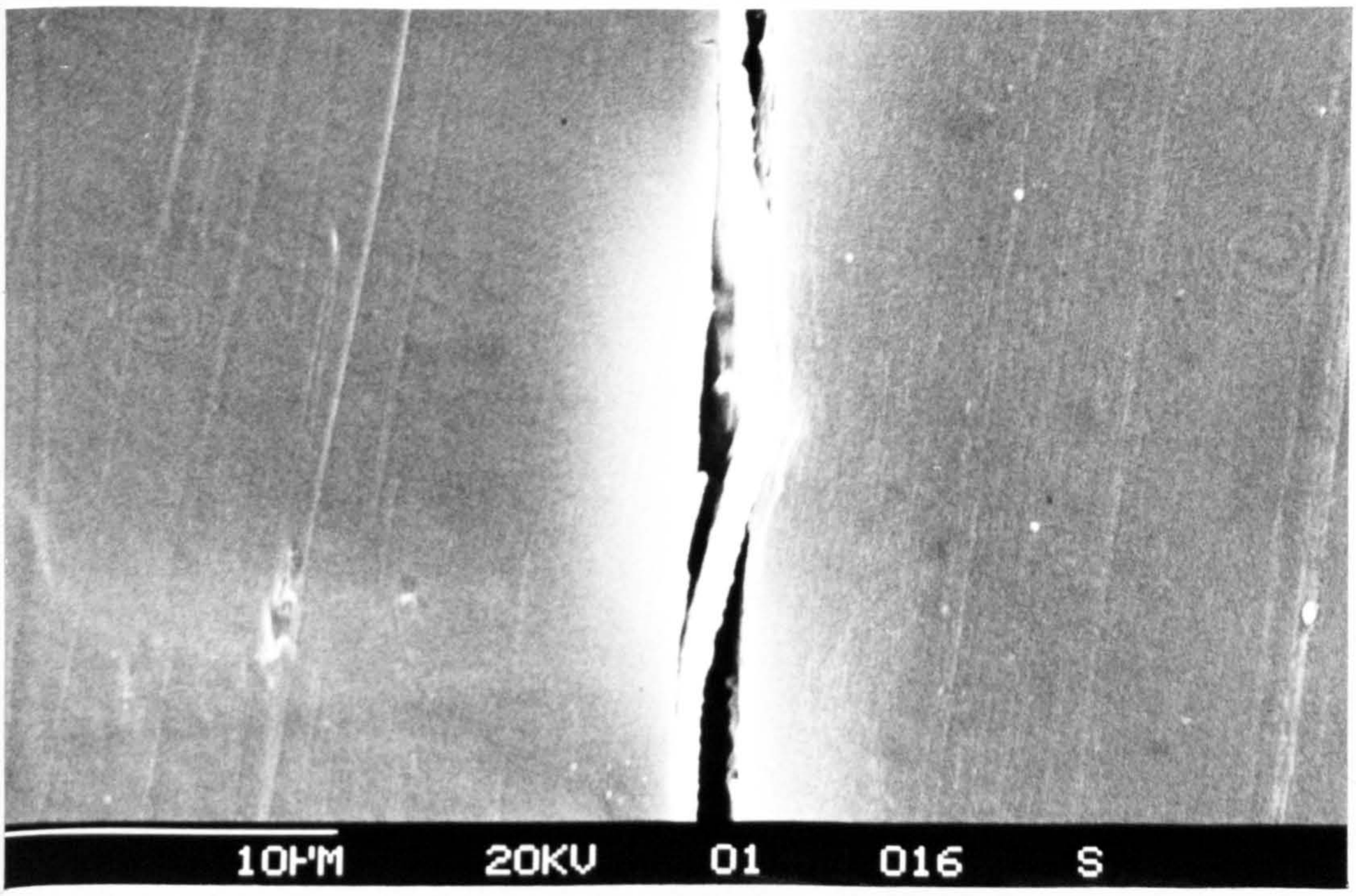

Plate 22. Delamination of silver coat from P(VF_2/VF_3) 60-40 copolymer film. Cross-sectional morphology typical of that found in region C of Fig. 64.

Thin matt deposits were also obtained at high silver nitrate concentrations (> 3%) for deposition potentials more cathodic than -0.7 V. This was caused by dendritic growth of silver as discussed in section 8.3.2.3.

Deposits in **region D** were highly reflecting, but had a discoloured or "burnt" appearance. This effect is common in electroplating and is a characteristic of deposition which exceeds the diffusion limited current density[16,231].

It is also interesting to note how the reflectivity of the reverse, (solution side) of the deposit varies as the deposition potential is stepped more cathodically. This was found to be highly dependent on the deposition potential, and to a much lesser extent on the concentration of Ag^+. The colour of the reverse side of the film varied through matt-silver (-0.2 V), silver (-0.3 V), silver/light grey (-0.4 V), dark grey (-0.5 V), charcoal grey (-0.6 V) and charcoal grey/black at potentials more cathodic than this.

Micrographs of cross-sectioned samples showed no evidence for any deposition other than metallic silver, hence it is believed that the colour of the reverse side of the film is an optical effect which is due to differences in light scattering from the metallic deposit as a result of different deposit morphologies. Indeed, from a visual inspection of the reflectivity, it is possible to ascertain a qualitative estimate of the surface roughness compared to liquid mercury, which by definition has unit roughness[228]. Surfaces with a mirror finish can be estimated to have a roughness factor of between 2-3. Grey surfaces have roughness factors of between 7-20, and black surfaces in between 80-200.

8.3.2.2 The Effect of the Volume Fraction of Acetonitrile on the Nature of the Silver Deposit.

The effect of varying the acetonitrile/methanol ratio on the silver deposit was investigated for acetonitrile concentrations between 2-20% vol./vol. Electrodeposition was carried out in the potential range -0.25 to -0.75 V, and results are detailed in Tables 13-15. Fig. 65 is a schematic illustration of the data obtained in this region.

Several regions, labelled A-E, may be identified. These are equivalent in physical characteristics and appearance to the corresponding regions labelled A-D in

Fig. 64, but with an additional region E, corresponding to the maximum limit of acetonitrile that can be added to the co-solvent without film degradation occurring. The boundary positions are only approximate for the same reasons which are described in section 8.3.2.1.

Excellent or good deposits were obtained over a wide concentration and potential range (regions A-C). A transition from deposits with a "burnt" appearance (region D), to good deposits (region B), was observed at around -0.65 V and 10% vol./vol. acetonitrile. This was due to the increased permeability of Ag^+ through the film at the higher acetonitrile and Ag^+ concentrations. **Region E**, ~18% vol./vol. acetonitrile, represents an upper limit of the amount of acetonitrile that can be added to the co-solvent mixture. At concentrations in excess of this, speckled, non-continuous deposits were obtained. This effect is characteristic of a dissolution and reprecipitation process[232], and is caused by the partial solubility of the polymer film at these concentrations of acetonitrile. Similar types of effects have been reported in swelling studies of sodium acrylate gels in water[232].

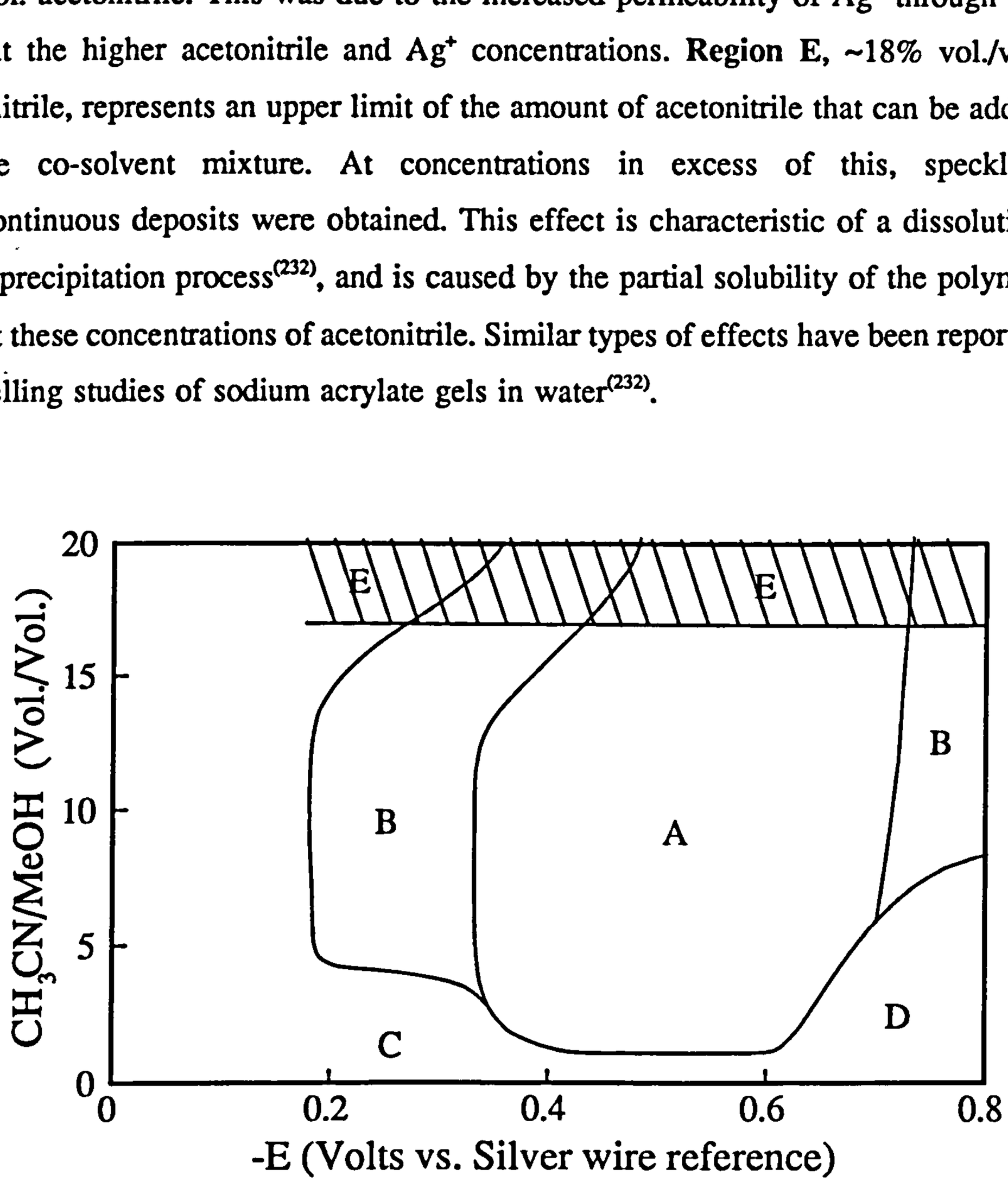

Fig. 65. Schematic representation of the results obtained for depositions with the acetonitrile/methanol/$AgNO_3$ co-solvent system.

Table 13. P(VF_2/VF_3) 60-40 copolymer, $AgNO_3$/methanol/acetonitrile (80/20 vol./vol.)

$AgNO_3$ (wt.%)	Potential V *vs.* Ag ref.	Duration (S)	Charge passed (mC)	Film thickness (μm)	wt. silver deposited (g)	Comment code
1.0	-0.45	1084	6983	27.80	3.86	M, T, Sp
1.0	-0.50	1044	5249	22.3	4.63	G, T, Sp
1.0	-0.55	537	5646	17.5	3.57	G, Sp
1.0	-0.60	549	5655	16.7	3.35	E, SSp
1.0	-0.65	858	5385	21.9	6.11	E, U
1.0	-0.70	783	5447	23.6	3.78	G, U
1.0	-0.75	666	5545	26.3	3.80	G, Sp

Key: M=Matt, T=Thin, SSp=Slightly Speckled deposit, Sp=Speckled deposit, G=Good deposit, E=Excellent deposit, U=Uneven deposit

Table 14. P(VF_2/VF_3) 60-40 copolymer, $AgNO_3$/methanol/acetonitrile (96/4 vol./vol.)

$AgNO_3$ (wt.%)	Potential V *vs.* Ag ref.	Duration (S)	Charge passed (mC)	Film thickness (μm)	wt. silver deposited (g)	Comment code
2.0	-0.40	2330	5046	28.0	2.03	G, D
2.0	-0.50	875	5005	19.6	1.07	E, D
2.0	-0.60	1210	5003	23.2	1.09	E, D
2.0	-0.70	1945	5071	28.0	0.96	E, D, B

Table 15. P(VF_2/VF_3) 60-40 copolymer, $AgNO_3$/methanol/acetonitrile (98/2 vol./vol.)

$AgNO_3$ (wt.%)	Potential V *vs.* Ag ref.	Duration (S)	Charge passed (mC)	Film thickness (μm)	wt. silver deposited (g)	Comment code
2.0	-0.40	1300	5032	25.3	1.08	P, D
2.0	-0.50	950	5059	24.6	0.60	P, D, T
2.0	-0.60	915	5007	34.6	2.27	E, D, T
2.0	-0.70	1500	5000	29.8	6.60	G, D, B

8.3.2.3 Cross-Sectional Morphology of Silver/P(VF_2/VF_3) 60-40 Copolymer Films.

As reported in section 8.3.2.2, a wide variety of surface morphologies were exhibited for silver coated polymer films prepared under the deposition conditions detailed in Tables 12-15. This section discusses typical cross-sectional morphologies that were obtained from depositions in acetonitrile/methanol/$AgNO_3$ solutions. Photomicrographs of cross-sections of samples were obtained according to the method previously detailed in section 3.8.

The cross-sectional morphology of silver/P(VF_2/VF_3) 60-40 copolymer composite films was found to be dependent on a combination of both the deposition potential and the concentration of $AgNO_3$ in the electrolyte solution. A wide range of morphologies of silver deposits were obtained which did not always correlate with the deposition conditions. However, the following general observations were made.

Silver deposited into P(VF_2/VF_3) 60-40 copolymer film at low concentrations of silver nitrate ($\leq$ 0.4%) and at deposition potentials less than -0.30 V tended to be thin, with metal deposition occurring mainly at the electrode surface/polymer film interface. A typical example of this type of morphology is shown in Plate 23 for silver deposited from a 1% wt./vol. solution of $AgNO_3$ at -0.25 V. At concentrations of $AgNO_3$ up to 1% and at deposition potentials in the range -0.30 to -0.60 V, depositions usually produced metal layers that were uniform, but which also penetrated into the thickness of the polymer matrix, thus providing good adhesion. This type of morphology is shown in Plate 24 for silver deposition at -0.60 V from 1% wt./vol. $AgNO_3$. With concentrations of $AgNO_3$ in excess of 1% wt./vol. or at deposition potentials more cathodic than -0.60 V, silver deposits were nodular or dendritic. Examples of each of these types of morphology are shown in Plates 24 and 25, for silver deposited at -0.65 V from 0.4% wt./vol. and -0.75 V from 4% wt./vol. $AgNO_3$ respectively.

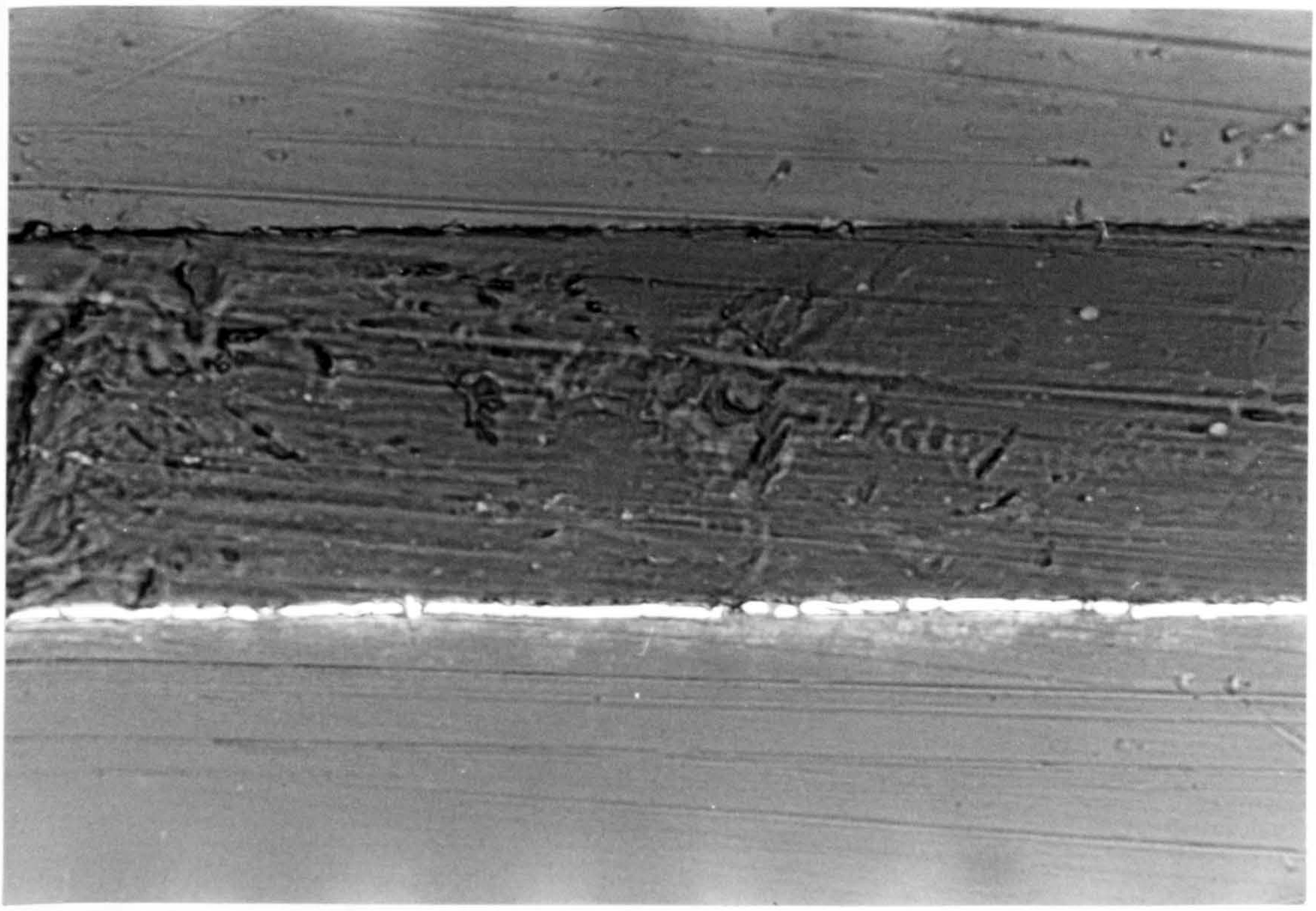

Plate 23. Cross-section of a silver/P(VF_2/VF_3) 60-40 copolymer film deposited from a 1% wt./vol. solution of $AgNO_3$ at -0.25 V.

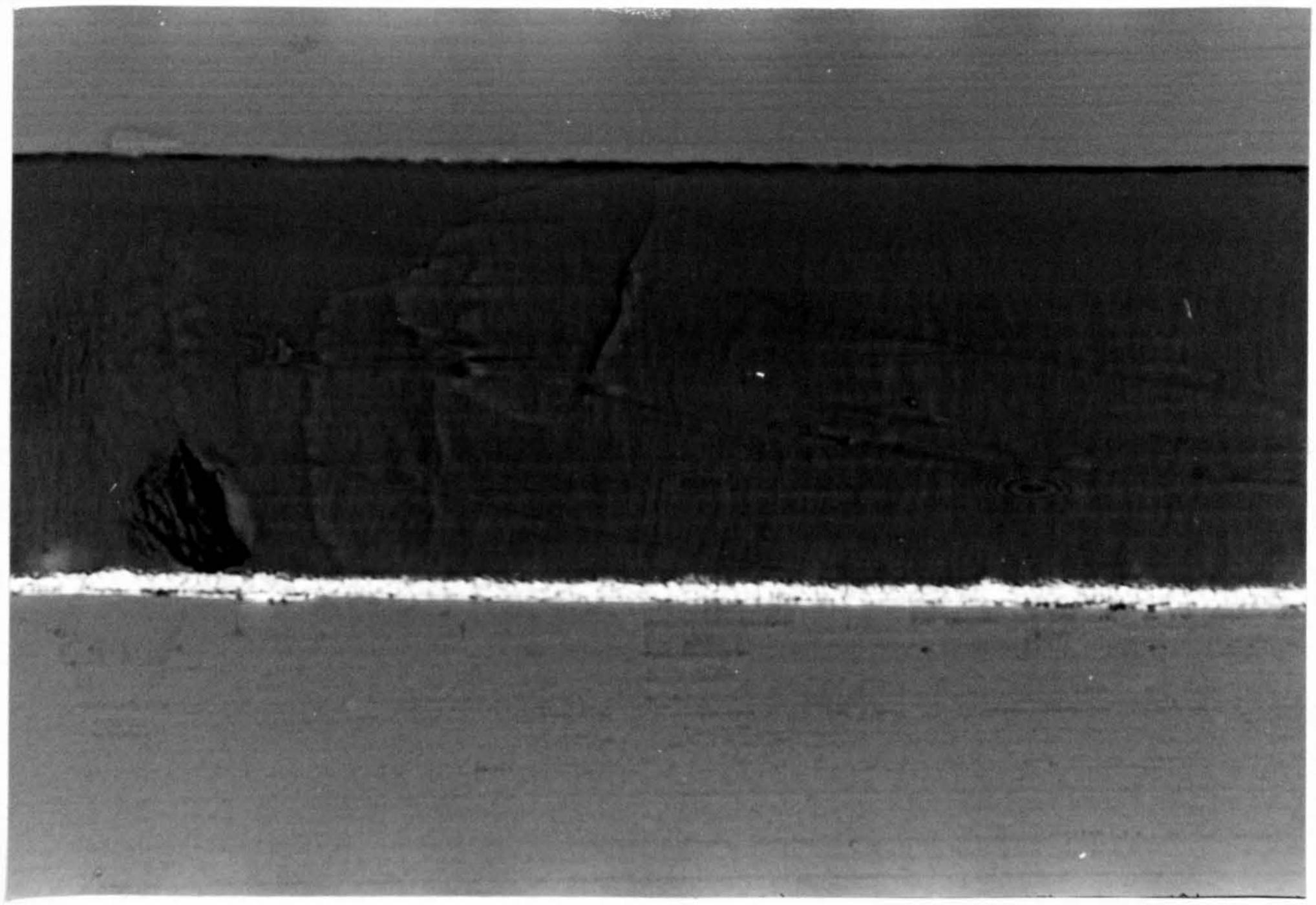

Plate 24. Cross-section of a silver/P(VF_2/VF_3) 60-40 copolymer film deposited at -0.60 V from 1% wt./vol. $AgNO_3$.

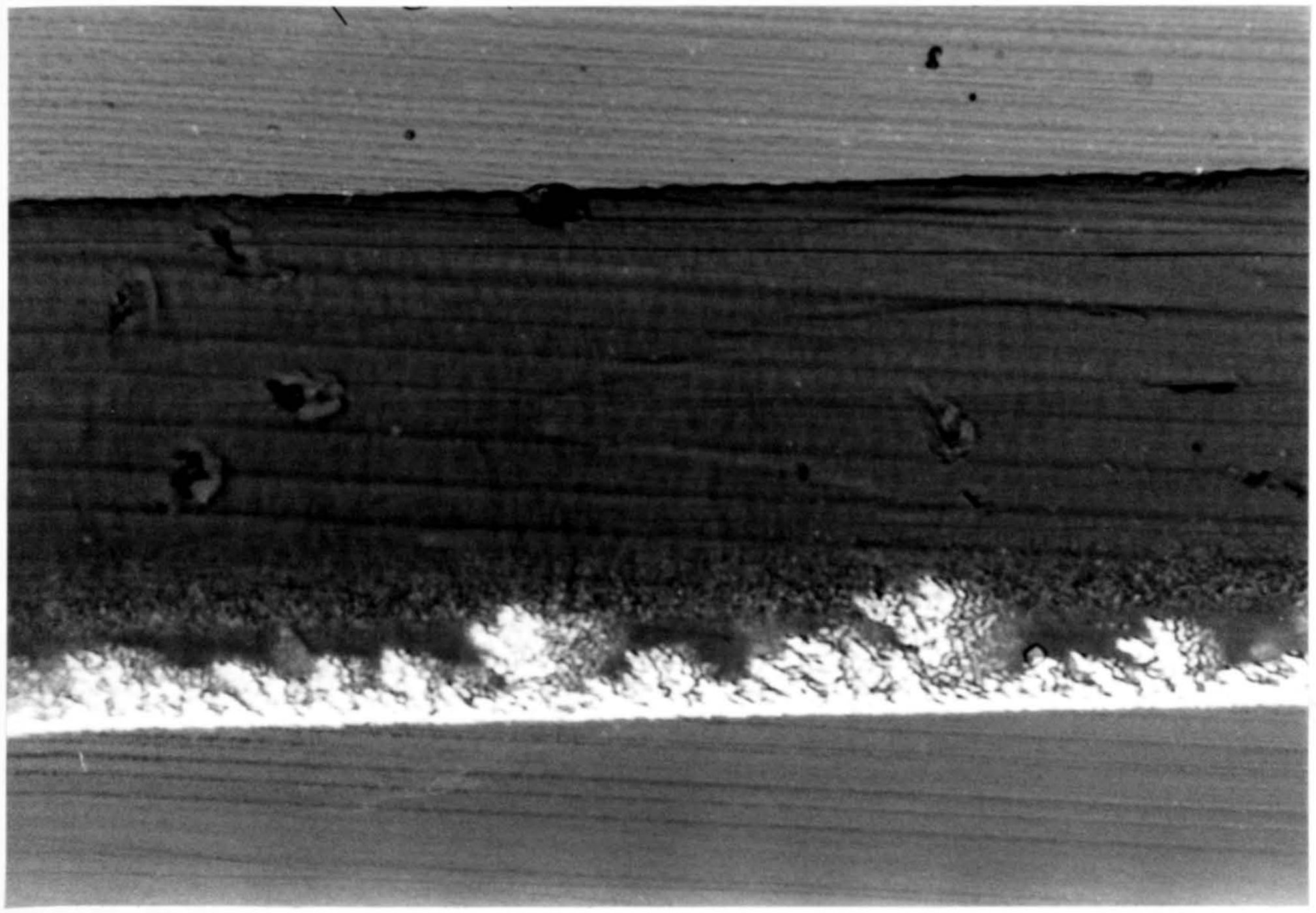

Plate 25. Cross-section of a silver/P(VF_2/VF_3) 60-40 copolymer film deposited at -0.65 V from 0.4% wt./vol $AgNO_3$ showing nodular growth.

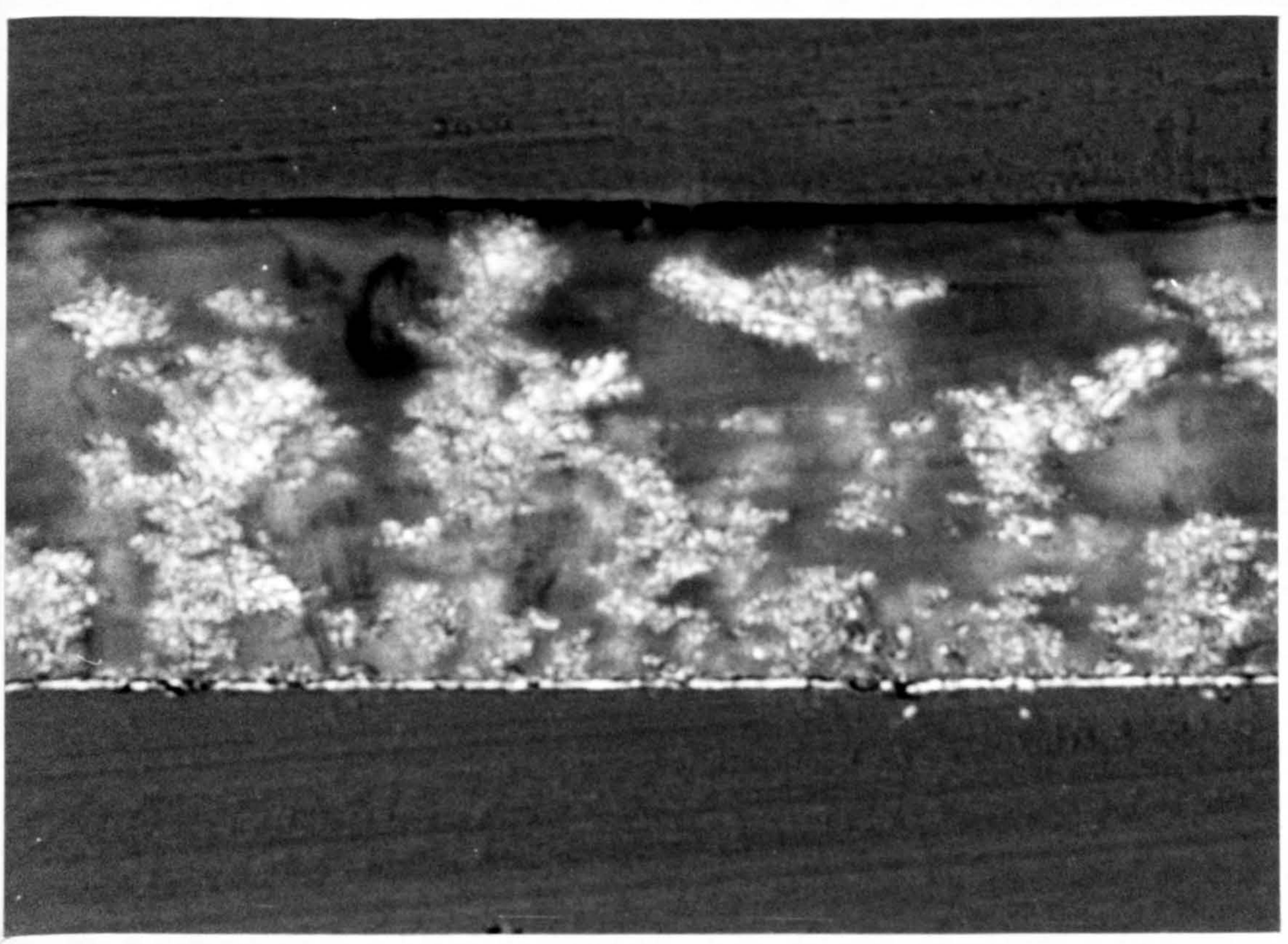

Plate 26. Cross-section of a silver/P(VF_2/VF_3) 60-40 copolymer film deposited at -0.75 V from 4% wt./vol. $AgNO_3$ showing dendritic growth.

Dendritic growth is highly undesirable, since growth is uncontrolled, and most of the charge passed during deposition is consumed in the formation of an unwanted metal deposit. Moreover, dendritic growth also limits the maximum thickness of metal deposit that is obtainable during deposition. Once dendritic growth is established, propagation occurs rapidly in the direction of increasing concentration of depositing ions (ie. into the solution)[186,194]. Dendrites then quickly penetrate the thickness of the polymer coat, thus short circuiting deposition through the film to the electrode surface. Deposition subsequently occurs predominantly at the points of penetration through the thickness of the film, giving rise to a rapid increase in current density. This penetration of dendrites through the polymer coat can be readily identified from inspection of the current-time transient during deposition.

A typical current-time transient for the deposition of silver into $P(VF_2/VF_3)$ 60-40 copolymer film (1% wt./vol. solution of $AgBF_4$ in acetonitrile/methanol, 90/10 vol./vol. at -0.70 V) is shown in Fig. 66.

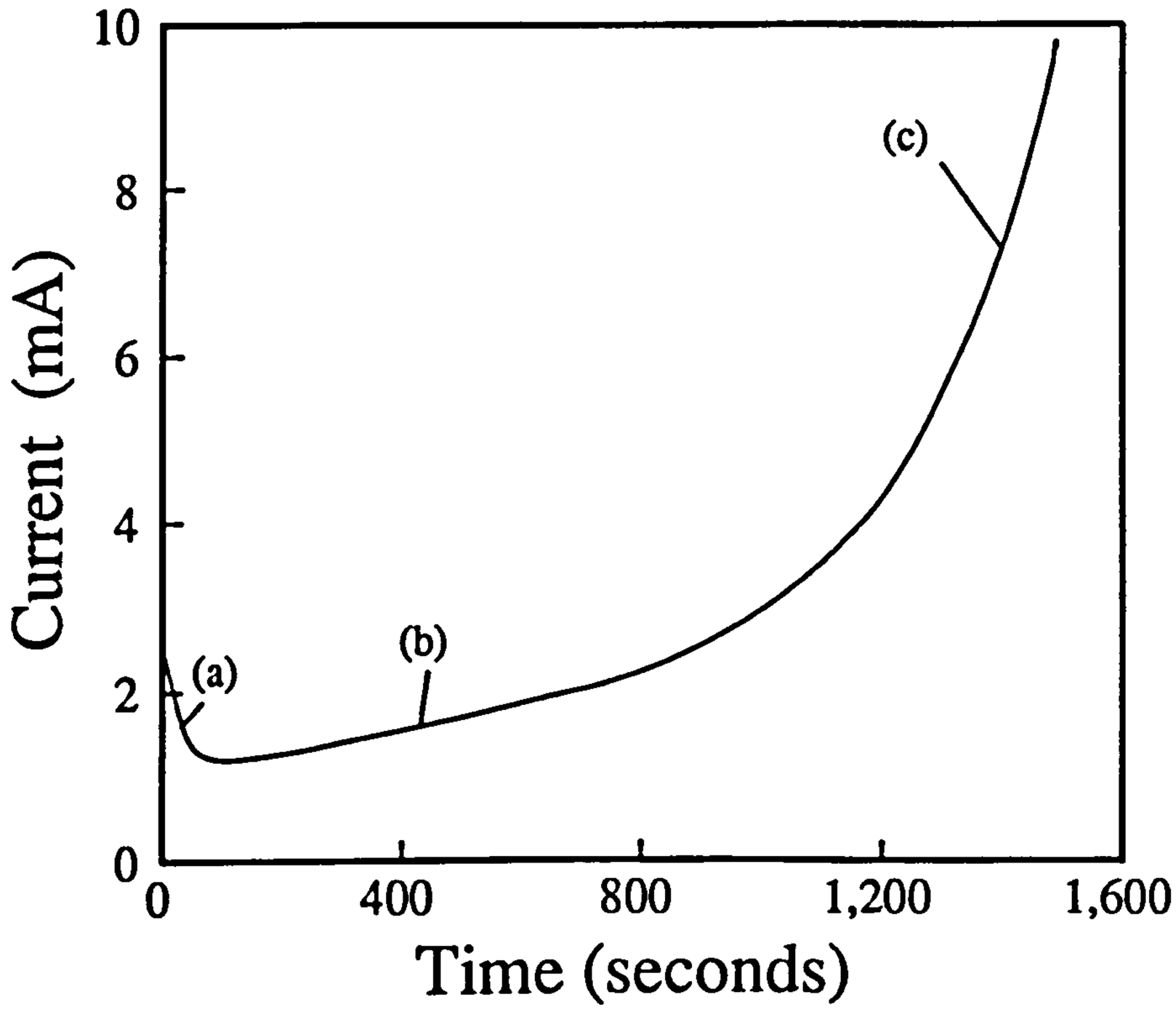

Fig. 66. A typical current-time transient for the deposition of silver into $P(VF_2/VF_3)$ 60-40 copolymer film (1% wt./vol. solution of $AgBF_4$ in acetonitrile/methanol, 90/10 vol./vol. at -0.70 V). (a) nucleation, (b) growth, (c) penetration of film by silver deposit.

Three different stages of growth, labelled A-C, may be identified. Stage A is the nucleation and growth of silver at the electrode surface. The decrease in current which is observed during the initial 40 seconds is caused by the depletion of silver ions in the vicinity of the electrode surface. Stage B, between 50 and 1000 seconds, is identified by a gradual increase in current. This is attributed to an increase in electrode area as silver deposition develops dendritic growth, and the shorter distance through which silver ions need to penetrate the film before deposition occurs[186,194]. Finally, the rapid increase in current in region C, is where the silver deposit penetrates the thickness of the polymer coat.

Another feature of dendritic growth is screening, whereby the outermost protrusions of dendritic growth form an effective shield to the diffusion of silver ions to the electrode surface. This effect is most pronounced where there is a close incidence of dendritic growth, and gives rise to thin deposits, and poorly adherent surface coats of metal. This type of growth is common to region D of Fig. 64, and an extreme example is shown in Plate 26.

The morphology of an electrodeposit is controlled by a combination of the flux of depositing ions to the electrode surface, and the kinetics of the charge transfer step. When the mass-transport of depositing ions to the electrode surface is rate determining, such as will be the case at highly cathodic deposition potentials or at low concentrations of Ag^+, the distribution of current is controlled by diffusion, and results in the amplification of surface irregularities[194]. Examples of this are nodular and dendritic growth, which are shown in Plates 25 and 26.

The growth of dendrites from $AgNO_3$ solutions has been thoroughly studied by a number of workers and the following observations have been made[186,194]; a critical overvoltage must be exceeded in order to provide dendritic growth, an induction period is exhibited before dendritic growth occurs, the incidence of dendrites increases with overall current density, not all dendrites grow at the same rate under the potential and concentration.

The results for depositions from the acetonitrile/methanol/$AgNO_3$ co-solvent system, for the deposition conditions listed in Tables 12-15 were found to be in general agreement with the above statements.

In summary, a consideration of the results obtained for deposition in Table 12-15, in combination with a study of surface and cross-sectional morphologies, shows that highly reflecting silver composites, with good adhesion and uniform metal thickness, may be achieved using the acetonitrile/methanol/$AgNO_3$ system. However, this requires that depositions should be carried out at concentrations of $AgNO_3$ less than 1% wt./vol. and at deposition potentials in the range -0.30 to -0.50 V.

8.4 Acetonitrile/Methanol/$AgBF_4$ System.

A small number of experiments were carried out using an acetonitrile/methanol co-solvent system, with silver fluoroborate ($AgBF_4$) rather than $AgNO_3$ as electrolyte. Deposition was carried out under conditions analogous to that used to deposit silver from silver nitrate based solutions, using 1% and 2% wt./vol. of $AgBF_4$ electrolyte. In common with deposition from solutions containing silver nitrate, the addition of 0.1 M supporting electrolyte caused a decrease in the reflectivity and homogeneity of the silver deposits. It is considered likely that this decrease in the quality of the film was due to inclusion of impurities from the electrolyte into the electrodeposit, as previously discussed in section 8.3.1. The results for deposition from $AgBF_4$ are presented in Tables 16 and 17.

Highly reflective and uniform metal films were obtained in the potential range -0.4 V to -0.7 V with 1 to 2% wt./vol. $AgBF_4$. Visual inspection of the films showed that the silver coats were more highly reflecting compared to that obtained with silver nitrate as electrolyte.

The major difference for depositions from silver nitrate and fluoroborate salts, was that deposits from silver fluoroborate were less dendritic. This is beneficial, since more compact and thicker deposits of silver can be obtained for the same amount of coulombs. A consequence of the less dendritic nature of deposits, is the increase in

deposition time compared to deposition from silver nitrate. However, deposition times are still short (see Table 16-17) in comparison with other methods of metallizing polymer films (see section 8.9.1).

From a consideration of the less dendritic morphology of cross-sections of films, coupled with the superior reflectivity of the silver coats deposited from $AgBF_4$ solutions, $AgBF_4$ was the preferred silver salt for depositions. However, the much higher cost of $AgBF_4$, in combination with the need for storage in anhydrous conditions and under a nitrogen atmosphere, means that $AgNO_3$ is likely to be the preferred choice for any industrial application. For this reason further studies were concentrated on depositions from $AgNO_3$ plating solutions.

Table 16. $P(VF_2/VF_3)$ 60-40 copolymer, $AgBF_4$/methanol/acetonitrile (90/10 vol./vol.)

$AgBF_4$ (wt.%)	Potential V *vs.* Ag ref.	Duration (S)	Charge passed (mC)	Film thickness (μm)	wt. silver deposited (g)	Comment code
1.0	-0.40	3300	5029	24.2	----	P/G, T
1.0	-0.50	2105	5015	25.9	----	E, D
1.0	-0.60	1740	5024	22.3	----	E, D
1.0	-0.70	1560	5049	21.3	----	E, D
1.0	-0.80	2200	5015	26.9	----	E, D, B

Table 17. $P(VF_2/VF_3)$ 60-40 copolymer, $AgBF_4$/methanol/acetonitrile (90/10 vol./vol.)

$AgBF_4$ (wt.%)	Potential V *vs.* Ag ref.	Duration (S)	Charge passed (mC)	Film thickness (μm)	wt. silver deposited (g)	Comment code
2.0	-0.30	1145	5018	20.6	3.40	M, T
2.0	-0.40	965	5039	19.2	----	E
2.0	-0.50	948	5001	17.8	1.71	E, D
2.0	-0.60	705	5104	20.0	1.81	E, D
2.0	-0.70	915	5069	27.5	3.08	E, D

Key: M=Matt, T=Thin, B=Burnt, P=Poor, G=Good, E=Excellent, D=Dendritic

8.5 Growth.

In order to establish a more complete understanding of the change in the reflectivity of the metal coat with the electrode potential and silver ion concentration, optical micrographs were taken of the growth after 250 mC of charge had been consumed.

8.5.1 Effect of Deposition Potential on Deposit Morphology.

Two distinct potential dependent types of silver deposit were obtained. The growth patterns of the silver aggregates deposited at -0.3 V were highly complex and unlike that which is typically observed for the deposition of silver from silver nitrate solution[233]. Growth was characterised by open, non space filling, randomly branched type structures as shown in Plate 27, and there appeared to be no crystalline symmetry, or any preferred axis of growth in any of the deposits.

In contrast to the open structure which resulted from deposition at -0.3 V, deposition at -0.6 V produced growth centres which were more compact and roughly circular in shape (Plate 28). However, a small number of growth centres still possessed the more complex random branched type structure associated with deposition at -0.3 V. One significant difference which was observed at the more cathodic deposition potential, was the coalescence of adjacent nuclei. This occurred even at low surface coverages of silver for depositions at -0.6 V. In contrast, boundaries between adjacent growth centres for deposition at -0.3 V could still be distinguished after 1500 mC of charge.

The cause of the transition from the more open type of structure which is observed at -0.3 V, to the essentially compact type of deposits which are obtained at -0.6 V, is not immediately obvious. Suggestions which have been proposed to account for this potential dependent growth behaviour have included the effects of migration and electrostatic interaction between charged ions[234,235], solvent breakdown, and agitation of the solvent in the vicinity of the electrode surface. In the present study, the effects of solvent breakdown can be disregarded, since the electrolyte solution is

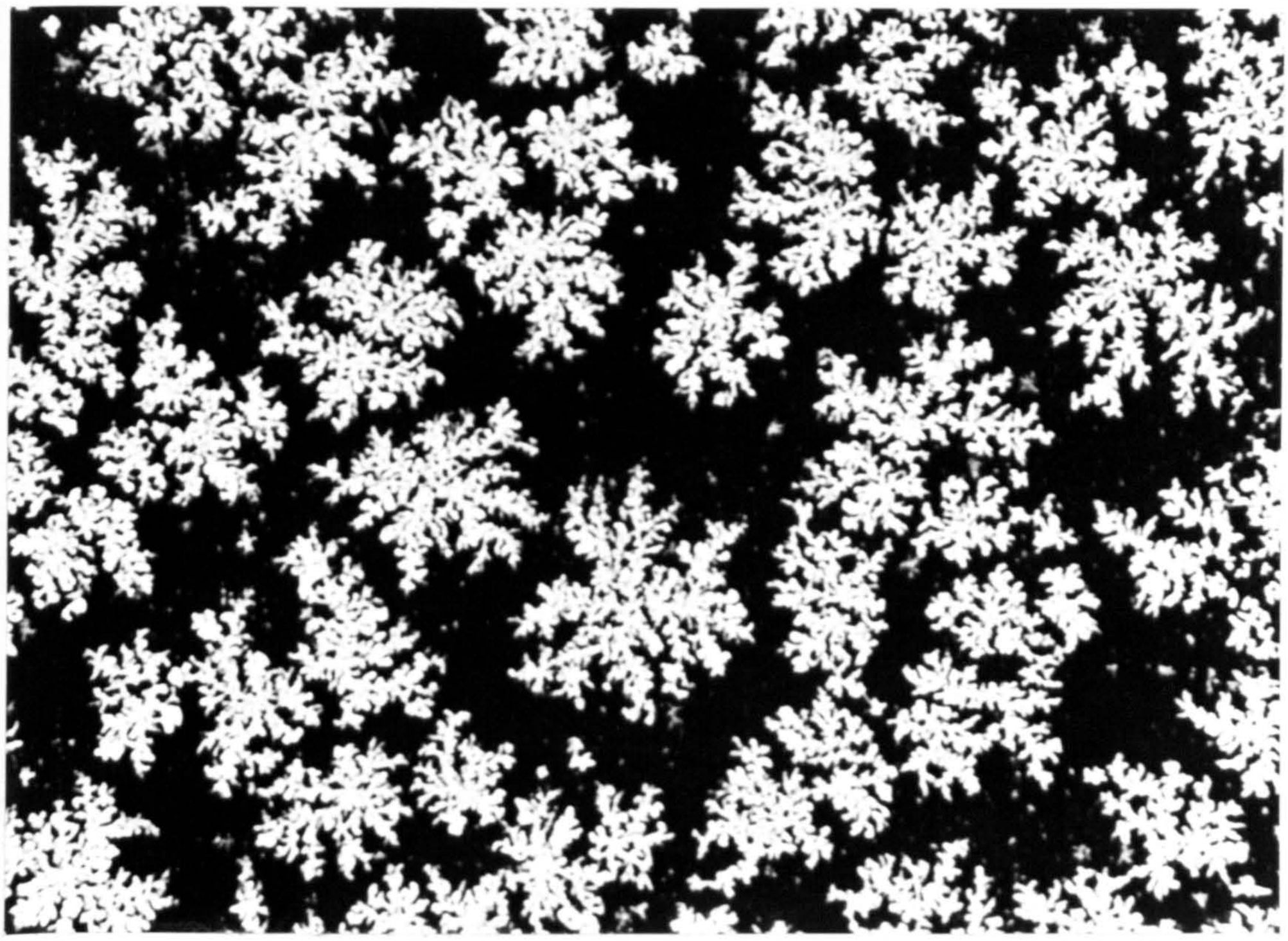

Plate 27. Surface morphology of silver/P(VF_2/VF_3) 60-40 copolymer film for 250 mC of charge, deposited at -0.3 V from 3% wt./vol. $AgNO_3$, showing 2D-diffusion limited type growth.

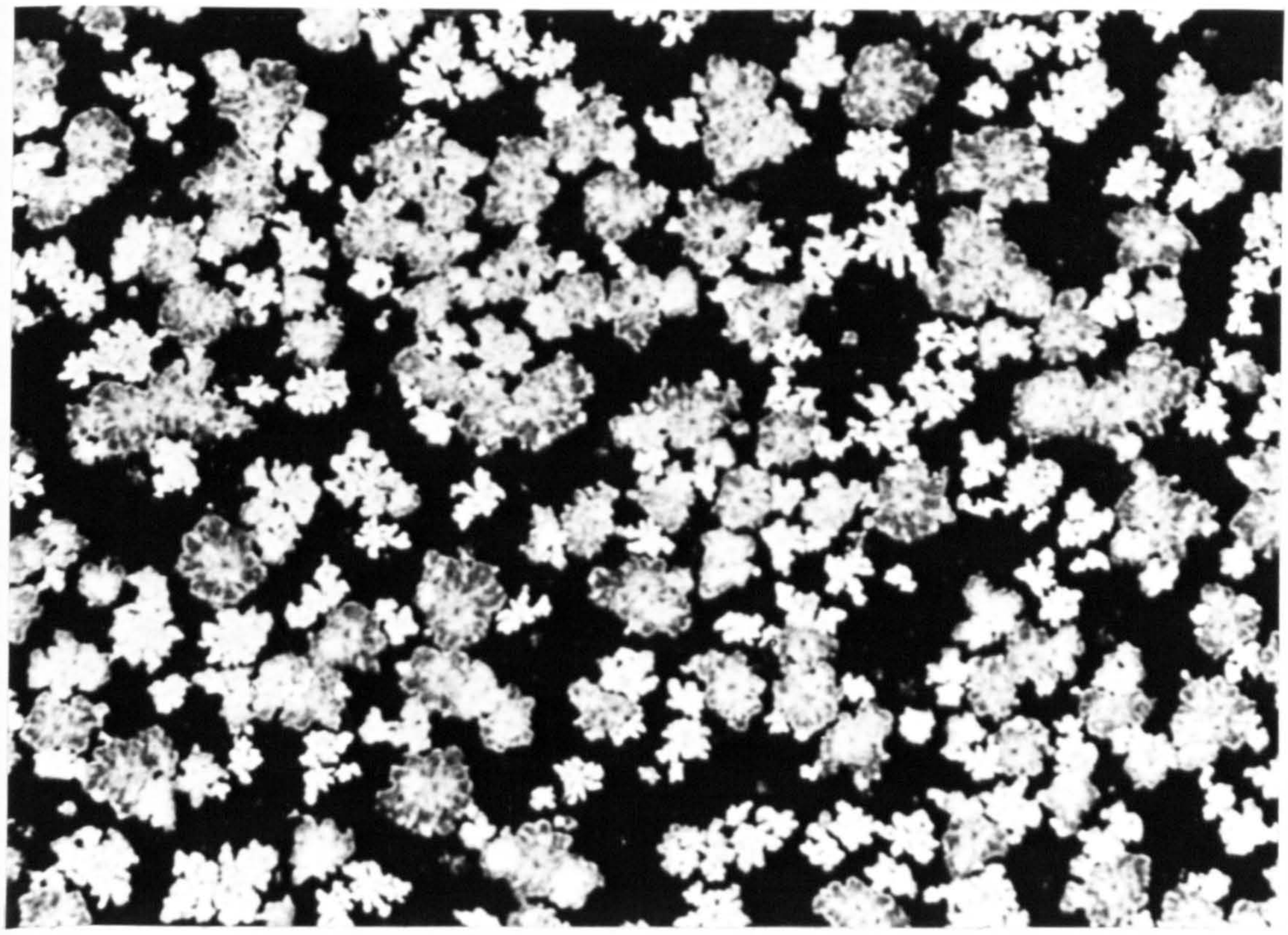

Plate 28. Surface morphology of silver/P(VF_2/VF_3) 60-40 copolymer film for 250 mC of charge, deposited at -0.6 V from 3% wt./vol. $AgNO_3$.

stable to decomposition for the above conditions of deposition. Agitation at the electrode surface would, presumably, be inhibited by the presence of the film. Electrostatic interactions can not be totally disregarded, however, it seems highly unlikely that charged ad-ions of silver would exist at -0.6 V, but not at -0.3 V.

Another possible explanation which has not received attention in the literature, are the effects of adsorption, either by solvent molecules, impurities which are present in solution, or the accompanying anion of the silver salt. This is a plausible explanation for the change of morphology, since it is known that even small amounts of foreign material can drastically alter the pattern of growth, and this is the basis for the addition of levellers and brighteners to plating solutions.

8.5.2 Computer Simulation of Growth from $AgNO_3$ Solution at -0.3 V.

The nature of the growth process from silver nitrate solution at -0.3 V was simulated using a custom written program, based on two-dimensional diffusion limited aggregation to growth centres[236].

The program allows the input of the number of growth centres to which diffusion can occur, the initial concentration of particles undergoing diffusion, and the random addition of further particles throughout diffusion. The addition of these extra particles was to simulate the conditions of diffusion of silver ions through the polymer film to the electrode surface during deposition. A typical simulation is shown in Fig. 67, for diffusion to three growth centres with a 10% initial surface coverage of particles, and with an additional 1.63 particles per cycle added at random positions on the lattice. The simulation was run for 5000 cycles, and it can be seen that there is excellent agreement with plate 27 for silver deposition at -0.3 V. This close resemblance between computer simulation and the initial stages of growth of silver at the polymer film/electrode interface, suggests that the mode of growth for the deposition at -0.3 V is by the random diffusion of adsorbed silver ions at the electrode surface. On this basis, it is proposed that depositing silver ions permeate the thickness of the polymer coat, become adsorbed at the electrode surface, followed by diffusion in the plane of the electrode until a favourable contact is made with a silver cluster where incorporation occurs.

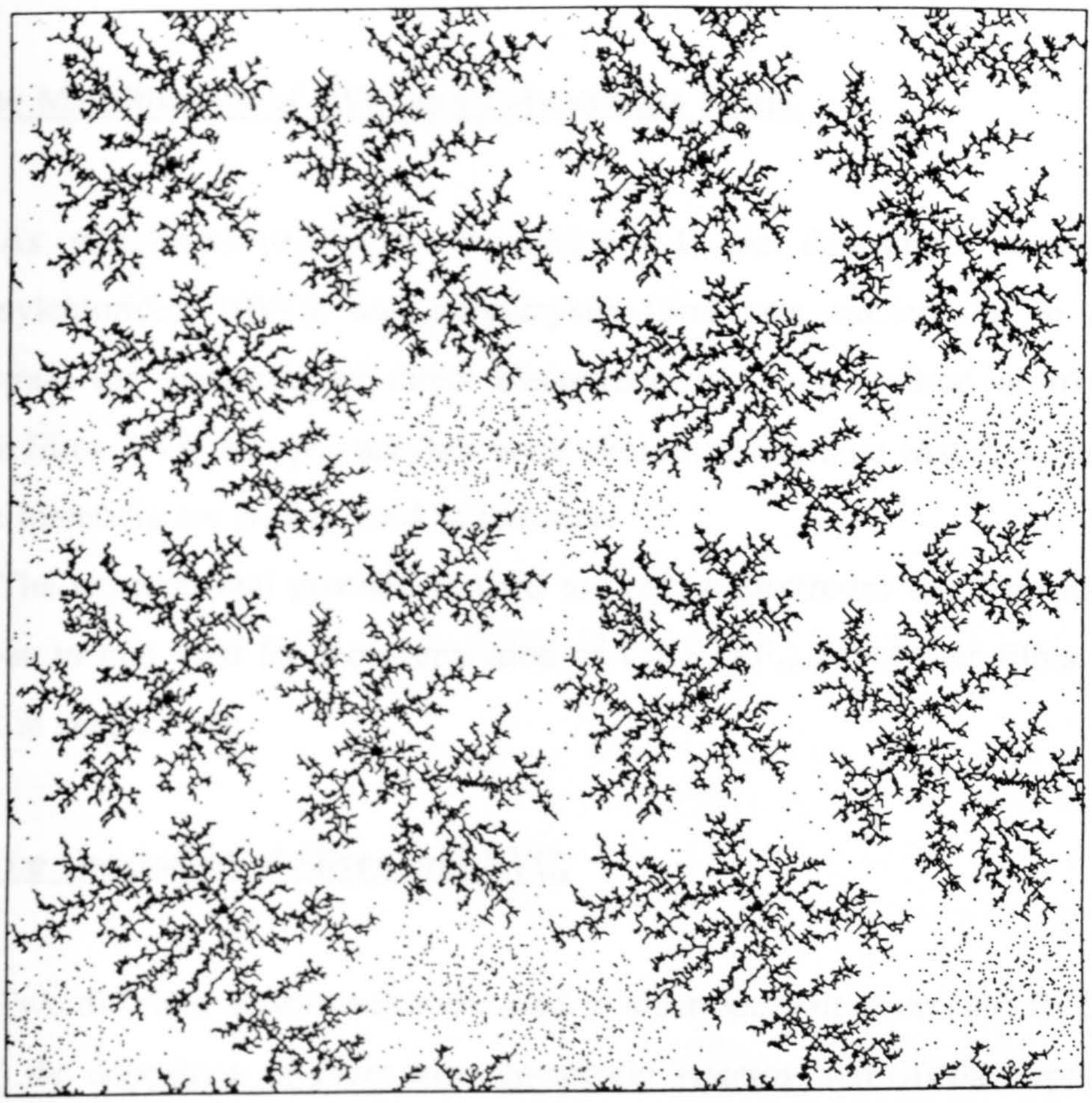

Fig. 67. Computer simulation of growth of silver from $AgNO_3$ at -0.3 V. Diffusion to three growth centres, with a 10% initial surface coverage of particles, with the random addition of 1.63 extra particles per cycle. After 5000 cycles.

8.6 The Metallization of PVC and Polyacrylate Films.

As mentioned previously in section 8.1, the deposition of silver into poly(vinylchloride), (PVC), and polyacrylate films was carried out in order to demonstrate the versatility of direct electroreduction as a method of metallizing polymer films. PVC and polyacrylate were chosen as substrate materials since both of these materials are widely used in industry.

The experimental procedures used to prepare electrodes for deposition were analogous to that used for the preparation of $P(VF_2/VF_3)$ copolymer films, and are detailed in section 3.6.

8.6.1 The Deposition of Silver into PVC.

Two different approaches were used to electrodeposit silver into PVC. These were, (i) the deposition of silver from co-solvent systems, and (ii) the deposition of silver into PVC blended with electrolyte. These methods proved necessary, since no single phase solvent/electrolyte combination was found that could swell PVC sufficiently to enable the deposition of silver films.

Co-solvent systems based on $AgNO_3$ dissolved in acetonitrile (CH_3CN), with tetrahydrofuran (THF), N,N'-dimethylacetamide (DMA) and N,N'-dimethylformamide (DMF) were investigated using the first approach. The co-solvent was chosen in order to swell the polymer substrate, thus increasing the permeability of the film to the silver nitrate electrolyte. Depositions were carried out on PVC films with thicknesses ranging from 31 to 47 μm, for deposition potentials between -0.5 to -1.1 V.

$AgClO_4$ and $TBABF_4$ were selected as electrolytes for blending into PVC, in experiments to determine the suitability of the second approach. This technique has previously been used to increase the rate of ingress of the electrolyte phase into polymer coated electrodes, with electropolymerization studies of polypyrrole[157].

8.6.1.1 Acetonitrile/Tetrahydrofuran Co-Solvent System.

Acetonitrile/tetrahydrofuran co-solvents with volume fractions of THF between 10 and 30% sufficiently swelled PVC to enable the rapid ingress of Ag^+. However, this combination of co-solvent and electrolyte yielded deposits that had poor adhesion to the PVC film and which rapidly tarnished on exposure to air. The results from depositions with this co-solvent system are listed in Table 18.

Table 18. PVC, $AgNO_3$/acetonitrile/tetrahydrofuran co-solvent system.

$AgNO_3$ (wt.%)	Potential V (*vs.* Ag ref.)	Solvent ratio (vol./vol.)	Comment code
2%	-0.60	90/10	G, Tsh
2%	-0.60	80/20	M, Tsh
2%	-0.60	70/30	E, Tsh

Comment code: M=matt deposit, G=good, semi-reflective deposit, Tsh=tarnish.

The incorporation of decomposition products of THF, or other impurities into the silver deposit was considered to be a likely cause of the tarnishing, since previous deposition studies with co-solvent systems based on acetonitrile and silver nitrate (see section 8.3.2) produced silver deposits that remained reflective. For this reason, attention was focused on the deposition of silver from co-solvent systems of acetonitrile containing DMA and DMF.

In order to effect the electroreduction of silver from co-solvents containing DMA and DMF, the deposition potential needed to be increased to more negative (cathodic) values. This is because DMA and DMF both complex more strongly to Ag^+ than acetonitrile. Deposition results from both these systems are given in Tables 19-21, and are described in section 8.6.1.2.

8.6.1.2 Depositions From Acetonitrile/Dimethylacetamide and Acetonitrile/Dimethylformamide Co-Solvent Systems.

Results for depositions with $AgNO_3$/acetonitrile/dimethylacetamide co-solvent system are listed in table 19.

Table 19. PVC, $AgNO_3$/acetonitrile/dimethylacetamide (90/10 vol./vol.) co-solvent system.

$AgNO_3$ (wt.%)	Potential V (*vs.* Ag ref.)	Solvent ratio (vol./vol.)	Comment code
2%	-0.50	90/10	N
2%	-0.60	90/10	M, T
2%	-0.75	90/10	M, T

Comment code: N=no deposit, M=matt deposit, T=thin deposit

The permeability of PVC to Ag^+ in CH_3CN/DMA and CH_3CN/DMF co-solvents was low, as evidenced by the low current densities (0.1 to 0.7 $mAcm^{-2}$), and long deposition times that were required to pass 5 C of charge (25 to > 60 minutes). Moreover, when the films were removed from the electrode surface and viewed under back illumination from a 1000 W tungsten lamp, the filament was still visible through the thickness of the coated films. This indicated that the silver coats were at most a few hundred Angstroms thick. If it is assumed that electrodeposition proceeds with 100% current efficiency, the thickness of the silver deposit should be ~1 μm thick. Thus, the thinness of the silver layer implies that a substantial fraction of the charge passed during deposition was consumed by other electrode processes. However, comparisons with other literature values for the cathodic current efficiency of the deposition of silver from organic plating solutions was not possible, due to the lack research that has been conducted in this area.

Table 20. PVC, $AgNO_3$/acetonitrile/dimethylformamide (90/10 vol./vol.)

$AgNO_3$ (wt.%)	Potential V *vs.* Ag ref.	Duration (S)	Charge passed (mC)	Film thickness (µm)	Comment code
3.0	-0.70	560	10168	18.5	G, T
3.0	-0.80	1635	5040	40.3	G, T
3.0	-0.90	4500	4370	42.3	P, T
3.0	-1.00	2100	10063	47.0	G, T

Table 21. PVC, $AgNO_3$/acetonitrile/dimethylformamide (80/20 vol./vol.)

$AgNO_3$ (wt.%)	Potential V *vs.* Ag ref.	Duration (S)	Charge passed (mC)	Film thickness (µm)	Comment code
3.0	-0.70	2930	5011	33.3	G, T
3.0	-0.80	1740	4993	30.6	G
3.0	-0.90	3750	5014	39.7	G
3.0	-1.00	1440	5032	41.3	M
3.0	-1.10	2140	5031	34.0	G, B

Comment code: M=Matt, T=Thin, B=Burnt, P=Poor, G=Good

Values for the weight of silver deposited by electrodeposition were not listed in Tables 19-21, since a net weight decrease was obtained with all depositions from acetonitrile/N,N'-dimethylacetamide and acetonitrile/N,N'-dimethylformamide co-solvents. This was attributed to the dissolution of PVC in both these co-solvents, since a similar weight loss (~1%) was also observed in a separate gravimetric study with PVC coated electrodes immersed with these co-solvent systems.

Deposition times for acetonitrile plating solutions containing 20% DMF and 3% wt. $AgNO_3$, were approximately 30 to 50% less than that for depositions from solutions containing 10% DMF and 2% $AgNO_3$. This reduction in plating time is considered to be due to the increased concentration of $AgNO_3$, and the greater permeability of the substrate towards Ag^+ at the higher concentrations of DMF[48]. However, it was not possible to reduce deposition times by further additions of $AgNO_3$ and DMF, due to excessive dendritic growth, and the fact that at increased concentrations of DMF, the PVC films tended to swell and detach from the electrode surface during deposition.

In general, depositions carried out in acetonitrile/dimethylacetamide (80/20 vol./vol.) produced the most highly reflective and coherent silver coats, with the best films being produced as the potential was increased through -0.7 to -1.0 V. Deposition at -1.1 V yielded deposits with a "burnt" appearance, caused by deposition under conditions of mass-transfer control[16,231].

8.6.1.3 Deposition of Silver into PVC Blended with Electrolyte.

The second approach that was used to metallize PVC, was the addition of electrolyte to the polymer solution. Analogous approaches have been utilized for the electropolymerization of pyrrole into PVC, and are reported to reduce deposition times and improve the uniformity of deposit[157,158]. The incorporation of ionic species into the film membrane serves two functions, firstly it reduces the ohmic resistance of the film, which is analogous in effect to increasing the electrode potential, and secondly, it aids the ingress of charged ions[157]. The advantage of this approach is that it permits the use of less complex (single-component) solvent systems for electrolysis.

Preliminary experiments were carried out with PVC substrates blended with ~0.5% wt. of (i) $AgClO_4$ and (ii) $TBABF_4$. $AgClO_4$ was chosen for its increased solubility in THF/PVC solution compared to $AgNO_3$, and was also chosen as the electrolyte, in order to reduce the number of deposition parameters.

PVC films containing both $AgClO_4$ or $TBABF_4$ were permeable to $AgClO_4$ dissolved in acetonitrile, as demonstrated by the instantaneous current (~1 to 2 $mAcm^{-2}$) that was obtained during deposition. In contrast, current densities obtained with the same electrolyte solution, for PVC films without added electrolyte were typically less than 0.02 $mAcm^{-2}$.

In spite of the increased current densities that were obtained by blending PVC with electrolyte, neither $AgClO_4$ nor $TBABF_4$ doped films produced silver deposits that were as continuous or reflective as those obtained using undoped PVC and co-solvent systems. One problem encountered using "doped" films, was that of poor adhesion of the film to the electrode surface during deposition. In the most extreme examples, films became detached, and deposition was effected at the electrode surface rather than in the matrix of the polymer film. Furthermore, PVC films blended with $AgClO_4$ tended to turn white in appearance on the addition of the electrolyte solution, possibly caused by leaching of $AgClO_4$ from the film into the bulk electrolyte. In view of these problems, attention was focused on the development of co-solvent systems from which to deposit silver.

8.6.2 The Deposition of Silver into Polyacrylate.

Initial deposition studies with polyacrylate were carried out on preformed films, with thicknesses of ~50 μm. The electrolyte solution was 1% wt. $AgClO_4$ dissolved in a methanol/1-2 dichloroethane co-solvent, with volume fractions of 1-2 dichloroethane between 4 and 10%. $AgClO_4$ was chosen for its solubility in methanol.

Preformed polyacrylate proved unsuitable as a substrate material, due to its low permeability to Ag^+ in the electrolyte solution. However, increasing the volume

fraction of 1-2 dichloroethane in excess of 0.1 resulted in excessive swelling and degradation of the film substrate, and did not aid deposition. In order to overcome the problems of the low permeability of preformed films, depositions were carried out on solution cast films with reduced thicknesses, ranging from 20 to 35 μm. However, these were degraded by the co-solvent at volume fractions of 1-2 dichloroethane in excess of only 4%. This decreased resistance of solution cast films to degradation by solvent, has been attributed to a decrease in crystallinity of solvent cast films compared to preformed films[48].

Depositions from the methanol/1-2 dichloroethane/silver perchlorate co-solvent system proved unsuccessful, even for high concentrations of 1-2 dichloroethane, in which polyacrylate was highly swelled. This failure to deposit silver was considered to be due to the low solubility of $AgClO_4$ in 1-2 dichloroethane (see Table 8). It is therefore apparent, that a film which is highly swelled by solvent is not a sufficient criterion to ensure deposition. In addition, the film must also be permeable to the electrolyte. This is only achieved if the metal salt is also soluble in the component of the co-solvent which is used to swell the film, as demonstrated by the above experiments. Thus, the solubility of the metal salt in the co-solvent which is used to swell the film is an additional factor which needs to be considered when determining the choice of co-solvent combination.

Having established these criteria, further depositions were carried out in methanol/acetonitrile co-solvent systems using $AgNO_3$ as electrolyte. This was considered to be the optimum combination, since $AgNO_3$ had already been proven to be highly soluble in acetonitrile, and furthermore, solution cast polyacrylate films proved stable to methanol/acetonitrile co-solvents with volume fractions of acetonitrile up to 20%.

Table 22. Polyacrylate, $AgNO_3$/methanol/acetonitrile co-solvent system.

$AgNO_3$ (wt.%)	Potential V (*vs.* Ag ref.)	Solvent ratio (vol./vol.)	Comment code
2%	-0.35	80/20[a]	G, T
2%	-0.40	80/20[a]	E
2%	-0.50	80/20[a]	E
2%	-0.60	80/20[a]	M
2%	-0.40	90/10[b]	N, B
2%	-0.50	90/10[b]	N, B
2%	-0.60	90/10[b]	P, B
2%	-0.40	90/10[c]	E
2%	-0.50	90/10[c]	E

Key: a=left to stand 10 minutes prior to commencing deposition, b=deposition commenced immediately, c=left to stand 20 minutes prior to deposition.

Comment code: N=no deposit, P=poor deposit, M=matt deposit, G=good, semi-reflective deposit, E=highly reflective deposit, T=thin deposit, B=burnt deposit

The deposition results in Table 22 show that the permeability of polyacrylate to silver nitrate was the crucial parameter in determining the nature of the silver deposit. Depositions that were commenced as soon as the electrode was immersed in electrolyte, yielded "burnt" deposits. These resembled those obtained for the deposition of silver into $P(VF_2/VF_3)$ copolymer, and PVC, when depositions were carried out in the limit of mass-transfer, at -0.7 V and -1.1 V respectively. This effect is considered to be due to the low permeability of the film to Ag^+, and was confirmed by the low current densities (< 0.02 $mAcm^{-2}$) that were obtained during deposition. In contrast, reflective and continuous silver deposits were obtained if the films were left to stand for ~20 minutes prior to commencing electrolysis. The increased permeability of the films to the electrolyte was demonstrated by an increase in the current density

(*ca.* 1 to 2 $mAcm^{-2}$) during deposition. Reflective and continuous silver deposits were also obtained in the potential range -0.35 to -0.6 V for co-solvent systems containing 20% vol. acetonitrile. In this case, the increase in permeability to Ag^+ is attributed to the increased volume fraction of DMF, which serves to increase the degree of swelling of the polyacrylate films.

8.6.3 Summary.

In summary, the versatility of direct electroreduction was demonstrated by the deposition of reflective and continuous metallic silver layers into PVC and polyacrylate films. Depositions carried out with both these films emphasised the importance of the permeability of the film substrate to the electroactive constituents in solution. Of the two different approaches that were used to electrodeposit silver, the use of co-solvent systems proved the superior to blending and yielded silver coats that were more reflective and uniform.

8.7 AC-Impedance Measurements of the Surface Roughness of Silver/P(VF_2/VF_3) 60-40 Copolymer Films.

Whilst optical microscopy is a useful method for studying the hidden (solution side) morphology of the silver deposit, it is limited by the time consuming process required for sample preparation. Moreover, it necessitates the destruction of part of the coated polymer film, and only reveals the morphology of a relatively small section of film. Ideally, the cross-sectional film morphology would be determined using a rapid and non-destructive technique.

This section describes the application of ac impedance as a method for determining the roughness of the hidden metal surface layer deposited into a polymer film. Apart from being non-destructive, it also enables the rapid determination of surface morphology over a much wider area than is possible with optical microscopy.

8.7.1 Theory of AC Impedance.

An electrochemical interface comprising an electrode in contact with an electrolyte solution may be represented by an equivalent circuit of resistors and capacitors, such as that illustrated in Fig. 68. The resistance $R_{(o)}$ represents the resistance of the electrolyte solution, and the capacitance (C) the double layer part of the impedance. The ac impedance of this circuit can then be described in complex number notation by the following Eqn 8.2,

$$Z(\omega) = Z'(\omega) + jZ''(\omega) \qquad (8.2)$$

where j is the complex number $\sqrt{-1}$, and w is the angular frequency. In the complex plane this equation has the form of a vertical line as shown in Fig. 68(b).

This description of the electrochemical interface holds well for a perfectly smooth homogeneous electrode surface, such as that produced by a liquid mercury electrode[237,239], and for electrode processes that are uncomplicated by faradaic processes or adsorption phenomena. These complications can be ignored in the present case, since measurements were carried out in inert electrolyte. However, the effect of a rough electrode surface-solution, such as that produced by silver with the above deposition conditions is to produce a non-ideal response[237-241]. In this case, the interfacial impedance has been found to vary with the frequency of the applied signal (w) according to:

$$Z^{-1} = A\,(j\omega)^{\alpha} \qquad (8.3)$$

Where A is a frequency independent real variable, and the exponent α is fractional and has a value between 1/2 and 1 for an ideally polarisable (blocking) electrode[237,238].

The equivalent electric circuit which represents this "non-ideal" behaviour is shown in Fig. 68(c). Here a frequency dependent element, referred to as a constant phase element, is substituted for the purely capacitive element. The effect of the

response in the complex plane is a clockwise rotation through an angle ϕ about the point ($R_{(\Omega)}$,0). This shift is termed the constant phase angle (CPA)[237-239].

CPA behaviour has recently been interpreted in terms of the fractal geometry of solid electrode surfaces. In particular, Nyikos and Pajkossy[237,238] have shown that the fractional exponent generated by a rough electrode surface is directly related to the Hausdorff (fractal) dimension D[242] , as:

$$\alpha = \frac{1}{(D-1)} \qquad (8.4)$$

α thus being a measure of the surface irregularity. When α is equal to 1/2, D = 2, and purely capacitive behaviour is observed, whereas when α is equal to 1, D = 3, which is a result previously deduced for the limiting case of a porous electrode[241].

Thus the magnitude of constant phase angle should enable the degree of surface roughness of the silver layer in the polymer film to be determined.

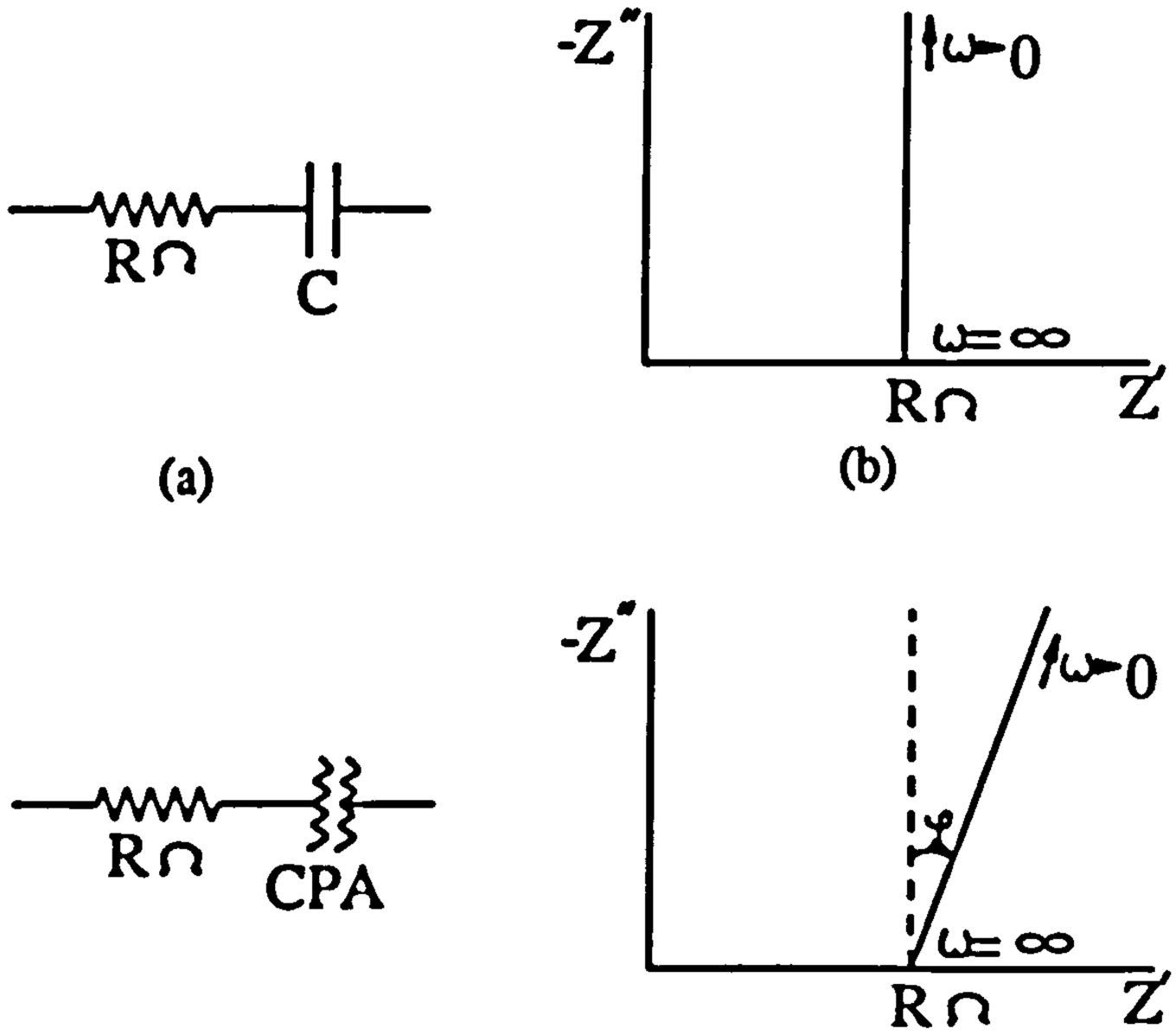

Fig. 68. (a) Equivalent circuit for a smooth electrode in contact with an electrolyte solution in the absence of a faradaic process. (b) Impedance plot corresponding to the circuit of Fig. 68(a). (c) Equivalent circuit representation of a rough solid electrode in contact with an electrolyte solution in the absence of a faradaic process. (d) Impedance plot corresponding to the circuit of Fig. 68(c) showing characteristic CPA behaviour.

8.7.2 Measurements of the Surface Roughness of Silver/P(VF_2/VF_3) 60-40 Copolymer Films.

The wide variety of cross-sectional morphology exhibited by silver/P(VF_2/VF_3) 60-40 copolymer films under typical deposition conditions was discussed in section 8.3.2.3. This section describes the application of ac impedance measurements to determine the fractal dimension of silver/P(VF_2/VF_3) 60-40 copolymer films. Depositions were carried out at constant potential in the range -0.3 to -0.7 V (*vs.* SCE). The electrolyte was a 1% wt./vol. solution of silver nitrate dissolved in methanol/acetonitrile (90:10 vol./vol.).

Following deposition, cross-sections of composite films were characterized by optical microscopy, using the procedure which is detailed in section 3.8. Typical results are shown in Plates 29(a-d). The compactness of the silver deposit obtained during deposition, coupled with the limits of resolution of optical microscopy precludes a quantitative analysis of the fractal dimension of the silver from micrographs.

Ac impedance measurements at an electrode/silver/polymer interface were performed according to the method described in section 3.7.1. The data corresponding to the four films shown in Plates 29(a-d) are shown in Figs. 69(a-d) in the form of complex plane impedance plots, i.e. a plot of Z'' versus Z' as a function of frequency, where Z'' and Z' are the imaginary and real impedances, respectively. The relationship between Z' and Z'' and the total impedance Z is given in Eqn. 8.3.

All the figures show a straight line inclined from the vertical axis as predicted by Eqn. 8.3. Imaginary impedance versus frequency data, from Figs. 69(a-d) were transformed into the form $\log(Z'')$ and $\log(\omega)$ using a simple computer program.

(a)

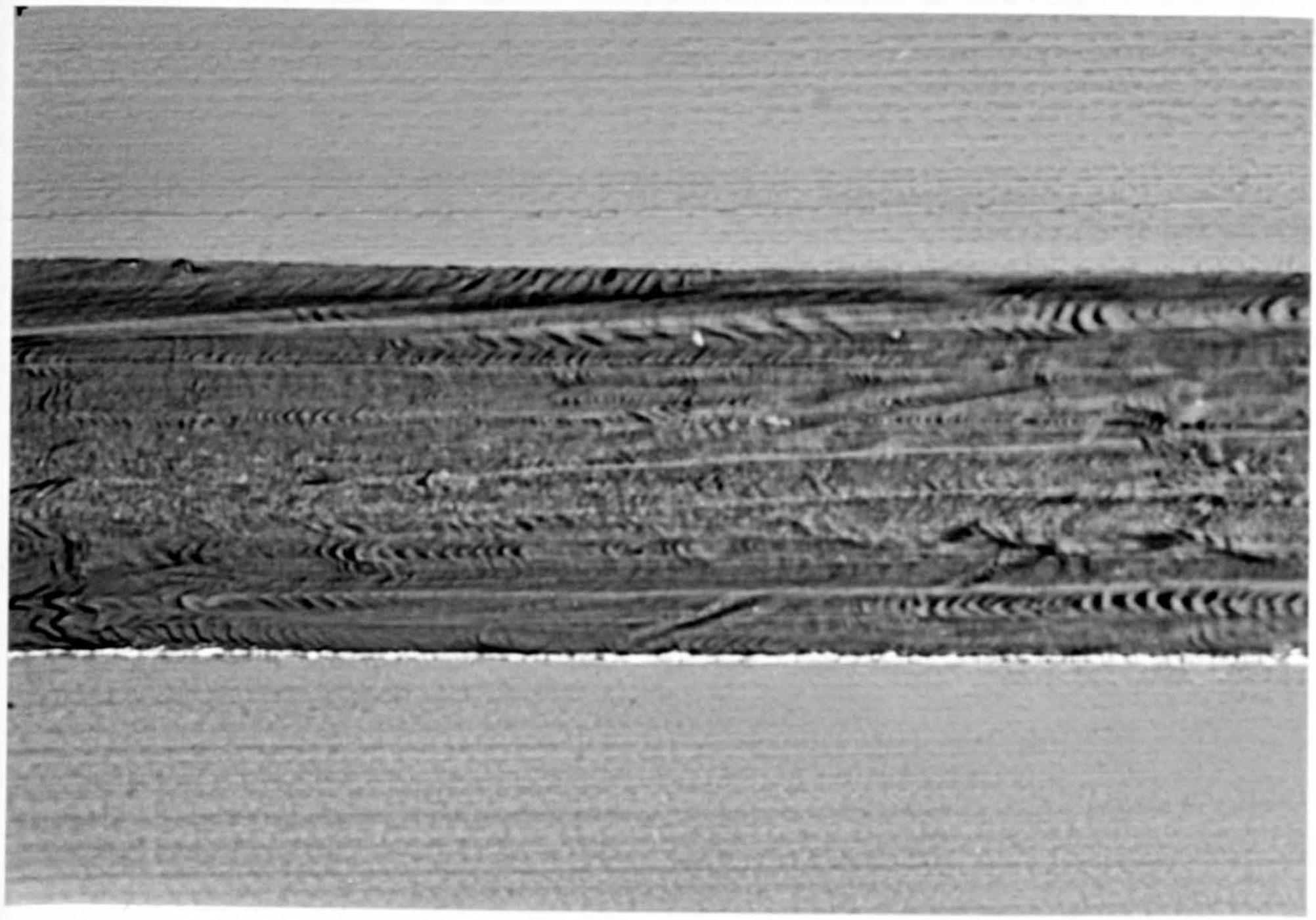

(b)

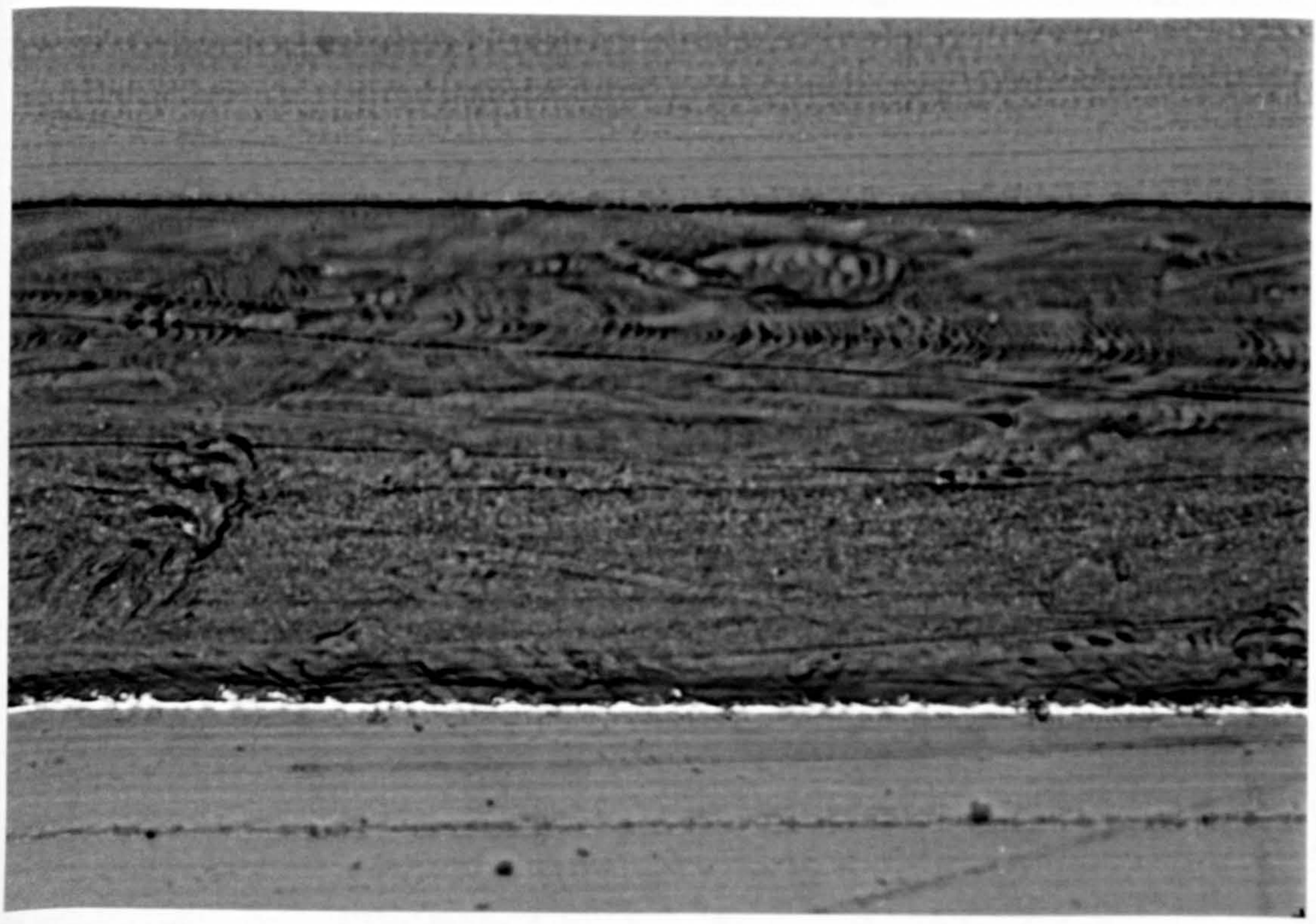

Plates 29(a-b). Cross-sections of silver/P(VF_2/VF_3) 60-40 copolymer film deposited at (a) -0.50 V, (b) 0.60 V (*vs.* SCE), with the passage of various amounts of charge. The fractal dimensions deduced from ac impedance measurements were (a) 2.14, (b) 2.22.

(c)

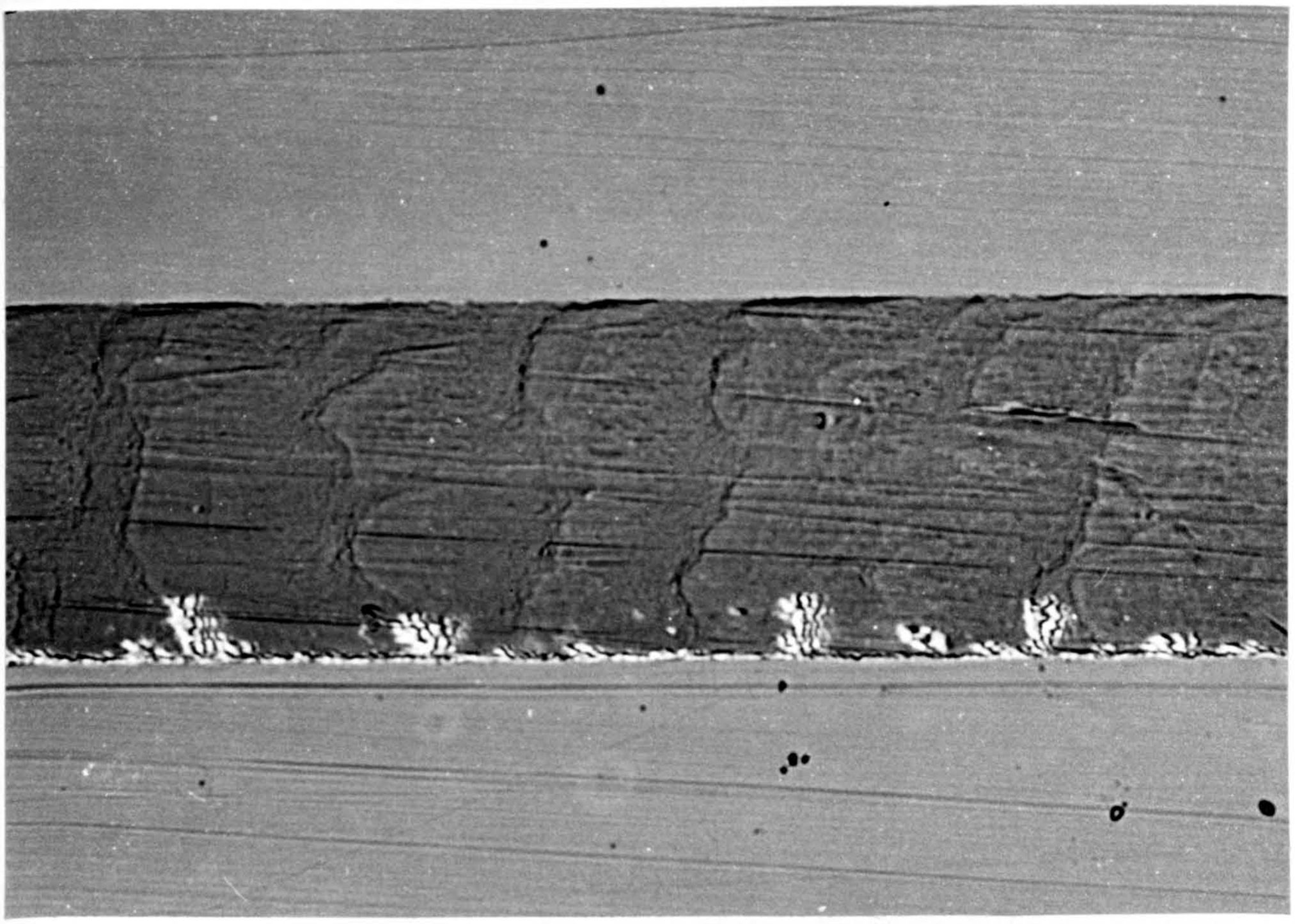

(a)

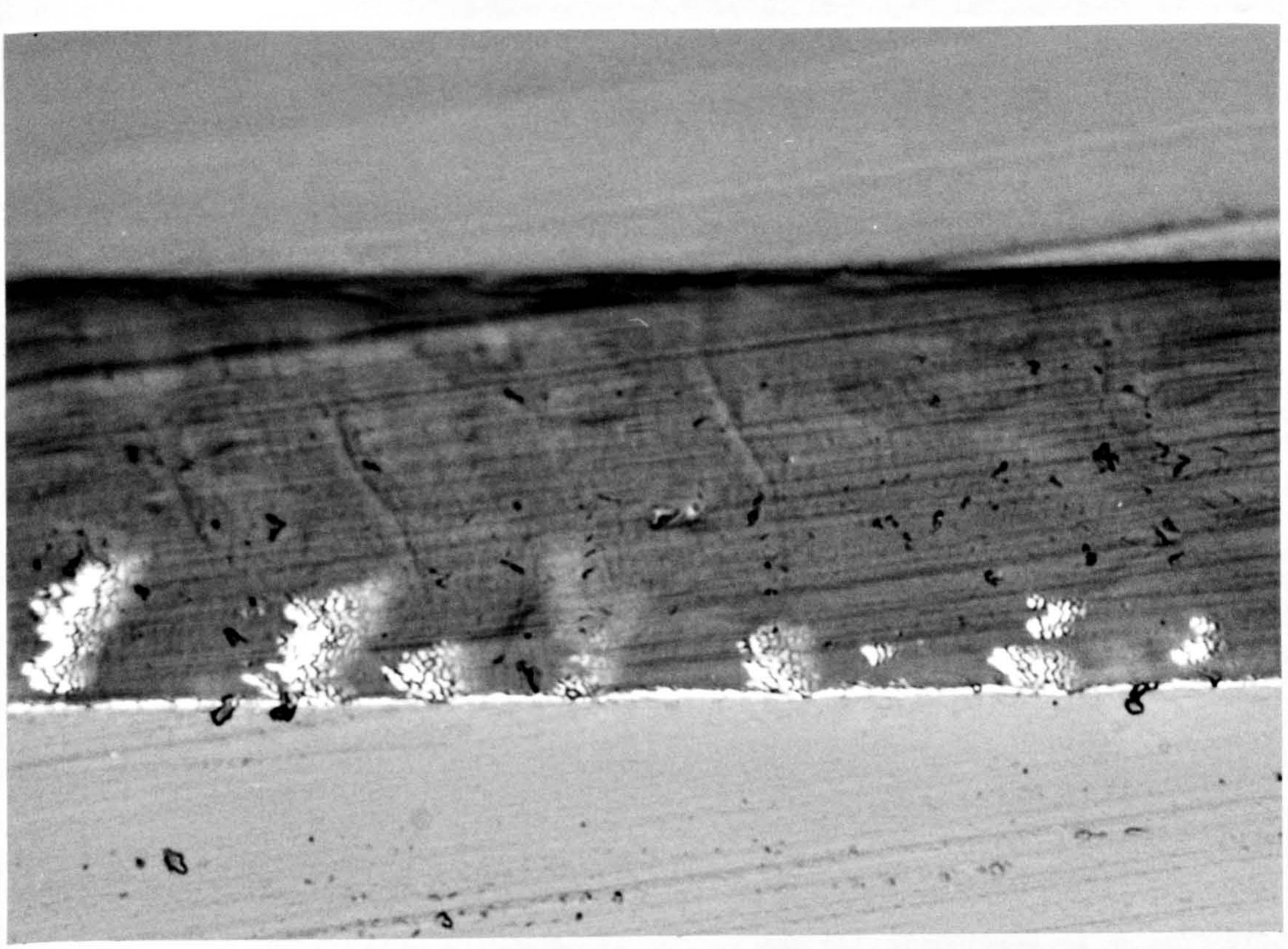

Plates 29. Cross-sections of silver/P(VF_2/VF_3) 60-40 copolymer film deposited at (c) -0.60 V, (d)-0.60 V (*vs.* SCE) with the passage of various amounts of charge. The fractal dimensions deduced from ac impedance measurements were (c) 2.35, (d) 2.39.

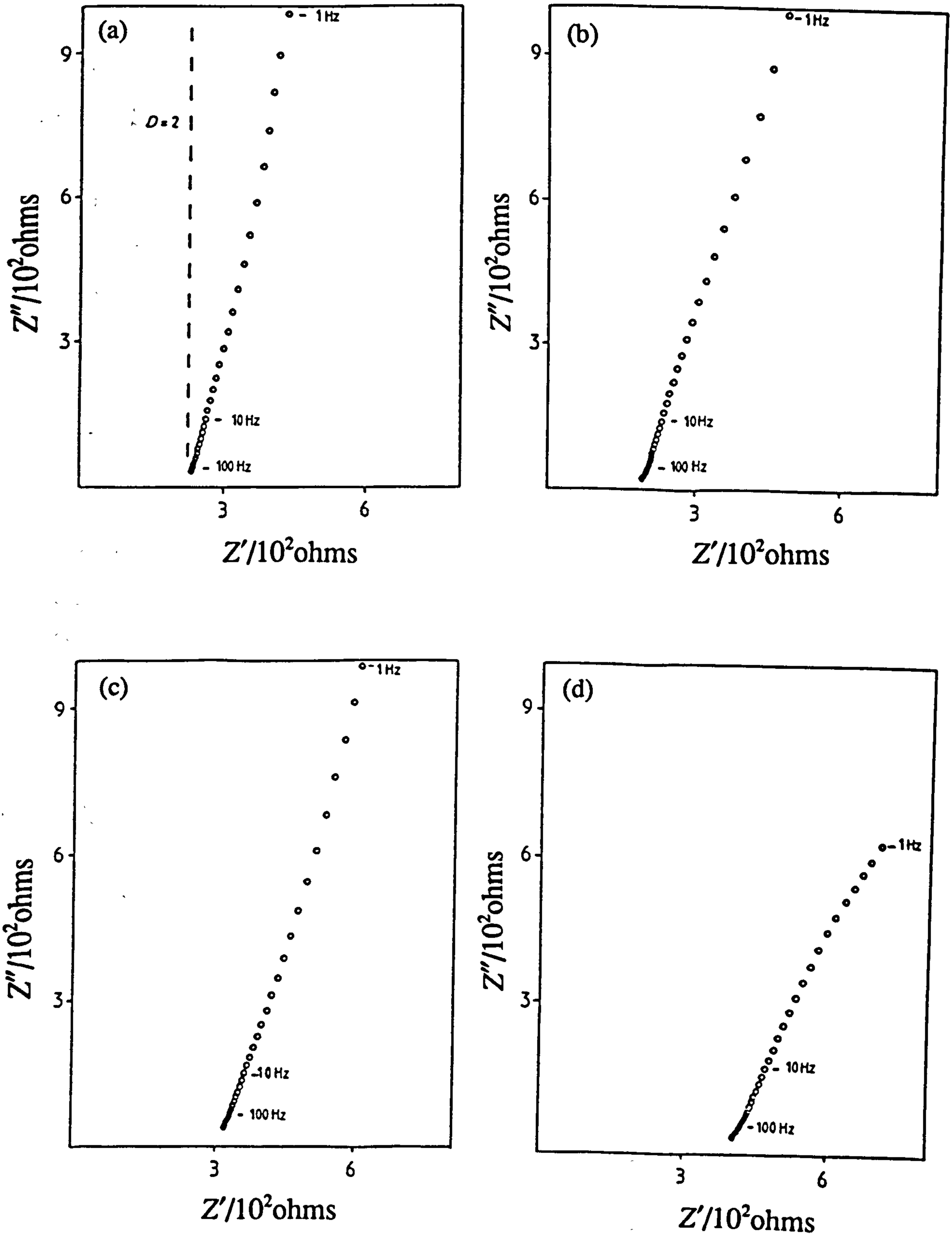

Fig. 69. Complex-plane impedance plots of a stainless steel electrode coated with polymer/silver films shown in Plates 29(a-d). Measured at a dc potential of 0.0 V *vs.* a SCE.

The fractal dimension (D) was then determined by plotting log(Z″) against log(ω). In this way the fractal dimensions shown in Figs. 69(a-d) were deduced as being 2.14, 2.22, 2.35, and 2.39 respectively. It can be seen that these values qualitatively correlate with the roughness observable in the plates. Ac impedance analysis of silver/P(VF_2/VF_3) 60-40 copolymer films can thus provide a quantitative measure of the fractal dimension of the metal surface and also offers a suitable non-destructive method for the examination of the surface geometry of metal layers grown within a polymer film.

8.8 Reflectance Measurements.

As was described in section 8.3.2.1, the observed reflectance of metallized films was used as a measure of film quality. Although somewhat crude, this method was deemed sufficient to enable an approximate classification of deposits into one of four categories. However, a more quantitative assessment of deposit quality was also determined using the apparatus which was detailed in section 3.16.

The results in Table 23 are of a silvered film deposited from an acetonitrile/methanol/$AgNO_3$ co-solvent system, and typical of that obtained in region A of Fig. 64. These give an average reflectivity of 94 ± 3%.

Table 23. Reflectance measurements.

Incident Power (I/W)	Reflected Power (I/W)
2.6	2.2
2.6	2.3
2.6	2.6
2.6	2.5
2.6	2.6
2.6	2.4

This high value of reflectivity is comparable to that obtained with bulk silver (94%), and is consistent with micrographs of cross-sections of silver coated films which reveal uniform and compact silver deposits (see Plate. 24). Moreover, the reflectivity of these films is significantly higher than that obtained using other methods of deposition (see Table 24), with the exception of polyimide film which was annealed at 400°C (95%)[49]. However, the high temperatures required to sinter polyimide films in order to obtain this degree of reflectivity, mean that the sintering process is only applicable to a few polymers. For this reason, the direct electrodeposition of silver is considered superior to polymer mediated deposition for obtaining highly reflecting silver coats.

Table 24. Comparison of silver coated films produced by alternative methods.

Deposition method	Polymer	Reflectivity (%)	Conductivity (Scm^{-1})	Ref.
Bulk silver	-------	94	$6.8x10^5$	243
Counter current diffusion of $AgBF_4/NaBF_4$ in acetonitrile.	ODA/PMDA* polyimide	*ca.* 30	$5x10^3$	47
Polymer-mediated electro-deposition, $AgBF_4$ in DMF.	ODA/PMDA* polyimide	6-36	10^2-$1.8x10^3$	48
Electrodeposition, $AgNO_3$ in CH_3CN/MeOH.	$P(VF_2/VF_3)$ copolymer	96	--------	This thesis

* ODA/PMDA, 4,4'-oxydianiline, pyromellitic dianhydride

8.9 Comparison of Direct Electrochemical Deposition with other Techniques of Metallizing Polymer Films.

As previously described in section 1.5, a number of alterative approaches to traditional tin/palladium based electroless procedures have been recently developed for the metallization of plastic films. These recent developments include the deposition of metals by both electrochemical and chemical techniques, and may be divided into the following categories; (i) electroless (counter-current) deposition, (ii) polymer-mediated electrodeposition, (iii) the doping of neutral polymer films with metal salts followed by chemical reduction, (iv) polymer-mediated chemical deposition, (v) carrier-mediated electrodeposition, and (vi) direct electrochemical deposition.

This section compares the direct electrochemical deposition of metals into polymer films, with each of the different approaches (i) to (vi) which are listed above.

Several criteria may be identified as requirements of any chemical or electrochemical technique which is used to deposit metal films either into, or onto polymer films. These can be listed as follows; (i) the technique should be rapid and simple to perform, (ii) versatile with respect to the combinations of polymer film substrate and metals that can be used, and (iii) comparable in cost to other methods of metallizing polymer films, such as vacuum deposition techniques. Depending on the envisaged application, the metal layer should also be continuous and reflective, and possess good adhesion to the substrate.

8.9.1 Electrochemical Methods of Deposition.

The direct electrochemical deposition of silver into polymer films is closely analogous to the procedure employed by Kuwana *et al*[43-45] to deposit palladium, silver, nickel, and cadmium onto polymer coated graphite substrates. However, a direct comparison of the resultant metal coated films is not valid, since the purpose of the experiments described by Kuwana was to study the catalytic activity of metal deposits towards the generation of hydrogen and the reduction of oxygen from aqueous

solution. Consequently, the choice of polymer film substrate and the nature of the metal deposit were adapted to suit this application, rather than to the preparation of reflective metal layers. Nevertheless, some general comparisons can be made.

The most significant difference between the systems described by Kuwana and those described in this thesis, was that the system employed by Kuwana was based on aqueous electrochemistry. This necessarily limits further application (if the method was adapted to the deposition of metal films) to polymer substrates which can be substantially swelled by water (hydrogels). Thus, these materials are expected to be unsuitable for use in anhydrous environments, and as a consequence, are likely to be restricted to few applications.

The procedures described by Kuwana[43-45] for the preparation of polymer coated substrates, were both complex and time consuming (> 16 hours). Furthermore, the thickness and reproducibility of the polymer coat was difficult to control, and was limited to the preparation of thin films (0.04 to 0.1 μm thick). In contrast, the droplet evaporation methods used to coat electrode substrates in this thesis was rapid and capable of preparing uniform polymer films, (5 to 50 μm) thick.

Depositions from the aqueous electrolytes employed by Kuwana[43-45] yielded only dispersions of metallic micro-particles (~0.1 μm diameter), even at high surface coverages of metal, where some degree of coalescence might be expected. From examination of the micrographs contained in the above references[43-45], it is considered likely that this type of morphology was due to the fact that "simple" (additive free) electrolyte metal plating solutions were used. In the case of silver, deposition from aqueous conditions without additives is known to produce isolated irregularly shaped deposits[233]. In contrast, continuous, highly reflective silver layers were deposited from co-solvent systems without the use of special additives.

It is therefore considered that the electrodeposition of metals using non-aqueous co-solvent systems and hydrophobic polymers is superior to analogous methods utilizing aqueous electrochemistry. Indeed, aqueous based systems would need to be substantially modified to produce continuous metallic films in free standing polymers.

Other methods of depositing metal films that are closely related to direct electrochemical deposition, are polymer-mediated electrodeposition (PMED), and carrier-mediated electrodeposition (CMED). The first of these methods requires that the polymer substrate is redox-active, and capable of transporting electrons from a cathode to metal ions in the polymer matrix. The second method relies on reduced electroactive solutes (organic molecules such as N,N'-ethylene-2-2, bipyridine[37] or quinones[48]) to effect metal reduction.

These methods have been utilized by several groups to effect the metallization of polymeric substrates[34,37,52]. However, comparison will primarily be focused on the techniques described by Mazur *et al*[52,244,245] and Levy *et al*[48], as these have demonstrated the preparation of reflective metal layers in polyimide, which is of commercial interest, and also in a variety of other common polymer matrices (PVC, PVDF and cellulose). The systems described by Pickup *et al*[37] and Wrighton *et al*[34,35] are essentially of scientific interest only, being limited to the preparation of specialized redox polymers with thicknesses of the order of 0.1 μm.

As previously stated in section 1.5.2, PMED requires that the polymer film being plated is electroactive. Therefore, the choice of substrate material for which the technique of PMED is applicable, is restricted to relatively few materials in comparison to direct electroreduction.

Silver layers produced by polymer-mediated electrodeposition may be deposited at the electrode surface/polymer film interface, or as interlayers within the matrix of polymer films. When metal is deposited at the polymer film/electrode interface, the method of metal deposition is analogous to direct metal deposition, and is governed by the same experimental parameters, namely the magnitude of diffusion coefficients, and the electrode potential. When metal is deposited as an interlayer, the rate of deposition is also governed by the diffusion coefficient of electrons (D_e) through the polymer, via the redox couple of the polymer film[37]. For ODA/PMDA polyimide, the value of D_e is substantially less than the permeability of typical metal ions[48]. This limits the maximum current density which can be employed in PMED, and as a consequence, increases the duration required for deposition.

Deposition times required to produce "continuous" metallic films by PMED with polyimide polymer films are comparable to that required for direct electroreduction with P(VF_2/VF_3) 60-40 copolymer films. However, a comparison of the polymer substrate thicknesses, shows that the polyimide films used in other studies were less than 50% as thick as P(VF_2/VF_3) copolymer film used in this thesis. Moreover, depending on the choice of redox-active polymer, deposition times can be substantially longer, requiring up to 20 minutes to deposit a 0.025 μm thick layer of silver[37], compared to several hundred seconds to deposit silver coats with thickness of ~ 1 μm by the method used in this thesis.

Both polymer-mediated electrodeposition and carrier-mediated electrodeposition produced dispersions of micro-particles, with particle diameters of the order of 0.015 μm and an upper metallic density of ~72% by volume. Moreover, these metal interlayers can be diffuse, occupying in some instances up to 70% of the total film thickness[244]. In contrast, silver deposits produced by direct electroreduction under optimized deposition conditions, provide compact, adherent and homogeneous metal layers with thicknesses greater that 1 μm. Furthermore, the values of reflectivity that are reported for metallized polymer films are less than 35%, compared to a value of 96% that was obtained for silver coated P(VF_2/VF_3) copolymer films in this study.

8.9.2 Chemical Methods of Deposition.

Chemical methods which have been developed to metallize polymer films include; electroless counter-current deposition, polymer-mediated chemical deposition, and the doping of neutral polymer films with metal salts followed by chemical reduction. These are detailed in section 1.5.

Chemical methods of preparing metallized polymer films possess certain possible advantages over electrochemical methods, namely shorter reaction times, due to the fact that reactants need in some instances only contact the outer surfaces of the substrate being plated[53,246,247], and the benefit of not being restricted in size and shape by the requirement of electrodes to effect reduction.

The metallization of neutral polymer films by impregnation with dissolved metal salts or metal salt complexes, followed by exposure to reducing agents does not generally produce reflective metallic coats[246-248]. Hence, these methods will not be discussed in further detail. In contrast, the doping of electroactive polymer films (polyimides) with metal salts of silver[55], and/or palladium[56], has been shown to produce reflective metal coated polymers. Although the nature of the metal deposits produced by this technique varies, the fact that reflective deposits are obtained in some instances, suggests that the surfaces of the metallized polyimides have almost 100% surface coverage by metal, and are smooth on the scale of microns. However, there are few micrographs in the literature to confirm this.

The metallization of polyimides by exposure to reducing agents, followed by subsequent immersion in metal salt solutions that have redox potentials more positive than that of the reduced polyimide film also produces reflective metal coats (see Table 25). Some measure of the strength of the reducing agents that are needed to reduce polyimide (poly(4,4'-diaminodiphenylether pyromellitimide), ODA/PMDA) is given by the redox potentials of the polymer, which are -0.73 and -1.13 V (*vs.* SCE)[249]. However, exposure of polyimide to such strong reducing agents has been reported to cause cleavage of imide linkages[53], and results in a degradation of the polymer surface. This in turn reduces the homogeneity and uniformity of the metal coated surface. In fact, polyimide films that are metallized after treatment with Zintle anions (alloys of polyatomic main group elements, such as germanium, tin, lead, arsenic or antimony, with alkali or alkaline earth metals) have metallic surfaces that are microporous. The non-metallized regions in the surface coat are thought to arise from areas of degradation caused during the chemical reduction stage[53], and from the finite number of reducible sites in the polyimide polymer film. As a consequence, polymer substrates may require the chemical reduction and re-oxidation stages to be repeated several times in order to achieve an "all over" surface coverage of metal[54]. In contrast, direct electrodeposition allows the amount of metal deposited to be accurately controlled by coulometry.

Silver has also been deposited as an interlayer within a variety of polymer films by a process of electroless (counter-current) deposition (CCD)[48]. This involves

diffusing a metal salt into one surface of a film whilst simultaneously diffusing a reducing agent in to the opposite surface. This procedure has been previously described in section 1.5.1.

The times required to deposit metallic silver interlayers using this technique are of the order of 60 minutes for a 0.5 μm thick silver interlayer, in a 10 μm thick polyimide polymer film. This is significantly longer than that required in direct electroreduction, where, under suitable reaction conditions, continuous metal silver layers can be deposited in as short a time as a few hundred seconds (see Table 12). Moreover, the reflectivity of silver interlayers produced by CCD (~30%) is significantly less than that obtained by electroreduction. This is due to the fact that silver interlayers are not continuous, but are comprised of a distribution of silver crystals, with sizes of the order of 6 nm. Both these factors mean that CCD is unlikely to be used to metallize polymer films on a commercial basis.

From a consideration of the criteria that were listed in section 8.9, direct electrodeposition is considered superior to chemical methods of depositing metal coats, since it is rapid, and under optimized conditions, produces uniform and highly reflective metal coats.

8.10 Summary.

The direct electrodeposition of silver into hydrophobic polymer films was investigated for a variety of polymer film substrates using non-aqueous plating solutions. Several different electrode substrate materials, electrolyte/solvent, and polymer film solvent combinations were investigated for deposition potentials in the range -0.2 to -1.1 V (*vs.* Ag wire ref.), and with silver salt concentrations between 0.2 and 4% wt./vol.

The permeability of the polymer film to the electroactive constituents in solution was found to be vital for metal deposition, and necessitated the use of co-solvent systems from which to deposit silver. This option was found to be superior to an alternative method of blending the polymer film with electrolyte, and under optimum conditions (-0.3 to -0.6 V, and silver salt concentrations of up to 1% wt.)

yielded highly reflective and continuous metal deposits that were resistant to tarnishing, and which possessed good adhesion to the polymer film.

A comparison with other chemical and electrochemical methods of metallizing polymer films, shows that under optimum conditions, direct electroreduction from non-aqueous solvents produces metallized films which are more compact and which have a greater reflectivity.

9. Conclusions.

The conclusions of the investigation described in this thesis are as follows:

1. GC-PPy electrodes with coats of polypyrrole in the range 0.05-5 μm were sufficiently conductive to be used as substrates for the deposition of copper and silver from aqueous electrolytes. Highly reflective and cohesive copper layers were also deposited onto thicker sectioned (~20 μm) free-standing films of polypyrrole from aqueous copper sulphate plating solutions containing 3-mercaptopropane-1-sulphonic acid. This is the first report of the metallization of polypyrrole with reflective metal coats. Metal deposition was shown to occur mainly at the polypyrrole surface, by a mechanism of instantaneous nucleation and growth. The effect of the polypyrrole layer is to retard nucleation, however, in the case of copper, deposition was diffusion controlled at scan rates up to 70 mVs^{-1}.

2. Polypyrrole was demonstrated to be porous to electroactive species in solution, via the incorporation of O_2 and Cu^{2+} ions. This result is in consensus with recent opinion. The reduction and oxidation of GC-$PPy^{+}(SO_4^{2-})$ in $CuSO_4/H_2SO_4$ was demonstrated to involve a competitive process of cation insertion and anion expulsion. This is more complex than the currently accepted redox mechanism which describes the redox process in terms of a loss and regain of the counteranion only.

3. The electroactivity of polypyrrole in oxygenated base solution in the range 0.0 to -0.75 V (*vs.* SCE) is consistent with the formation of $PPy(-H)^{\circ}\cdots O_2$ or $PPy(-H)^{+}O_2^{-}$ and is not due to the PPy^{+}/PPy° redox couple as proposed by other workers. The loss of electroactivity of base treated polypyrrole in the potential range 0 to -0.75 V is due to the formation of $PPy(-H)^{\circ}$ and is not caused by significant disruption of π-conjugation as a result nucleophilic attack by OH^{-}. The electroactivity of base treated polypyrrole is almost completely restored by treatment with protic acids.

4. A novel process for metallizing polypyrrole was developed. Reflective metal coats of copper and silver were deposited onto base treated polypyrrole following immersion in solutions containing; acidified copper sulphate, copper sodium potassium tartrate at 40°C, or ammoniacal silver nitrate solution.

5. A novel method for metallizing non-electroactive polymer films, based on the electroreduction of Ag^{+} from non-aqueous co-solvent solutions was developed. The reflectivity of metallized films prepared under optimum conditions was 96%, which is comparable to that of bulk silver. This is significantly higher than that reported for other electrochemical or chemical techniques.

6. The permeability of the polymer film to the Ag^{+} was crucial to the deposition of reflective metal films, and necessitated the use of mixed-solvent systems. Co-solvent systems, based on acetonitrile were developed to plate silver into $P(VF_2/VF_3)$ 60-40 copolymer, PVC and polyacrylate films. The optimum deposition conditions for metallizing $P(VF_2/VF_3)$ 60-40 copolymer, was an acetonitrile/methanol co-solvent, with volume fractions of methanol in the range 2-18% vol., and with silver nitrate system or silver fluoroborate electrolyte dissolved at concentrations of up to 1% wt. The optimum deposition potential for preparing uniform and coherent metal deposits was in the range -0.3 to -0.6 V *vs.* a silver wire reference.

7. The choice of the working electrode substrate material was found to be critical for metal deposition. Only stainless steel substrates enabled the preparation of silver deposits that were uniform and which had good adhesion to the polymer film.

8. AC impedance analysis of metallized polymer films was demonstrated to be a suitable non-destructive method for the examination of the surface geometry of metal layers grown within a polymer film.

10. Future Work.

The work carried out in this thesis has demonstrated the successful metallization of conducting polymers, both in film form and impregnated into the surfaces of polymer substrates. Non-electroactive polymer films have also been metallized with silver. However, whilst the principles of metallization have been demonstrated, further work is recommended in order to achieve optimum deposition conditions, and to extend these techniques to additional polymer substrate/metal combinations. Potential applications of this technology should also be investigated.

10.1 Optimisation of Preparative Conditions.

The major area in which future work is required, is in the optimisation of preparative conditions for the impregnation of plastics with conducting polymer. This will facilitate the preparation of highly reflective and coherent metal deposits of optimum quality. Such improvements may be realised through a more comprehensive study of experimental parameters, such as reactant concentrations, impregnation temperature, and the choice of oxidant. This should permit the preparation of smooth conductive surface coats of conducting polymer without causing degradation to the plastic substrate material.

Further improvements in the quality of plating may also be achieved by the utilization of commercial plating solutions, since these contain additives to improve both the deposit morphology and visual appearance.

An alternative approach to the use of additives in controlling deposit morphology is the use of pulsed plating. This may be especially useful for the metallization of polymer films where the polymer matrix may restrict the diffusion of additives to the electrode surface.

The electroless deposition of copper from formaldehyde plating solutions was inhibited by a decrease in conductivity of polypyrrole, caused by deprotonation. It is considered that the use of an alternative hypophosphite electroless plating solution

which can operate at pH's in the range 4 to 7, may overcome this loss of conductivity and thus permit autocatalytic metal deposition to occur. This would enable the metallization of complex shaped objects which are not easily electroplated.

Although the studies in this thesis were concerned primarily with the deposition of copper and silver onto polypyrrole coated electrodes, and the deposition of silver into non-electroactive polymer films, unpublished preliminary work has also shown that polyaniline may be used as a substrate for the electrodeposition of copper and silver. This is considered to be advantageous for potential commercial applications, due to the lower cost of aniline compared to pyrrole, and hence, further studies of the metallization of polyaniline are recommended.

Preliminary studies have also demonstrated the metallization of P(VF_2/VF_3) 60-40 copolymer and PVC films with highly reflective and continuous copper layers. Such studies could be further extended to the deposition of other metal/polymer film combinations.

10.2 Applications of Metallized Substrates.

Future studies should also be extended to the investigation of potential applications of the techniques developed in this thesis. In particular, the ability to metallize polymer mouldings and coaxial cable composites has important benefits for the integration of electromagnetic screening into electronic assemblies, especially with future changes in legislation.

A suitable adaptation of the techniques described for the photoelectrochemical deposition of metals at semiconductor electrode surfaces[250,251], would enable the electrodeposition of metal patterns into polymer films. Possible applications of patterned films may include flexible conductive circuits, or use in lithography[39].

REFERENCES

1. S. Wein
Metallizing Non-Conductors, Finishing Publ., Inc., Westwood, USA, 1945

2. W. Goldie
Metallic Coating of Plastics, Vol. 1 and 2, Electrochemical Publications Ltd., England 1968, 1969.

3. H. Narcus
Metallizing of Plastics, Reinhold Publishing Corp., New York, 1960.

4. J. Christoph
Electroplating of Plastics: Handbook of Theory and Practice, Middlesex, Finishing Publications, 1977.

5. Plastics, Pt. 1, p. 12, 1938.

6. H. Narcus
Metalloberflache, Vol 17, p. 284, 1963.

7. E. B. Saubestre, C. J. Durney, J. Hajdu and E. Bastenbeck
Plating, Vol. 86, p. 112, 1964.

8. C. R. Holt and B. J. Jensen
Plastverarbeiter, Vol. 2, p.17, 1965.

9. J. McDermott
Plating of Plastics with Metals, New Jersey, Noyes Data Corporation, Chemical Technology Review 27, 1974.

10. K. Heymann, W. Riedel and G. Woldt
Galvanotechnik, Vol. 61, p. 221, 1970.

11. J. I Duffy (ed.)
Electroplating Technology: Recent Developments, New Jersey, Noyes Data Corporation, Chemical Technology Review 187, 1981.

12. Metallization of Polymers
ACS Symposium Series 440, (E. Sacher, J. J Pireaux, S. T. Kowalczyk, Eds.), Amer. Chem. Soc., Washington, DC, 1990.

13. G. C. Van Tilburg
Plating and Surf. Fin., Vol. 71, p. 78, 1984.

14. B. F. Walker
Plating, Vol. 37, p. 384 and 755, 1950.

15. K. Heyman, W. Riedel and G. Woldt
Prod Finish., Vol. 24, p. 20, 1971.

16. A. F. Lowenheim
Electroplating, American Electroplaters Society, McGraw-Hill, Inc., 1978.

17. J. Christoph
in Electroplating of Plastics: Handbook of Theory and Practice, Middlesex, Finishing Publications, Chapter 4, 1977.

18. A. F. Lowenheim
in Electroplating, American Electroplaters Society, McGraw-Hill Inc., Chapter 19, 1978.

19. J. Henry
Metal Finishing, Vol. 82, Pt. 1, p. 93, 1984.

20. A. Brenner and G. E. Riddell
Proc. AES, Vol. 33, p. 23, 1946.

21. A. Brenner and G. E. Riddell
Proc. AES, Vol. 34, p. 156, 1946.

22. J. Henry
Metal Finishing, Vol. 82, Pt. 3, p. 47, 1984.

23. G. Muller and D. W. Baudrand
in Plating on Plastics; a Practical Handbook, 2nd edn., Draper, Chapter 2, 1971.

24. T. Ogura, M. Malcomson and Q. Fernando
Langmuir, Vol. 6, p. 1709, 1990.

25. P. Bindra and J. Roldan
J. Appl. Electrochem., Vol. 17, p. 1254, 1987.

26. K. Nichimura, K. Machida and M. Enyo
J. Electroanal. Chem. Interfacial Electrochem., Vol. 251, p.103, 1988.

27. R. M Lukes
Plating, Vol. 51. p. 1066

28. Product Engineering, Vol. 19, p.81, 1966.

29. R. G. Wedel
Plating, Vol. 58, p. 225, 1971.

30. W. Poppe
J. Adhesion, Vol. 2, p. 114, 1970.

31. W. P. Innes
Electroplating and Metal Finishing, Vol. 22, No. 5, p. 29, 1969.

32. W. Saxer
Galvanotechnik, Vol. 75, Pt. 9, p. 1112, 1984.

33. R. S Potember, R. C. Hoffman, H. S. Hu, J. E. Cocchiaro, C. A. Viands, R. A. Murphy and T. H. Poehler
Polymer, Vol. 28, p. 574, 1987.

34. R. A. Simon, T. E. Mallouk, K. A. Daube and M. S. Wrighton
Inorg. Chem., Vol. 24, p. 3119, 1985.

35. J. A. Bruce, T. Murahashi and M. S. Wrighton
J. Phys. Chem., Vol. 86, p. 1552, 1982.

36. P. G. Pickup and R. W. Murray
J. Am. Chem. Soc., Vol. 105, p. 4510, 1983.

37. P. G. Pickup, K. M. Kuo and R. J. Murray
J. Electrochem. Soc., Vol. 130, p. 2205, 1983.

38. G. K. Chandler and D. Pletcher
J. Appl. Elect., Vol. 16, p. 62, 1986.

39. D. H. Craston, C. W. Lin and A. J. Bard
J. Electrochem. Soc., Vol. 135, p. 785, 1988.

40. F. Bedioui, M. Voisin, J. Devynck and C. Bied-Charreton
J. Electroanal. Chem., Vol. 297, p. 257, 1991.

41. G. Tourillon and F. Garnier
J. Phys. Chem. Vol. 88, p. 5281, 1984.

42. H. Y. Liu and F. C. Anson
J. Electroanal. Chem., Vol. 158, p. 181, 1983.

43. W. H. Kao and T. Kuwana
J. Am. Chem. Soc., Vol. 106, p. 473, 1984.

44. D. E. Weisshaar and T. Kuwana
J. Electroanal. Chem., Vol. 163, p. 395, 1984.

45. D. E. Bartak, B. Kazee, K. Shimazu and T. Kuwana
Anal. Chem., Vol. 53, p. 2756, 1986.

46. S. Holdcroft and B. L. Funt
J. Electroanal. Chem., Vol. 240, p. 89, 1988.

47. L. E. Manring
Polymer Communications, Vol. 28, p. 68, 1987.

48. M. Levy, L. E. Manring and S. Mazur
J. Electrochem. Soc., Vol. 135, p. 2479, 1988.

49. S. Reich, S. Mazur, P. Avakian and F. C. Wilson
J. Appl. Phys. Vol. 62, p. 287, 1987.

50. D. J. Harrison and M. S. Wrighton
J. Phys. Chem., Vol. 88, p. 3932, 1984.

51. J. A. Bruce, T. Murahashi and M. S. Wrighton
J. Phys. Chem. Vol. 86, p. 1552, 1982.

52. S. Mazur and S. Reich
J. Phys. Chem., Vol. 90, p. 1365, 1986.

53. R. C. Haushalter and J. J. Krause
Thin Solid Films, Vol. 102, p. 161, 1983.

54. A. Viehbeck, C. A. Kovac, S. L. Buchwalter, M. J. Goldberg and T. J. Watson
in Metallization of Polymers; ACS Symposium Series 440,
(E. Sacher, J. J Pireaux, S. T. Kowalczyk, Eds.), Amer. Chem. Soc.,
Washington, DC, Chapter 29, 1990.

55. A. Auerbach
J. Electrochem. Soc., Vol. 131, p. 937, 1984.

56. R. D. Macfarlane, D. Uemura, K. Ueda and Y. Hirata
J. Am. Chem. Soc., Vol. 102, Pt. 2, p. 876, 1980.

57. S. Asavapiriyanont, G. K. Chandler, G. A. Gunawardena and D. Pletcher
J. Electroanal. Chem., Vol. 177, p. 229, 1984.

58. D. D. Erickson, W. H. Smyrl and D. S. Ginley
J. Electrochem. Soc., Vol. 133, p. 1985, 1986.

59. A. Fontaine, E. Dartyge and G. Tourillon
Proc. of Am. Int. Conf., p. 403, 1984.

60. D. Guay, G. Tourillon and A. Fontaine
Faraday Discuss. Chem. Soc., Vol. 89, p. 41, 1990.

61. H. S. White, G. P. Kittlessen and M. S. Wrighton
J. Am. Chem. Soc., Vol. 106, p. 5375, 1984.

62. D. Fichou, G. Horowitz, Y. Nishikitani and F. Garnier
Synthetic Metals, Vo. 28, C723, 1989.

63. H. Koezuka and A. Tsumura
Synthetic Metals, Vol. 28, C753, 1989.

64. H. Shirakawa, E. G. Louis, A. G. MacDiarmid, C. K. Chiang and A. J. Heeger
J. Chem. Soc. Chem. Commun., p. 578, 1977.

65. M. Tanaka, A. Watanabe, H. Fujimoto and J. Tanaka
Chem. Lett., p. 907, 1980.

66. J. F. McAleer, S. Pons, H. B. Mark and G. Dunmore
J. of Molecular Electronics, Vol. 2, p. 183, 1986.

67. R. H. Baughman
in Conductive Polymers, (R. B. Seymour ed.), Plenum Press, New York, 1981

68. J. Bargon, S. Mohmand and R. J. Waltman
IBM. J. Res. Develop., Vol. 27, p. 330, 1983.

69. A. G. MacDiarmid, W. S. Huang and B. D. Humphrey
J. Chem. Soc.: Faraday Trans., Vol. 82, p. 2385, 1986.

70. A. F. Diaz and K. K. Kanazawa
J.C.S. Chem. Comm., p. 635, 1979.

71. A. F. Diaz and J. I. Castillo
J.C.S. Chem. Comm., p. 397, 1980.

72. G. Tourillon
in Handbook of Conducting Polymers, (T. A. Skotheim ed.),
Dekker, New York, Vol. 1, Chapter 9, 1986.

73. Handbook of Conducting Polymers, (T. A. Skotheim ed.),
Dekker, New York, Vol. 1 and 2; 1986

74. D. Bloor and B. Movaghar
IEE. Proc., Vol. 130, Pt. 1, p. 225, 1983.

75. B. D. Malhotra, N. Kumar and S. Chandra
Prog. Polym. Sci., Vol. 12, p. 179, 1986.

76. A. F. Diaz and K. K. Kanazawa
in Extended Linear Chain Compounds, (J.S Miller, ed.),
Plenum, New York, Vol. 3, p. 417, 1982.

77. G. Bidan
Materials Sci. Forum., Vol. 21, p. 21, 1987.

78. K. K. Kanazawa, A. F. Diaz, W. D. Gill, P. M. Grant, G. B. Street,
G. P. Gardini and J. F. Kwak
Synthetic Metals, Vol. 1, p. 329, 1979/1980.

79. K. K. Kanazawa, A. F. Diaz, R. H. Geiss, W. D. Gill, J. F. Kwak, J. A. Logan,
J. F. Rabolt and G. B. Street
J.C.S. Chem. Comm., p. 854, 1979.

80. K. J. Wynne and G. B. Street
Macromolecules, Vol. 18, p. 2361, 1985.

81. R. Noufi, A. J. Nozik, J. White and L. F. Warren
J. Electrochem. Soc., Vol. 129, p. 2261, 1982.

82. A. Dall'Olio, Y. Dascola, V. Varacca and V. Bocchi
Comptes Rendus, C267, p. 433, 1968.

83. A. F. Diaz and J. Bargon
in Handbook of Conducting Polymers, (T. A. Skotheim ed.), Dekker,
New York, Vol. 1, Chapter 3, 1986.

84. S. J. Hahn, W. E. Stachina, W. J. Gadia and P. O. Vogelhut
J. Electron. Mater., Vol. 15, p. 145, 1986.

85. M. Ogasawara, K. Funahashi and K. Iwata
Mol,. Cryst. Liq. Cryst., Vol. 118, p. 159, 1985.

86. T. F. Otero, R. Tejada and A. S. Elola
Polymer, Vol. 28, p. 651, 1987.

87. A. F. Diaz and B. Hall
IBM. J. Res. Develop., Vol. 27, p. 342, 1983.

88. L. J. Buckley, D. K. Roylance and G. E. Wenk
J. Polym. Sci, Pt. B, Polym. Phys., Vol. 25, p. 2179, 1987.

89. Bianting Sun, J. J. Jones, R. P. Burford and M. Skyllas-Kazacos
J. Electrochem. Soc., Vol. 136, p. 698, 1989.

90. D. T Glatzhofer, J. Ulanski and G. Wenger
Polymer, Vol. 28, p. 449, 1987.

91. D. Bloor, R. D. Hercliffe, C. G. Galiotis and R. J. Young
in Electronic Properties of Polymers and Related Compounds, Solid State
Sciences, Springer-Verlag. Vol. 63, p. 179, 1985.

92. K. M. Cheung, D. Bloor and G. C. Stevens
Polymer, Vol. 129, p. 1709, 1988.

93. J. Chapples
M.Sc. Thesis, Cranfield Institute of Technology, Nov. 1986.

94. A. Witkowski, M. S. Freund and A. Brajter-Toth
Anal. Chem., Vol. 63, p. 622, 1991.

95. R. Noufi, D. Tench and L. F. Warren
J. Electrochem. Soc., Vol. 127, p. 2310, 1980.

96. R. Noufi, A. J. Frank and A. J. Nozik
J. Am. Chem. Soc., p. 1849, 1981.

97. J. Prejza, I. Lundstrom and T. Skotheim
J. Electrochem. Soc., Vol. 129, p. 1685, 1982.

98. P. Burgmayer and R. W. Murray
in Handbook of Conducting Polymers, (T. A. Skotheim ed.),
Dekker, New York, Vol. 2, Chapter 15, 1986.

99. G. B. Street, T. C. Clarke, M. Krounbi, K. K. Kanazawa, V. Lee, P. Pfluger,
J. C. Scott and G. Weiser
Mol. Cryst. Liq. Cryst., Vol. 83, p. 253, 1982.

100. A. F. Diaz
Chem. Scripta, Vol. 17, p. 145, 1981.

101. R. Qian and J. Qiu
Polymer Journal, Vol. 19, p. 157, 1987.

102. M. Takakubo
Synthetic Metals, Vol. 18, p. 53, 1987.

103. W. Wernet, M. Monkenbusch and G. Wenger
Mol. Cryst. Liq. Cryst., Vol. 1181, p. 193, 1985.

104. G. Mengoli, M. M. Musiani, M. Fleischmann and D. Pletcher
J. Appl. Electrochem., Vol. 14, p. 285, 1984.

105. M. Satoh, M. Tabata, F. Uesugi, K. Kaneto and K. Yoshino
Synthetic Metals, Vol. 14, p. 289, 1986.

106. W. Wernet and G. Wegner
Makromol. Chem., Vol. 188, p. 1465, 1987.

107. M. Salmon, A. F. Diaz, A. J. Logan, M. Krounbi and J. Bargon
Mol. Cryst. Liq. Cryst.; Vol. 83, p. 265, 1982.

108. R. Qian, Y. Li, B. Yan and H. Zhang
Synthetic Metals, Vol. 28, C51, 1989.

109. W. Wernet, M. Monkenbusch and G. Wegner
Macromol, Chem., Rapid Commun., Vol. 5, p. 157, 1984.

110. G. K. Chandler and D. Pletcher
Chem. Soc. Spec. Period Rep. Electrochem., Vol. 10, p. 117, 1985.

111. A. F. Diaz, A. Martinez, K.K. Kanazawa and M. Salmon
J. Electroanal. Chem., Vol. 130, p. 181, 1980.

112. E. M. Genies, G. Bidan and A. F. Diaz
J. Electroanal. Chem., Vol. 149, p. 101, 1983.

113. G. B. Street, T. C. Clark, R. H. Geiss, A. Nazzal and J. C. Scott
Journal De Physique, Vol. 44, p. 599, 1983.

114. A. F. Diaz, J. I. Castillo, J. A. Logan and W. Y. Lee
J. Electroanal. Chem., Vol. 129, p. 115, 1981.

115. S. Kuwabata, H. Yoneyama and H. Tamura
Bull. Chem. Soc. Jpn., Vol. 57, p. 2247, 1984.

116. Y. Li and R. Qian
Synthetic Metals, Vol. 28, C127, 1989.

117. T. Shimidzu, A. Ohtani, T. Iyoda and K. Honda
J. Electroanal. Chem., Vol. 224, p. 123, 1987.

118. M. Iseki, K. Saito, K. Kuhara and A. Mizukami
Synthetic Metals, Vol. 40, p. 117, 1991.

119. Z. Cai and C. R. Martin
J. Electroanal. Chem., Vol. 300, p. 35, 1991.

120. R. M. Penner and C. R. Martin
J. Phys. Chem., Vol. 93, p. 984, 1989.

121. R. M. Penner, L. S. Van Dyke and C. R. Martin
J. Phys. Chem., Vol. 92, p. 5274, 1988.

122. P. G. Pickup and R. A. Osteryoung
J. Electroanal. Chem., Vol. 195, p. 271, 1985.

123. N. Mermilliod, J. Tanguy and F. Petiot
J. Electrochem. Soc., Vol. 133, p. 1073, 1986.

124. J. Tanguy, N. Mermilliod and M. Holcet
Synth. Met., Vol. 18, p. 7, 1987.

125. S. W. Feldburg
J. Am. Chem. Soc., Vol. 106, p. 4671, 1984.

126. S. W. Feldman, P. Burgermayer and R. W. Murray
J. Am. Chem. Soc., Vol. 107, p. 872, 1985.

127. M. M. Castillo-Ortega, M.B. Inoue and M. Inoue
Synthetic Metals, Vol. 28, p. C65, 1989.

128. R. E. Myers
J. Electron Mat., Vol. 15, p. 61, 1986.

129. M. Salmon, K. K. Kanazawa, A. F. Diaz and M. Krounbi
J. Polym. Sci., Polym. Lett. Ed., Vol. 20, p. 187, 1982.

130. A. Ohtani and T. Shimidzu
Bull. Chem. Soc. Jpn., Vol. 62, p. 234, 1989.

131. J. A. Walker, L. F. Warren and E. F. Witucki
J. Polym. Sci., Pt. A, Polym. Chem., Vol. 26, p. 1285, 1988.

132. G. Ciamician and P. Silber
Chem. Ber., Vol. 45, p. 1842, 1912.

133. A. Angeli and L. Alessandri
Gazz, Chim. Ital., Vol. 46, p. 283, 1916.

134. G. P. Gardini
Adv. Heterocycl. Chem., Vol. 15, p. 67, 1973.

135. G. Plancher
Atti. Accad. Naz. Linceri, Vol. 12, p. 490, 1904.

136. R. B. Bjorklund and I. Lundstrom
J. Electron Mat., Vol. 13, p. 211, 1984.

137. R. B. Bjorklund, H. Gustavsson, I. Lindstrom and B. Nygren
U.S. Patent, 4,521,450, 1985.

138. H. Naarmann, W. Heckmann, G. Kohler and P. Simak
U.S. Patent, 4,567,250, 1986.

139. V. Bocchi, G. P. Gardini and S. Rapi
J. Mat. Sci. Lett., p.1283, 1987.

140. V. Bocchi and G. P. Gardini
J. Chem. Soc., Chem. Commun., p. 148, 1986.

141. E. Ruckenstein and J. S. Park
J. Appl. Polym. Sci., Vol. 42, p. 925, 1991.

142. R. V. Gregory, W. C. Kimbrell and H. H. Kuhn
Synthetic Metals, Vol. 28, C823, 1989.

143. A. Pron, Z. Kucharski, C. Budrowski, M. Zagorska, S. Krichene, J. Suwalski, G. Dehe and S. Lefrant
J. Chem. Phys., Vol. 83, p. 5923, 1985.

144. M. Zagorska, A. Pron, S. Lefrant, Z. Kucharski and P. Bernier
Synthetic Metals, Vol. 18, p. 43, 1987.

145. A. Pron, J. Suwalski and S. Lefrant
Synthetic Metals, No. 18, p. 25, 1987.

146. G. Dascola, C. Giori, V. Varacca and L. Chierici
C. R. Acad. Sci., Ser. C 262, p. 1617, 1966.

147. A. Watanabe, K. Mori, M. Mikuni, Y. Nakamura and M. Matsuda
Macromolecules, Vol. 22, p. 3323, 1989.

148. E. M. Genies, A. A. Syed and C. Tsintavis
Mol. Cryst. Liq. Cryst. Vol. 121, p. 181, 1988.

149. D. E. Stilwell and S. M. Park
J. Electrochem. Soc., Vol. 135, p. 2491, 1988.

150. O. Niwa and T. Tamamura
J. Chem. Soc., Chem. Commun., p. 817, 1984.

151. M. A. De Paoli, R. J. Waltman, A. F. Diaz and J. Bargon
J. Chem. Soc., Chem. Commun., p. 1015, 1984.

152. M. A. De Paoli, R. J. Waltman, A. F. Diaz and J. Bargon
J. Polym. Sci: Polym. Chem. Ed., Vol. 23, p. 1687, 1985.

153. G. Ahlgren and B. Krische
J. Chem. Soc., Chem. Commun., p. 946, 1984.

154. S. E. Lindsey and G. B. Street
Synthetic Metals, Vol. 10, p. 67, 1984/85.

155. H. Lindenberger, S. Roth and M. Hanack
in 'Electronic properties of polymers and related Compounds',
Solid State Sciences, Springer-Verlag, Vol. 63, p. 194, 1985.

156. M. Hikita, O. Niwa, S. Sugita and T. Tamamura
Jpn. J. Appl. Phys., Vol. 24, p. L79, 1985.

157. T. T. Wang, S. Tasaka, R.S. Hutton and P. Y. Lu
J. Chem. Soc., Chem. Commun., p. 1343, 1985.

158. R. M. Penner and C. R. Martin
J. Electrochem. Soc., Vol. 133, p. 310, 1986.

159. F. F. Fan and A. J. Bard
J. Electrochem. Soc., Vol. 133, p. 301, 1986.

160. E. Ruckenstein and J. H. Chen
Polymer, Vol. 32, p. 1230, 1991.

161. R. B. Bjorklund and B. Liedberg
J. Chem. Soc., Chem. Commun., p. 1293, 1986.

162. D. R. Rueda, C. Arribas, F. J. Balta Calleja and J. M. Palacios
Synthetic Metals, No. 28, C77, 1989.

163. A. Yassar, J. Roncali and F. Garnier
Polym. Commun., Vol. 28, p. 103, 1987.

164. Y. Chen, R. Qian, G. Li and Y. Li
Polymer Commun., Vol. 32, p. 189, 1991.

165. A. Pron, W. Fabianowski, C. Budrowski, J. B. Raynor, K. Kucharski,
J. Suwalski, S. Lefrant and G. Fatseas
Synthetic Metals, Vol. 18, p. 49, 1987.

166. T. Ojio and S. Miyata
Polymer J., Vol. 18, p. 95, 1986.

167. A. Mohammadi, I. Lundstrom, O. Inganas and W. R. Salaneck
Polymer, Vol. 31, p. 395, 1990.

168. S. P. Armes and M. Aldissi
Polymer, Vol. 31, p. 569, 1990.

169. H. Munstedt
Polymer, Vol. 27, p. 899, 1986.

170. H. Munstedt, H. Naarman and G, Kohler
Mol. Cryst. Liq. Cryst. Vol. 118, p. 129, 1985.

171. O. Inganas, R. Erlandsson, C. Nylander and I. Lundstrom
J. Phys. Chem. Solids, Vol. 45, p. 427, 1984.

172. Y. Li and R. Qian
Synthetic Metals, Vol. 26, p. 139, 1988.

173. G. Gustaffson, I. Lundstrom, B. Liedberg, C. R. Wu and O. Inganas
Synthetic Metals, Vol. 31, p. 163, 1989.

174. R. Qian, J. Qiu and D. Shen
Synthetic Metals, Vol. 18, p. 13, 1987.

175. G. Wegner, W. Wernet, D. T. Glatzhofer, J. Ulanski and M. Mohammadi
Synthetic Metals, Vol. 18, p. 1, 1987.

176. Y. Li and R. Qian
Synthetic Metals, Vol. 28, C. 126, 1989.

177. C. K. Mann
in Electroanalytical chemistry, (A. J. Bard ed.),
Marcel Dekker, New York, Vol. 3, 1969.

178. R. C. Larson, R. T. Iwamoto and R. N. Adams
Anal. Chim. Acta, Vol. 25, p. 1161, 1961.

179. M. Hayes
in Techniques in Electrochemistry, Corrosion and Metal Finishing: A Handbook
(A. T. Kuhn ed.), John Wiley and Sons, Chichester, Chapter 1, 1987.

180. G. Milazzo and S. Caroli
Tables of Standard Electrode Potentials, Wiley-Interscience, New York, 1977.

181. H. Block, M. A. Cowd and S. M. Walker
Polymer, Vol. 19, p. 531, 1987.

182. A. G. MacDiarmid, S. L. Mu, N. L. D. Somasiri and W. Wu
Mol. Cryst. Liq. Cryst., Vol. 121, p. 173, 1985.

183. A. F. Diaz, J. M. Vasquez Vallejo and A. M. Duran
IBM. J. Res. Develop., Vol. 25, p. 42, 1981.

184. A. J. Bard and L. R. Falkner
Electrochemical Methods: Fundamentals and Applications, New York,
John Wiley and Sons, p. 222, 1980.

185. Encyclopaedia of Electrochemistry of the Elements,
(A.J. Bard, Ed.), Marcel Dekker, New York, Vol. 2, 1976.

186. A. R. Despic
in Deposition and dissolution of Metals and Alloys,
Pt. B. Mechanisms, Kinetics, Texture, and Morphology
(B. E. Conway, J. O'M. Brockris and E. Yeager Eds.)
Chapter 7, p. 451, 1983.

187. T. Inoue and T. Yamase
Bull. Chem. Soc. Jpn., Vol. 56, p. 985, 1983.

188. F. A. Cotton and G. Wilkinson
Advanced Inorganic Chemistry: A Comprehensive Text, (4th ed),
John Wiley & Sons, New York, p. 801, 1980.

189. A. J. Bard and L. R. Falkner
Electrochemical Methods: Fundamentals and Applications, New York,
John Wiley and Sons, p. 417, 1980.

190. J. B. Schlenoff and J. C. W. Chien
J. Am. Chem. Soc., Vol. 109, p. 6269, 1987.

191. J. H. Kaufman, K. K. Kanazawa, and G. B. Street
Phys. Rev. Lett., Vol. 53, p. 2461, 1984.

192. M. Slama and J. Tanguy
Synthetic Metals, Vol. 28, C171, 1989.

193. T. Iyoda, A. Ohtani, T. Shimozu and K. Honda
Chem. Lett., p. 687, 1986.

194. A. R. Despic and K. I. Popov
in Modern Aspects of Electrochemistry,
(B. E. Conway and J. O'M Brokris eds.)
Plenum Press, New York, No. 7, 1972.

195. A. J. Bard and L. R. Falkner
Electrochemical Methods: Fundamentals and Applications, New York,
John Wiley and Sons, p. 412, 1980.

196. S. Asavapiriyanont, G. K. Chandler, G. A. Gunawardena, and D. Pletcher
J. Electroanal. Chem., Vol. 177, p. 245, 1984.

197. A. J. Bard and L. R. Falkner
Electrochemical Methods: Fundamentals and Applications, New York,
John Wiley and Sons, p. 222, 1980.

198. P. Pfluger, M. Krounbi, G.B. Street and G. Weiser
J. Chem. Phys., Vol. 78, p. 3213, 1983.

199. Encyclopaedia of Electrochemistry of the Elements,
(A.J. Bard, Ed.), Marcel Dekker, New York, Chapter 2, Vol. 2, 1976.

200. E. Scholtens
U.S. Patent 4 478 690, 1984.

201. R. J. Taylor and A. A. Humffray
J. Electronal. Chem., Vol. 64, p. 63, 1975.

202. J. P. Hoare
in Encyclopaedia of Electrochemistry of the Elements, (A.J. Bard, Ed.), Marcel Dekker, New York, Chapter 5, Vol. 2, 1976.

203. S. Antoniadou, A. D. Jannakaoudakis and E. Theordoridou
Synthetic Met., Vol. 30, p. 283, 1989.

204. P.K. Adanuvor and R. E. White
J. Electrochem. Soc., Vol. 135, p. 2509, 1988.

205. J. O'M. Brockris, J. A. Ammar and A.K.M.S. Huq
J. Phys. Chem., Vol. 61, p. 879, 1957.

206. E. T. Kang, K. G. Neoh, Y. K. Ong, K. L. Tan and B. T. G. Tan
Polymer, Vol. 32, p. 1354, 1991.

207. J. C. Scott, M. T. Krounbi, P. Pfluger and G. B. Street
Physical Review B, Vol. 28. p. 2410, 1983.

208. K. Shigehara and F. C. Anson
J. Phys. Chem., Vol. 86, p. 2776, 1982.

209. D. A. Buttry and F. C. Anson
J. Am. Chem. Soc., Vol. 104, p. 4824, 1982.

210. W. S. Huang, B. Humphrey and A. G. MacDiarmid
J. Chem. Soc., Faraday Trans., Vol. 82, p. 2385, 1986.

211. B. Zinger, S. Shkolnik and H. Hocker
Polymer, Vol. 30, p. 628, 1989.

212. J. Christoph
in Electroplating of Plastics: Handbook of Theory and Practice, Middlesex, Finishing Publications, p. 24 and 153, 1977.

213. D. F. Foust and W. V. Dumas
in Metallization of Polymers: ACS Symposium Series 440, (E. Sacher, J. J Pireaux, S. T. Kowalczyk, Eds.), Amer. Chem. Soc., Washington, DC, Chapter 35, 1990.

214. Standards and Guidelines for Electroplated Plastics
Third Ed., American Society of Electroplating Plastics, Prentice Hall, Chapter 10, p.110, 1984.

215. G. Muller and D. W. Baudrand
in Plating on Plastics; a Practical Handbook, 2nd edn., Draper, Chapter 4, 1971.

216. Hydrogels in Medicine and Pharmacy, Fundamentals,
(N. A. Peppas ed.), CRC Press, Inc, Florida, Vol. 1, 1986.

217. A. Brenner
J. Electrochem. Soc., Vol. 103, p. 652, 1956.

218. T. Takei
Surface Technology, Vol. 8, p. 543, 1979.

219. H. E. Patten and W. R. Mott
Trans. Electrochem, Soc., Vol. 15, p. 529, 1909.

220. I. A. Menzies
Trans. Inst. Metal Finishing, Vol. 39, p. 172, 1962.

221. R. N. Adams
in Electrochemistry at Solid Electrodes, Marcel Dekker, New York, 1969.

222. E. H. Lyons
in Modern Electroplating, (3rd. edn), New York and London,
Electrochemical Society Series, John Wiley & Sons, 1974.

223. M. Fleischmann and H. R. Thirsk
in Advances in Electrochemistry and Electrochemical Engineering,
(P. Delahay ed.), Interscience Publishers, John Wiley & Sons, Chapter 3, 1963.

224. Metals Handbook, Desk Edn.
(H. E. Boyer and T. L. Gall eds.), American Society for Metals, Ohio, 1984

225. B. Linford and O. D. Feder
Plating, Vol. 41, p. 397, 1954.

226. E. Raub and K. Muller
Fundamentals of Metal Deposition, London, Elsevier, Chapter 5, 1967.

227. E. Raub and K. Muller
Fundamentals of Metal Deposition, London, Elsevier, Chapter 3, 1967.

228. A. T. Kuhn
in Techniques in Electrochemistry, Corrosion and Metal Finishing: A Handbook
(A. T. Kuhn ed.), John Wiley and Sons, Chichester, Chapter 7, 1987.

229. A. R. Despic and K. I. Popov
J. Appl. Electrochem., Vol. 1, p. 275, 1971.

230. N. Ibl
Surface Technology, Vol. 10, p. 104, 1980.

231. D. S. Carr
in Techniques of Electrochemistry, (E. Yeager, A. Salkin, Eds.),
Wiley Interscience, New York, Vol. 3, Chapter 6, p. 495, 1978.

232. T. Komori, H. Takahashi and N. Okamoto
Colloid. Polym. Sci., Vol. 266, p. 1181, 1988.

233. E. Raub and K. Muller
Fundamentals of Metal Deposition, London, Elsevier, Chapter 4, p. 135, 1967.

234. M. Matsushita, M. Sano, Y. Hayakawa, H. Honjo and Y. Sawada
Phys. Rev. Lett., Vol. 53, p. 287, 1984.

235. Y. Sawada, A. Dougherty and J. P. Gollub
Phys. Rev. Lett., Vol. 56, p. 1260, 1986.

236. A. Clarke
Personal communication, Kodak Ltd, Harrow, England. 1991.

237. L. Nyikos and T. Pajkossy
Electrochim. Acta., Vol. 30, p. 1533, 1985.

238. T. Pajkossy and L. Nyikos
J. Electrochem. Soc., Vol. 133, p. 2061, 1986.

239. W. H. Mulder and J. H. Sluyters
Electrochimica Acta. Vol. 33, p. 303, 1988.

240. W. Schelder
J. Phys. Chem., Vol. 79, p. 127, 1975.

241. R. De Levie
Electrochim. Acta., Vol. 10, p. 113, 1965.

242. B. B. Mandelbrot
The Fractal Geometry of Nature, Freeman, San Francisco, 1977.

243. M. Born and E. Wolf
Principles of Optics; Electromagnetic Theory of Propagation interference and Diffraction of Light. Pergamon Press, sixth edn. p. 621, 1987.

244. G. T. Dee, L. E. Manring and S. Mazur
J. Phys. Chem., Vol. 91, p. 6699, 1987.

245. S. Mazur
U.S. Patent 4 512 855, 1985.

246. C. Yen, C. J. Huang and T. C. Chang
J. Appl. Polym. Sci., Vol. 42, p. 439, 1991.

247. C. J. Huang, C. C. Yen and T. C. Chang
J. Appl. Polym. Sci., Vol. 42, p. 2237, 1991.

248. V. C. Carver, L. T. Taylor, T. A. Furtsch and A. K. St. Clair
J. Amer. Chem. Soc., Vol. 102, p. 876, 1980.

249. S. Mazur and S. Reich
in Integration of Fundamental Polymer Science and Technology, Elsevier, Amsterdam, p. 265, 1985.

250. T. L. Rose, R. H. Micheels, D. H. Longendorfer and R. D. Rauh
Mat. Res. Soc. Symp. Proc., Vol. 17, p. 265, 1983.

251. R. H. Micheels, A. D. Darrow and R. D. Rauh
Appl. Phys. Lett., Vol. 39, p. 418, 1981.